INTERNATIONAL COLLOQUIUM

STABILITY OF STEEL STRUCTURES

HUNGARY, BUDAPEST 1990

PRELIMINARY REPORT

VOLUME II.

TECHNICAL UNIVERSITY OF BUDAPEST

HUNGARIAN ACADEMY OF SCIENCES

STRUCTURAL STABILITY RESEARCH COUNCIL

INTERNATIONAL ASSOCIATION FOR BRIDGE
AND STRUCTURAL ENGINEERING

INTERNATIONAL COLLOQUIUM
EAST-EUROPEAN SESSION

STABILITY OF STEEL STRUCTURES

PRELIMINARY REPORT

VOLUME II.

EDITED BY
M. IVÁNYI
B. VERŐCI

HUNGARY, BUDAPEST
APRIL 25-27, 1990

Címlap
részlet Somogyi Győző
rajzából

Cover
a piece of Győző Somogyi's
drawing

ISBN 963-421-487-8 Ö.

ISBN 963.420.219.5 R 2 1.

MC109.788/2
ORSZ. SZÉCHÉNYI KÖNYVTÁR
1990

Felelős szerkesztők: Dr. Iványi Miklós
Dr. Verőci Béla
Kiadja: a Budapesti Műszaki Egyetem
Acélszerkezetek Tanszék
A kiadásért felelős: az Acélszerkezetek
Tanszék vezetője
Készült: a Budapesti Műszaki Egyetem
Sokszorosító Üzemében
Felelős vezető: Miszori Sándor
Példányszám: 350, Méret: B/5

SESSION 6

PLATE & BOX GIRDERS

(1)
BALÁŽ, Ivan (1)

EFFICIENT CALCULATION OF BOX GIRDER SECTION MODULUS

INTERNATIONAL COLLOQUIUM
STABILITY OF STEEL STRUCTURES
BUDAPEST, HUNGARY, 1990
PRELIMINARY REPORT

SUMMARY: A new way of section modulus calculation is presented which could be very useful and efficient tool in the design of thinwalled structures when repeated calculation of section modulus is needed. Numerical examples show how it is possible to calculate:
(i) the section modulus of the effective cross-section from the known section modulus of the gross cross-section and from the given effective flange area ratios in the case when the area of girder tension flange is to be reduced due to effect of shear lag and/or the area of girder compression flange is to be reduced due to shear lag, local and global buckling;
(ii) the section modulus of another gross cross-section with the same shape, same area of the webs, but with the different areas of the upper and/or bottom girder flange.

NOTATION:

$\varrho_{W_i} = W_{e,i}/W_i$	is effective section modulus ratio ($i = u,b$ for upper and bottom flange, respectively)
$\varrho_{A_i} = A_{e,i}/A_i$	is effective flange area ratio ($i = u,b$)
ϱ_{ef}	is reduction coefficient accounting for shear lag
ϱ_{np}, ϱ_{nf}	are reduction coefficients accounting for compressed isotropic plate and orthotropic flange buckling, respectively
$\varrho_{bn} = (bt\,\varrho_{np} + n\,A_{st})/(bt + n\,A_{st})$	is partial efficiency factor
n, A_{st}	is number of long. stiffeners and long. stiffener area, respectively.

(1) Ing.,CSc., Stavebná fakulta SVŠT Bratislava, ČSSR
(M.Sc., Ph,D., Faculty of Civil Engineering,
Slovak Technical University Bratislava, Czechoslovakia)

(2)

INTRODUCTION The SNP bridge across the Danube in Bratislava will be used in numerical examples. It has 15 cross-sections with the same shape which differ in t_i (Fig. 1). Location some of the cross-section types can be found in Fig. 4. The way of section modulus calculation will be demonstrated on the cross-section No 1 with: $t_1 = t_3 = t_4 = t_6 = t_7 = 12$, $t_2 = 6$, $t_5 = 36$, $t_8 = t_9 = 25{,}2$ mm, $A_u = 0{,}443\ 44\ m^2$ (including long. stiffener and cantilever areas), $A_b = 0{,}192\ 86\ m^2$, $W_u \equiv W_{153} = 1{,}972\ m^3$, $W_b \equiv W_{47} = 1{,}261\ m^3$ (location of the points 153, 47 is shown in Fig. 2).

The variation of the effective section modulus ratios ϱ_{W_i} of the cross-section No 1 as a function of the two variables ϱ_{A_u} and ϱ_{A_b} is shown in Fig. 3. Note that functions

$\varrho_{W_u} = f(\varrho_{A_u})$ for $\varrho_{A_b} = \text{const.}$ and $\varrho_{W_b} = f(\varrho_{A_b})$ for $\varrho_{A_u} = \text{const.}$

are linear (Fig. 3). It is valid also for the cross-sections with different shape. The functions ϱ_{W_i} can be very good approximated in for us interesting area (e.g. in area defined by $\varrho_{A_u} > 0{,}6$, $\varrho_{A_b} > 0{,}5$) by the functions

$$\varrho_{W_i} = C_{1,i}\,\varrho_{A_u}\varrho_{A_b} + C_{2,i}\,\varrho_{A_u} + C_{3,i}\,\varrho_{A_b} + C_{4,i} \qquad (1)$$

Now we have to calculate ϱ_{W_u} and ϱ_{W_b} for four cross-sections (including gross cross-section) to determine $C_{k,i}$. The values ϱ_{W_u}, ϱ_{W_b} which were obtained for cross-section No 1 can be found in Fig. 3 and they enabled us to write

$$\varrho_{W_u} = 0{,}115\,\varrho_{A_u}\varrho_{A_b} + 0{,}019\,\varrho_{A_b} + 0{,}735\,\varrho_{A_u} + 0{,}131 \qquad (2)$$

$$\varrho_{W_b} = 0{,}065\,\varrho_{A_u}\varrho_{A_b} + 0{,}577\,\varrho_{A_b} + 0{,}0475\,\varrho_{A_u} + 0{,}3105 \qquad (3)$$

Knowing two values $W_{e,i} = \varrho_{W_i} W_i$ ($i = u,b$, where in our case $u = 153$, $b = 47$) we can obtain (Fig. 2):

(i) $W_{e,s} = I_e / z_e(s)$ for every point of the cross-section ($s = 1, 2, \ldots 296$),

(ii) the shift of the neutral axis Δz from the following formulae:

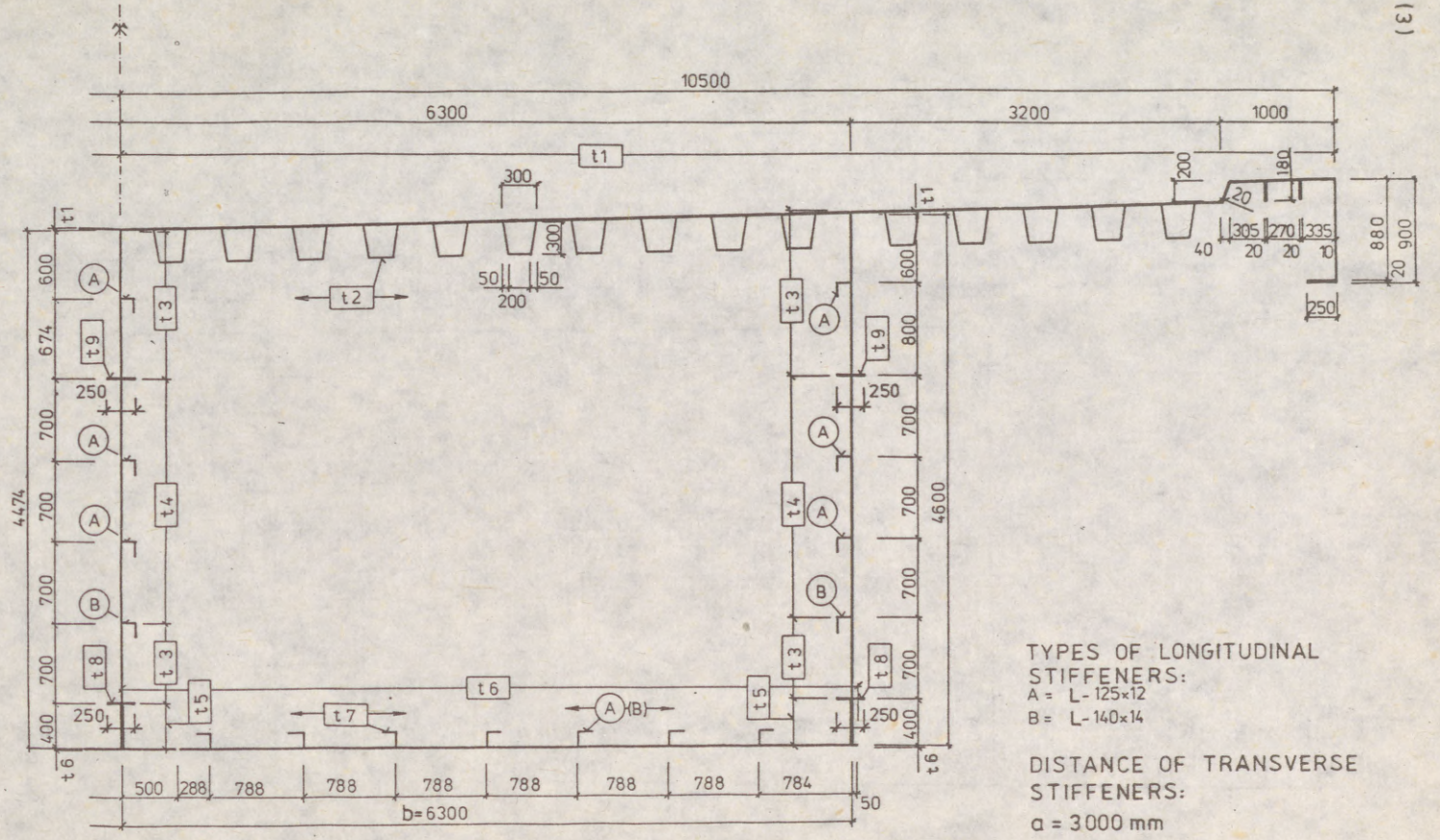

TYPES OF LONGITUDINAL STIFFENERS:
A = L-125×12
B = L-140×14

DISTANCE OF TRANSVERSE STIFFENERS:
a = 3000 mm

FIG. 1 TYPICAL CROSS SECTION OF THE SNP BRIDGE ACROSS THE DANUBE IN BRATISLAVA, ČSSR

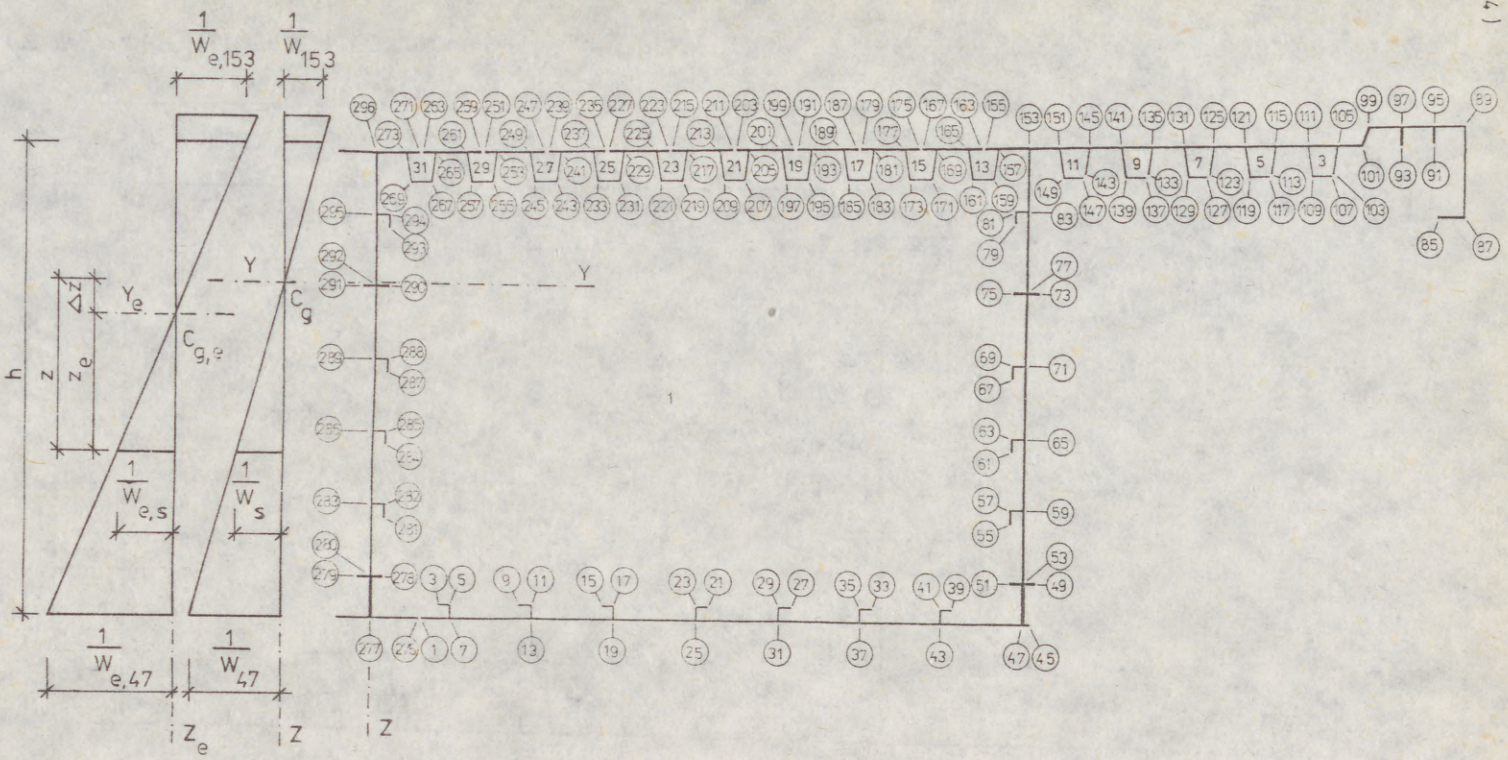

FIG. 2 TO THE CALCULATION OF EFFECTIVE SECTION MODULUS $W_{e,s}$. LOCATION OF 296 POINTS AND 32 CELLS OF THINWALLED BRIDGE BOX GIRDER CROSS SECTION.

(5)

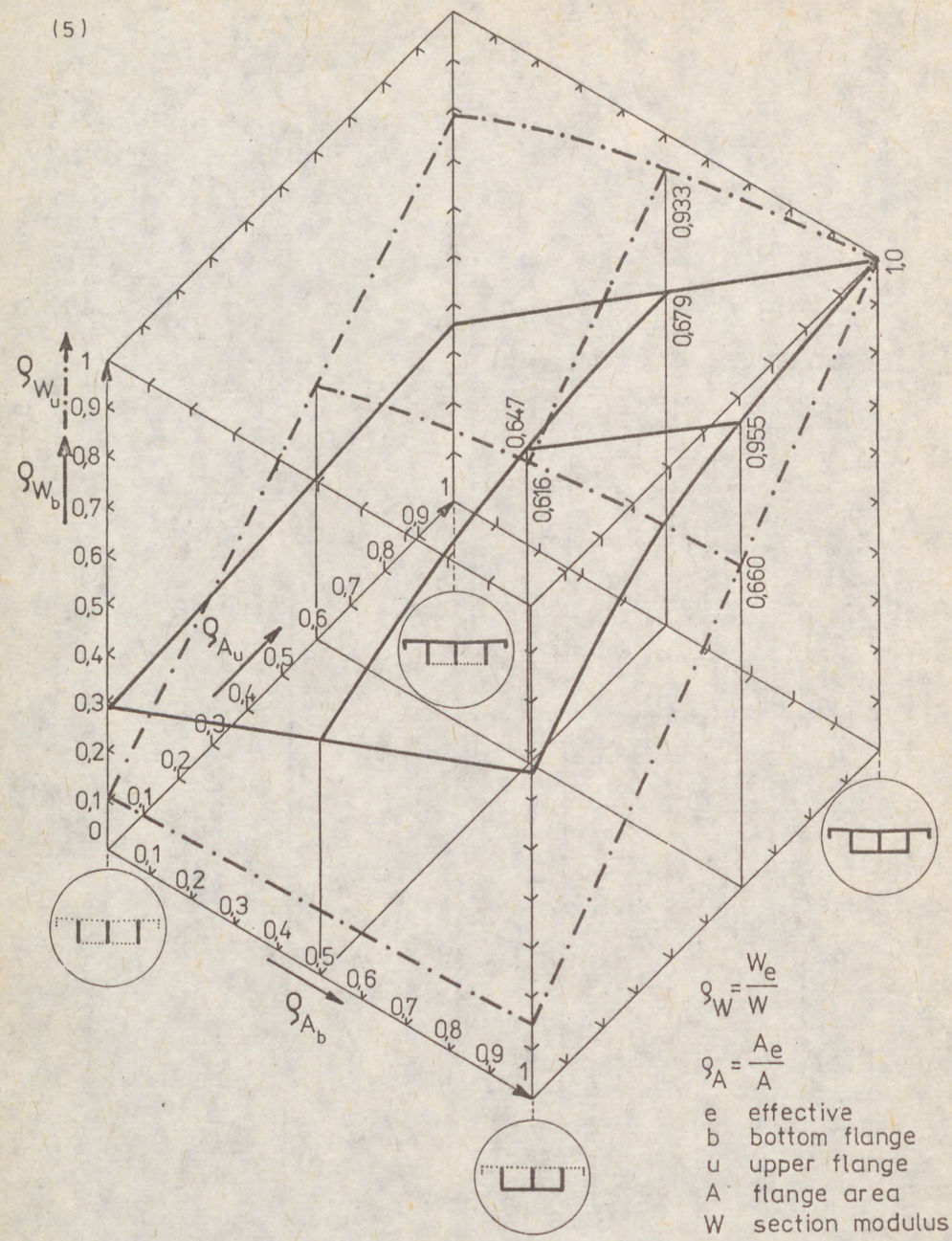

FIG 3 VARIATION OF EFFECTIVE SECTION MODULUS RATIOS ϱ_{W_u} AND ϱ_{W_b} AS A FUNCTION OF TWO VARIABLES ϱ_{A_u} AND ϱ_{A_b} (EFFECTIVE FLANGE AREA RATIOS)

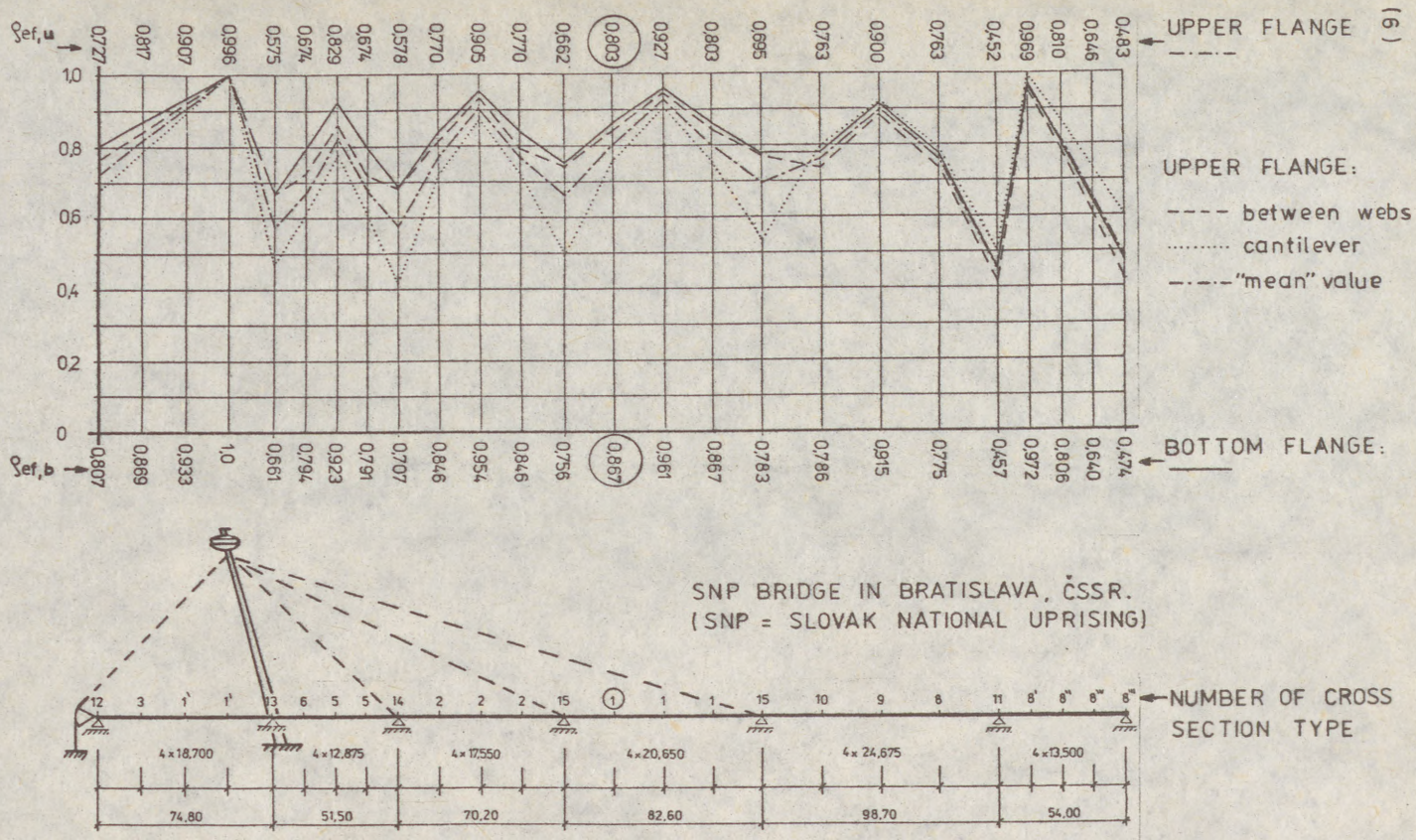

FIG. 4 VARIATION OF STRESS EFFECTIVE BREADTH RATIOS ϱ_{ef} ALONG SPAN OF CABLE STAYED BRIDGE FOR UNIFORM LOAD. IN APPROXIMATE CALCULATION THE BRIDGE WAS REPLACED BY SIX SPAN CONTINUOUS GIRDER ON RIGID SUPPORTS WITH ϱ_{ef} - VALUES ON THE SAFE SIDE, OBTAINED FROM [3].

(7)

$$\frac{1}{W_{e,s}} = \left[1 - \frac{z_{47} - z}{h}\left(1 + \frac{\rho_{W_b} W_b}{\rho_{W_u} W_u}\right)\right] \frac{1}{\rho_{W_b} W_b} \qquad (4)$$

$$\Delta z = \frac{h}{1 + (W_b/W_u)} - \frac{h}{1 + (\rho_{W_b} W_b / \rho_{W_u} W_u)} \qquad (5)$$

Only z or Δz can be negative in eqns (4), (5).

EXAMPLE 1: Evaluate $W_{e,u} \equiv W_{e,153}$ for the cross-section No 1 which has $\rho_{ef,u} = 0{,}803$, $\rho_{ef,b} = 0{,}867$ (Fig. 4).

In the chosen section the bottom flange is in compression due to bending moment and normal force. Reduction coefficients accounting for local and global buckling of the flange were calculated according to [1, 2] using criterion a/ together with $\sigma_{max} = R_d = 290$ MPa. Simple design formulae derived by the author in [1] can be found also in [5]. For initial local and global curvature of the flange $W_0^P = b_{st}/200$ and $W_0^L = a/500$, respectively, we obtained $\rho_{nf,b} \cdot \rho_{bn,b} = 0{,}73$ (Fig. 5).

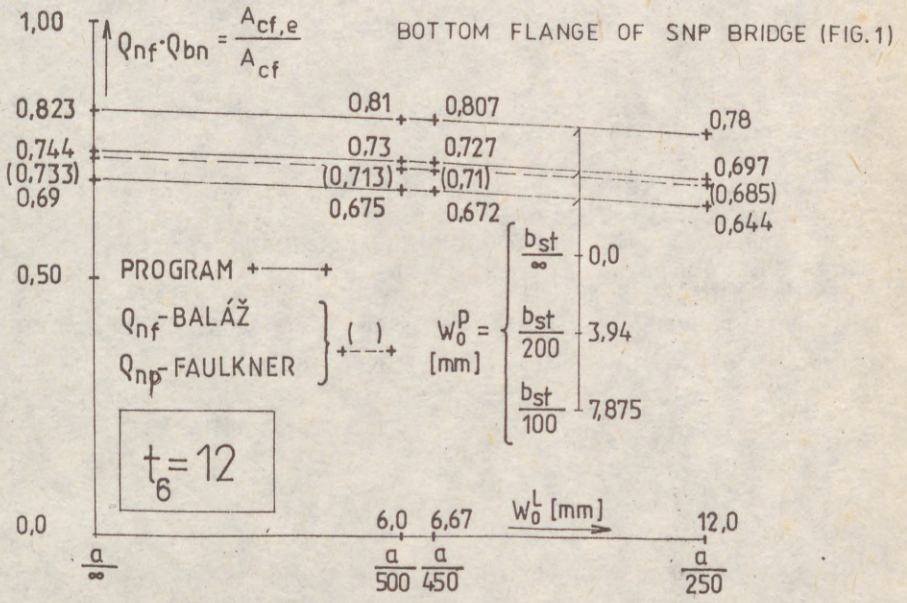

FIG.5 INFLUENCE OF INITIAL DEFLECTIONS OF LONGITUDINAL STIFFENERS w_o^L AND/OR PLATE PANELS w_o^P ON THE EFFECTIVE FLANGE AREA RATIO. COMPRESSION FLANGE IS CALCULATED USING PROGRAM "ORTHO" OR SIMPLE DESIGN FORMULAE [1, 2].

(8)

According to code ČSN 73 6205 we can write now for the bottom flange

$$\varrho_{A_b} = \varrho_{nf,b} \cdot \varrho_{bn,b} \sqrt{\varrho_{ef,b}} = 0,73 \cdot \sqrt{0,867} = 0,68 < \varrho_{ef,b} = 0,867$$

and for the upper flange (it is compressed due to big normal force, but no local or global buckling occurs in it)

$$\varrho_{A_u} = 1. \sqrt{0,803} = 0,896 > \varrho_{ef,u} = 0,803 \Rightarrow \varrho_{A_u} = \varrho_{ef,u} = 0,803$$

Substituting ϱ_{A_b} and ϱ_{A_u} in eqn (2) we obtain

$\varrho_{W_u} = 0,797$ and then $W_{e,u} = \varrho_{W_u} W_u = 0,797 \cdot 1,972 = 1,572 \ m^3$

EXAMPLE 2: Evaluate $W_b \equiv W_{47}$ for the cross-section No 2 which differs from No 1 only in $t_6 = 14$ mm. The cross-section No 2 has $A_u = 0,443\ 44\ m^2$, $A_b = 0,218\ 26\ m^2$, $W_b = 1,369\ m^3$, $W_u = 1,996\ m^3$.

$\varrho_{A_b} = A_b^{(2)} / A_b^{(1)} = 0,218\ 26 / 0,192\ 86 = 1,131\ 7$, $\varrho_{A_u} = 1$

Substituting ϱ_{A_b} and ϱ_{A_u} in eqn (3) we obtain

$\varrho_{W_b} = 1,0845$, $W_b^{(2)} = \varrho_{W_b} W_b^{(1)} = 1,0845 \cdot 1,261 = 1,368\ m^3$

The error is negligible (compare approximate value 1,368 with exact value 1,369).

ACKNOWLEDGEMENTS. The paper is part of the work "Load carrying capacity of the SNP bridge" which was done under the supervision of Associated Professor Eugen CHLADNÝ at the Slovak Technical University Bratislava. The author wishes to thank Mr. Daniel GOMBA, student of the STU Bratislava, for computation of ϱ_{ef} values in Fig. 4 and Mr. Steve KOTLEBA of the JKC International Los Angeles for his helpful advice.

(9)

REFERENCES:

[1] BALÁŽ, I.; 1977, Post-Critical Behaviour of Stiffened Compression Flanges and Torsion of Large Box Girder Bridges, Ph.D. Thesis, Sloval Academy of Sciences Bratislava.

[2] BALÁŽ, I., 1987, Ausgesteifte Druckgurte von Kastenträgerbrücken, Stahlbau, Heft 5, pp. 145-154.

[3] MOFFATT, K.R., DOWLING, P.J., 1975, Shear Lag in Steel Box Girder Bridges, Struct. Eng. London 53, No.10, pp. 439-448.

[4] MURRAY, N.W., 1986, Introduction to the Theory of Thin-Walled Structures, Clarendon Press, Oxford.

[5] World View, 1989, Stability of Metal Structures, 2nd Edition, Vol.1, pp. 170-171.

(1)
CHRÓŚCIELEWSKI, Jacek (1)
CYWIŃSKI, Zbigniew (2)
SMOLEŃSKI, Witold (3)

POSTBUCKLING BEHAVIOUR OF HYBRID PLATE GIRDERS WITH WEB OPENINGS

INTERNATIONAL COLLOQUIUM
STABILITY OF STEEL STRUCTURES
BUDAPEST, HUNGARY, 1990
PRELIMINARY REPORT

Summary: Within certain case study, the practical conduct of initially imperfect, geometrically and statically identic hybrid and homogeneous I-beams with rectangular web openings, under bending and shear, has been investigated theoretically by special FEM procedure - in order to settle the qualitative consequence of flange steel nature on the postbuckling carrying capacity of those beams. For simple loading and support conditions, depending upon the opening longitudinal location, the bending or shear modes of failure have been found essential, showing a substantial effect of flange steel quality among the bending, and little such effect among the shear modes, respectively.

BACKGROUND AND GOAL

Perforated I-beams have been focus of research, both theoretical and experimental, throughout many years whereby castellated beams and beams with web openings (more or less individual in nature), as shown by Cywiński in 1984 and 1987, appeared to be two main types of that beam cathegory; for reasons of some structural requirements of tall buildings and bridge constructions, the second type of perforated beams became point of special interest, to mention only many studies headed by Redwood, the experimental one of 1978, in particular.

(1) Assistant Professor of Structural Engineering, Technical University of Gdańsk, Poland;
(2) Professor of Structural Engineering, as (1);
(3) Instructor of Structural Engineering, as (1).

(2)

Analysing the research discussed by Cywiński in 1987 and that published later, it can be characterized, as follows:

- in the past the theoretical approach was based, predominantly, on the classic theory of elasticity and simplified design models, as well as - upon the conventional buckling theory, whereby elastic treatment has been found uneconomical because of high stress concentrations at the cut-outs;
- extensive experimental investigations have been performed to interpret the beam structural performance, finding the theoretical simplifications unfit to account for the real stress-states, in particular - as far as the opening zones are concerned;
- space modelling respecting different initial imperfections, together with plastic approach, has been found prerequisite to describe the actual nonlinear behaviour of the beams considered.

Mentioned three-dimensional, nonlinear treatment was used first in the analysis of other structures, e.g. ribbed plates examined by Chróścielewski in 1983; obviously, its character could be numerical and, accordingly, individual only, and had to base upon proper FEM procedures, as shown by Bathe,1982. It was demonstrated twice in 1987 by Chróścielewski et al. that similar theoretical treatment could be referred also to I-beams with isolated rectangular web-openings; the compliance of the developed theoretical with the existing experimental results of Redwood et al., 1978, has been found encouraging. More perfect results in that field have been obtained by Chróścielewski et al. in 1989. Hereby two main observations have been made:

- that together with the increase of the number of finite elements (from 86, over 210, to 400) the real, experiment related, beam carrying capacity was approached, and
- that the magnitude and the form of the initial imperfections had little influence on the beam postbuckling final performance, just slightly effecting the value of the critical load at the initiation of the beam buckling process.

Since two decades, at least, it is well known that hybrid steel I-beams are much stronger in bending than similar homogeneous beams. As a proper reference the paper of Cywiński, first of 1978, can be quoted, where a hybrid beam, with the ratio of yield stresses for flanges and web equal 2.78, was found 89 % stronger than a homogeneous one, the ratio of which was equal 1.00; naturally, the precondition was the development of full plastic moment and lateral support of those beams. Another magnification of the bending strength can be achieved by transforming the normal I-beam into the castellated one. As shown by Cywiński in the second paper of 1978, when combining the effects of hybridity and castellation, a considerable increase of the beam bending strength could be obtained.

Obviously, all those considerations, since based upon simplified assumptions, must be regarded as rather approximate.

(3)
Therefore, recent studies on ordinary I-beams, like that of Dunai, 1986, or on those with web openings of Chrôścielewski et al., 1987 and 1989, had to be more accurate. An adjustment of the last mentioned for the problem of hybrid beams is being approached in the present report, whereby the main objective of the undertaken research was to find the qualitative difference in the beam structural behaviour, relative to cases of perforated homogeneous and hybrid I-beams, as a basis for future examination of similar castellated beams.

SUBSTANCE

The investigations in question concentrated on the I-beam given in Fig. 1. This beam has been analysed numerically by FEM, according to the procedure developed by Chrôścielewski in 1983, and later adapted by Chróścielewski et al. in 1987 and 1989. It should be underlined alone, that due to the assumed purely qualitative character of analysis the subdivision into discrete elements could be pretty rough, producing 114 elements for one half of the beam. The yield stresses have been taken 248.4 kN/m^2 for homogeneous beams and for the webs of hybrid beams, but 690 kN/m^2 - for flanges of the last mentioned. For other details of the computational side, readers are adviced to return to the above quoted authors' earlier publications.

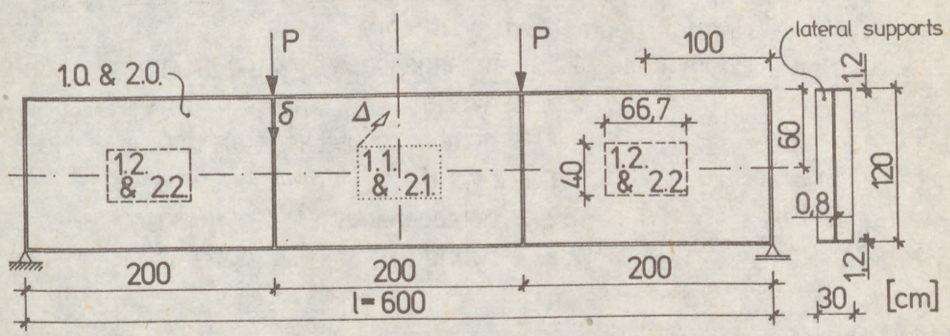

Fig 1. I-beam investigated

As indicated on Fig. 1, within two basic types of I-beams: 1.-homogeneous, and 2.-hybrid, three particular cases have been considered: 0.-no openings, 1.-one opening at 1/2, and 2.-symmetrical openings at 1/6; the corresponding description is: 1.0., 1.1., 1.2. and 2.0., 2.1., 2.2. the horizontally oriented initial imperfection Δ=0.4 cm (half of web thickness) was imposed on the particular web point given in Fig. 1. The obtained P-δ relations, with δ as the vertical deflection under P, are illustrated, with reference to classic theory, in Fig. 2; corresponding ultimate loads are evident. Figs. 3, 4, and 5 show the associated deformation forms.

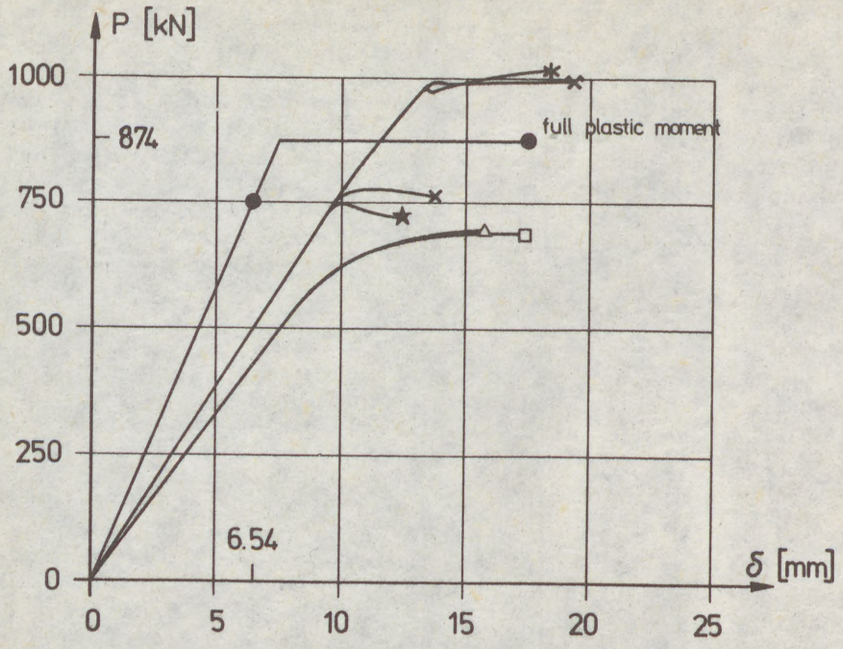

Fig. 2. P–δ relations

- ●: Normal beam, classic theory
- ×: Beam case 1.0. – homogeneous, no openings
- ⚒: 2.0. – hybrid, no openings
- ★: 1.1. – homogeneous, 1 opening
- ✱: 2.1. – hybrid, 1 opening
- △: 1.2. – homogeneous, 2 openings
- □: 2.2. – hybrid, 2 openings

CONCLUSIONS

The executed analysis permits to specify the following practical conclusions:

1. Homogeneous and hybrid I-beams without web openings, or with openings located within the central zone of beam span (1 opening), fail by deformation due to bending action – showing the hybrid against homogeneous beams remarkably stronger, and the unperforated against perforated beams comparably strong.
2. Beams with web openings located at zones next to the supports (2 openings), fail by deformation due to shear action – showing the hybrid against homogeneous beams similarly strong.

(5)

1.0.

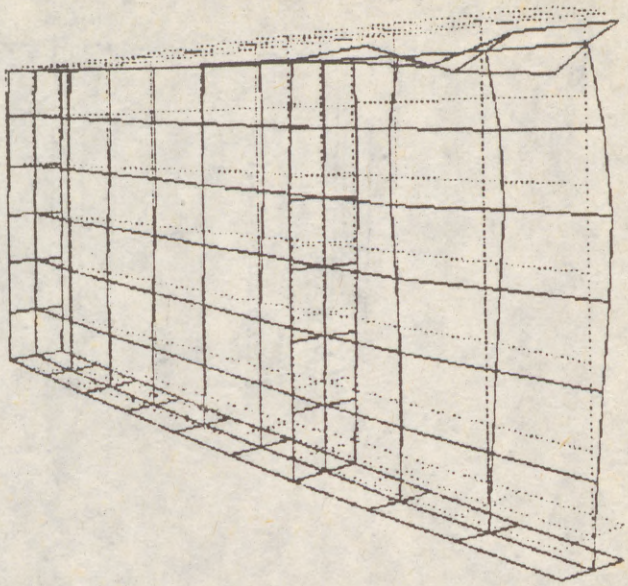

2.0.

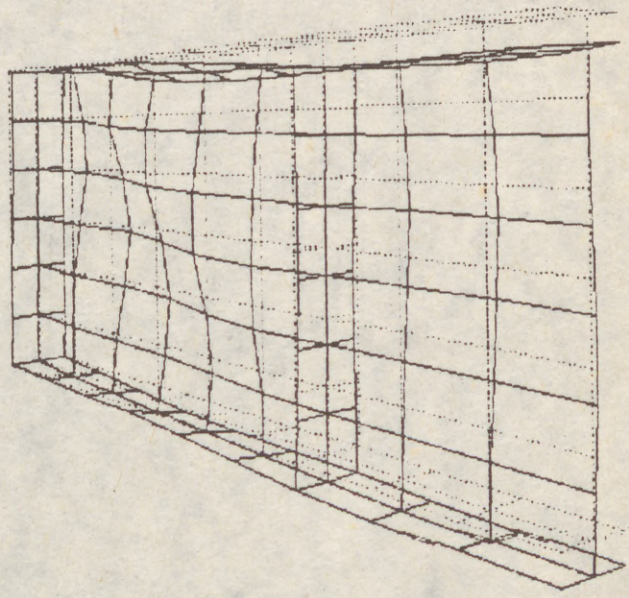

Fig. 3. I-beam deformation forms:
1.0. Homogeneous, no openings
2.0. Hybrid, no openings

(6)

1.1.

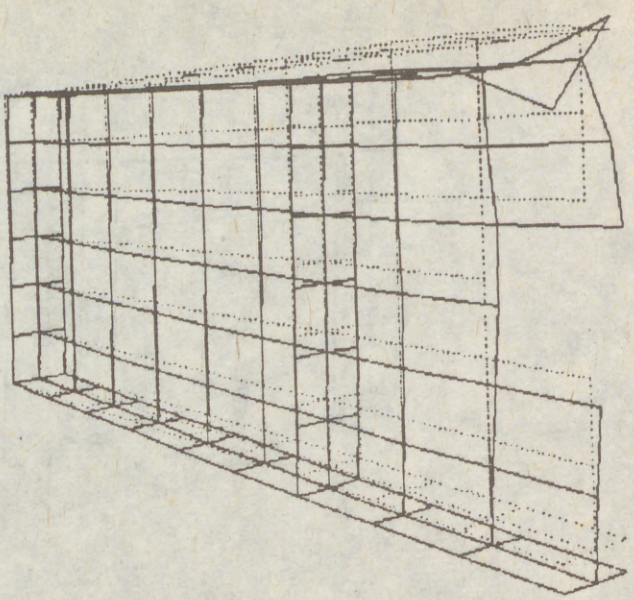

2.1.

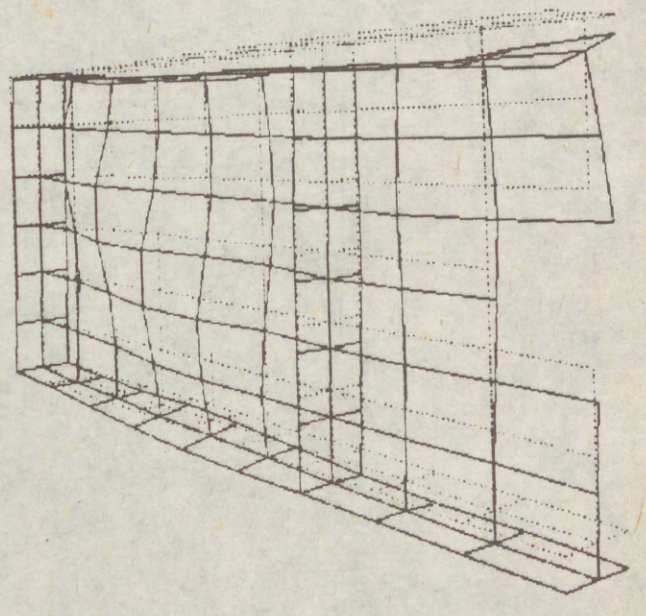

Fig. 4. I-beam deformation forms:
1.1. Homogeneous, 1 opening
2.1. Hybrid, 1 opening

(7)

1.2.

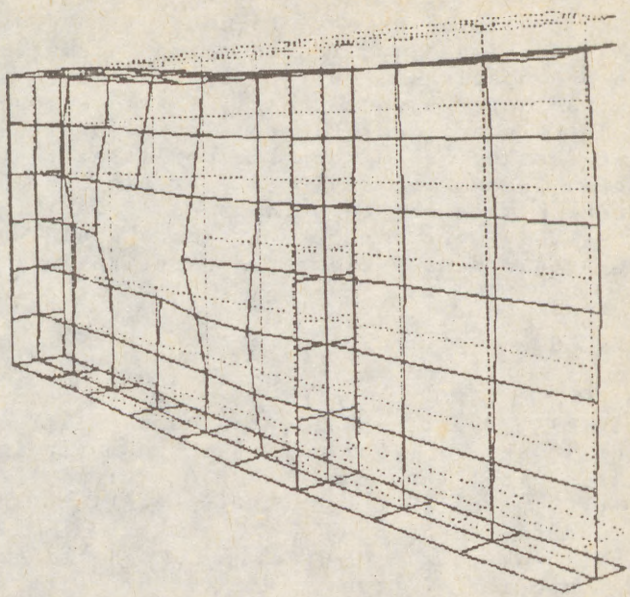

2.2.

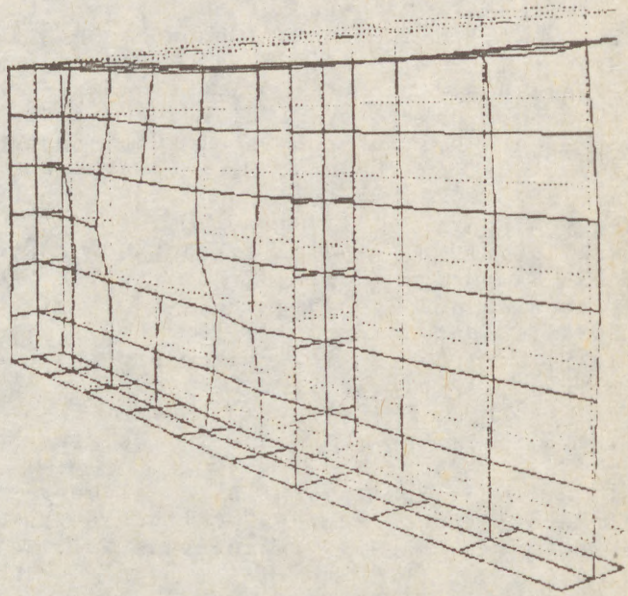

Fig. 5. I-beam deformation forms:
1.2. Homogeneous, 2 openings
2.2. Hybrid, 2 openings

(8)

3. Classic bending theory, together with conventional plasticity assumptions, applied to normal beams (homogeneous, without web openings), brings up the P-δ relation which envelopes, as upper bound, those for homogeneous beams resulting from the non-linear theory. It follows that traditional plastic design, based upon the development of full plastic moments, seems to result in certain overestimation of beam strength which appears to be ca. 1.2 of the real one. A quantitatively more rigorous estimate would be possible, if based upon a densed element discretization.

REFERENCES

Bathe, K.-J. 1982. Finite element procedures in engineering analysis. Prentice-Hall, Englewood Cliffs, New Jersey.

Chrõścielewski, J. 1983. FEM based numerical analysis of ribbed plates within the range of geometrical and material nonlinearity (in Polish). Doctor Dissertation, Technical University of Gdańsk, Gdańsk.

Chróścielewski, J. - Cywiński, Z. - Smoleński, W. 1987. Carrying capacity of steel plate girders with web openings modelled as space structures. International AMSE Conference "Modelling & Simulation", Cairo (Egypt), Proceedings Vol. 3A, 3-12.

Chróścielewski, J. - Cywiński, Z. - Smoleński, W. 1987. Computer aided limit design of an I-beam with web opening (in Polish). VIII Conference "Computer Methods in Structural Mechanics", Jadwisin (Poland), Proceedings Vol. I, 131-138.

Chrõścielewski, J. - Cywiński, Z. - Smoleński, W. 1989. Nonlinear space analysis of highrise building floor beams with web openings. International Conference on Highrise Buildings, Nanjing (China), Proceedings

Cywiński, Z. 1978. On collapse loads of hybrid I-beams. Stavebnícky časopis 26, 117-128.

Cywiński, Z. 1978. Bending strength of castellated hybrid beams. IABSE Symposium "Main Trends in the Development of Steel Structures and Modern Methods for Their Fabrication", Moscow (USSR), Final Report, 151-155.

Cywiński, Z. 1984. Review of research on castellated beams (in Polish). Inżynieria i Budownictwo 41, 457-460.

Cywiński, Z. 1987. Review of research on beams with openings (in Polish). Zeszyty Naukowe Politechniki Gdańskiej 406, 285-296.

Dunai, L. 1986. Nonlinear finite element analysis of steel I-girders. Second Regional Colloquium on Stability of Steel Structures, Hungary, Proceedings Vol. I/1, 67-74.

Redwood, R.G. - Baranda, H. - Daly, M.J. 1978. Tests of thin-webbed beams with unreinforced holes. Journal of the Structural Division, ASCE, 104, 577-595.

(1)
DJUBEK Jozef (1)

STABILITY OF WEB WITH TENSILE CRACK CONCENTRATION

INTERNATIONAL COLLOQUIUM
STABILITY OF STEEL STRUCTURES
BUDAPEST, HUNGARY, 1990
PRELIMINARY REPORT

Summary: The backround of the discussed problem has been given by Hutchinson J.W. [6] and Čerepanov G.P. [5]. The analysis which follows take account on large web deflection.

The Papkovich method is used in a solution to the formulated problem (the differential eq. of deformation compatibility is solved exactly, while the differential equation of equilibrium of Kármán-Marguerre eqs. is solved approximately). The maximum tensile stress for a slender web σ_x^{max}, which corresponds to the yielding stress f_y in linear fracture mechanics, is calculated for a initial web imperfection $w_{0_{max}} = 0.7\,(b/t)^2/100$ according to the reduction factor $m_M = p_x/\sigma_x$.

Singular behaviour at the crack tip (part 4) follows Hutchinson´s results. A power hardening relationship between the plastic strains and stresses is assumed in simple tension $\varepsilon = \sigma + \alpha\sigma^n$, where α is a material constant. Only membrane stresses are considered in the study.

1. Crack-Tip Stress Fields for Elastic Material

The redistribution of stress in a body due to introducing a crack or notch is done by (linear) elastic stress analysis. The greatest attention is paid to the stresses of the crack tip which will usually be accompanied by some plasticity and other non-linear effects.

The correct stress field near crack tips can be divided into real parameters, each of which is associated with a local mode or deformation (Fig. 1).

I. Tension (for $K_{II} = K_{III} = 0$ and $K_I \neq 0$)

The opening mode I, is associated with local displacement in which the crack surfaces move directly apart (symmetric with respect to the x - y and x - z planes).

---

(1) Assoc.Prof. of Civil Engineering, D.Sc., Institut of Construction and Architecture of SAS, Bratislava, Czechoslovakia.

II. Shear in transverse direction (for $K_I = K_{III} = 0$ and $K_{II} \neq 0$).

The mode II is characterized by displacements symmetric with respect to the x - y plane and skew-symmetric with respect to the x - z plane.

III. Shear in longitudinal direction (for $K_I = K_{II} = 0$ and $K_{III} \neq 0$).

Mode III tearing, finds the crack surfaces sliding with respect to one another parallel to the leading edge (skew-symmetric with respect to the x - y and x - z planes).

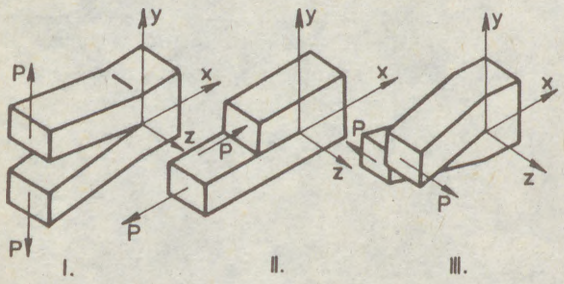

Fig.1 Basic Modes of Crack Surface Displacements

The most general three dimensional case of local crack-tip deformation and stress field is obtained by the superposition of the three modes.

The resulting stress and displacement field are given in corresponding references, e.g. (Siratori [2]).

For mode I we have, e.g.:

$$\sigma_x = \frac{K_I}{(2\pi r)^{1/2}} \cos\frac{\theta}{2}\left(1 - \sin\frac{\theta}{2}\sin\frac{3\theta}{2}\right) + \sigma_{x0} + 0(r^{1/2}).$$

The parameters K_I, K_{II} and K_{III} for corresponding three modes are called crack tip stress (field) intensity factors. Since K_I, K_{II} and K_{III} are not functions of the coordinates r, θ they represent the strength of the stress field surrounding the crack tip. Mathematically they may be viewed as the strengths of the stress singularities at the crack tip. From a physical viewpoint stress intensity factor may be regarded as a parameter reflected redistribution of stresses in the body in surrounding crack. Finally it is significant to note that stress intensity factors have units of: force x length $^{-3/2}$.

2. Plastic Area at the Top of the Crack

Let us have the Mises yield condition

$$(\sigma_1 - \sigma_2)^2 + (\sigma_2 - \sigma_3)^2 + (\sigma_3 - \sigma_1)^2 = 2 f_y^2 \qquad (2)$$

or

$$\left[(1 - n)^2 + (n - m)^2 + (1 - m)^2\right] \sigma_1^2 = 2 f_y^2 \qquad (3)$$

where $\sigma_2 = n\,\sigma_1$ and $\sigma_3 = m\,\sigma_1$.

Coefficient of plastic deformation $\varkappa$ is

$$\varkappa = \sigma_1 / f_y = (1 - n - m + n^2 + m^2 - mn)^{-1/2} \qquad (4)$$

If we use the stress component in the crack tip stress field (in principal coordinates) for $\theta = 0$ we get

$$\text{for plane stress at } \begin{matrix} n = 1 \\ \varkappa = 1 \end{matrix} \quad \text{and} \quad m = 0 \tag{5}$$

$$\text{for plane strain at } \begin{matrix} m = 1 \\ \varkappa = 1/(1 - 2\nu). \end{matrix} \quad \text{and} \quad m = 2\nu \tag{6}$$

For Poisson's ratio $\nu = 0.3$ for plane strain we get

$$\sigma_{max} = \sigma_1 = \varkappa f_y \doteq 3\, f_y \tag{7}$$

With f_y as a representative value of the initial tensile yield stress, the maximum value of the normal tensile stress occuring ahead of the tip of a plane strain crack is $\varkappa f_y$, where $\varkappa$ ranges from about 2.5 for a low hardening material and to about 5 for a high hardening material (Fig. 2).

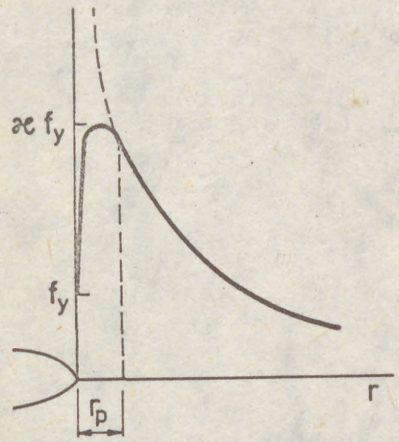

Fig. 2 Stress relation at the Top of Crack Tip for Plane Strain

This elevation in tensile stress is due to the high constraint in plane strain ahead of the tip and the resulting state of high stress triaxiality (see Rietchie [4]).

3. Equations for the Tensile Crack

The non-linear elastic-plastic behaviour is considered and the tensile stress-strain relations are suggested. The stress quantities, if unbarred, will be non-dimensionalized by a yield stress $\bar{f}_y$ throughout the paper and unbarred strain quantities will be normalized by a yield strain $\bar{\varepsilon}_y = \bar{f}_y/E$, where E is the elasticity modul in tension.

In either plane stress or plane strain equilibrium is ensured for stresses derived from a stress function

$$\begin{aligned} \sigma_r &= r^{-1}\Phi' + r^{-2}\,\Phi'' \\ \sigma_\theta &= \Phi'' \\ \tau_{r\theta} &= -(r^{-1}\Phi')', \end{aligned} \tag{8}$$

where cylindrical coordinates r and θ [$(\;)' = \frac{\partial}{\partial r}$ and $(\;)^{\cdot} = \frac{\partial}{\partial \theta}$] are used.

In the plane stress, dealt in the paper the effective stress

$$\sigma_e = (\sigma_r^2 + \sigma_\theta^2 - \sigma_r \sigma_\theta + 3\,\tau_{r\theta}^2)^{1/2} \tag{9}$$

and the strains are considered

(4)

$$\varepsilon_r = \sigma_r - \nu\sigma_\theta + \alpha\sigma_e^{n-1}\left(\sigma_r - \frac{1}{2}\sigma_\theta\right)$$

$$\varepsilon_\theta = \sigma_\theta - \nu\sigma_r + \alpha\sigma_e^{n-1}\left(\sigma_\theta - \frac{1}{2}\sigma_r\right) \qquad (10)$$

$$\varepsilon_{r\theta} = (1+\nu)\,\tau_{r\theta} + \frac{3}{2}\,\alpha\,\sigma_e^{n-1}\,\tau_{r\theta}$$

where n is the power hardening coefficient and α can be regarded as a material constant.

The compatibility equation can be written in the form

$$r^{-1}(r\varepsilon_e)'' + r^{-2}\,\varepsilon_r'' - r^{-1}\,\varepsilon_r' - 2\,r^{-2}\,(\varepsilon_{\theta r}\,r)' =$$

$$= \frac{1}{2}\,L\,(w_0, w_0) - \frac{1}{2}\,L\,(w_0 + w,\ w_0 + w) \qquad (11)$$

where the right hand side is in Cartesian coordinates, w and w_0 are the initial and additional web deflections and the operator

$$\frac{1}{2}\,L\,(w,w) = \frac{\partial^2 w}{\partial x^2}\,\frac{\partial^2 w}{\partial y^2} + \left(\frac{\partial^2 w}{\partial x \partial y}\right)^2 . \qquad (12)$$

The boundary conditions on the crack can be taken in the form

$$\Phi = \Phi' = 0. \qquad (13)$$

In the paper the strain concentration by crack or notches in tensile stresses is considered. An assymptotic expansion of a stress function Φ is attempted in the form

$$\Phi = K_1\,r^s\,\Phi_1(\theta) + K_2\,r^t\,\Phi_2(\theta) \qquad (14)$$

where the first term as the dominant one is considered, e.g.

$$\Phi = K\,r^s\,\tilde{\Phi}(\theta) \qquad (15)$$

In the stress function the amplitude K and parameter s should be determined according to J-integral.

The stresses can be written as

$$\sigma_e = K\,r^{s-2}\,\tilde{\sigma}_e(\theta) = K\,r^{s-2}\,(\tilde{\sigma}_r^2 + \tilde{\sigma}_\theta^2 - \tilde{\sigma}_r\tilde{\sigma}_\theta + 3\,\tilde{\tau}_{r\theta}^2)^{1/2}$$

$$\sigma_r = K\,r^{s-2}\,\tilde{\sigma}_r(\theta) = K\,r^{s-2}(s\tilde{\Phi} + \tilde{\Phi}'') \qquad (16)$$

$$\sigma_\theta = K\,r^{s-2}\,\tilde{\sigma}_\theta(\theta) = K\,r^{s-2}\,s\,(s-1)\,\tilde{\Phi},$$

$$\tau_{r\theta} = K\,r^{s-2}\,\tilde{\tau}_{r\theta}(\theta) = K r^{s-2}\,(1-s)\,\tilde{\Phi}',$$

where $\tilde{\sigma}_r$, $\tilde{\sigma}_\theta$, $\tilde{\tau}_{r\theta}$ are the stresses of the function θ only.

Path - independent line integral discovered by J.R. Rice [1] in Cartesian coordinates is

$$J = \int_{\Gamma} (W\, dy - \tilde{T}\, \frac{\partial \tilde{u}}{\partial x}\, ds) \qquad (17)$$

where W is the strain energy density for a linear or nonlinear material, Γ is a curve surrounding the notch tip, $\tilde{T}$ is a traction vector ($T_i = \sigma_{ij}\, n_j$) $\tilde{u}$ is the displacement vector and ds is an element of arc length along Γ.

Let us consider the closed circuit $\Gamma = \Gamma_1 + \Gamma_2$ (Fig. 3). The area integral vanishes, and so

$$\int_{\Gamma} (W\, dy - \tilde{T}\, \frac{\partial \tilde{u}}{\partial x}\, ds) = 0 \qquad (18)$$

This is the case for any closed curve Γ. Since the total integral vanishes, the integral about Γ_1 is identical to that about Γ_2. More details for J integral can be found in (Rice [1]).

For the tensile crack under consideration, if we use dimensionless quantities

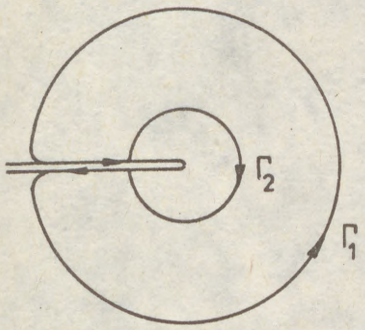

Fig.3 Two Closed Circuits

$$\int_{\Gamma_2} (W\, dy - \sigma_{ij}\, n_j\, u_{i,x}\, ds) = \pi\sigma_{\infty}^2 \qquad (19)$$

where σ_{∞} is uniform remote tensile stress.

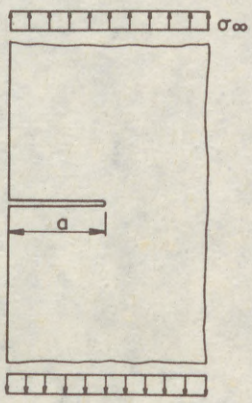

In the distance from the crack the normal stresses are uniformly divided (Fig. 4). It is not necessary to consider that the right part of the equation (19) for small or large web deflections should have the value $\pi\sigma_{\infty}^2$. Quite sufficiently is to believe that the right side of (19), has a some finite quantity.

The path in the tensile stress singularity ahead of the crack (the path Γ_2) is chosen such that it lies in fully plastic region. This integral is evaluated for the parameter s and the amplitude K.

Fig. 4 Narow Notch or Crack of Length in an Infinite Body. Uniform Remote Stress σ_{∞}.

4. Strain Energy Density in Plastic Region. Singular Term for Plane Stress [1]

The strain energy density is

$$W = \frac{n}{n+1} (\sigma_r \varepsilon_r + \sigma_\theta \varepsilon_\theta + 2 \tau_{r\theta} \varepsilon_{r\theta}) \tag{20}$$

or using $s = \frac{2n+1}{n+1}$ (Siratori [2], p.116)

$$W = \alpha \frac{n}{n+1} K^{n+1} r^{(s-2)(n+1)} \tilde{\sigma}_2^{n+1} = \alpha \frac{n}{n+1} K^{n+1} r^{-1} \tilde{\sigma}_e^{n+1} \tag{21}$$

and

$$\sigma_{ij} n_j u_{i,x} = \sigma_r n_1 \left(\frac{\partial u_r}{\partial r} \cos\theta - \frac{1}{r} \frac{\partial u_r}{\partial \theta} \sin\theta\right) + \tau_{r\theta} n_1 \left(\frac{\partial u_\theta}{\partial r} \cos\theta - \frac{1}{r} \frac{\partial u_\theta}{\partial \theta} \sin\theta\right). \tag{22}$$

Following the (10) and (16) we find

$$\frac{\partial u_r}{\partial r} = \alpha K^n r^{-n/n+1} \tilde{\sigma}_e^{n-1} \left(\tilde{\sigma}_r - \frac{\tilde{\sigma}_\theta}{2}\right), \tag{23}$$

and

$$u_r = \alpha K^n r^{1/n+1} \tilde{u}_r(\theta) + f(\theta), \tag{24}$$

where

$$\tilde{u}_r(\theta) = (n+1) \tilde{\sigma}_e^{n+1} \left(\tilde{\sigma}_r - \frac{\tilde{\sigma}_\theta}{2}\right).$$

Similarly we can find $\tilde{u}_\theta$, u'_θ and $\tilde{u}'_r$.

The final form of the path integral on Γ_2

$$\int_{\Gamma_2} (W\, dy - \sigma_{ij} n_j u_{i,x}\, ds) = \alpha K^{n+1} r_2^{(n/n+1 - n/n+1)} \cdot I \tag{25}$$

where (Hutchinson [5])

$$I = \int_{-\pi}^{\pi} \left[\frac{n}{n+1} \tilde{\sigma}_e^{n+1} - \left\{\sin\theta(\tilde{\sigma}_r (\tilde{u}_\theta - \tilde{u}'_r) - \tilde{\tau}_{r\theta} (\tilde{u}_r + \tilde{u}'_\theta)) + \frac{1}{n+1} (\tilde{\sigma}_r \tilde{u}_r + \tilde{\tau}_{r\theta} \tilde{u}_\theta) \cos\theta\right\}\right] d\theta$$

The function of Φ is chosen as the maximum value when σ_e is equal one (Fig. 5).

The path independent integral must be equal to the value obtained from the Γ_1 integration. Thus

---

[1] In singular term large web deflections are neglected.

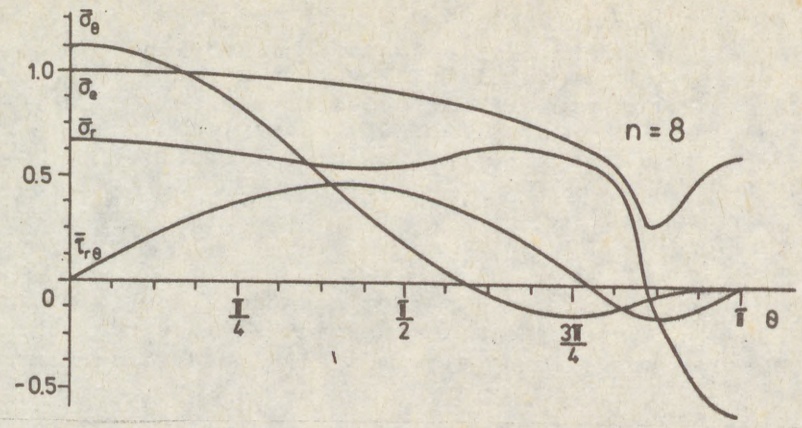

Fig. 5 θ-Variation of Stresses at Crack Tip for Plane Stress

$$\alpha\, K^{n+1}\, r_2^{(n+1)(s-2)+1} \,.\, I = \pi\sigma_\infty^2 \qquad (26)$$

or as $$s = \frac{2n+1}{n+1}\,, \quad \alpha K^{n+1}\, I = \sigma_\infty^2\,. \qquad (27)$$

The important piece of information can also be obtained from path integral, namely the amplitude K. If we use (27), then

$$K = \left(\frac{1}{\alpha}\right)^{1/n+1} \left(\frac{\pi}{I}\right)^{1/n+1} \sigma_\infty^{2/n+1} \qquad (28)$$

where α depends on the initial and additional web deflection w and w_0. If $w = w_0 = 0$ the material constant α is equal to 0.02 (Hutchinson [5]).

Further if we put (26) into (21), then after some rearrangements we get the strain energy density by

$$W = \frac{n}{n+1}\,\frac{\pi}{I}\,\frac{\sigma_\infty^2}{r}\,\tilde{\sigma}_e^{\,n+1}\,. \qquad (29)$$

Numerical results of I for various values of n for plane stress and plane strain tensile crack are given in Table 1. Some θ variations of stresses at crack tip for plane stress for n = 8 we can find in Fig. 5.

Table 1

n =	3	5	9	13
Tensile crack				
Plane stress	3.86	3.41	3.03	2.87
Plane strain	5.51	5.01	4.60	4.40

5. A Slender Rectangular Web Subjected to Compression and Bending

In part 4 singular term for plane stress was discussed. We did not yet considered the problem of stresses which arises

in slender rectangular webs.

This part presents a solution of the non-linear problem of the deformation of slender initially curved rectangular webs which are stiffened along their edges by elastically stiffeners, flexible in the web plane. The Papkovich method is successfully used in a solution to the formulated problem.

Let us define the reduction factor (Djubek, [6], p.98)

$$m_M = \frac{p_x}{\sigma_x^{max}} \qquad (30)$$

where p_x express the maximum tensile stress due to external loading and σ_x^{max} is the normal maximum tensile stress which corresponds to the yielding stress f_y in linear fracture mechanics.

Example. Let us have

$$a_f = a'_f = \frac{A_f}{bt} = 0.25, \qquad \sigma_E = \frac{\pi^2 E t^2}{12(1-\nu^2)b^2} \qquad (31)$$

where E is Young's modulus of elasticity of flange (or web) material and ν Poisson's ratio.

In [6], p. 105 for bending we have

p_x/σ_E	11.94	23.88	47.76	71.64	95.62
m_M	0.91	0.828	0.69	0.62	0.58

The reduction coefficient m_M was calculated for an initial imperfection $w_0 = 0.7(b/t)^2/100$, and for tensile or compressive stress in slender rectangular web subjected to bending the reduction coefficient is practically the same (the difference is less than 1%).

Author wants to mark his gratitude to Dipl.Ing. Jozef Kriváček, Ph.D. who computerized the result given on the Figure 5.

References

[1] J.R. RICE, 1968: A Path Independent Integral and the Approximate Analysis of Strain Concentration by Notches and Cracks. Journ.of Appl.Mech.,p.379-386.

[2] M. SIRATORI, T.MIJESI, Ch.MACUSITA, 1986: Vyčisliteľnaja mechanika razrušenija. Per.iz jap. M.: Mir.

[3] P.O. RIETCHIE, J.F. KNOTT and J.R. RICE, 1973: On the Relationship Between Critical Tensile Stress and Fracture Toughness in Mild Steel. J.Mech.Phys. Solids 21,395.

[4] G.P. CEREPANOV, 1967: O razpredelenii treščin v splošnej srede. Prikladnaja matematika i mechanika 31, vyp. 3.

[5] J.W. HUTCHINSON, 1968: Singular Behaviour at the End of a Tensile Crack in a Hardening Material. J.Mech.Phys.Solids, Vol.16, pp.13-31.

[6] J.DJUBEK, R.KODNÁR, M. ŠKALOUD, 1983: Limit State of the Plate Elements of Steel Structures. Birkhäuser Verlag Basel-Boston-Stuttgart.

(1)
DRDÁCKÝ, Miloš (1)

ON TWO PARTICULAR PROBLEMS OF PLATE GIRDER WEBS UNDER PARTIAL EDGE LOADS

INTERNATIONAL COLLOQUIUM
STABILITY OF STEEL STRUCTURES
BUDAPEST, HUNGARY, 1990
PRELIMINARY REPORT

Summary: The experimental data from tests conducted to study i) the effect of eccentricities of the load with respect to the idealized web plane and ii) the influence of variable repeated loads on the behaviour of thin unstiffened webs are reported in this paper. Eccentricity varies from -16 mm to +24 mm, loads are applied through a rigid cylindrical bar placed on the top flange. Considerable increase in web surface stresses is observed due to the increase of the eccentricity. Pilot tests on steel webs subjected to compressive variable repeated loads pulsating at frequency of 3 Hz are described. The initiation and progression of plastic areas in web are detected by means of thermal measurements.

1. Introduction

The behaviour of slender plate-girder webs subjected to partial edge loadings has been investigated in the Institute of Theoretical and Applied Mechanics of the Czechoslovak Academy of Sciences for more than twenty years. The attention has been concentrated to the study of the influence of different structural and loading parameters on the buckling phenomena and the load-carrying capacity of thin-walled plate girders, (DRDÁCKÝ 1989).

Important loading characteristics for crane-way girders are i) the eccentricity of the applied load with regard to an idealized web plane and ii) the repetition of loading cycles. The contribution presents some experimental data concerning those two problems.

/1/ Ph.D. Civ. Eng., Head of the Central Laboratory of Experimental Mechanics (CLEM), Vice-Director, Institute of Theoretical and Applied Mechanics, Czechoslovak Academy of Sciences, Prague

(2)

2. Plate Girder Webs Under Eccentric Patch Loads

A series of tests with different loading configurations was performed on the test specimen the details of which are given in Fig. 1. In the first step of the tests the central panel was loaded centrically. Then five further loading arrangements were completed with gradually increased eccentricity to the both positive, (e = +8, +16, +24 mm), and negative, (e = -8, -16 mm), deviations from the middle web plane. The counterward direction to the maximum initial web deflection was chosen to be the positive deviation. Contour lines of the initial web deflection of the test girder and the details of loading arrangement are given in Fig. 2 and Fig. 3 respectively. At the third loading series the changes of web deflections and web stresses were studied for small positive deviations from the middle plane (e = +1, +2, +4 mm). The specimen was loaded in steps by means of an electronic testing machine Testatron and strains were measured using resistance strain gages and a measurement unit Peekel Autolog controlled by a PC. The deflections of web and flanges were measured by a system of dial gages on one web face.

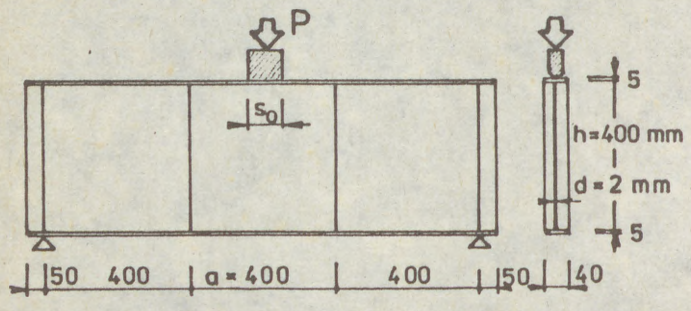

Fig. 1

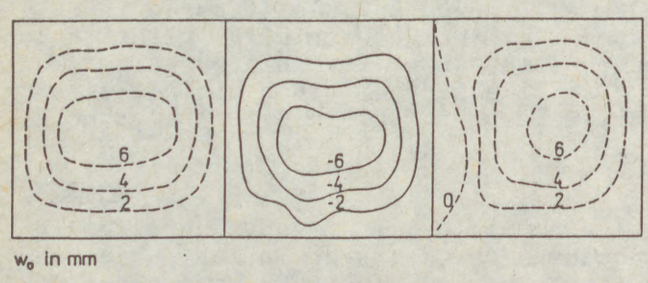

Fig. 2

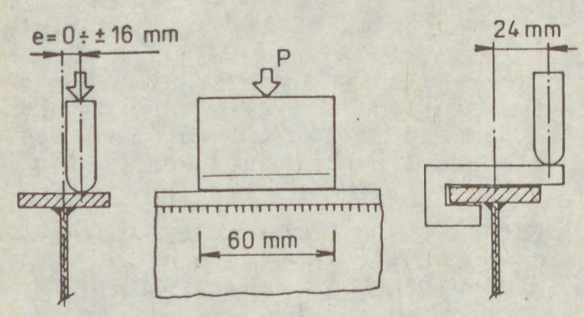

Fig. 3

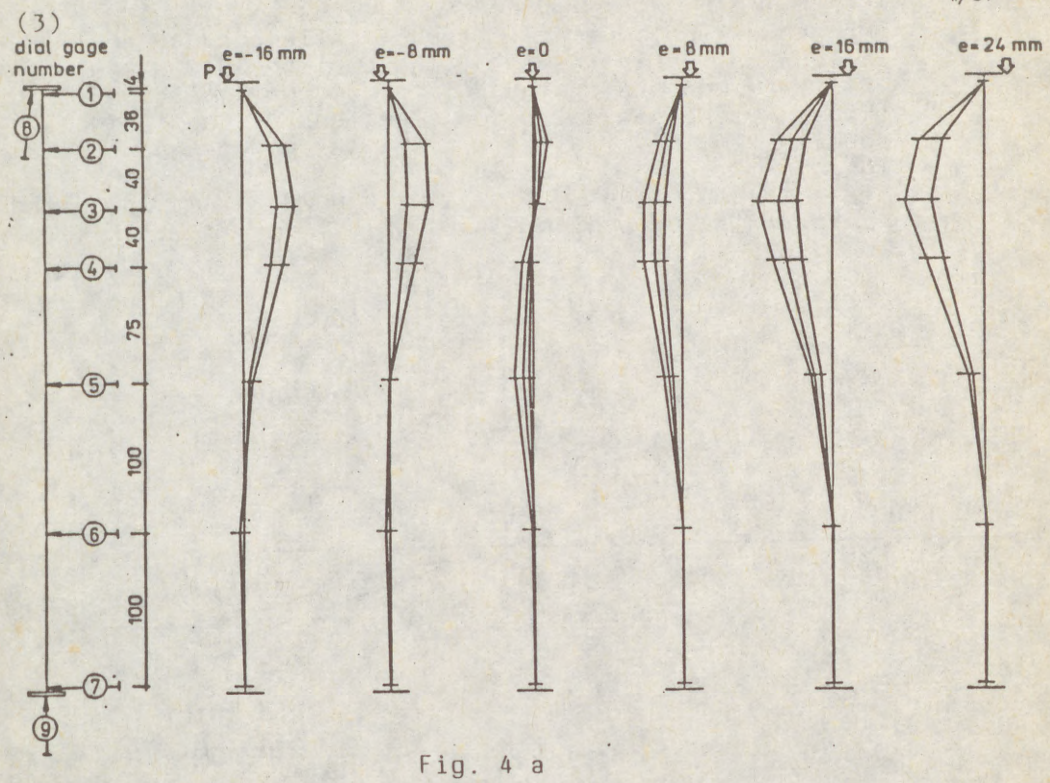
(3)
dial gage number
1
2
3
4
5
6
7
8
9
38
40
40
75
100
100
14
P
e=-16 mm
e=-8 mm
e=0
e=8 mm
e=16 mm
e=24 mm

Fig. 4 a

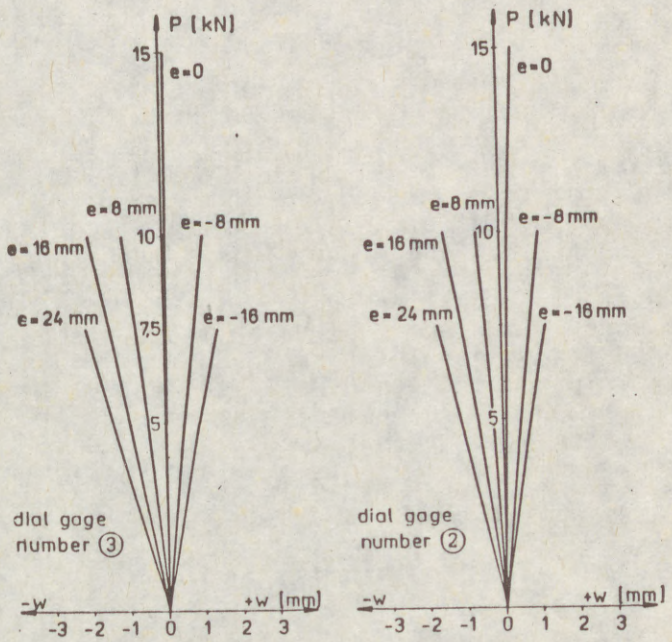
P [kN]
15
e=0
e=8 mm
e=-8 mm
10
e=16 mm
e=24 mm
7,5
e=-16 mm
5
dial gage number (3)
-w
+w [mm]
-3 -2 -1 0 1 2 3
P [kN]
15
e=0
e=8 mm
e=-8 mm
10
e=16 mm
e=24 mm
e=-16 mm
5
dial gage number (2)
-w
+w [mm]
-3 -2 -1 0 1 2 3

Fig. 4 b

(4)

The main test results and observations can be summed up as follows:

a) The web deflections are strongly influenced by an increase of eccentricity of the applied load at only little dependence on the initial web deflections. (Figs. 4 a, b present web deflections of the test specimen in the middle cross-section under the applied load.).

b) The increase of web deflections depends linearly on the eccentricity of applied loads (Fig. 5).

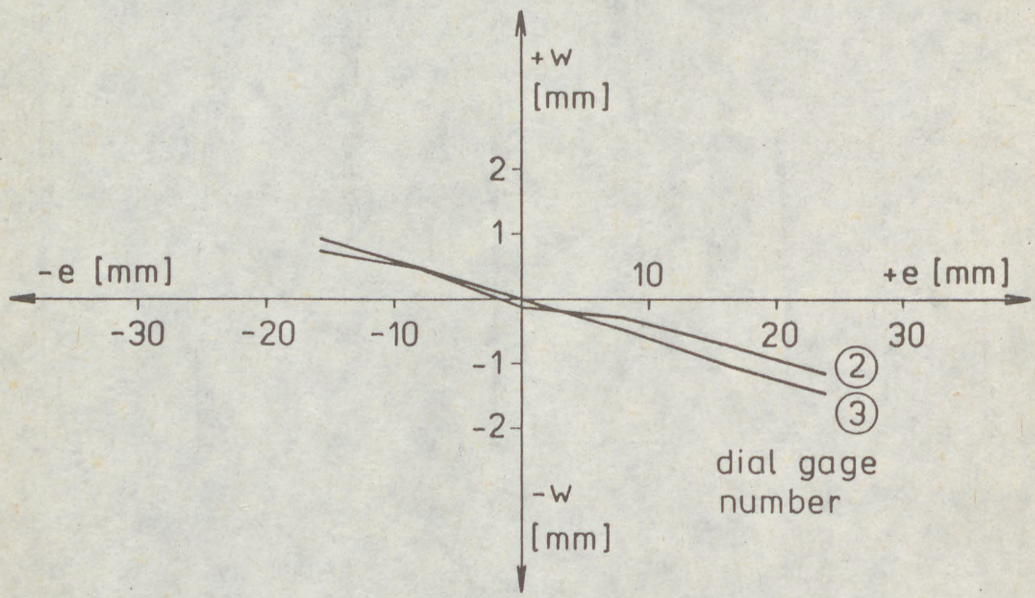

Fig. 5

c) Similar behaviour was observed as far as strains or stresses are concerned. In Figs. 6 a, b the changes in vertical surface strains can be followed, (measured in the middle cross-section of the test panel).

d) The change of stresses along vertical central cross-section against the eccentricity of the applied load is shown in Fig. 7. It is also approximatively linear. However, the relative increase of surface (bending) stresses in the web depends on the distance z from the loaded flange and this dependency based on experimental data is presented graphically in Fig. 8. There exists a fairly good agreement with a theoretical estimate of the increase of web surface stresses under the loaded flange due to the eccentrical load application in the form

$$\Delta\sigma = \pm e \frac{P d a}{0,75 J_t h} \quad /N\ mm^{-2}/, \qquad /1/$$

(5)

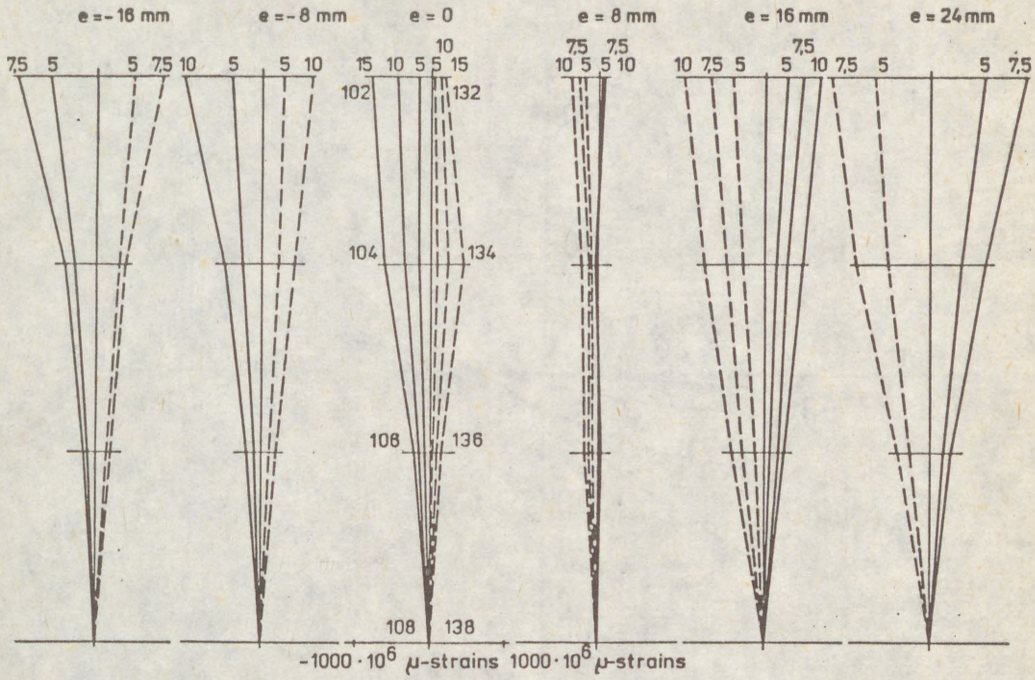

Fig. 6a

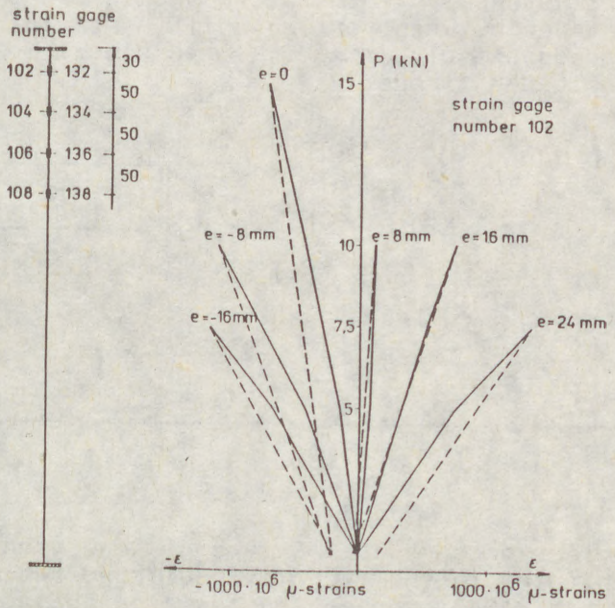

Fig. 6b

(6)

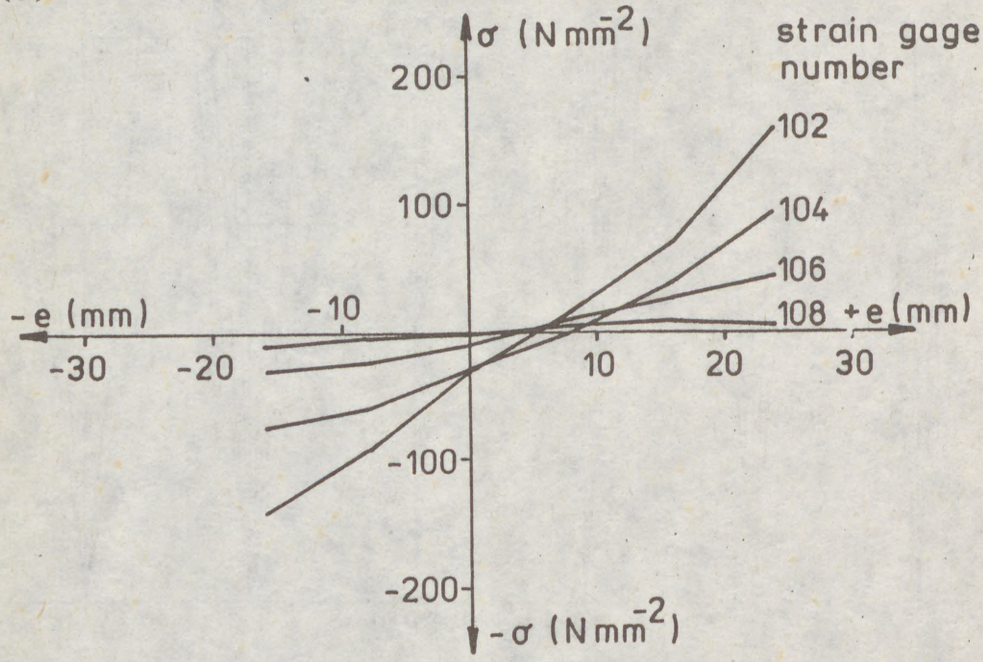

Fig. 7

were P denotes the applied load /N/, d the thickness of the web /mm/, a, h distance between vertical stiffeners in the web and the web depth respectively /mm/, J_t the torsional moment of inertia of the loaded flange.

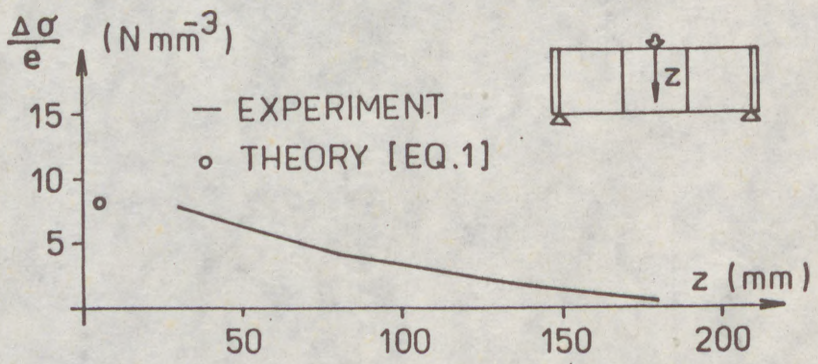

Fig. 8

The behaviour depends on the type of load transfer to the top flange according to the recently published results by ELGAALY and NUNAN (1989) concerning tests on rolled beams.

(7)

3. Plate-Girder Web Under Variable Repeated Loads

From some of previous experiments, (ŠKALOUD, DRDÁCKÝ, ZÜRNEROVÁ - 1974), on thin-walled plate-girder panels it follows that the repeated loading and the incremental collapse rarely lead to any significant reduction in ultimate loads of structural elements under consideration.

Nevertheless, a web in the vicinity of the applied load is higly stressed beyond the elastic material limit even at the early stage of loading (DRDÁCKÝ - 1986). Therefor, low-cycle fatigue may occur, which was observed at one of the above mentioned tests. There was formed a crack there in a web in the plastic hinge developed just under the loaded flange. This transcrystalline crack was initiated on the tension surface of the web and exhibited typical signs of low-cycle-fatigue failure.

To study this, to date only partially solved, problem of thin webs a series of tests is being under preparation. Let us mention two pilot tests on panels of the same nominal geometry as described in Fig. 1. Specimens were repeatedly loaded by means of the MTS servohydraulic testing system in load blocks presented in Fig. 9, at frequency of pulses being 3 Hz.

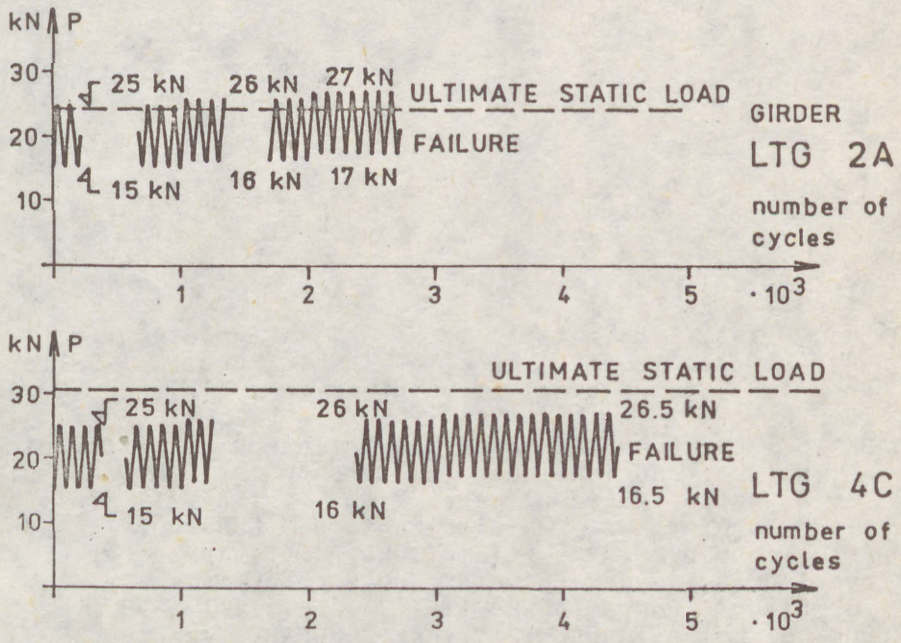

Fig. 9

The beginning and the progression of plastification of the web material was determined by means of thermal surface measurements. The attached illustrative example, (Fig. 10), shows that the released heat at similar experiments is

(8)
sufficient for application of measurement techniques detecting temperature changes of 0.1 K. Further, at the described tests the plastic region remain limited to the plastic hinge developed in the closest vicinity of the loaded flange.

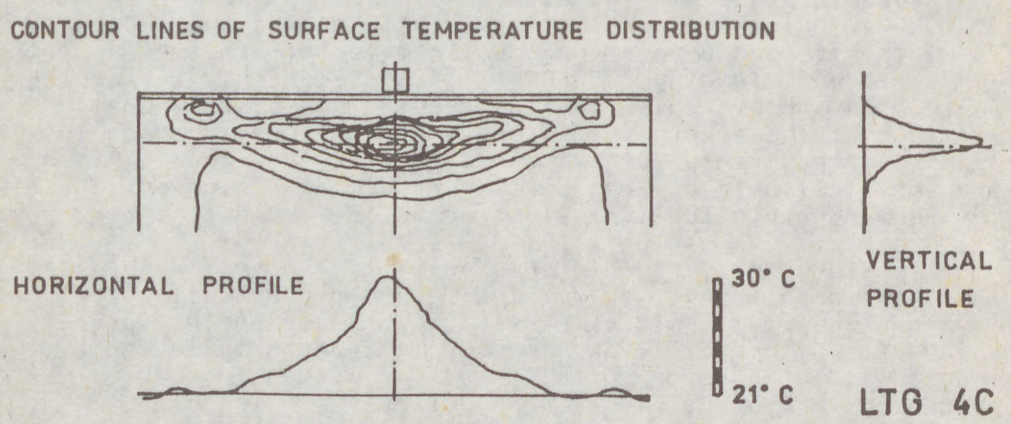

Fig. 10

4. References

DRDÁCKÝ, Miloš, 1986, Limit states of steel plate girder webs under patch loading, Proc. of the II. Regional Colloq. on Stability of Steel Structures, Vol. II/1, pp. 49-56, Budapest.

DRDÁCKÝ, Miloš, 1989, Tests of the influence of different structural and loading parameters on the behaviour of thin -walled plate girders, Proc. of the VIII. Int. Sci. Tech. Conference - Metal Structures, Gdańsk.

ELGAALY, Mohamed; NUNAN, William, L., 1989, Behaviour of rolled section web under eccentric edge compressive loads, J. Struct. Engrg, ASCE, 115 (7), pp. 1561-1578.

ŠKALOUD, Miroslav; DRDÁCKÝ, Miloš; ZÜRNEROVÁ, Marie, 1974, Post-buckled behaviour of webs under partial edge loading, Report ÚTAM - ČSAV, 66 p., Prague.

(1)
JANUŠ, Karel (1)
KUTMANOVÁ-KÁRNÍKOVÁ, Irena (2)
ŠKALOUD, Miroslav (3)

DESIGN OF LONGITUDINALLY STIFFENED THIN WEBS UNDER PATCH LOADING

INTERNATIONAL COLLOQUIUM
STABILITY OF STEEL STRUCTURES
BUDAPEST, HUNGARY, 1990
PRELIMINARY REPORT

Summary: The objective of the contribution is to sum up all of the formulae for the ultimate loads of longitudinally stiffened plate girder webs subject to (i) stationary (ii) variable repeated (cyclic) patch loading, which has recently been established by the authors. Some information about the size of the optimum longitudinal stiffening of the webs is also presented. All formulae given in the paper were derived on the basis of the results and conclusions of the authors' experimental investigation into the problem, which has been under way in Prague for several years now.

1. Introduction

Over the last years, the authors carried out several experimental investigations into the ultimate load behaviour of steel plate girder webs under the action of a partial edge load. The first stage of the research was concentrated on the performance of webs subject to a stationary patch load, while the attention of the other (started three years ago) stage turned to the "breathing" of webs under variable repeated partial edge loading. A lot of data about the deformation, stress state and failure mechanisms of the girders tested

(1) Ph.D., C.E., Czech Technical University, Building Research Institute, Prague
(2) D.Sc., Ph.D., C.E., Czech Technical University, Building Research Institute, Prague
(3) Assoc. Prof., D.Sc., Ph.D., C.E., Institute of Theoretical and Applied Mechanics, Czechoslovak Academy of Sciences, Prague

(2)
resulted from the experiments; the main of them can be found in [Škaloud, Novák, 1975], [Škaloud, Kárníková, 1985], [Januš, Kárníková, Škaloud, 1988] and [Kutmanová, Škaloud, Januš, 1990].

On the basis of the results obtained and the conclusions drawn, the authors established a number of formulae for the ultimate strengths of longitudinally stiffened plate girder webs subject to (i) stationary, (ii) variable repeated patch loading and for the optimum rigidity of quasi-rigid longitudinal ribs. These formulae are presented herebelow.

2. Stationary Loading

2.1. Effect of the size of the loaded flange

At collapse, three plastic hinges in the loaded flange and a segmental line plastic hinge in the web sheet develop in a steel plate girder subject to a stationary partial edge load. The plastic hinges in the loaded flange occur (i) at mid-span, i.e. under the partial edge load, and (ii) at those flange sections from which the segmental line plastic hinge in the web sheet emanates. The distance of the outer hinges from the central one is influenced by the flange size; i.e. the larger the size of the flange, the greater is the distance of the outer hinges.

M. Drdácký established in [Drdácký, 1982] the following condition for the formation of outer plastic hinges:

$$(1) \qquad I_f/a^3 t_w < 3.10^{-5},$$

where I_f is the moment of inertia of the loaded flange with respect to its centroidal axis perpendicular to the web plane, a is the web width and t_w the thickness of the web sheet.

This criterion has the following meaning: When condition (1) is satisfied, the outer flange hinges form between the adjacent transverse stiffeners, i.e. within the web panel under consideration. As the presence of a longitudinal stiffener brings about a reduction of the distance of the outer hinges from the central one, the above criterion remains valid even in the case of web plates fitted with longitudinal stiffening, which is one of the results of the authors' tests.

Then, as flexible we regard those flanges in which all three plastic hinges do form between the two adjacent transverse stiffeners; if the opposite is the case, the flange is regarded as rigid.

An examination of the obtained results further indicates that the effect of the size of the loaded flange upon the load-bearing capacities of the webs (and of the whole plate

(3)
girders) is very significant. It considerably influences the dispersion of the load in the web, its buckling and even the collapse mechanism of the plate girder.

2.2. Effect of the size (and rigidity) of the longitudinal rib

The effect of the size (and rigidity) of the rib is pronounced only in the range of flexible ribs, where the curve plotting the relationship between ultimate load and stiffener rigidity exhibits a conspicuous rising tendency. In the domain of larger stiffeners, the curve is flat, so that the growth of ultimate strength with a further increase in stiffener size and rigidity is very slow.

On the basis of the experimental results obtained, the authors established the following formula for the optimum moment of inertia, $I_{st,r}^{opt}$, of a rigid (i.e. not deflecting in the course of web buckling and, therefore, able to provide the buckling sheet with rigid support until the ultimate strength of the girder has been exhausted) longitudinal stiffener positioned at $b_1 \leq 0.2b$:

$$(2) \qquad I_{st,r}^{opt} = 0.1 b t_w^3 \varkappa \gamma^*.$$

There I_{st} is the moment of inertia of the longitudinal stiffener (calculated for a cross-section consisting of (i) the stiffener proper and (ii) an effective portion of the web sheet having a width of $2 \times 15 t_w \sqrt{240/R_{y,w}}$ with respect to its centroidal axis parallel with the web plane, γ^* the optimum rigidity resulting from linear buckling theory and $\varkappa$ a coefficient according to Table 1, which respects the effect of initial imperfections and of post-buckled behaviour.

Table 1

λ	≤ 90	≥ 230	Between the values of $\lambda = 90$ and
$\varkappa$	2.25	4.0	$\lambda = 230$ can be linearly interpolated.

However, when examining the curves "Ultimate load versus stiffener rigidity", it was found that for larger rigidities these curves were very flat. This led to the conclusion that a major reduction of stiffener rigidity would lead to only an insignificant reduction of ultimate load. This conclusion was further confirmed by the authors evaluating the relation of the experimental ultimate loads to the predicted ones for those of the test girders whose webs were stiffened by ribs the moment of inertia of which was less than $I_{st,r}^{opt}$ according to formula (2).

Therefore, the writers came to the conclusion that, at least as far as strength considerations were concerned, a less strict

(4)
formula would do for the calculation of the optimum stiffener rigidity, viz.

$$(3) \quad I_{st}^{opt} = 0.5 I_{st,r}^{opt}.$$

And this is also the formula the authors recommend to be used in design.

It should be noted, however, at this juncture that, unlike Eq.(2), formula (3) is not able to ensure for the stiffener to be rigid during the whole "life" of the plate girder, so that the stiffener then more or less deflects with the buckling sheet and even the buckled pattern of the web sheet is more pronounced.

2.3. Ultimate loads and onset-of-yielding loads of test girders, ultimate limit state definitions

The average values of the experimental load-carrying capacities of all girders tested are shown, in terms of the position of the longitudinal rib, in Fig.1.

By way of analysing the measured strains (and related stresses), the writers found out the loads that corresponded to the onset of plasticization, whether this be surface (load $P_{y,w}^{su}$) or membrane (load $P_{y,w}^{me}$) plastification, in the individual test girders. They also ascertained the quantities $P_{2\varepsilon}^{su}$, $P_{3\varepsilon}^{su}$, $P_{2\varepsilon}^{me}$ and $P_{3\varepsilon}^{me}$, which are related to unitary deformation ε equal to twice or three times the strains corresponding to the onset of surface and membrane plastification. The average values of loads $P_{y,w}^{su}$ (black portions of columns) and $P_{3\varepsilon}^{me}$ (dashed portions of columns) are shown in Fig.1.

These results show that the position of the longidudinal rib substantially affects the stress state in the webs and particularly the role of the individual stress components. For example, while in the case of a web with a stiffener at $b_1=0.2b$ pronounced buckling becomes manifest in the upper web panel and is accompanied with the occurrence of significant bending stresses, with webs stiffened by a rib at $b_1=0.1b$ little buckling occurs in the top web panel, so that the stress state in the panel is practically determined by membrane stresses. This fact was reflected in the writers' limit state considerations, as will be seen below.

Thus, the ultimate limit state of a web subject to a patch load and reinforced by a longitudinal stiffener placed at one fifth of web depth, i.e. in the case where - as said above - significant bending stresses developed in the upper web panel, was defined by the onset of surface yielding. For the ultimate loads, $P_u(x=0.2)$, of webs fitted with rigid ribs, the authors derived the following formula:

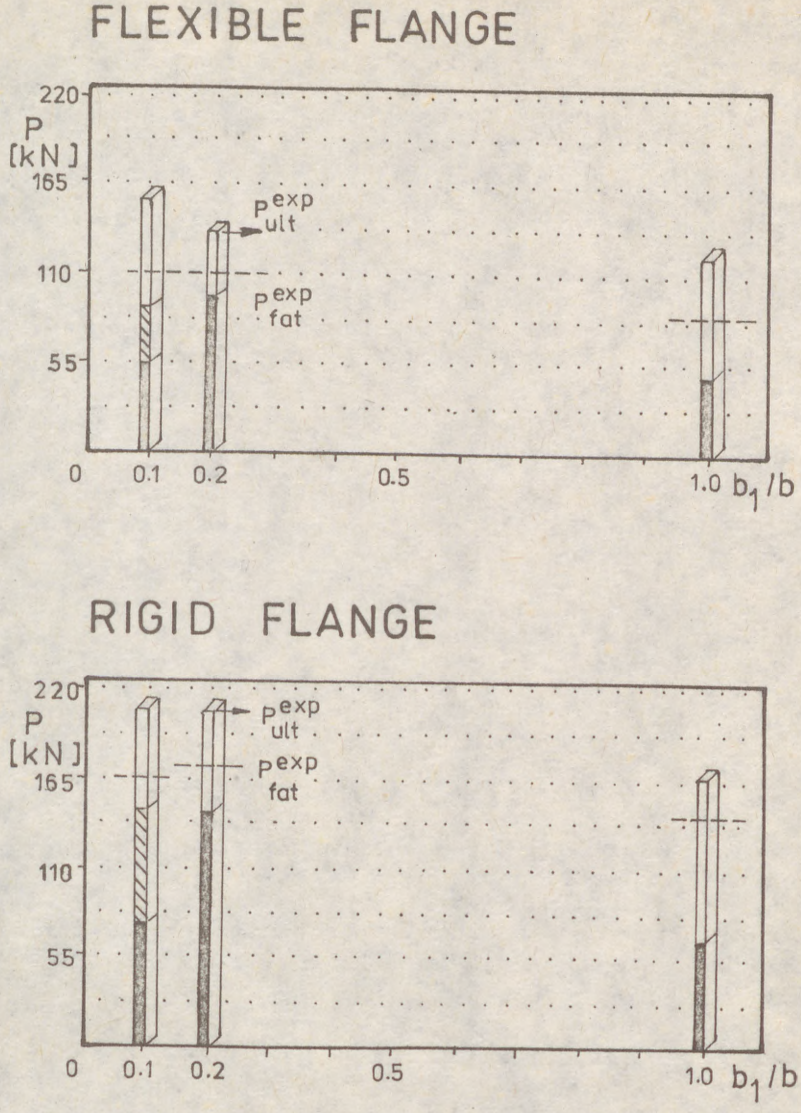

Fig.1

$$(4) \qquad P_u^r(x=0.2) = A.R_{y,w}.t_w^2\left(1+0.004\frac{c}{t_w}\right)\left(\frac{I_f}{t_w^4}\sqrt{\frac{R_{y,f}}{240}}\right)^B,$$

where A and B are coefficients having the values $A = 13.9$, $B = 0.153$; all other symbols were defined above.

(6)

When establishing formula (4), the authors strove - in order to introduce some continuity into the design of webs under partial edge loading - to make its structure similar to that of the formula given in [Drdácký, 1982] for longitudinally unstiffened webs; but, of course, the coefficients A and B, derived via non-linear regression, were different from their counterparts in [Drdácký, 1982] in order to allow for the beneficial presence of the longitudinal stiffener. Moreover, the effect of flange material was also inserted into the formula.

In the light of the currently held Limit State Design philosophy, when - among other things - yield stresses, R_y, are replaced by design strengths, R_d, formula (4) can be rewritten as follows:

$$(5)\quad P_u^r(x=0.2) = 15.9 R_{d,w}\, t_w^2 \left(1+0.004\frac{c}{t_w}\right)\left(\frac{I_f}{t_w^4}\sqrt{\frac{R_{d,f}}{210}}\right)^{0.153},$$

with $R_{d,w}$ denoting the design strength of the web material and $R_{d,f}$ that of the flange material.

So far we have been dealing with the performance of webs stiffened by a longitudinal rib at $b_1=0.2b$. Let us now generalize the task by introducing the effect of the position of the rib into it. For this purpose, the authors established, again by analysing their experimental results and using non-linear regression, this formula:

$$(6)\quad P_u(x) = P_u(0)[0.958-0.123\ln(b_1/b)],$$

where $x=b_1/b$ and $P_u(0)$ is the ultimate load of the related longitudinally unstiffened web.

Conversely, from Eqs 5 and 6, the load-carrying capacity of a web without longitudinal stiffening can be obtained (if again written for the design strength $R_{d,w}$ and $R_{d,f}$) as follows:

$$(7)\quad P_u(0) = 13.8 R_{d,w}\, t_w^2 \left(1+0.004\frac{c}{t_w}\right)\left(\frac{I_f}{t_w^4}\sqrt{\frac{R_{d,f}}{210}}\right)^{0.153}.$$

In conclusion, the writers established a formula for the ultimate load of a web subject to a partial edge load and stiffened by a longitudinal rib placed at $b_1=0.1b$:

$$(8)\quad P_u(x=0.1) = 17.1 R_{d,w}\, t_w^2 \left(1+0.004\frac{c}{t_w}\right)\left(\frac{I_f}{t_w^4}\sqrt{\frac{R_{d,f}}{210}}\right)^{0.153}.$$

As in this case, as said above, only insignificant bending stresses occurred in the upper web panel, the formula was derived so as to correspond to a restricted degree [$3\varepsilon_{me}$] of membrane plastification in the web.

(7)

3. Variable Repeated Loading

3.1. Ultimate limit state definition

On the basis of the tests conducted to date, low-cycle fatigue curves were plotted, and a maximum limit load, P_{fat}^{exp}, was determined such that under this load no failure of the girders occurred in the course of the 5.10^4 loading cycles applied.

The results are given in Fig.1, in comparison with the stationary loading test results.

Summing up all information obtained during their tests on girders under the action of a repeated partial edge load, in the course of which the "breathing" of the girder webs and the cumulation of damage in the webs and the whole girders was studied, the authors concluded that the ultimate limit state of webs under the aforesaid loading conditions could safely be defined (until further evidence makes it possible to employ a less strict definition) on the basis of the onset of surface plastification.

Moreover, the experiments confirmed (see Fig.1) that the optimum position of the longitudinal stiffener was at 0.2 web depth (measured from the loaded flange), since for other stiffener positions a marked decrease in the onset-of-surface yielding load occurred.

With due regard to the above definition of the ultimate limit state, summarizing all data obtained, the writers established the following formula for the ultimate load, P_u, of a web fitted with a longitudinal rib at the distance $b_1=0.2b$ from the loaded flange and subject to a variable repeated patch load:

$$(9)\quad P_u = A.R_{d,w}.t_w^2\left(1+0.004\frac{c}{t_w}\right)\left(\frac{I_f}{t_w^4}\sqrt{\frac{R_{d,f}}{210}}\right)^B.$$

There $R_{y,w}$ is the yield stress of the web material, $R_{y,f}$ that of the flange material, I_f the second moment of area (with respect to the centroidal axis perpendicular to the web plane) of the loaded flange, and A and B are (experimentally verified) coefficients. For the case under consideration (i.e., for a web with a longitudinal stiffener at $b_1=0.2b$), $A=15.9$ and $B=0.153$. For webs without longitudinal stiffening, the same formula may be used, but with $A=9.9$ and $B=0.132$.

4. Combined Action of a Partial Edge Load and a Bending Moment

If the web under study is subject to the combined action of a patch load and a bending moment, the ultimate loads resulting from the formulae given above in secs 2 and 3 are multiplied by a reduction factor

(8)

$$(10) \quad \eta_b = \sqrt{(1 - \frac{\sigma_{b,w}}{Rd,w})^2} \,,$$

where $\sigma_{b,w}$ is the bending stress at the extreme (i.e. adjacent to the loaded flange) fibres of the web and Rd,w is the design strength of the web material.

References:

[1] Drdácký, M.; 1982: Steel webs with flanges subjected to partial edge loading. Chalmers University of Technology, Göteborg.

[2] Januš, K., Kárníková, I. and Škaloud, M.; 1988: Experimental investigation into the ultimate load behaviour of longitudinally stiffened steel webs under partial edge loading. Acta technica ČSAV, No. 2, pp. 158 - 195.

[3] Kutmanová-Kárníková, I., Škaloud, M. and Januš, K.; 1990: "Breathing" of thin webs under variable repeated patch loading. Colloquium on Stability of Steel Structures, Hungary.

[4] Škaloud, M. and Kárníková, I.; 1988: Experimental research on the limit state of the plate elements of steel bridges. Transactions of the Czechoslovak Academy of Sciences, Series of Technical Sciences, Vol. 95, No. 1, Academia, Prague, pp. 123 - 139.

[5] Škaloud, M. and Novák, P.; 1975: Post-buckled behaviour of webs under partial edge loading. Transactions of the Czechoslovak Academy of Sciences, Series of Technical Sciences, Vol. 85, No. 3, Academia, Prague, pp. 1 - 94.

(1)

WITOLD KAKOL*.

PARAMETRIC STUDIES OF COMPRESSED STIFFENED PLATES

INTERNATIONAL COLLOQUIUM
STABILITY OF STEEL STRUCTURES
BUDAPEST, HUNGARY, 1990
PRELIMINARY REPORT

Summary: The elastic stability analysis of stiffened plates by means of the finite strip method is presented. The modified Marguarre's large deflection theory of shallow shells, giving nonlinear strain-displacement relations, is used to solve the problem. Thus all possible buckling modes that may occur in the problem considered are contained in the buckling model. The compound finite strip element with one internal nodal line is applied. Numerical parametric studies of the buckling strength of stiffened plates in compression are carried out covering a range of plate and stiffener slenderness.. The nonlinear analysis is then performed to analyse the post-locally as well as interactive buckling behaviour of stiffened plates.

1. INTRODUCTION

The paper presents a part of the systematic studies of buckling strength of stiffened plates to provide design curves as a function of plate and stiffener slenderness.
The finite element and finite difference programs have been developed in recent years to study both plates and stiffened panels. However these programs are so time consuming that it is expensive to undertake parametric studies, a necessary input to any design formulation.
The finite strip method has proved to be accurate and efficient tool for analysing the structures that have constant cross sectional properties along one axis. In the finite strip method a two-dimensional problem is reduced to a one-dimensional problem and it results in considerable reduction of computational costs involved in the analysis.
The finite strip method has been used with success for analysis the elastic critical and post-buckled strength of both plates and plate assemblages, [Yoshida 1971], [Graves-Smith 1978],

* Ass. Professor, Department of Civil Engineering, Technical University of Poznan, Poland

(2)

[Gierlinski 1984], [Benito 1985]. Most of the previous applications of the finite strip method used lower order strips. In the paper higher order strips are used.

2. FINITE STRIP FORMULATION

For the standard form of the finite strip method, the structure is discretized into strips, whose displacement field is described by harmonic functions in the longitudinal direction and polynomials in the transverse direction. If higher order polynomial functions are used to represent the transverse variation of displacements, it becomes possible to reduce the number of strips required for a given degree of accuracy. The finite strip with one additional nodal line (at mid-width) has been used with success in the static and dynamic analysis of elastic plates and bridges, [Cheung 1972]], [Loo 1978]. The displacement function in the transverse direction incorporates a fifth and second order polynomials for the bending and in-plane actions, respectively.
For a strip with one auxiliary nodal line (Fig.1), the assumed displacement interpolation function may be written as:

$$u = f_{1m}(\eta)\ U_m(\xi)$$
$$v = f_{2m}(\eta)\ V_m(\xi) \qquad (1)$$
$$w = f_{3m}(\eta)\ W_m(\xi)$$

where $\eta = y/b$ $\xi = x/l$.

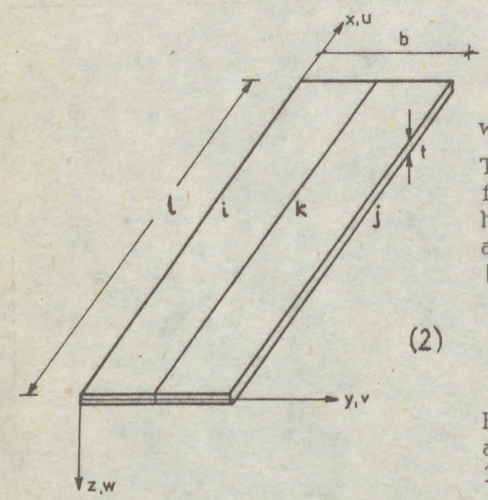

Fig.1 Finite strip with one internal line

The shape functions $f_{im}(\eta)$ may be found in [Cheung 1976]. The harmonic functions in eq.(1) are assumed the same as those used by [Maeda 1982]:

$$U_o = 1, \quad V_o = 1 - 2\xi, \quad W_o = 1,$$
$$U_m = \cos(m\pi\xi) \quad V_m = \sin(m\pi\xi) \qquad (2)$$
$$W_m = \sin(m\pi\xi) \quad m = 1, 3, 5 \ldots$$

Basic assumptions made in the analysis are as follows:

1. Large deflection theory of thin shallow shells, due to von Karman-Marguerre is employed.
2. The material is elastic, isotropic and obeys Hooke's law.
3. Linearized curvatures assumptions are used. This limits the magnitude of the bending slopes to remain small.
4. The load is static and conservative.

In von Karman theory of thin plates only those nonlinear terms which depend on the slopes of w are retained. Although the omission of nonlinear terms due to u and v considerably simplifies analysis, this assumption may not be satisfactory for plates which undergo in-plane buckling displacements. Hence the Green strain tensor is employed in the form:

(3)

$$\varepsilon_x = u,x + 1/2(v,x + 2v^{\circ},x)v,x + 1/2(w,x + 2w^{\circ},x)w,x - zw,xx$$

$$\varepsilon_y = v,y + 1/2(v,y + 2v^{\circ},y)v,y + 1/2(w,y + 2w^{\circ},y)w,y - zw,yy$$

$$2\varepsilon_{xy} = u,y + v,x + 1/2(v,x + 2v^{\circ},x)v,y + 1/2(w,x + 2w^{\circ},x)w,y +$$
$$1/2(v,y + 2v^{\circ},y)v,x + 1/2(w,y + 2w^{\circ},y)w,x - 2zw,xy \qquad (3)$$

where u°, v°, w° define the shape of the initial stress-free middle surface of the plate element which is assumed in the form similar to eq.(1).
The corresponding Kirchhoff's stress tensor is:

$$Sx = \frac{E}{1-\nu^2}(\varepsilon_x + \nu\varepsilon_y) \quad Sx = \frac{E}{1-\nu^2}(\varepsilon_y + \nu\varepsilon_x) \quad Sx = \frac{2E}{1+\nu}\varepsilon_{xy} \qquad (4)$$

where E denotes Young's modulus and ν is Poisson's ratio.

3. SOLUTION PROCEDURE

The Total Lagrangian Description was used to develop the governing equations of the equilibrium of the body. Based on the principle of incremental virtual work the linearized equilibrium equation for a structure modelled with finite strips with respect to the incremental displacement U_m was obtained in the form [Kakol 1987]:

$$\sum_n ({}^tK^0_{mn} + {}^tK^1_{mn} + {}^tK^2_{mn}) U_m = {}^{t+\Delta t}R_m - {}^tF_m \qquad (5)$$

where ${}^tK^0_{mn}$ is the stiffness matrix for linear, stable behaviour, ${}^tK^1_{mn}$ is the initial-stress or geometric stiffness matrix being a linear function of displacements, and ${}^tK^2_{mn}$ is the initial- displacement stiffness matrix - a second order function of displacements (all of them derived at time t), ${}^{t+\Delta t}R_m$ is the vector of externally applied nodal line loads at time t+Δt, ${}^tF_m$ is the vector of nodal line forces equivalent to the element stresses at time t.
The complete nonlinear response of the structure can be determined by solving the assembled resulting nonlinear equations with an incremental loading procedure together with Newton's iterative method.

4. PARAMETRIC STUDIES

The analysis is carried out for panels of fixed plate slenderness (b/tp) and changing the height (d) and the thickness of the stiffeners (ts). The flat bar type of stiffeners, angle and tee sections will be considered. Consider wide stiffened plate reinforced with equal spaced ribs. Due to the symmetry of the buckling mode it is sufficient to analyse only typical panel with one longitudinal stiffener with its associated plating. Finite strip nonlinear analysis involves firstly performing a buckling analysis to determine the local buckling stress and buckling half wavelength. The nonlinear analysis is then carried out for a section equal in length to

4)

the half wavelength of the local buckle. The shape of the geometrical imperfections has been assumed to be the same as the buckling mode.

The results of buckling analysis for three types of stiffeners are shown in Fig.2. It can be observed that the sensitivity of both depth and thickness of stiffeners to buckling stress is basically of the same nature for all panels considered. For flat bar stiffeners the buckling plots attain clearly their maximum and beyond these points the buckling stress decreases rather rapidly. Note that for all types of stiffeners and for $t_s > t_p$ the buckling strength practically does not differ from each other, except the case of flat bar stiffener. It is seen also that the stiffeners should be thicker than the plating to obtain the maximum buckling strength.

The nonlinear analysis was then performed for the panels considered above. The panels were subjected to uniform in-plane displacements in order to pursue the post-buckling behaviour. In all of the following examples the panels were assumed to be imperfect. The amplitude δ of geometrical imperfections was assumed to be of 0.1 of the thickness of the main plate. The reduction of the stiffness due to buckling phenomena can be expressed as tangents to load-end-shortening curves. The ratio of post-buckling compressional stiffness to that before buckling is given by the ratio E^*/E, where E^* is often called a reduced effective Young's modulus. For the perfect panel this ratio is equal to unity in the entire range below the classical buckling load. However even for small imperfections the stiffness decreases significantly at relatively low loads.

Fig.3 shows plots of the ratio E^*/E versus the normalized load P/P_L for few panels considered (P_L is the load corresponding to bifurcation buckling of the panel).

It can be easily found that tee type stiffeners have the highest post-buckling stiffness. However the differences between the angle and tee sections are not very remarkable.

To solve the problem of the interactive buckling the tangent stiffness of the locally deformed stiffened plate is required. The reduced effective stiffness of the panel is computed from the finite strip analysis of isolated panel in similar way as above. For a given load intensity resolution of the nonlinear eq.(5) is performed due to changes of the stiffness. Along uncoupled path in which local type of deflections are initially small local buckling may occur and the plate bifurcates into the coupled lateral-torsional mode. This point is called a compound bifurcation point [Reis 1977].

The results of analysis of wide stiffened plate reinforced with flat bar stiffeners with $b/t_p=62$, $d/t_p=18$ and $t_p=t_s$ are presented in Fig.4. The results are plotted in nondimensional form, in the P/P_L and w/t_p coordinates, where w is the lateral displacement of the junction of the plate and the rib. The overall sinusoidal geometrical imperfections were assumed in two directions: towards the stiffener ($\Delta>0$) and away from the stiffener ($\Delta<0$). The case of the ratio of P_L to P_E equal to unity is shown in Fig.4. Post-buckling paths are everywhere

(5)

unstable regardless of the direction of imperfections. For the less ratio of P_L/P_E compound bifurcation point may be stable or unstable in dependence on both the magnitude and direction of the imperfections, [Kakol 1987].

5. CONCLUSIONS

In the paper the buckling and post-buckling analysis of stiffened plates was carried out with the use of finite strips. The buckling strength analysis carried out for the types of stiffeners used in actual structures has shown that it is difficult to choose the optimal ratio of the stiffener slenderness to the plate slenderness. The nonlinear analysis is required if post-buckling behaviour is taken into consideration at the design process.

The interaction between local and global buckling modes reduces the buckling stress obtained for the perfect structures. The reduction of buckling load may be as much as 30% of that of the perfect plate for nearly coincident buckling loads.

Further parametric studies are needed, especially for nonlinear behaviour of the considered structures. Work is in progress to extend the method to elasto-plastic analysis.

6. REFERENCES

Benito R., Sridharan S., 1985, Interactive buckling analysis with finite strips, Int.J.Num.Meth.inEng.,vol.21, pp.145-161.

Cheung M.S.,Cheung Y.K., 1972, Static and dynamic behaviour of rectangular plates using higher order finite strips, Build. Sci.,vol.7, pp.151-158.

Cheung Y.K., 1976, Finite strip method in structural mechanics, Oxford, Pergamon.

Gierlinski J.T.,Graves-Smith T.R., 1984, The geometric non-linear analysis of thin-walled structuresby finite strips, Thin Walled Structures, 2, pp.27-50.

Graves-Smith T.R., Sridharan S., 1978, A finite strip method for the post-locally-buckled analysis of plate structures, Int.J.of Mech.Sciences, vol.20,pp.833-842.

Kakol W., 1987, Nonlinear stability analysis of rectangular stiffened plates, Ph.D. Thesis, Technical University of Poznan.

Kakol W., 1987, Interactive buckling of plates stiffened with ribs, Proc. ECCS Int. Coll. on Stability of Plate and Shell Structures, Ghent University, 6-8 April pp. 151-156.

Loo Y.C., Cusens A.R., 1978, The finite strip method in bridge engineering, Slough, Viewpoint.

Maeda Y., Hayashi M., Mori K., 1981, Finite displacement analysis of thin plates by finite strip method, Proc.JSCE, 316(12), pp.23-36.

Reis, A.J., Roorda, J., 1977, The interaction between lateral torsional and local plate buckling in thin walled beams, Second Int.Coll.on the Stability of Steel Struct., Liege, pp. 415-25.

Yoshida K., 1971, Buckling analysis of plate structures by the strip elements, Proc.Jap.Soc.of Naval Architects,130,pp.161-171

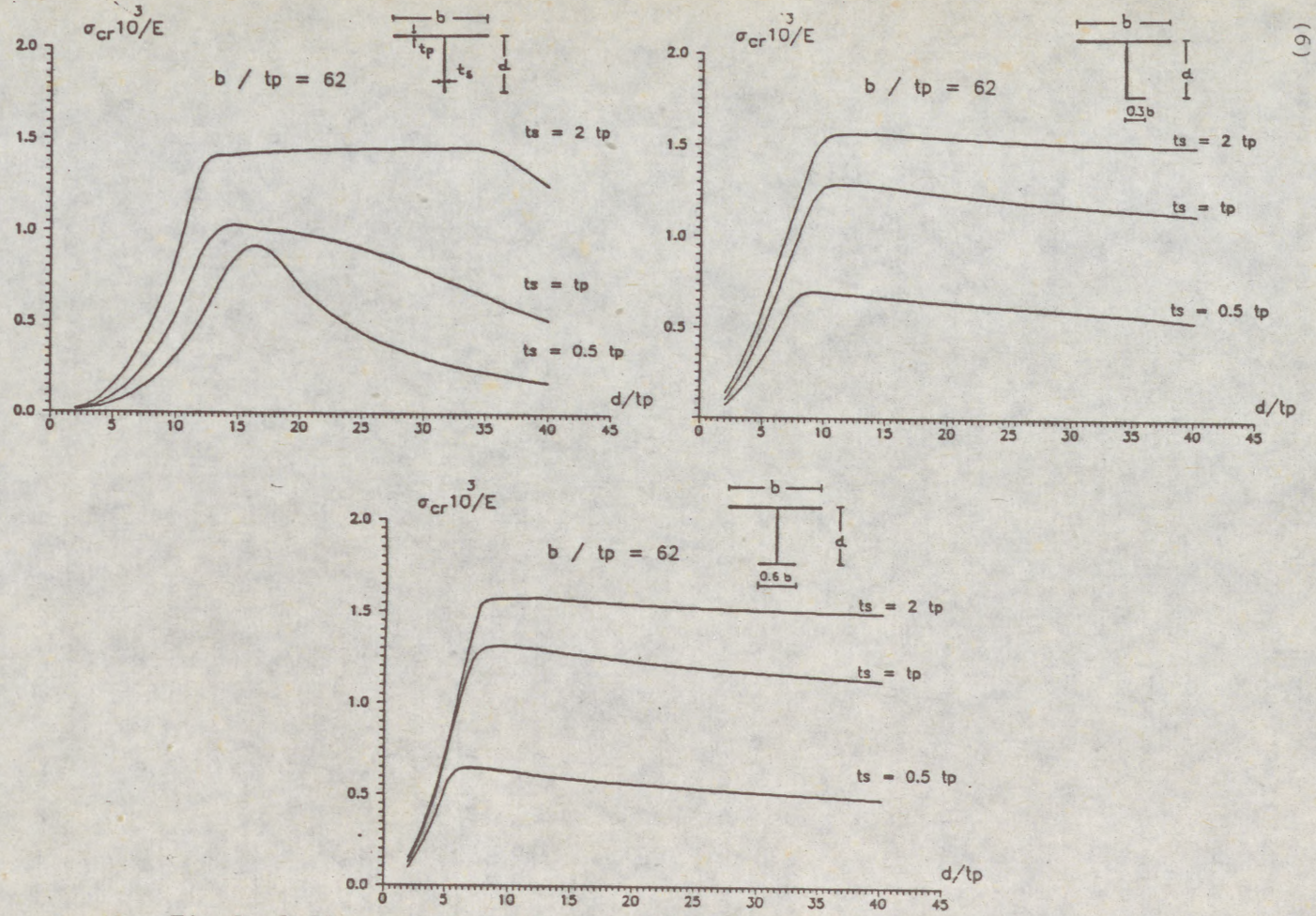

Fig.2. Influence of depth and thickness of stiffeners on buckling stress for a) flat, b) angle c) tee type of stiffeners.

(6)

$$d = b$$

(7)

stress for a) flat, b) angle c) tee type of stiffeners.

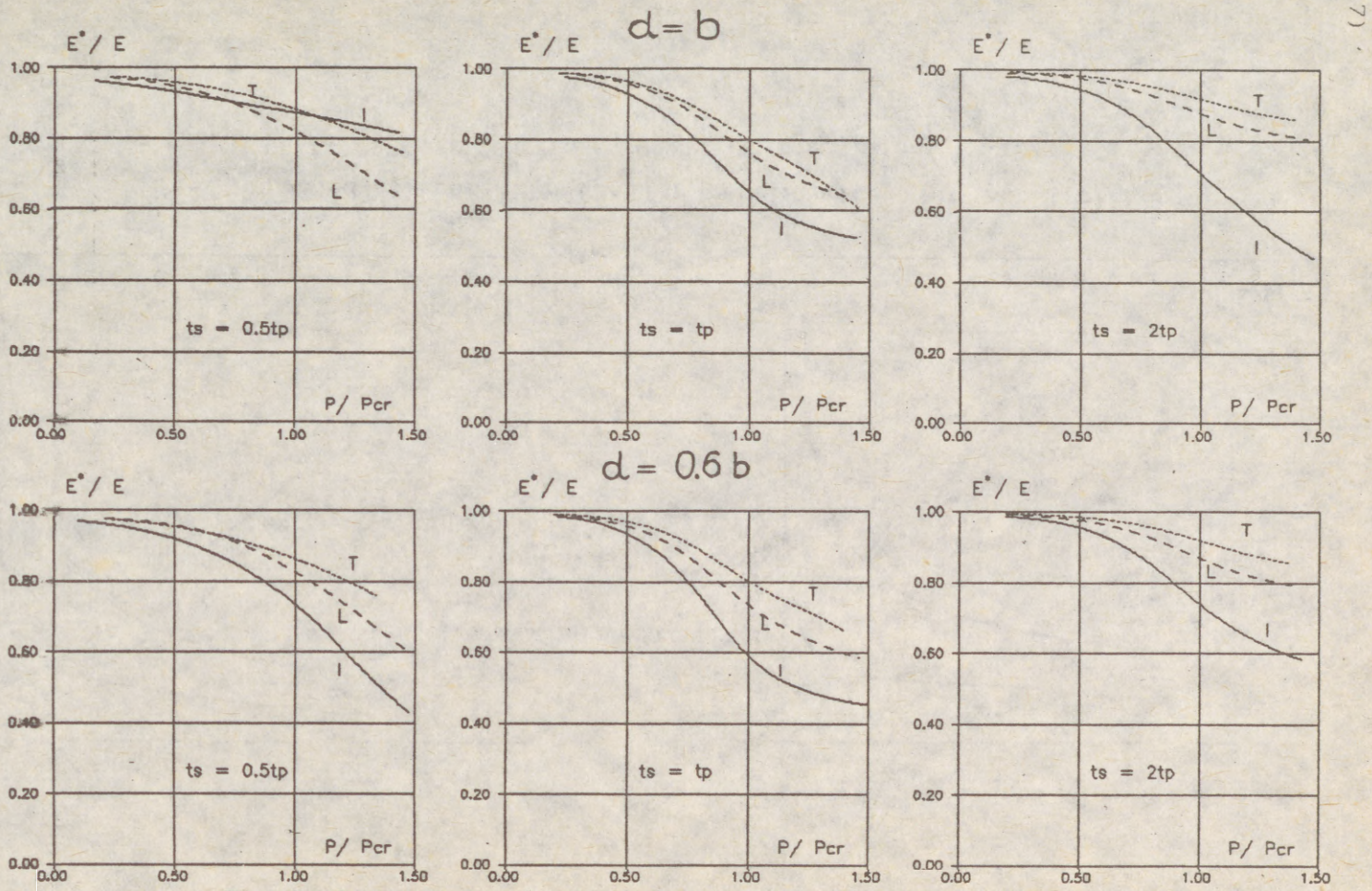

Fig.3. Comparison of effective Young's modulus for bar, angle and tee type stiffeners for d=b and d=0.6b.

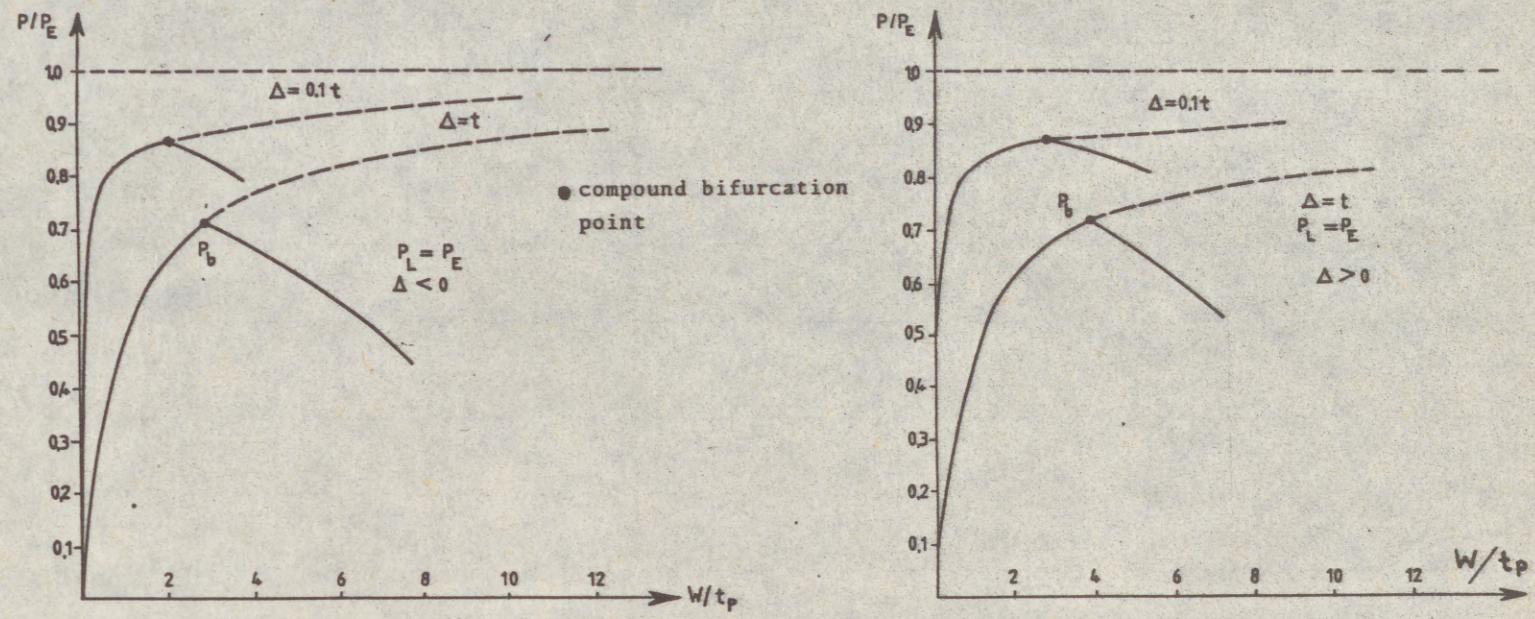

Fig.4. Load-displacement paths for panels with flat bar type stiffeners.

(1)
KALYONOV, Vladimir (1)

THE TEST OF FULL-SCALE ROOF-BLOCK WITH THIN-WALLED GIRDERS WITHOUT STIFFENERS

INTERNATIONAL COLLOQUIUM
STABILITY OF STEEL STRUCTURES
BUDAPEST, HUNGARY, 1990
PRELIMINARY REPORT

Summary: The paper presents some results of roof-block investigations in which girders with high slenderness of the web, without stiffeners were used. New constructive form of roof operates as supporting, safeguarding and technological constructions i.e. fulfils the principles of functions coincidence. This solution in comparison with that traditional has considerable economical effect. The investigations have shown that post-buckling behaviour of girder webs don't influence on the serviceability of roof construction and confirm real ability of their practical use.

New construction of roof for plants has been worked out in the USSR for the case when because of technology requirements powerful system of large air conduicts is necessary. Construction of roof is designed for the conditions of large block erection. Fig.1 shows the scheme of assembled roof block. Thin-walled girders without stiffeners (with slenderness ratio $\lambda = h/t = 320$, where h - depth of beam, t - thickness of web) are used as main trusses. Girders are supported by secondary trusses. Corrugated steel sheeting installed on top and bottom flanges of girder and webs of girders form closed spaces, which are used as communication tunnels and ventilation skips, calculated for the excessive air pressure of 0.1 atm. There are no lateral ties in roof constructions because corrugated steel sheeting on top and bottom flanges of girder provides necessary space rigidity. New roof construction in comparison with the

---

(1) Cand.Sc.(Eng.), Head of Department "Structures and Assembly Connections", VNIPIPromstalconstruktsiya, Moscow, USSR

(2)
traditional one, reduces steel rate for 30 % and time of roof erection for 30-40 % .

Tests of the full-scale roof-block have been carried out with the purpose to study real behaviour and to set correspondence between real and theoretical load-carrying capacity and deformativity of new type roof construction.

Test block (Fig. 1) consisted of four main girders with span 24m which were placed in 4m; cross-section of girders was constant along the length and consisted of web 1900 x 6 mm and flanges 360 x 14 mm. There were 4 holes with diameter 800 mm for the attending personnel to pass from one compartment to another during exploitation; hole edges were not stiffened. Steel corrugated sheeting was installed on top and bottom flanges of beams. Fastenings of sheeting were made with the help of self-tapping screws.

Tests of roof-block included two schemes of loading: step-by-step loading of uniformly-distributed load q up to design value and subsequent unloading;step-by-step loading q up to ultimated values, combined with action of loads imitated air pressure upon the beam webs.

Scheme of roof loading for uniformly-distributed load is given in Fig. 1.

Influence of air pressure upon webs of tests girders was imitated with the equivalent concentrated loads. Transfer of concentrated actions upon the webs of test girders was made with the help of tackle block, according to scheme in Fig.2. Design force in rope of tackle block was:

Design of load-carrying capacity and deformativity of roof girders was made according to [1]. The design has shown that section 7-7 (Fig.1) located in zone of bending determines load-carrying capacity of girders. Ultimate value of moment taken by girder in this section was determined according to design scheme (Fig.2) by formula:dd

$$M_{ult} = F_n \sigma_T (R + t_n) + 30 t^2 \sigma_n (1 - D/R)[R - 30t(1 - D/R)]$$

where F_n - area of flange cross section,
σ_T - yield stress of flange steel,
t_n - thickness of flange,
D - diameter of hole.

Ultimate value of bending moment calculated with account to actual mechanical properties of test girder steel was taken equal to 2935 kN m, designed, according to method of limit states - 2232 kN m; corresponding values of distributed load: ultimate - 40.3 kN/m, designed - 31.4 kN/m.

Analysis of test results has shown the following. Characteris-

(3)
tic feature of test girder is the presence of considerable initial web deformations. Maximum initial deformations in web for test girder B-1 were up to 0.031 m i.e. 2.7 times more than it was assumed. Initial deformations in web didn't influence much upon the behaviour of webs and load-carrying capacity of girders on the whole, but defined direction of webs' deflections in post-buckling stage of their behaviour. Deflections in webs because of action of critical loads upon girders had elastic character. Maximum deflections, for example, in girder B-2 were 0.023m (Fig.4). Forces upon the web, imitating air pressure, practically didn't influence on character of web wave-formation and didn't change deflections of web more than for 0.005 - 0.008m (Fig.3).

Fig.4 shows designed and experimental maximum deflections caused by external load in test girder B-2. The diagram shows that vertical deflections in test girders up to design loads are of linear character.After being unloaded there were practically no residual deflections in girders. Maximum value of vertical deflections in girders caused by action of design loads (without taking into consideration own weight of construction) was 0.0511m for girder B-2 or 1/450 of girder span that fulfils the requirements of Building Code [2]. Experimental deflections of girder B-2 were about 10 % more than their theoretical values. Discrepancy could be explained by the presence of holes in the web d=800m having weakened to some degree bending rigidity of the girder. This diagram has also shown the deflections of girder B-2 during the second loading scheme. The diagram shows that when the load exceeds 1.14 times the designed one, character of deflections changes. It could be explained by the reduction of girder shear and bending rigidity because of increase of lateral web deflections. It could be also explained by the beginning of development of elastic-plastic deformations in some sections of girder. At action of loads close to those ultimate theoretical - 40.3 kN/m, maximum deflections of girder B-2 were equal to 0.076 and were 0.86 of theoretical ones.

Theoretical critical loads which caused buckling of webs in girders due to primary bending and shear actions were not large. They were correspondingly 3.7 kN/m and 8.5 kN/m. Taking into account considerable initial deformations of web, it buckled practically just after the loading of block. Post buckling behaviour of girder webs characterized by the development of diagonal field of tensile strains. Fig.5 shows distribution curve of main membrane stresses σ_1 and σ_2 in sections 1,2 and 3 during loading, equal to 37.6 kN/m (without taking into account the own weight of construction); maximum tensile stresses developed in sections 1 and 2 (i.e. in the zone of web mainly subjected to shear); vectors of stress σ_1 practically coinsided with the direction of diagonal folds of the wall and exceeded critical tangent stresses approximately 10 - 11 times. Growth of main compressed stresses σ_2 occured in the zone of web adjacent to support, where stiffeners and flanges form rigid

(4)

contour. Here the excess of measured stresses σ_2 is 3.6 times more than critical stresses. It is less considerable in the other parts of the web. The presence of diagonal field of stresses influenced upon the character of distribution of membrane stresses σ_x and τ_{xy}. Fig.6 shows experimental stresses σ_x and τ_{xy} in typical sections girder: in zones mainly subjected to shear (section 1-1), combined shear and bending (section 3-3),mainly subjected to bending (section 9-9). Type of distribution of stresses σ_x and τ_{xy} completely corresponds with the representation about stress state in thin-walled girders without stiffeners, studied in detail in some papers, for example [3], [4].

Comparison of curves for normal membrane stresses- σ_x and shear - τ_{xy}, obtained during the loading of experimental block, according to schemes 1 and 2 (in particular at the time of action of linear design load q equal to 31 kN/m) has shown that the action upon girder webs of lateral forces, imitating air pressure (the second scheme of loading) hasn't influenced much upon quantitative and qualitative distribution of membrane stresses σ_x and τ_{xy}.

It has already been mentioned that load-carrying capacity of girders was determined by strength of beam in section 7, weakened by the hole in the wall. Fig.6 shows stress curves σ_x of this section,received during the girder loading of linear loads 18.4, 29.3 and 37.6 kN/m (without taking into account the own weight of construction). Presence of the hole has caused redistribution of forces in girder section. As a result there was some lag of stresses development in tensile flange in comparison with the compressed one. At loading 37.6 kN/m stresses in compressed flange were some 13 % greater than in that tensile and were equal to 238 MPa. On the whole stress curves in section 7 during action of loads close to ultimate ones confirm the design scheme (Fig.2). When maximum linear load upon the girder was equal to 40.3 kN/m (taking into account the own weight of construction per each girder) the construction of roof block kept its load-carrying capacity.

So, the experimental investigations on the full-scale roof block confirmed the high level of safety of new roof construction and allowed to recommend it for exploitation.

REFERENCES

[1] Руководство по проектированию стальных тонкостенных балок. ЦНИИПроектстальконструкция.Москва,1980.

[2] СНиП II-23-81* Строительные нормы и правила.Нормы проектирования.Стальные конструкции.Москва,1988.

[3] Мельников Н.П.,Левитанский И.В.,Каленов В.В. :Тонкостенные балки- эффективный вид строительных конструкций. Промышленное строительство №10,1973,Москва.

[4] Каленов В.В. : Основные положения проектирования тонкостенных балок без ребер жесткости.Реферативная информация,серия VIII,выпуск 5,ЦНИИС,1976.

Fig.1. Test roof-block. 1 - thin-walled girders; 2 - secondary trusses; 3,4 - corrugated steel sheeting on top and bottom flanges;5 - tackle block, imitating load upon girder webs due to air pressure; 6 - supports;7 - vertical distributed load; 0 - apparatus used to record deflections of girders.

(6)

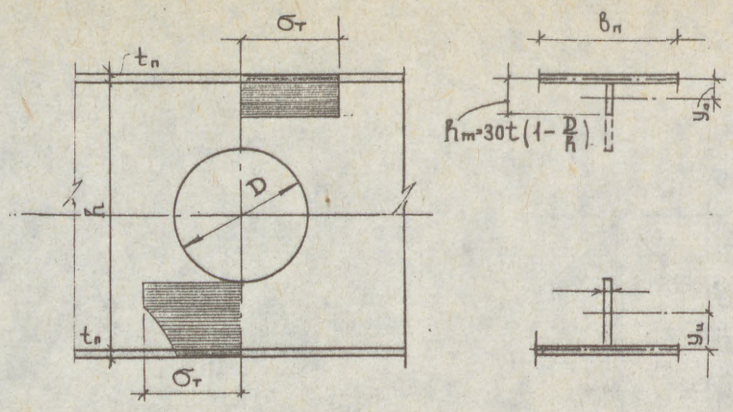

Fig.2. Design scheme for determination of girder ultimate bending moment with account of hole presence in the web.

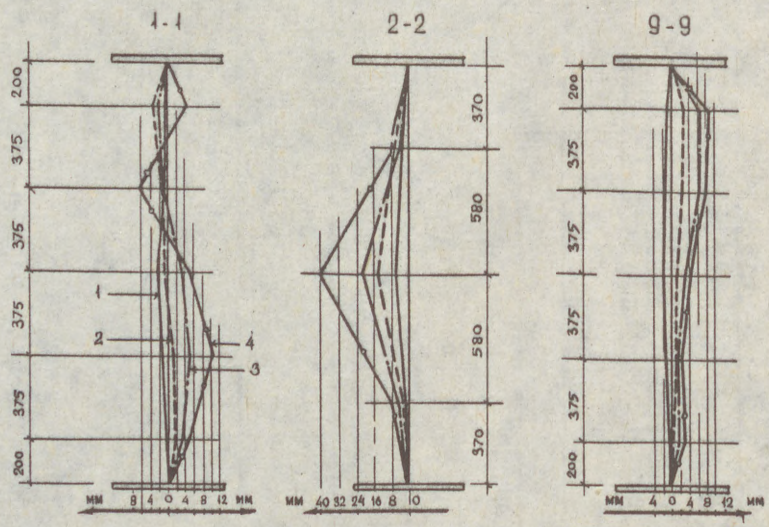

Fig.3. Lateral deflections of girder's web B-2 1 - initial web deflections;2 - deflections at load 18.4 kN/m;3 - the same,29.3 kN/m;4 - the same, 37.6kN/m.

(7)

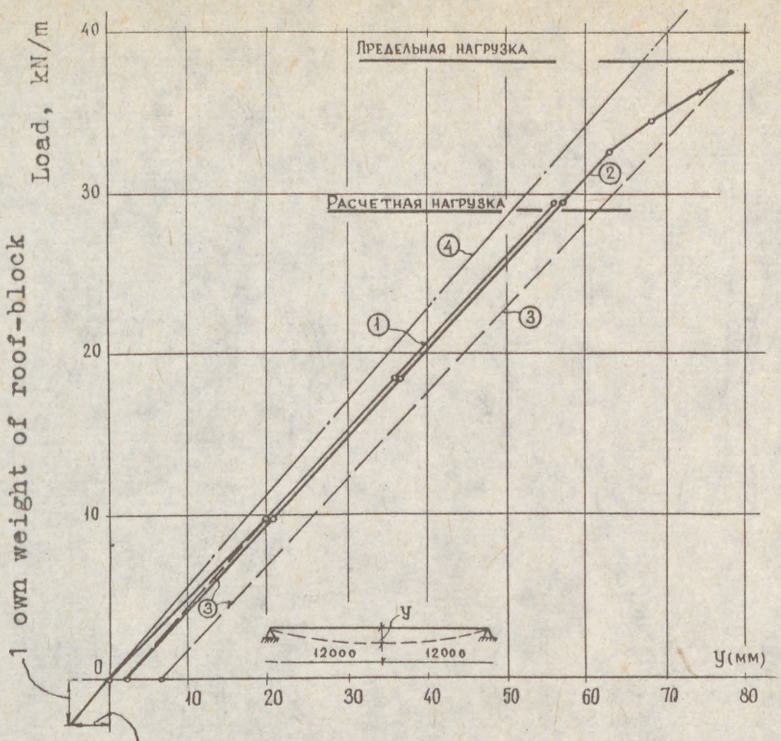

Fig.4. Maximum deflections of girder B-2.
1 - at loading scheme I;
2 - at loading scheme II;
3 - unloading;
4 - theoretical values of deflections.

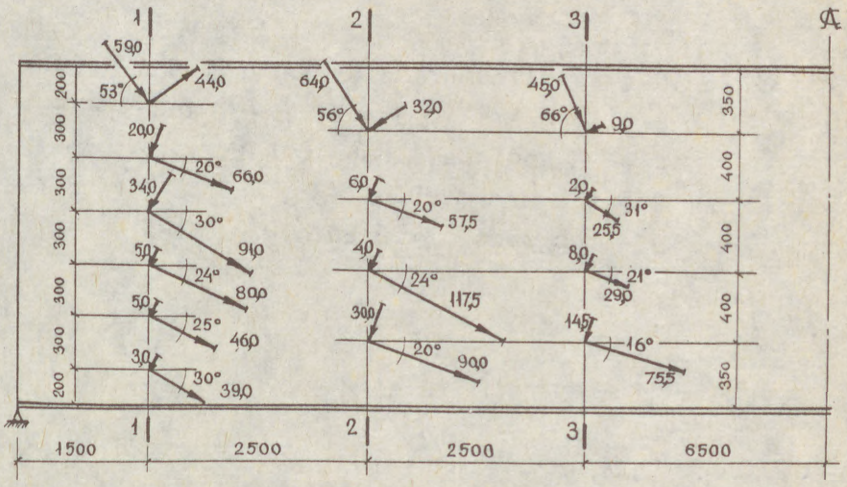

Fig.5. Main membrane stresses and (MPa) in sections 1 - 1, 2 - 2, 3 - 3 at load 37.6kN/m

(8)

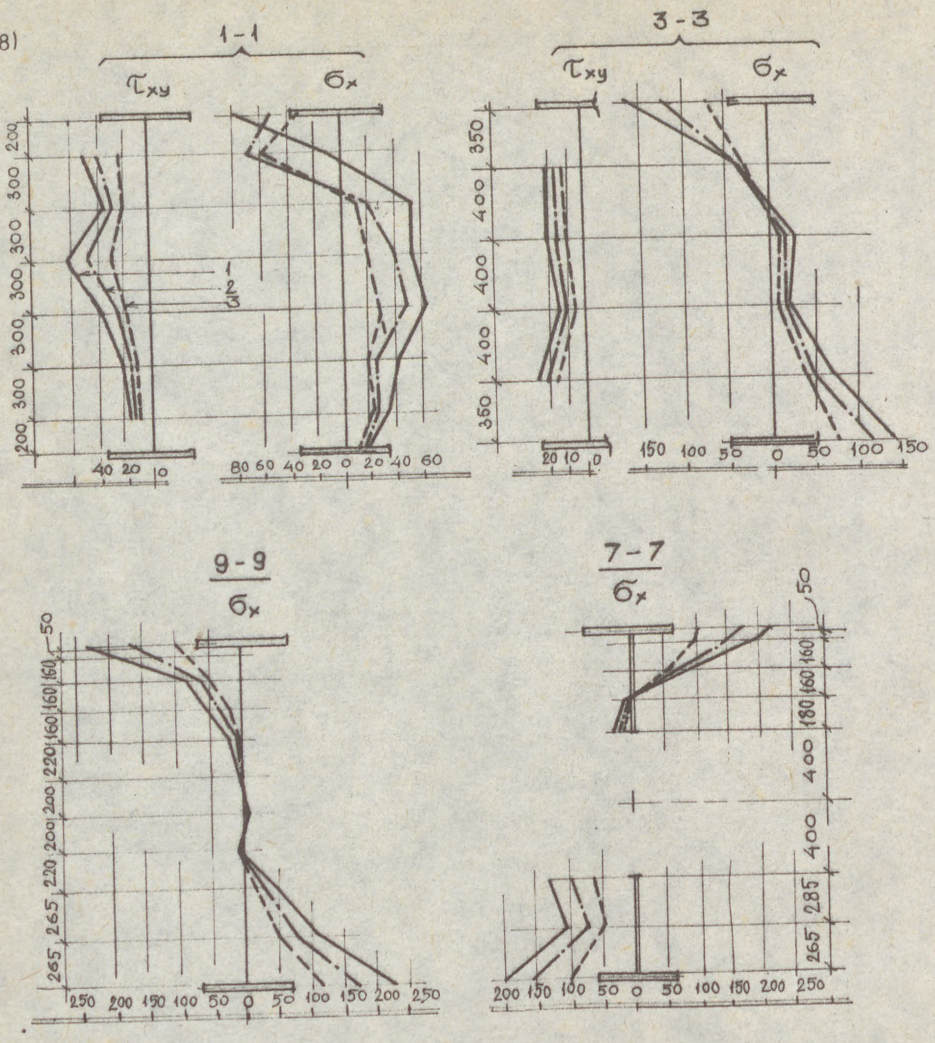

Fig.6. Curves of membrane stresses and (MPa) in sections 1 - 1, 3 - 3, 7 - 7 and 9 - 9
1 - and at load 18.4 kN/m,
2 - the same, 29.3 kN/m,
3 - the same, 37.6 kN/m

(1)
KITADA, Toshiyuki (1)
NAKAI, Hiroshi (2)
FURUTA, Tomiyashu (3)

EXPERIMENTAL STUDY ON ULTIMATE STRENGTH OF STIFFENED PLATES SUBJECTED TO LONGITUDINAL TENSION AND TRANSVERSE COMPRESSION

INTERNATIONAL COLLOQUIUM
STABILITY OF STEEL STRUCTURES
BUDAPEST, HUNGARY, 1990
PRELIMINARY REPORT

Summary: The ultimate strength of steel plates with longitudinal stiffeners of open or closed cross section subjected to both longitudinal tension and transverse compression is experimentally investigated in this study. Four stiffened plate specimens on scale 1/3 corresponding to that of the steel deck plate in an actual Nielsen Lohse bridge were tested by using an experimental apparatus newly developed for this study. The test results verify a practical design method which the authors developed for predicting the ultimate strength of stiffened plates subjected to biaxial in-plane forces.

1. Introduction

Wide steel deck plates of arch bridges are subjected to both longitudinal in-plane tension in the direction of the bridge axis, as in the case of tie members, and significant transverse in-plane compression in the direction perpendicular to the bridge axis, as in the case of compression flanges of cross girders. Since the steel deck plate is usually stiffened by longitudinal stiffeners arranged in the direction of the bridge axis, it is necessary to check the buckling stability of these steel deck plates by regarding them as stiffened plates subjected to longitudinal tension in the direction of the stiffeners and transverse in-plane compression in the direction perpendicular to the stiffeners, as shown in Fig. 1.

---

(1)Associate Professor of Civil Engineering, Osaka City University
(2)Professor of Civil Engineering, Osaka City University
(3)Research Student of Postgraduate School, Osaka City University

(2)

However , there is no available design criteria for these stiffened plates subjected to biaxial in-plane forces in the current Japanese Specifications for Highway Bridges (1980). Such stiffened plates are, therefore, designed on the basis of the elastic buckling analysis or elasto-plastic and finite displacement analysis (Taido, Hayashi, Kitada and Nakai, 1985).

For these stiffened plates a design provision is codified in the BS 5400 part 3 (1982). In this code, the interaction curve for the ultimate strengths of the plate panel of stiffened plate and the design method for the longitudinal stiffeners are stipulated. Nevertheless, this design code tends to lead to comparatively heavy longitudinal stiffeners.

Through a parametric study on the basis of the elasto-plastic and finite displacement analysis by the finite element method (Komatsu and Kitada, 1980), the interaction curve on the ultimate strengths of stiffened plates subjected to biaxial in-plane forces is developed and a practical design method for predicting the ultimate strengths using the interaction curve and the longitudinal and transverse ultimate strengths of stiffened plate under respectively uni- longitudinal and -transverse compressions was proposed by Kitada, Nakai, Furuta and Suzuki (1988) as well as Furuta, Kitada and Nakai (1988). In this practical design method, the longitudinal ultimate strength is calculated by the column approach proposed by Taido, Hayashi, Kitada and Nakai (1985), and the table and figure on ultimate strength curves are available for the transverse ultimate strength.

In this study, the buckling tests of two stiffened plate specimens subjected to longitudinal tension and transverse compression and two stiffened plate specimens under transverse compression only are carried out in order to investigate the ultimate strength of these stiffened plates and examine the validity of the practical design method mentioned above..

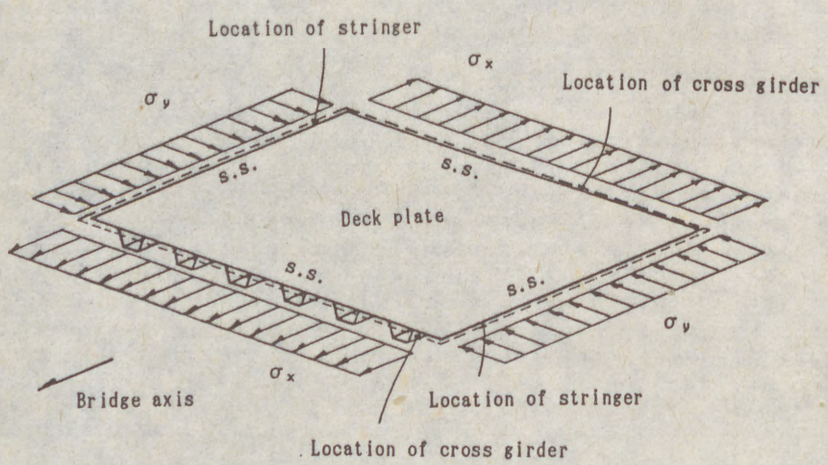

Fig.1 Stiffened Plate Subjected to Longitudinal Tension and Transverse Compression

(3)

2. Experimental Apparatus and Test Specimens

An experimental apparatus illustrated in Fig.2 and Fig.3 has been developed to satisfy the boundary condition of simple support at the edges of a stiffened plate specimen and apply longitudinal tension and transverse compression to them simultaneously. Longitudinal tension and transverse compression are produced by a hydraulic jack with capacity, 600tf and 12 hydraulic jacks with capacity, 25tf, respectively.

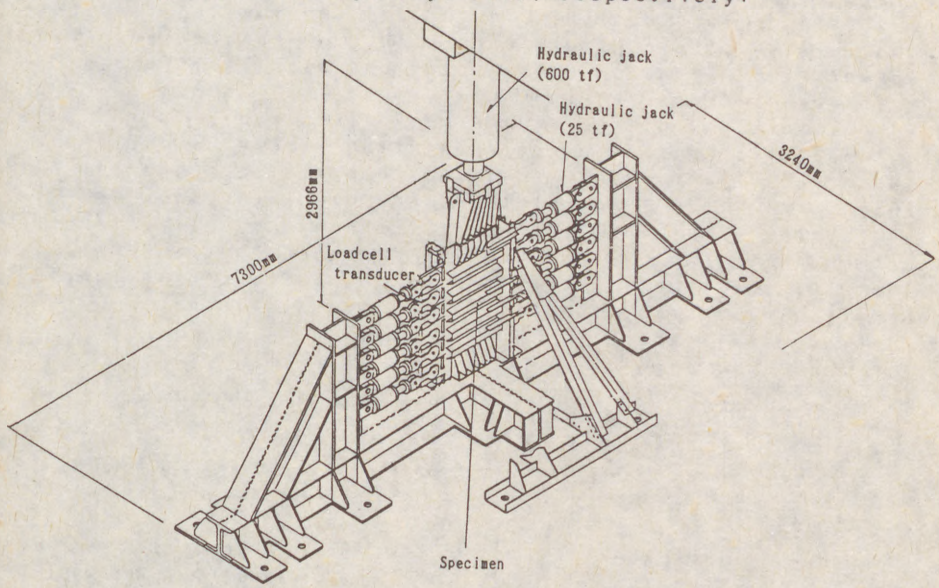

Fig.2 Experimental Apparatus for Stiffened Plate Subjected to Longitudinal Tension and Transverse Compression

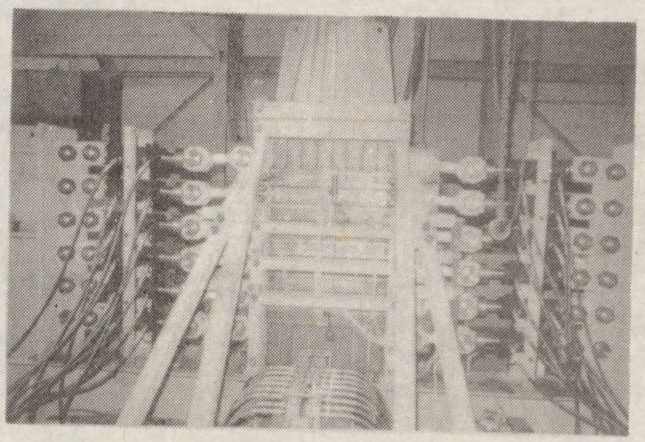

Fig.3 General View of the Experimental Apparatus and Stiffened Plate Specimen

(4)

The four stiffened plate specimens built for the buckling test are listed in Table 1, together with the type of stiffeners and loading conditions. The general view of the specimen No.TCT and the cross-sections of the stiffeners are shown in Fig.4 and Fig.5, respectively. The out-of-plane displacement at the transverse edges $\overline{AB}$ and $\overline{CD}$ of stiffened plate specimen are restrained by special rigs without disturbing the rotation of specimen at the edges to realize the condition of simple support. Slits of 2mm width are installed between the anchor plates with a hole for setting a load cell transducer and tension jack, so that the anchor plates make negligible contribution toward resisting the transverse compression. The specimens with stiffeners of closed (trough) cross-section correspond to one-third the stiffened plate panel of the wide steel deck plate in an actual Nielsen Lohse bridge. The elastic buckling stress of stiffened plate specimen subjected to transverse compression alone is 331 N/mm^2, that is, 1.1 times the yield stress of plate panel and is determined by the local buckling of plate panel among stiffeners. The specimens with open stiffeners are designed to investigate the effect of the type of stiffener on the ultimate strength. The geometrical moment of inertia of an open stiffener is half that of a closed stiffener.

Table 1 Stiffened Plate Specimens

Specimens	Type of stiffener	Loading condition
NCO	Open	C
NCT	Trough	C
TCO	Open	TC
TCT	Trough	TC

C : Transverse compression only
TC: Both longitudinal tension and transverse compression

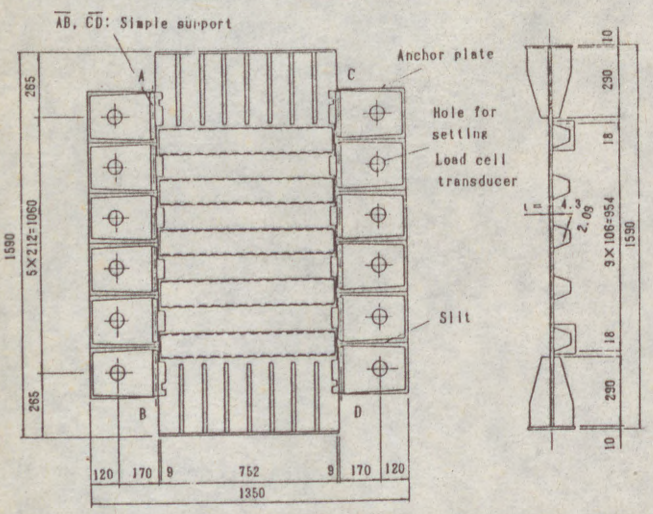

(a) Plan (b) Cross-section

Fig.4 Stiffened Plate Specimen No.TCT (dimensions in mm)

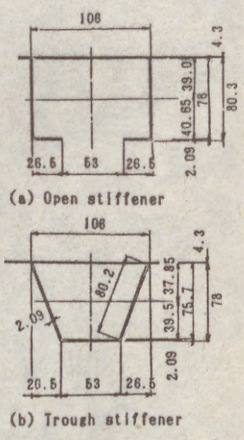

Fig.5 Cross-Sections of Stiffeners (dimensions in mm)

(5)

The material properties of steel plates used are shown in Table 2. The plate panels and stiffeners of the specimens are made of the steel plates A and B, respectively.

Table 2 Material Properties of Steel Plates

Steel plates	Thickness t (mm)	Young's modulus E (N/mm^2)	Poisson's ratio	Yield stress σ_Y (N/mm^2)	Tensile strength σ_u (N/mm^2)
A	2.09	2.20×10^5	0.260	301	376
B	4.30	2.08×10^5	0.271	294	470

3. Initial Imperfections

The maximum values of initial deflections of plate panels and stiffeners in the specimens are shown in Table 3.

The distribution of the transverse residual stress, σ_{ry}, along the longitudinal direction of plate panel is shown in Fig.6, for one of the two specimens measured. It can be seen from the figure that the transverse bending residual stress is large, but the transverse in-plane residual stress, which is the average of the values at the surfaces of plate panel, is small in the plate panel except for the parts near the transverse edges.

Table 3 Maximum Values of Initial Deflections

Specimens / Initial deflection	NCO	NCT	TCO	TCT
δ_{1max}/b_1	1/106	1/133	1/141	1/265
δ_{glmax}/a	1/313	1/859	1/289	1/396

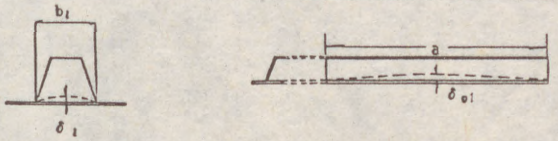

(a) Initial deflection of plate panel

(b) Initial deflection of stiffener

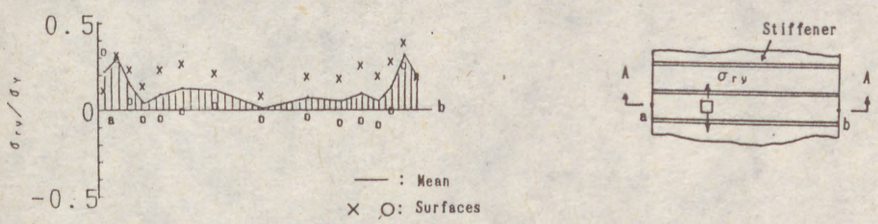

(a) Distribution of residual stress σ_{ry} along line AA

(b) Residual stress σ_{ry}

Fig.6 Residual Stress Distribution

(6)

4. Buckling Test

The buckling test was carried out, after it was confirmed through an elastic test that the expected stress condition could be simulated. In the buckling test, after the expected longitudinal in-plane tension was applied to a stiffened plate specimen, the transverse in-plane compression was gradually increased up to the ultimate state of the specimen by keeping the longitudinal tension constant.

As illustrated in Fig.7, the local buckling of plate panels among stiffeners is predominant in the specimens Nos. NCO and NCT with transverse compression alone, while the overall buckling of stiffened plate and the local buckling of plate panels are observed to coexist , as shown in Fig.8, in the case of the specimens Nos. TCO and TCT with biaxial in-plane forces.

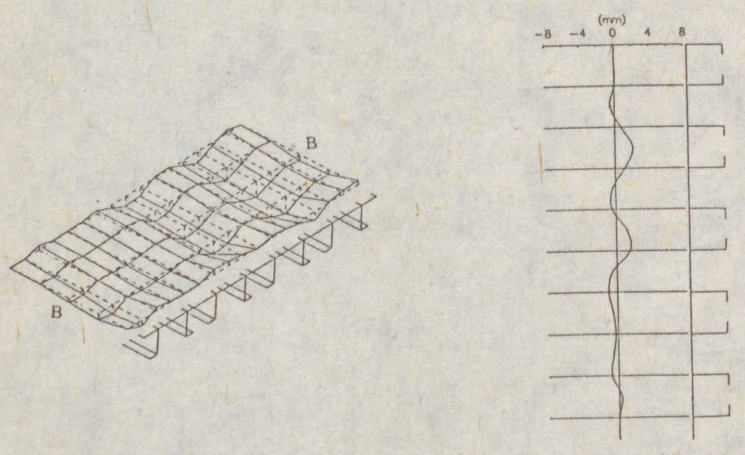

(a) Residual deformation (b) Residual deflection along cross-section $\overline{BB}$

Fig.7 Residual Deformation of Specimen No.NCO after Buckling Test

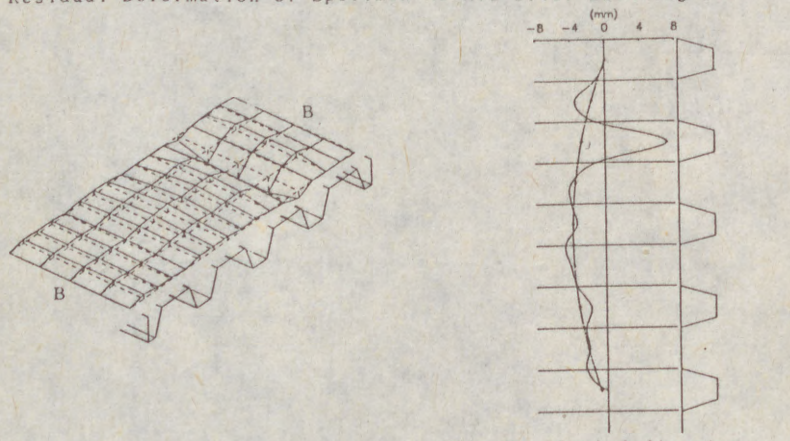

(a) Residual deformation (b) Residual deflection along cross-section $\overline{BB}$

Fig.8 Residual Deformation of Specimen No.TCT after Buckling Test

(7)

The experimental ultimate strengths are shown in Table 4 and Fig.9. The von Mises' yield criterion and the interaction curve of ultimate strength predicted by the practical design method proposed by the authors (1988) are also plotted in Fig.9. It can be seen from Fig.9 that the predicted interaction curve for ultimate strengths fits well the experimental results and falls within the safety region. That is to say, the experimental results show the validity of the practical design method. It can also be observed from Fig.9 that the influence of the type of stiffener cross-section upon the ultimate strength is small.

Table 4 Experimental Ultimate Strength

Specimens	Transverse ultimate stress σ_{ym}/σ_Y	Longitudinal ultimate stress σ_{xm}/σ_Y
NCO	0.654	0.0
NCT	0.629	0.0
TCO	0.650	- 0.500
TCT	0.584	- 0.500

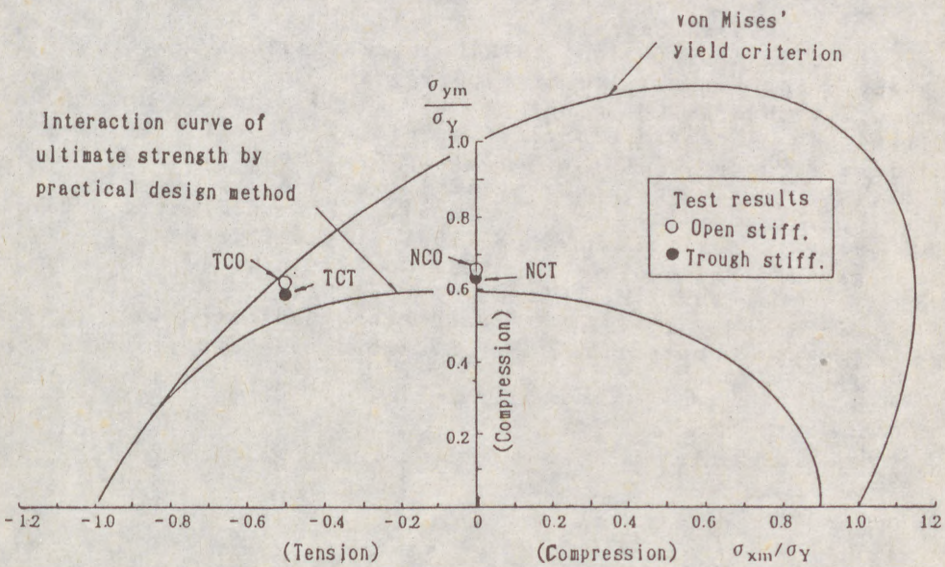

Fig.9 Comparison of Experimental Results with Interaction Curve for Ultimate Strengths by the Practical Design Method

(8)

5. Conclusion

The verification of the practical design method for predicting the ultimate strength of stiffened plates subjected to biaxial in-plane forces, proposed by the authors, is shown through the buckling test of stiffened plate specimens under longitudinal tension and transverse compression.

Acknowledgments

This research was supported by Osaka Third Constructional Division of Hanshin Expressway Highway Public Corporation.

The authors would like to express their gratitude to Mr. Miyasaka and Mr. Nakamoto of Hanshin Expressway Highway Public Corporation for their valuable supports in conducting this research, Mr. Hori and Mr. Takase of Komai-Harumoto Cooperative Fabricator of Kanzaki River Nielsen Lohse Bridge for fabricating the experimental apparatus and test specimens, as well as Mr. Hatano, graduate student of Osaka City University for his help during the experiment.

References

British Standard Institution (1982), BS 5400 Part 3, Code of practice for design of steel bridges.

Furuta, T., Kitada, T. and Nakai, H. (1988), "Ultimate Strength of Stiffened Plates Subjected to Biaxial In-Plane Forces", Proceedings of 1988 Annual Technical Session, Structural Stability Research Council, pp.269-280.

Japanese Road Association (1980), Japanese Specifications for Highway Bridges, Part II, Steel Bridges.

Kitada, T., Nakai, H., Furuta, T. and Suzuki, H. (1988), "Ultimate Strength of Stiffened Plates Subjected to Biaxial In-plane Forces", Journal of Structural Engineering, Japanese Society of Civil Engineers (JSCE), Vol.34A, pp.203-214

Komatsu, S. and Kitada, T. (1980), "Elasto-Plastic Finite Displacement Analysis of Longitudinally Stiffened Plates in Compression", Proceedings of JSCE, No.269, pp.1-12

Taido, Y., Hayashi, H., Kitada, T. and Nakai, H. (1985), "A Design Method of Wide Stiffened Plate Subjected to Uniaxial and Biaxial Compression", Der Stahlbau, 54 Jahrg., Heft 5, S.149-155

(1)
KUTMANOVÁ-KARNÍKOVÁ, Irena (1)
ŠKALOUD, Miroslav (2)
JANUŠ, Karel (3)

"BREATHING" OF THIN WEBS UNDER VARIABLE REPEATED PATCH LOADING

INTERNATIONAL COLLOQUIUM
STABILITY OF STEEL STRUCTURES
BUDAPEST, HUNGARY, 1990
PRELIMINARY REPORT

Summary: The paper describes an experimental investigation, conducted by the authors, into the ultimate load behaviour of slender steel webs subject to variable repeated partial edge loading, the aim being to look into the "breathing" of webs and its effect on the failure mechanism and ultimate limit state of the plate girders tested. On the basis of 80 experiments conducted to date, the authors were able to establish (i) the effect of the cyclic character of the partial edge load upon the initiation and propagation of cracks at the junction of the loaded flange with the breathing web and (ii) a curve of low-cycle fatigue strength for the girders under study.

1. Introductory Remarks

One of the stability problems that attracted plenty of attention over the last years was that of the ultimate load behaviour of thin steel webs subject to partial edge loading. Several years ago, the second author, jointly with V. Křístek and P. Novák, carried out an extensive investigation into the problem (see [Škaloud, Novák, 1975] and [Škaloud, Křístek, 1981]). These studies, representing the first stage of our research on the performance of the plate girders under the action of a patch load, were concerned mainly with the ultimate limit state of webs without longitudinal stiffeners.

(1) D.Sc., Ph.D., C.E., Czech Technical University, Building Research Institute, Prague
(2) Assoc. Prof., D.Sc., Ph.D., C.E., Institute of Theoretical and Applied Mechanics, Czechoslovak Academy of Sciences, Prague
(3) Ph.D., C.E., Czech Technical University, Building Research Institute, Prague

(2)

However, the webs of deep plate girders are often stiffened by longitudinal ribs. Then, of course, the question arises whether the presence of longitudinal stiffening can also favourably influence the behaviour of a web if this is loaded by a patch load, or by such a combination of loading in which the effect of patch loading predominates.

Little information was available in regard to this problem; therefore, the authors decided to contribute to its solution. Desiring to look profoundly into the progression of plastification in the web and the whole girder, and into its effect upon the ultimate limit state, and bearing in mind that a theoretical treatment of such a problem would be very complex and time-consuming, they chose the experimental way of investigation.

The first stage of the research - comprising 152 tests - dealt with the performance of steel webs under the action of a stationary patch load. In conclusion, the authors established formulae for (i) the optimum rigidity of the longitudinal rib and (ii) the predicted ultimate loads of webs subject to partial edge loading and stiffened by a longitudinal rib (see [Škaloud, Kárníková, 1985], [Januš, Kárníková, Škaloud, 1988] and [Kárníková, Škaloud, 1989]).

Three years ago, the second stage of research started, which comprises a campaign of tests on steel webs subject to a variable repeated (cyclic) patch load, the aim being to look into the "breathing" of the webs and its effect on the failure mechanism and ultimate limit state of the plate girders tested. On the basis of 80 experiments conducted to date, the authors were able to establish (i) the effect of the cyclic character of the partial edge load upon the occurrence of cracks at the junction loaded flange/breathing web and (ii) a curve of low-cycle fatigue strength for the plate girders under study. Further experiments are under way.

2. Test Girders

80 test girders subject to variable repeated patch loading have been tested to date, their webs being fitted with a longitudinal stiffener positioned at (i) one-tenth, (ii) one-fifth of the web depth. For comparison, a few girders without stiffening were tested, too.

The test girders had the same dimensions, and were fabricated from the

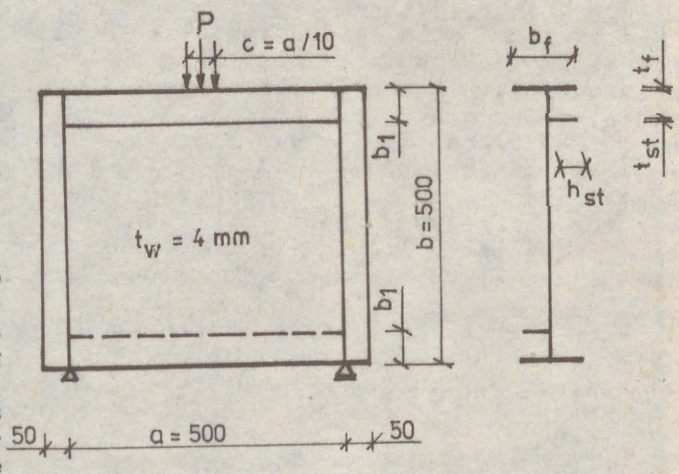

Fig.1: Test girders

(3)
same material, as those used in the stationary patch loading tests, this being so as to enable the authors to compare the results (ultimate loads, onset-of-yielding loads, etc.) of both respective experimental series.

In all experiments, the load length, c, was constant, $c=a/10$. The general details of the test girders can be seen in Fig. 1, their main characteristics are listed in Table 1.

3. Test Set-Up and Experimental Apparatus

The variable repeated loading was materialized by means of a 1000 kN AMSLER pulsator, the frequency of loading cycles being of 3.75 Hz.

The following quantities were registered during the tests:

(i) the initial imperfections of the experimental girders,
(ii) the values of deflections and strains at a number of selected places,
(iii) the initiation and propagation of cracks, and
(iv) the acoustic emission in the web in the neighbourhood of the applied load.

The load P cycled between (i) zero and (ii) a value P_{max}, which in turn was varied between α) the statical ultimate load P^{exp}_{ult} and β) the onset-of-surface yielding load, detected also in the related stationary test. Thus, under the above loading, the webs of the girders tested behaved in the elasto-plastic range and, consequently, their performance was expected to be governed by low-cycle fatigue. Therefore, the basic number of loading cycles was chosen so as to be equal to 5.10^4.

In the case of girders where after 5.10^4 cycles no failure (whether through initiation of cracks or through excessive plastic buckling of the girder web) occurred, the experiment was continued under a higher load level. If, however, a crack appeared in a certain loading cycle, the experiment went on, under the same (i.e. unchanged) load level, as long as the load-carrying capacity of the test girder was exhausted.

The test set-up is seen in Fig.2.

4. Main Results of the Tests

4.1. Failure mechanisms of the girders

The failure mechanism of each test girder was very attentively studied during the experiments. In doing so, the authors concluded that this mechanism was in principle very similar to that they had previously observed in their stationary tests, viz. it consisted of a set of three plastic hinges in the loaded flange and of a segmental line plastic hinge in the adjacent zone of the web sheet.

However, in addition to that, in the case of most cyclic loading tests, the initiation of a crack in the zone immediately adjacent to the applied load was detected. This phenomenon was significantly influenced by the position of the longitudinal rib.

(4)

Table 1: The Main Charakteristics of Test Girders

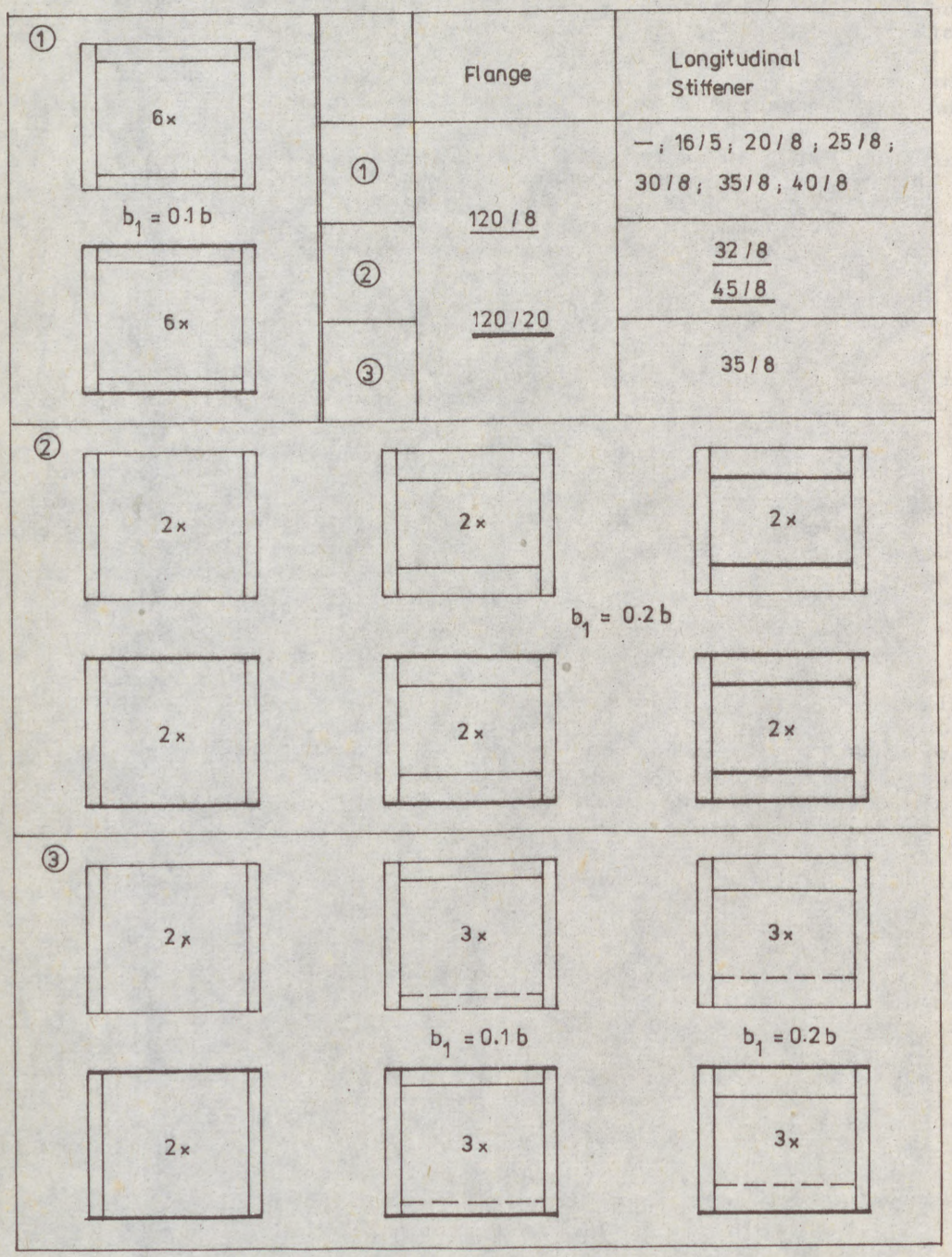

	Flange	Longitudinal Stiffener
①	120 / 8	—; 16/5; 20/8; 25/8; 30/8; 35/8; 40/8
②	120/20	32/8 45/8
③		35/8

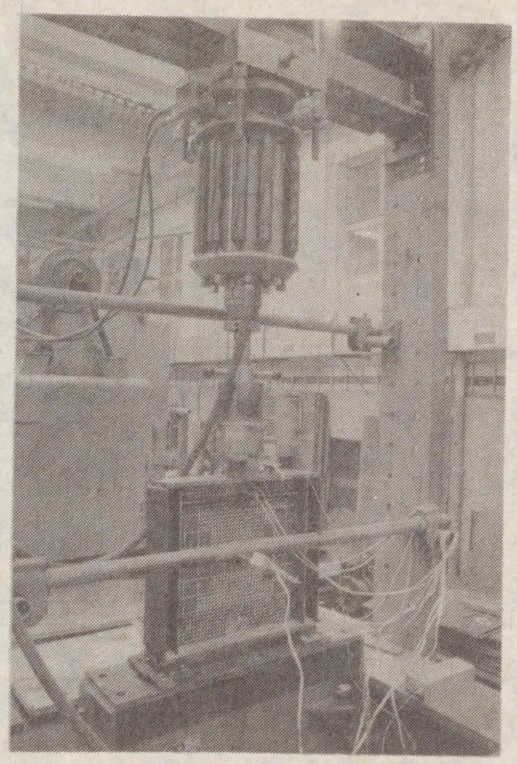

Fig.2: Test set-up

With girders having a rib at the distance $b_1=0.1b$ from the loaded flange, such a crack appeared (with the exception of two tests) as late as the girder was collapsing, the crack initiating in the web sheet either in the segmental line hinge or close to the weld underneath the loaded flange. In the case of some girders, no crack developed at the collapse of the girder.

Conversely, with girders having a stiffener at $b_1=0.2b$, a crack practically always (i.e., barring one case) initiated close to the weld, and the test girder concerned was able to sustain thereafter even a high number (of the order of 10^5) of loading cycles before its load-bearing capacity was exhausted.

A typical failure mode of test girders, with a crack underneath the weld connecting the web with the loaded flange, is seen in Fig. 3.

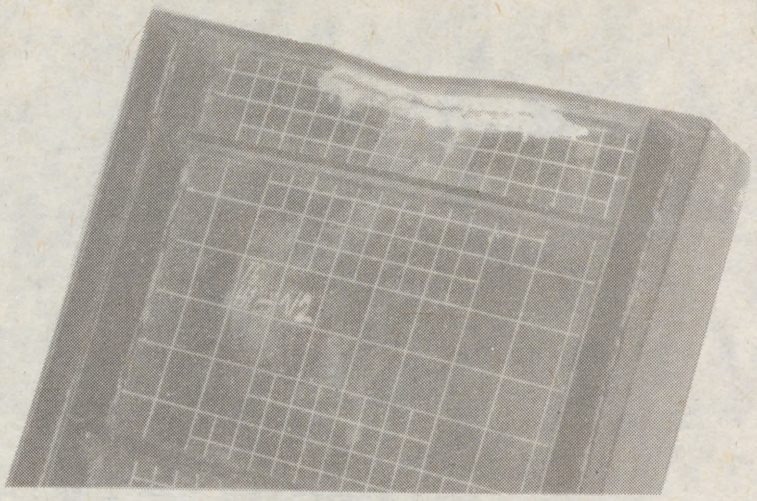

Fig.3: Failure mechanism with a crack

4.2. The magnitude of load versus the number of loading cycles

On the basis of the tests conducted to date, low-cycle fatigue curves were plotted, and a maximum limit load, P^{exp}_{fat}, was determined such that under this load no failure of the girders occurred in the course of the 5.10^4 loading cycles applied.

The main data obtained are listed in Fig. 4, where - in dependence on the placing of the longitudinal rib and the size of the loaded flange - the following quantities are given for all girders tested:

a) the experimental (resulting from stationary tests) ultimate loads, P^{exp}_{ult}, the onset-of-surface-yielding loads, P^{su} (the black portion of the columns), and the loads $P^{me}_{3\varepsilon}$, which is related to unitary deformation equal to three times the strains corresponding to the onset of membrane plastification (the dash portions of the columns),
b) the low-cycle fatigue limit loads, P^{exp}_{fat}, resulting from cyclic load tests.

5. Conclusions

Summing up all information obtained during their tests on girders under the action of a repeated partial edge load, in the course of which the "breathing" of the girder webs and the cumulation of damage in the webs and the whole girders was studied, the authors have concluded that the ultimate limit state of webs under the aforesaid loading conditions can safety be defined (until further evidence makes it possible to employ a less strict definition) on the basis of the onset of surface plastification.

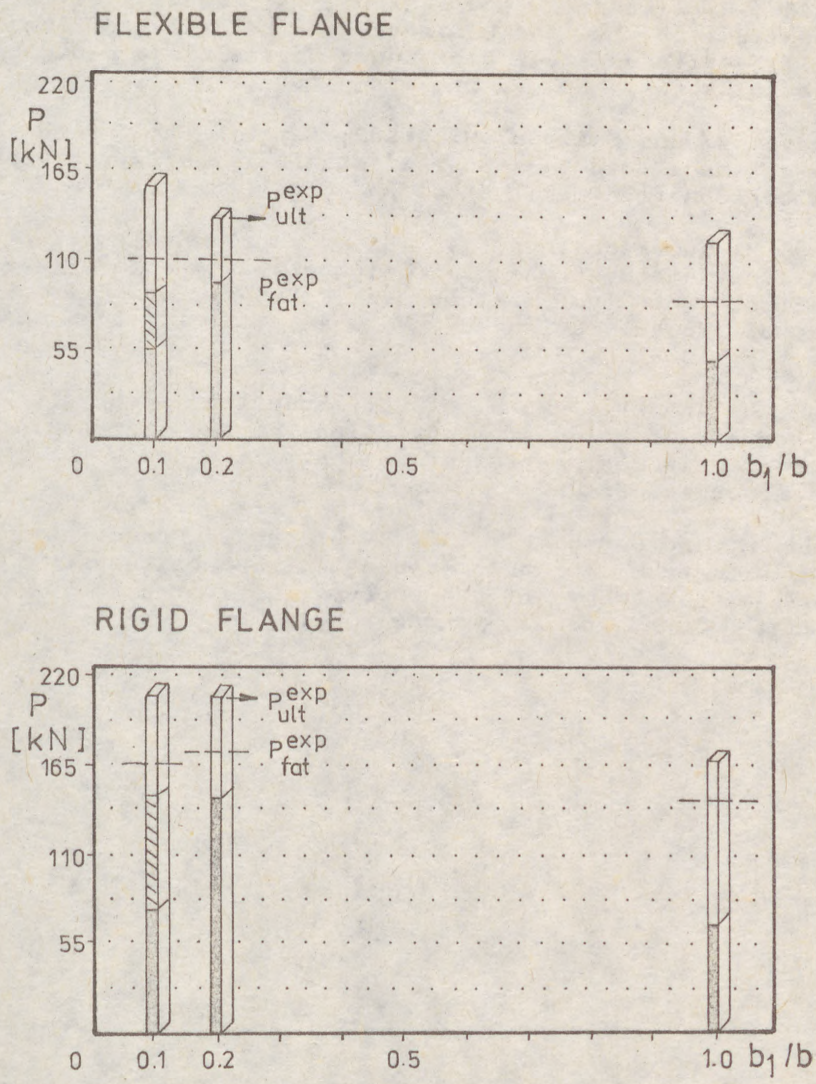

Fig. 4: Main data obtained

Moreover, the experiments have confirmed (see Fig. 4) that the optimum position of the longitudinal stiffener is at 0.2 web depth (measured from the loaded flange), since for other stiffener positions a marked decrease in the onset-of-surface yielding load occurs.

(8)

5. References

[1] Januš, K., Kárníková, I. and Škaloud, M.; 1988: Experimental investigation into the ultimate load behaviour of longitudinally stiffened steel webs under partial edge loading. Acta technica ČSAV, No. 2, pp. 158 - 195.

[2] Kárníková, I. and Škaloud, M.; 1989: Experimental research on the ultimate load behaviour of steel plated structures. Journal of Constructional Steel Research, Vol. 12, No. 1.

[3] Škaloud, M. and Kárníková, I.; 1985: Experimental research on the limit state of the plate elements of steel bridges. Transactions of the Czechoslovak Academy of Sciences, Series of Techn. Sciences, Vol. 95, No. 1, Academia, Prague, pp. 123-139.

[4] Škaloud, M. and Křístek, V.; 1981: Stability problems of steel box girder bridges. Transactions of the Czechoslovak Academy of Sciences, Series of Techn. Sciences, Vol. 91, No. 1, Academia, Prague.

[5] Škaloud, M. and Novák, P.; 1975: Post-buckled behaviour of webs under partial edge loading. Transactions of the Czechoslovak Academy of Sciences, Series of Techn. Sciences, Vol. 85, No. 3, Academia, Prague.

(1)
MACHÁČEK, Josef (1)

STRENGTH OF STIFFENED PLATING UNDER COMPRESSION

INTERNATIONAL COLLOQUIUM
STABILITY OF STEEL STRUCTURES
BUDAPEST, HUNGARY, 1990
PRELIMINARY REPORT

Summary: Results of large parametric studies of compression plates with longitudinal stiffeners are presented. The results are based on large deflection elasto-plastic analysis of more than 200 plates and allow for internationally recommended initial deflections and residual strains due to welding. Effects of initial deflection modes, longitudinal continuity, material properties and number of stiffeners are described. Elastic and elasto-plastic strengths are defined and simple analytical expressions are suggested to determine the appropriate strength for an arbitrary set of geometrical data, grade of steel and welding residual strain level within chosen intervals.

I. Introduction.

Two conceptions for dealing with stiffened compression plates are currently employed in design practice |1|. First it is the "conception of rigid stiffeners", where stiffeners of rigidity $m \cdot \gamma^*$ are introduced to calculate strength of the stiffened plate from strength of panels between stiffeners, and second the "conception of non-rigid stiffeners", where strut |2|-|8|, orthotropic plate |9|-|13|, or discretely stiffened plate approaches are used to analyse the behaviour and strength of stiffened plates.

As mentioned in |14|, the strut or orthotropic approaches cannot provide a rigorous basis for representing the actual inelastic behaviour of all the components of a stiffened plate. The full inelastic analysis, using a discretely stiffened plate approach, is the only way to deal correctly with the problem |15|-|18|. Such approach, based on principles given by Basu et al. |19|, is used in this paper.

II. Theory.

The three-dimensional problem of stiffened plating, Fig. 1, is reduced to two-dimensional isotropic plate subject to external loading and interactive forces simulating the effect of stiffening, and one-dimensional stiffener, Fig. 2.

Simplified version in comparison with |18|,|19| was used, neglecting the torsional and lateral flexural rigidities of stiffeners, thus leaving interactive forces F_x and F_z only. However, as shown in |20|, for the stiffeners with open cross-sections is this simplification justified and, in case of differences, should give slightly conservative results.

(1) research fellow, MSC, PhD, Faculty of Civil Engineering,
Czech Technical University in Prague, Czechoslovakia

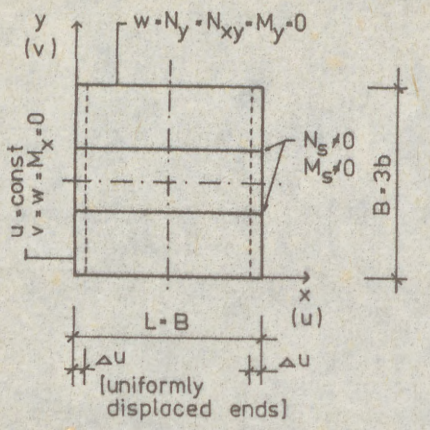

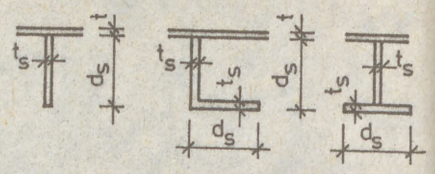

Fig. 1. Stiffened plate geometry and stiffener cross-sections considered.

To exclude local stiffener web or flange instabilities, lateral torsional buckling and premature plasticity by tripping, suitable plate depth-to-thickness ratios, i.e. $d_s/t_s = 10$ ("compact sections") were suggested in accordance with experimental and other results |20|.

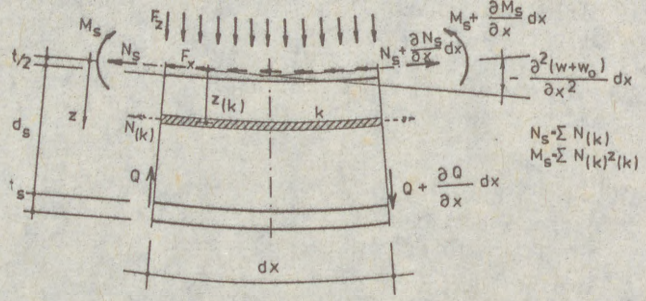

Fig. 2. Interacting and internal forces acting on a deformed element of a stiffener.

Theoretical formulation and numerical solution are described in |20|, |21|. Isotropic plate subject to above given loading is solved according to the Saint-Venant (von Karman) equilibrium equations, modified by Marguerre to include initial out-of-flatness. The elasto-plastic behaviour is based on incremental "flow" theory, using Crisfield's single layer ("area") approach and Ivanov's approximation of Ilyushin's yield surface for shallow shells |22|. In stiffeners only longitudinal stresses are considered and plasticity in volume elements is treated.

Boundary conditions are shown in Fig. 1. The edge load is supposed to be smeared uniformly to the plate and stiffeners, thus making it possible to vary, with loading history, the position of the neutral axis ($N_s \neq 0$, $M_s \neq 0$) |20|.

Numerical solution uses central finite differences (FD) with rectangular interlacing network (Fig. 3), and dynamic relaxation (DR). Some details of numerical procedures concerning stiffener nodes are given in |20|, |21|, extending |22|.

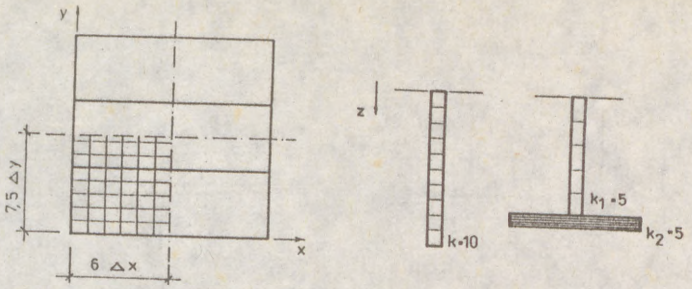

Fig. 3. Optimum principal mesh and stiffener division used for parametric studies.

III. Preliminary and parametric studies.

Comparisons with other theories |17|, |18| and experiment |23| showed excellent agreement (see |20|). As a main result, the average stress-strain curve for each of the stiffened plate studied was obtained, Fig. 4. The following design strengths, suitable for common application in accordance with Czechoslovak Standards (based on Limit State Design), were proposed:

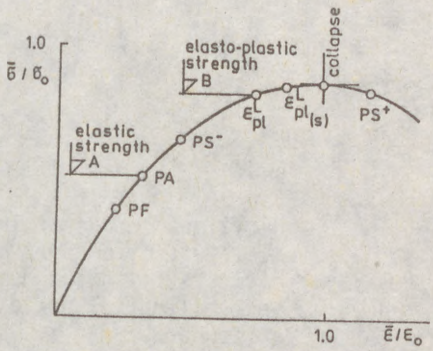

Fig. 4. Characteristic average stress-average strain curve and proposal for determining of the design strengths.

A. Elastic strength - point PA, $PS^{\mp}$ (point PF appears to be too severe)

B. Elasto-plastic strength - point ε^{L}_{pl} or real collapse (whichever is reached sooner).

In the study of initial imperfections |20| internationally recommended amplitudes of deflections were introduced, namely $w^{s}_{o,max} = \pm L/500$ for stiffeners and $w^{l}_{o,max} = \pm b/200$ for panels between them. Residual strains due to welding, if considered, were as shown in Fig. 5. Initial equilibrium accompanied with longitudinal shrinkage or elongation of an initially deflected stiffened plates was solved, keeping amplitudes of stiffeners and panels within 3 % and 10 % of their prescribed values. 8 probable modes of initial deflections - formed from half-sine waves - were studied for two plate geometries (both residual strain free or residually strained) and resulting "critical" ones (giving the least strengths) are shown in Fig. 6.

Following experimental measurements, for flats and rolled angle-sections the "positive" initial bow of stiffeners may usually be supposed. The critical modes from |20| are $2a^{+}$ or 3^{+}. For welded T sections, however, the "negative" initial bow of stiffeners must be considered next to "positive" ones and mode $2b^{-}$ usually is the "critical" one.

(4)

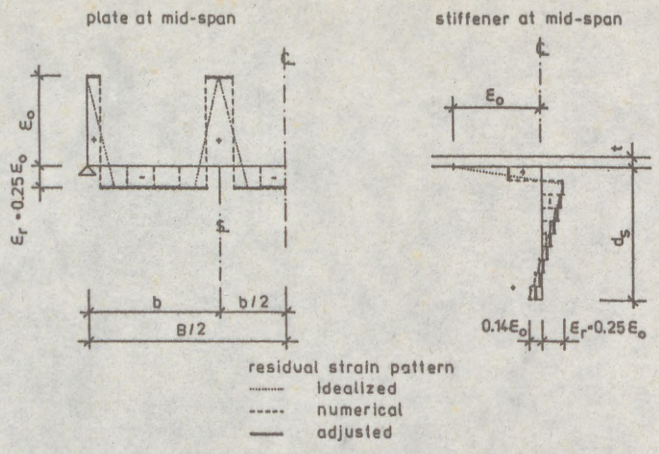

Fig. 5. Welding residual strains used in parametric studies.

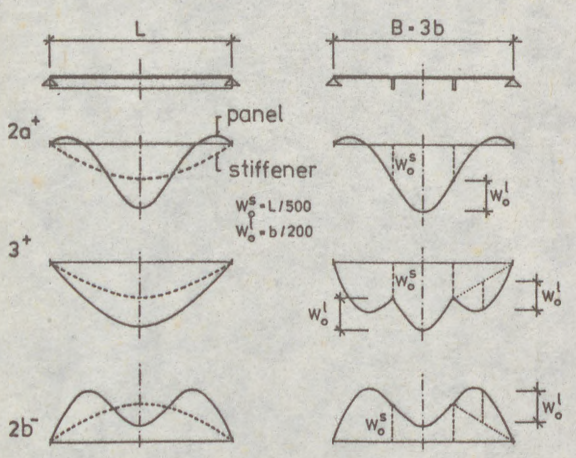

Fig. 6.
"Critical" modes of initial deflection for "positive" (+) and "negative" (-) initial bow of stiffeners.

The effect of continuity of stiffened plates over several spans (between cross-frames) was studied in |21|. Several modes of stiffener initial deflections was fully investigated for two plate geometries, Fig. 7. It was concluded, that strength of continuous plates with prevalent "positive" bays (1^{+-+}, 1^{+++}, 1^{+}) may be found from "positive" single-span analysis and that of prevalent "negative" bays (1^{-+-}, 1^{-}) from "negative" single-span analysis. Since possible decrease in the strength of the continuous plate with prevalent "negative" bays in comparison with the result of single-span analysis was found, the latter analysis with $w_{o,max}^s = -\ L/500$ corresponds to continuous plate with lower "negative" amplitudes. More details concerning influence of initial deflections and residual strains may be found in |20|, |21|.

A limited study was undertaken to show the influence of material properties. The non-dimensional stiffener and panel slendernesses α, β were proved to be the ones that govern the behaviour |24|.

The large parametric study of single-span plates stiffened by 2 flats or T-section stiffeners (according to Fig. 1, with $L = B$) was carried out

(5)

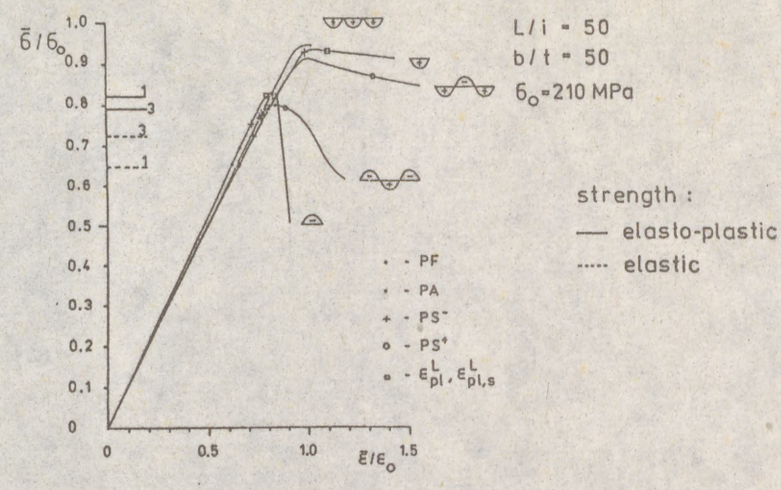

Fig. 7. Average stress-average strain curves for single and three-bay residual strain free stiffened plates.

for the above mentioned initial deflections $2a^+$, 3^+, $2b^-$ and 2 levels of residual strains ($\varepsilon_r = 0$, $\varepsilon_r = 0.25\varepsilon_o$, Fig.5). The full set of stress--strain curves covering intervals $\alpha\ \varepsilon \langle 0.95 ; 3.16 \rangle$, $\Omega\ \varepsilon \langle 0.95 ; 2.53 \rangle$, may be found in |25|, (see Fig. 8).

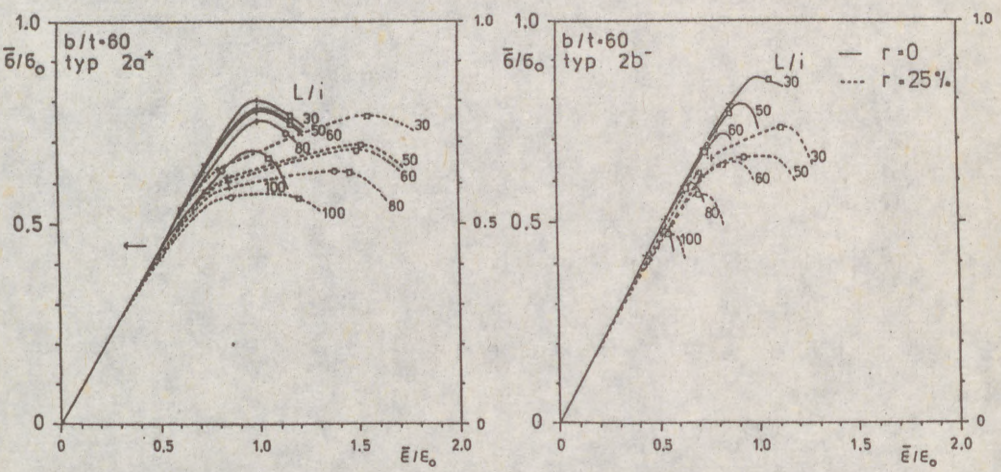

Fig. 8. Example of results of parametric study , σ_o = 210 MPa.

After evaluating elastic and elasto-plastic strengths of all these charts the extremes for "positive" initial deflections of stiffeners (group $2a^+$, 3^+) and for arbitrary sign of stiffener amplitudes (group $2a^+$, 3^+, $2b^-$) were found, Fig. 9.

Analytical formulas for both strengths were formulated, approximating the extremes within 3 % (in the given intervals) or on safe side |24|.Another study showed, that the results for elasto-plastic strengths are valid at least for plates with aspect ratio $B/L \geq 0.4$ (otherwise may be slightly conservative) :

(6)

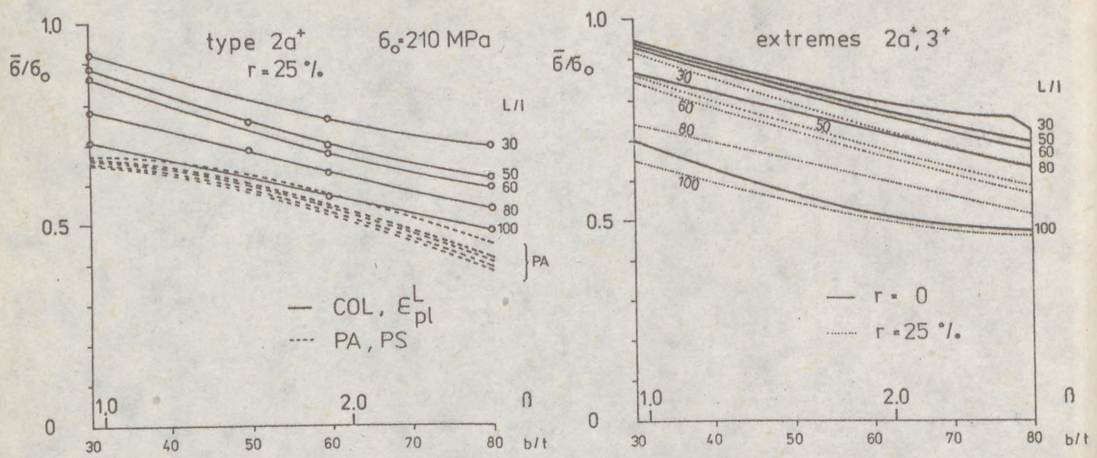

Fig. 9. Elastic and elasto-plastic strengths for mode $2a^+$ (in the left) and extremes of elasto-plastic strengths for "positive" amplitudes of stiffeners (in the right).

"Positive" amplitudes of stiffeners (group $2a^+$, 3^+) - flats, rolled stiffeners:

elastic strength:

(1) $\psi^{el}_{(o)} = 0.595 - 0.051(\alpha - 1.9) - 0.032(\alpha - 1.9)^2 - |0.044 + 0.021(\alpha - 1.9) + 0.015(\alpha - 1.9)^2|(n - 1.9)$

(2) $\psi^{el}_{(25)} = 0.5 - 0.046(\alpha - 1.9) - |0.165 - 0.008(\alpha - 1.9) - 0.03(\alpha - 1.9)^2|(n - 1.9)$

elasto-plastic strength:

(3) $\psi^{pl}_{(o)} = 0.77 - 0.101(\alpha - 1.9) - 0.066(\alpha - 1.9)^2 - |0.15 - 0.006(\alpha - 1.9)|(n - 1.9)$

(4) $\psi^{pl}_{(25)} = 0.67 - 0.097(\alpha - 1.9) - 0.018(\alpha - 1.9)^2 - |0.165 - 0.031(\alpha - 1.9) - 0.011(\alpha - 1.9)^2|(n - 1.9)$

Arbitrary amplitudes of stiffeners (group $2a^+$, 3^+, $2b^-$) - welded stiffeners:

elastic strength:

(5) $\psi^{el}_{(o)} = 0.585 - 0.072(\alpha - 1.9) - 0.043(\alpha - 1.9)^2 - |0.032 - 0.006(\alpha - 1.9)|(n - 1.9)$

(6) $\psi^{el}_{(25)} = 0.485 - 0.061(\alpha - 1.9) - |0.145 - 0.033(\alpha - 1.9) - 0.041(\alpha - 1.9)^2|(n - 1.9)$

elasto-plastic strength:

(7) $\psi^{pl}_{(o)} = 0.684 - 0.131(\alpha - 1.9) - 0.023(\alpha - 1.9)^2 - |0.09 - 0.062(\alpha - 1.9) + 0.025(\alpha - 1.9)^2|(n - 1.9)$

(8) $\psi^{pl}_{(25)} = 0.625 - 0.11(\alpha - 1.9) - |0.1 - 0.037(\alpha - 1.9)|(n - 1.9)$

(7)

If other compressive residual strain level is to be considered, linear interpolation within interval $r \in \langle 0 ; 25 \rangle$ may be used:

$$(9) \qquad \Psi_{(r)} = \Psi_{(0)} + (\Psi_{(25)} - \Psi_{(0)}) \cdot r/25$$

The beneficial influence of a plate behaviour is, however, lost in plates stiffened by 4 and more stiffeners. Results of another study |24| led to reducible coefficients K for such plates:

$$(10) \qquad \Psi_{(4 \text{ and more stiffeners})} = K \cdot \Psi_{(2 \text{ stiffeners})}$$

Coefficients proved to be α, β and sign of the stiffener amplitude dependent:

"positive" amplitudes (group $2a^+$, 3^+) - flats, rolled stiffeners:

$$(11) \qquad K = 0.98 - 0.046(\alpha - 1.9) - 0.046(\alpha - 1.9)^2 + |-0.035 + 0.052(\alpha - 1.9) + 0.073(\alpha - 1.9)^2|(\beta - 1.9) \leq 1$$

arbitrary amplitudes (group $2a^+$, 3^+, $2b^-$) - welded stiffeners:

$$(12) \qquad K = 0.96 - 0.043(\alpha - 1.9) + |0.042 + 0.044(\alpha - 1.9)|(\beta - 1.9) \leq 1$$

The resulting strengths were compared with existing formulas and charts given by Czechoslovak (strut approach) and American (second-order inelastic analysis) Standards. The formula (4) gives good agreement with values of both Standards. However, the unsufficiency of these regulations is clearly seen from the limited entry data regardless of the level and mode of initial imperfections |24|.

Author has the pleasure to inform the readers about the full analytical evaluation of numerical results presented in |26|. The simple formulas, given in |27|, cover isolated isotropic compression plates and flanges of box girders under various loading. The formulas of elastic and elasto-plastic strengths , based on amplitude of initial deflection b/200, are residual strain dependent for interval $r \in \langle 0 ; 25 \rangle$.

IV. Notation.

γ^* - optimum value of relative flexural rigidity of a stiffener (linear buckling theory)

m - factor ensuring sufficient rigidity of stiffeners up to collapse

N_s, M_s - stiffener axial resultant and moment with respect to plate mid-plane

σ_o, ε_o - yield stress, yield strain

$\bar{\sigma}$ - average of longitudinal stresses over plate cross-section (including stiffeners)

$\bar{\varepsilon}_L$ - applied edge strain

$\varepsilon^L_{pl}, \varepsilon^L_{pl_s}$ - plane plastic strain limit or stiffener uniaxial plastic strain limit (=0.002)

$\alpha = L/i \cdot \sqrt{\sigma_o/E}$ - non-dimensional stiffener slenderness

$\beta = b/t \cdot \sqrt{\sigma_o/E}$ - non-dimensional panel slenderness

i - radius of gyration of stiffener cross-section with panel of width b

r - compressive residual strain level |%|

$\Psi_{(r)} = \bar{\sigma}/\sigma_o \ (r)$ - "buckling coefficient" of a stiffened plate with compressive residual strain level r

(8)

Abbreviations:

PF - onset of panel extreme fibre plasticity
PA - onset of panel "area" (single layer) plasticity
PS^-, (PS^+) - onset of stiffener extreme fibre plasticity in compression (tension)
COL - collapse

V. Notation.

|1| Škaloud,M.; 1982: Design of webs and their stiffeners according revised design code ČSN 73 6205, Staveb.čas., Vol.30, No.10, pp. 749-774

|2| Faltus,F. - Škaloud,M.; 1973: Crashes of steel bridges and instructions resulted of them. Inžen.stavby, Vol. 21, No.2, pp. 49-58

|3| Little, G.H.; 1976: Stiffened steel compression panels - theoretical failure analysis. The Struct.Eng., Vol. 54, No. 12, pp. 489-509

|4| Moolani,F.M. - Dowling,P.J.; 1977: Ultimate load behaviour of stiffened plates in compression. Steel Plated Struct., Crosby Lockwood Staples, London, pp. 51-88

|5| Chatterjee,S. - Dowling,P.J.; 1977: The design of box girder compression flanges. Steel Plated Struct., Crosby Lockwood Staples, London

|6| Carlsen,C.A.; 1980: A parametric study of collapse of stiffened plates in compression. The Struct.Eng., Vol. 58B, No. 2, pp. 33-40

|7| Šertler,H. - Vičan,J.; 1987: Elasto-plastic analysis of behaviour of continuous longitudinal stiffener in compression. Proc.Conf. Bridge Theory and Structures, B.Bystrica, pp. 39-46

|8| Šertler,H.; 1988: Design of longitudinal stiffeners of wide flanges. Inžen.stavby, Vol. 36, No. 2, pp. 96-100

|9| Massonnett,Ch. - Maquoi,R.; 1973: New theory and tests on the ultimate strength of stiffened box girders. Proc.Int.Conf. Steel Box Girder Bridges, Imperial College London, pp. 131-143

|10| Baláž,I. - Djubek,J.; 1982: Load-carrying capacity of stiffened compression flanges according to revised ČSN 73 6205 draft. Staveb.čas., Vol. 30, No. 10, pp. 775-797

|11| Baláž,I.; 1986: On the limit state of the stiffened compression flanges of steel bridges. Proc.2nd Reg.Coll. Stability of Steel Struct., Hungary, pp. II/3-12

|12| Jetteur,P.; 1983: A new design method for stiffened compression flanges of box girders. Thin-Walled Structures 1, pp. 189-210

|13| Škaloud,M.; 1985: The effect of shear lag in the light of various definitions of the ultimate limit state of stiffened compression flanges. Thin-Walled Structures 3, pp. 283-292

|14| ECCS, TWG 8.3 -Plated Structures; 1986: Behaviour and design of steel plated structures. ECCS Pub., ed. P.Dubas and E.Gehri, Zürich

|15| Crisfield,M.A.; 1976: Large-deflection elasto-plastic buckling analysis of eccentrically stiffened plates using finite elements. TRRL Rep. No. 725, Crowthorne

|16| Søreide,T.H. - Bergan,P.G. - Moan,T.; 1977: Ultimate collapse behaviour of stiffened plates using alternative finite element formulations. Steel Plated Struct., Crosby Lockwood Staples, London

|17| Djahani,P.; 1977: Large-deflection elasto-plastic analysis of discretely stiffened plates. PhD thesis, Imperial College, London

|18| Webb,S.E. - Dowling,P.J.; 1980: Large-deflection elasto-plastic behaviour of discretely stiffened plates. Proc.Instn.Civ.Engrs, Part 2, 69, pp. 375-401

(9)

|19|

|20|

|21|

|22|

|23|

|24|

|25|

|26|

|27|

|28|

(9)

|19| Basu,A.K. - Djahani,P. - Dowling,P.J.; 1977: Elastic post-buckling behaviour of discretely stiffened plates. Int.Coll. on Stability of Steel Struct., Liege, pp. 433-438

|20| Macháček,J.; 1988: Study on imperfections of stiffened plating. Acta technica ČSAV, Vol. 33, No. 5, pp. 582-605

|21| Macháček, J.; 1989: Effect of longitudinal continuity in steel stiffened compression plating. Acta technica ČSAV, Vol. 34, No. 1, pp. 99-117

|22| Macháček,J.; 1985: Unstiffened plating under in-plane loading. Acta technica ČSAV, Vol. 30, No. 5, pp. 551-574

|23| Komatsu,S. - Nara,S.; 1980: Elasto-plastic analysis of orthogonally stiffened plates with initial imperfections under uniaxial compression. Comp. and Struct., Vol. 11, pp. 429-437

|24| Macháček,J.; 1989: Formulas for strength of steel stiffened plates under compression. Staveb.časopis (in print)

|25| Macháček,J.; 1988: Parametric study and minimum strengths of steel stiffened plates. Staveb.časopis (in print)

|26| Macháček,J.; 1986: Elasto-plastic buckling of unstiffened plates in compression. Proc.Reg.Coll. Stability of Steel Structures, Tihany, Hungary, pp. II/99-107

|27| Macháček,J.; 1988: Design of steel compression plates and flanges. Acta polytechnica, Czech Techn.University, I/1, pp. 31-52

|28| Wolchuk, R.; 1981: Proposed American specification for steel box girder bridges. IABSE Proc., No. 2, P41/81

(1)
PIEKARCZYK,Marek (1)
SIEPAK,Jerzy S. (2)
CHRÓŚCIELEWSKI,Jacek (3)

EXPERIMENTAL AND NUMERICAL ANALYSIS OF THE POST-BUCKLING BEHAVIOUR OF A BOX-GIRDER IN BENDING AND SHEAR

INTERNATIONAL COLLOQUIUM
STABILITY OF STEEL STRUCTURES
BUDAPEST, HUNGARY, 1990
PRELIMINARY REPORT

Summary:The results of an experimental and numerical analysis of the behaviour in bending and shear of a single-cell,narrow-flange,slender-web steel box-girder with diaphragms are presented in the paper.The experimental model was made in a semi-commercial scale.The numerical calculations were based on the finite element method.The influence of large initial deformations of the webs on the post-buckling behaviour of the girder was examined.

1. Introduction

The analytical investigation of the post-buckling behaviour of slender- web steel box-girders under bending and shear is possible thanks to the approximate numerical solutions which take into account an interaction of flanges,webs and stiffenings in the conditions of large elasto-plastic

(1) M.Sc.,C.E.,Postgraduate,Technical University,Cracow
(2) Assist.Prof.,Ph.D.,C.E.,Technical University,Cracow
(3) Ph.D.,C.E.,Technical University, Gdansk

(2)

displacements (Puthli et al. 1978, Chróścielewski et al. 1989). A comparison between the results of a numerical analysis and an experimental study gave satisfactory results in the case of a small-scale model of the slender-web box-girder (Chróścielewski et al. 1989). A verification of this relation for a semi-commercial model was the aim of the work.

2. Experimental model

The experimental model was made of thin, low-carbon steel sheets joined by gas welding. The cross-section of the girder as well as the aspect ratio and the thickness of the diaphragms were chosen in order to guarantee the satisfactory stiffnesses of the flanges and the diaphragms for a tension-field action in the webs. The geometric and material data of the model and the test stand with the instrumentation for the measurement of deflections are presented in Fig.1 and Fig.2. A plexiglass plate with a network of holes was used as a reference line for the dial indicator readings of the perpendicular displacements of the web in one quarter of the girder.

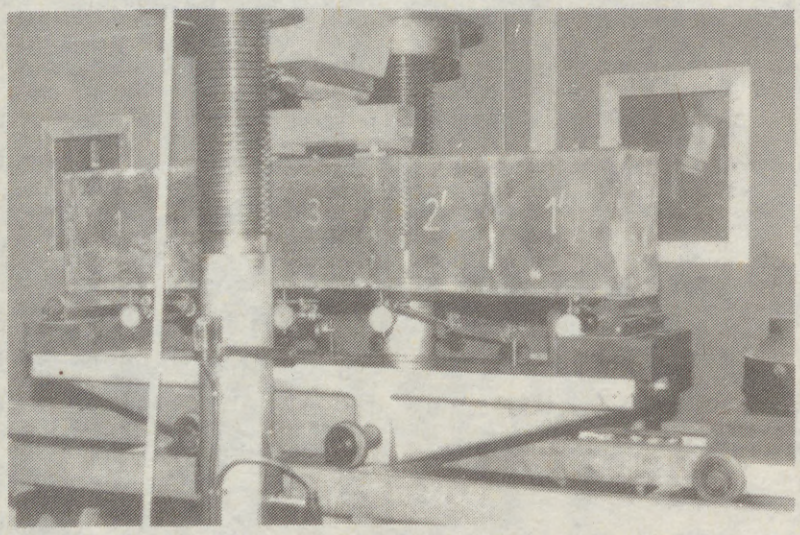

Fig.1

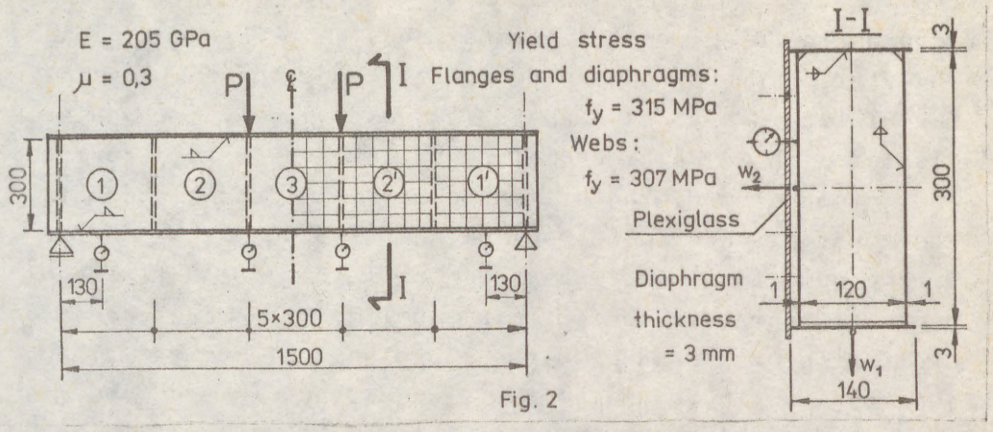

Fig. 2

3. Numerical model

Numerical modelling was carried out according to the assumptions of the program BOX (Chróścielewski et al. 1989). In this

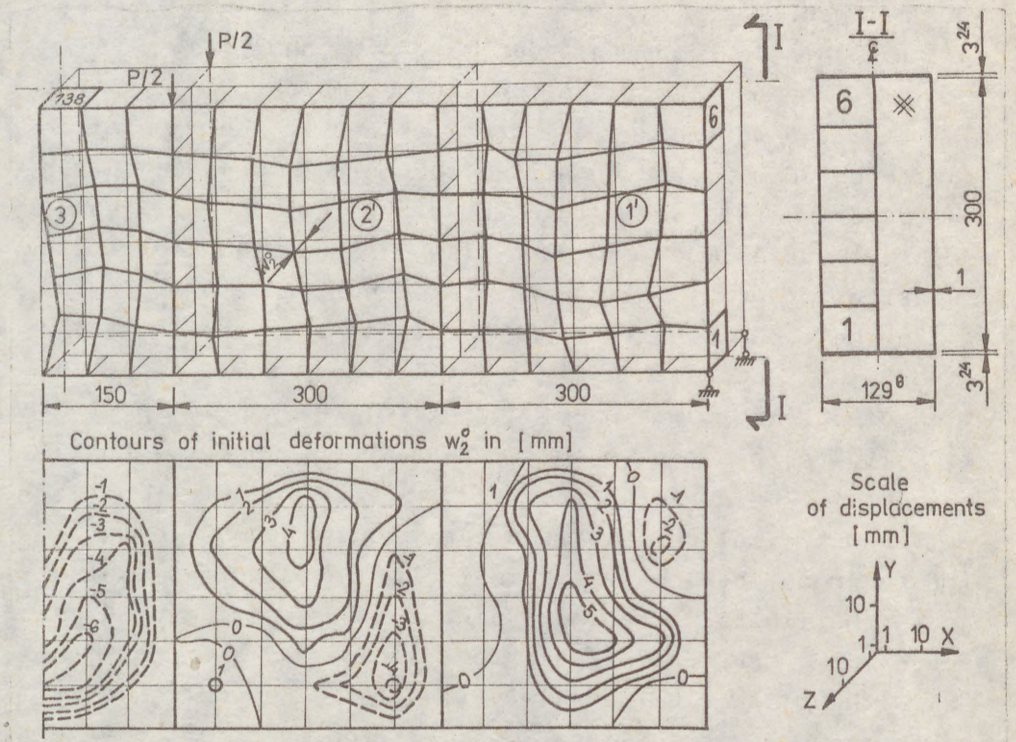

Fig. 3

(4)

program the displacement form of the finite element method, the stationary Lagrangian description and the incremental formulation are adapted and a four-node,plane,rectangular element with 24 degrees-of-freedom is used for digitizing. The integration of the stiffness matrix of the element is done by the Gaussian method in the 3x3x5 scheme.

The numerical model is presented in Fig.3.138 finite elements of geometric and material nonlinearity were used for digitizing with regard to the two planes of symmetry.The junctions at the edges of the flanges,the webs and the diaphragms fulfilled the conditions of a complete stitching.

The dimentions of the cross-section were chosen so as the areas and the slenderness ratios of the flanges and the webs were the same in the numerical model and the experimental one.The ideally elastic-plastic physical model of the body was assumed.

4. Scope and results of the analysis

As a consequence of the applied technology of joining the sheets large initial deformations arised in the webs of the test model Fig.3 . Nevertheless,the authors decided tu run the experiment in order to examine the influence of these deformations on the behaviour of the girder and to test the numerical program for such initial conditions.

In the experiment the observation of the behaviour of the girder,the measurements of its deflections and the registration of perpendicular displacements of the web in the fields 1,2,3(to the plane of symmetry)were conducted for certain values of the loading P.

The numerical calculations were done by use of a IBM PC for the real model with the initial deformations of values as in the fields where the experimental recording of displacements was carried out(solution "a")and for an ideal model without imperfections(solutions "b"). The confrontation of the results of the experiment and the numerical analysis is given in Tabl.1, Fig.4 and Fig.7.

Displacements of the web perpendicular to its plane in the fields 3,2',1', contours in [mm]

Fig. 4

(6)

Tabl.1

P kN	Experiment	Numerical solution "a"
15.0	A jump in the webs 1,1′, a noticeable increase of displacements in 2,2′ towards the diagonal	Elastic behaviour, a little increase of displacements in the web 2′ towards the diagonal, a noticeable change of displacements in 1′.
17.5		First plastifications in the webs.
30.0	Tension fields arise in the webs 1,1′,2,2′.	Propagation of plastic zones in all the webs, in 2′ a tension field comes into being.
40.0	A jump in the panel 1′,1, a tension field action in the webs 1,1′,2,2′, large displacements.	A change in the distribution of plastic zones in all the webs, a distinct tension-field in 2′, an increase of displacements in 1′.
45.0	A delamination of the weld at the top flange--web connection in the panel 1′, a failure of the model.	A tension field action in the webs 1′,2′, further propagation of plastification in the webs.
68.9		Buckling of the compression flange in the panel 3, the boundary of the carrying-capacity.

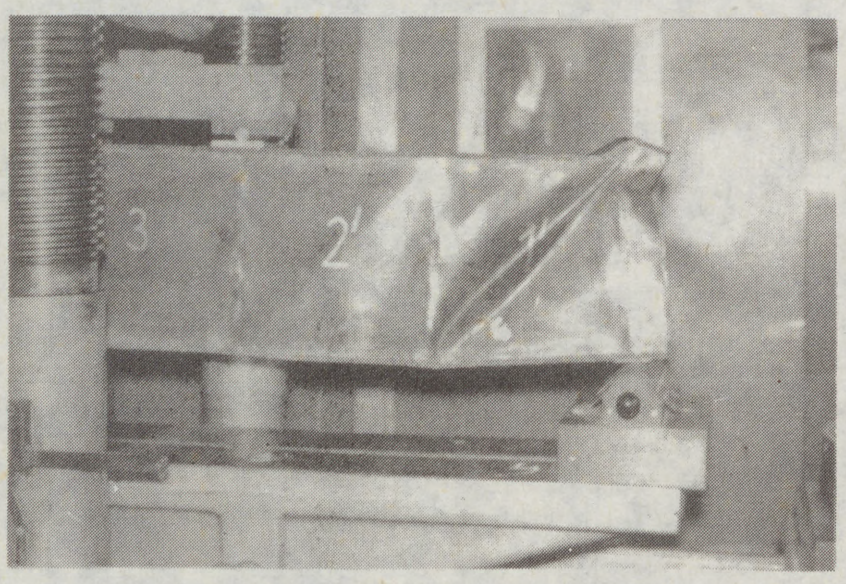

Fig.5

(7)

Numerical solution „b"

P = 40,0 kN

Numerical solution „a"

P = 40,0 kN

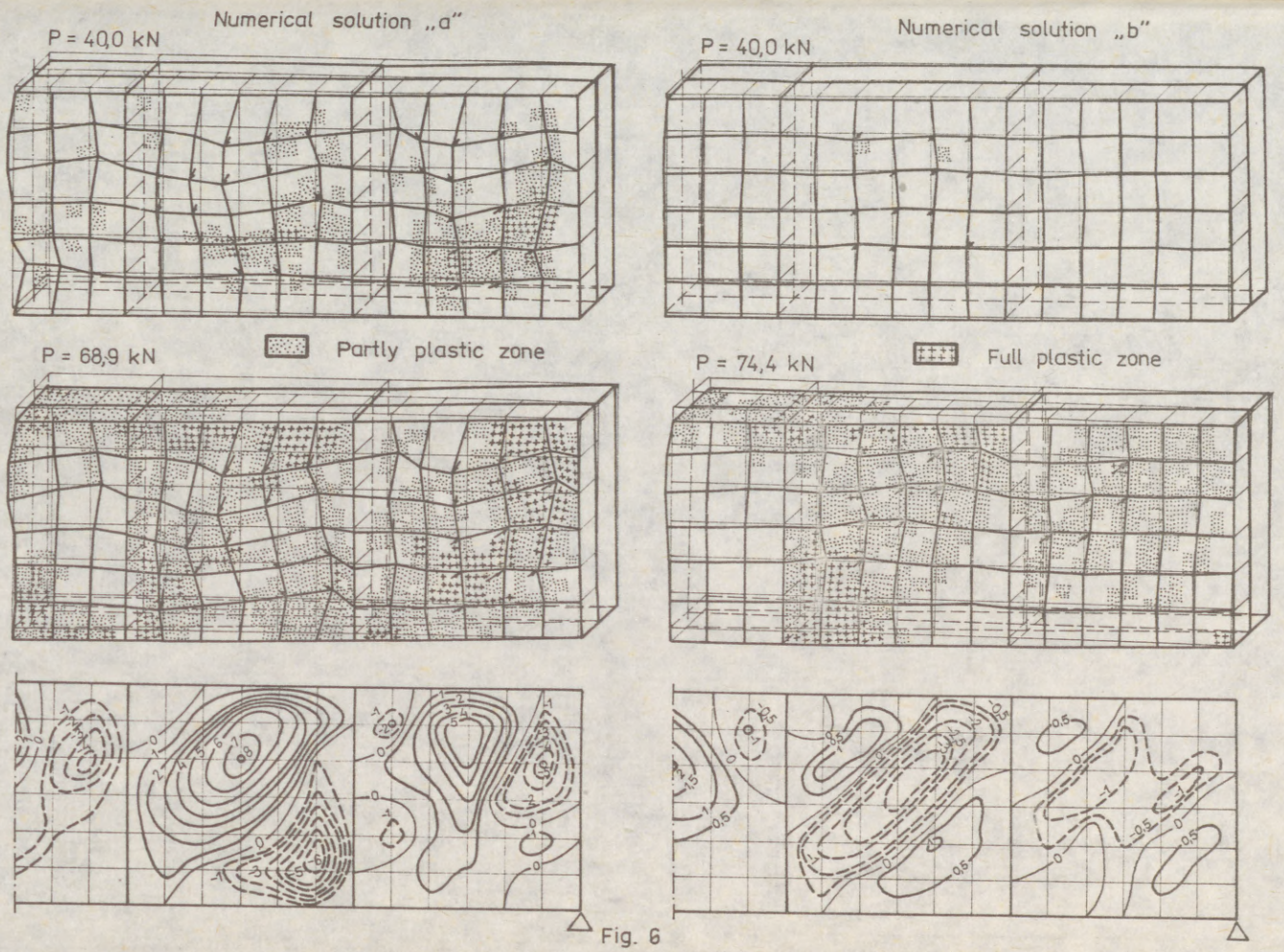
Numerical solution „a"
P = 40,0 kN
Numerical solution „b"
P = 40,0 kN
P = 68,9 kN
Partly plastic zone
P = 74,4 kN
Full plastic zone

Fig. 6

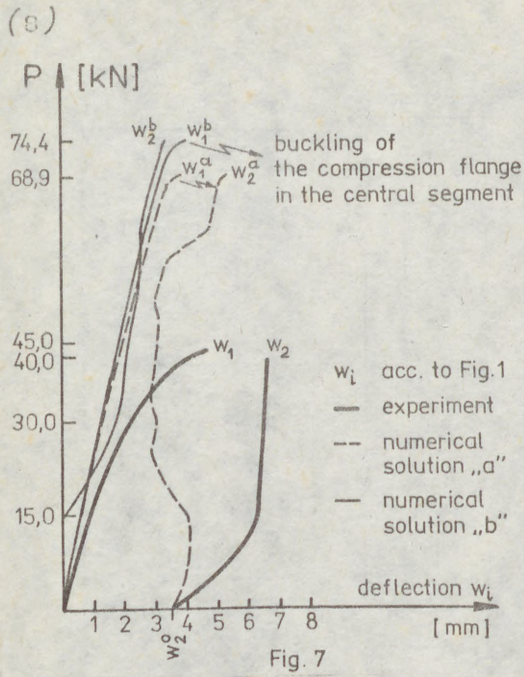

Fig. 7

The mode of failure of the test model is shown in Fig.5. Some chosen phases of the numerical simulations "a" and "b" are presented in Fig.6.

5.Conclusions

The initial deformations of the webs, the sizes of which exceeded allowable values several times had a substantial influence on the behaviour of the girder as it is seen in the P-w_1 diagram(Fig.7). The occurence of jumps and the sooner creation of tension fields was closely connected with the configuration of these deformations.In the presence of the prematurc failure of the experimental model essential quantitative conclusions cannot be formulated.On the other hand the qualitative comparison of the results of the experimental analysis and the numerical one shows a good adequacy particularily in the observed panels 2 and 3.The numerical analysis showed that imperfections in the web,where only pure bending exists and the failure takes place(panel 3),have an influence on the carrying-capacity of the girder.The making of semi-commercial thin-walled models requires the electric welding which will allow to avoid big imperfections.

References:

1. Chróścielewski J.,Piekarczyk M.,Siepak J.S.,1989,Numerical Analysis of the Post-Buckling Behaviour of a Steel Box Girder,Proc.of VIII Int.Sci.Conf.Metal Structures Gdańsk, p.44-52.
2. Puthli R.S.,Supple W.J.,Crisfield M.A.,1978,Collapse Behaviour of Rectangular Steel Box Girders,Structural Engineer,vol.56 B,No4,p.75-84.

(1)
ŠERTLER, Hynek (1)
VIČAN, Josef (2)

DESIGN OF THE COMPRESSED STIFFENED PLATES OF RAILWAY BRIDGES

INTERNATIONAL COLLOQUIUM
STABILITY OF STEEL STRUCTURES
BUDAPEST, HUNGARY, 1990
PRELIMINARY REPORT

Summary: In this paper the simplified check and its theoretical basis of the stiffened compressed plates of railways bridges is described, elaborated in the Departement of Structures and Bridges of the Technical University of Transport and Communications in Žilina (ČSSR). The check has been included in the standard for checking steel railway bridges and calculation of their load-carrying capacity. The check is based on the modified bar simulation analogy. Evolution and successive improvement in this method is described.

(1) Professor of Steel Structures and Bridges DrSc., Technical University of Transport and Communication in Žilina, Czechoslovakia

(2) Assistent-Professor of Steel Structures and Bridges, TUTC in Žilina, Czechoslovakia

(2)

NOTATION

A_L, A_{st}	cross sectional area of a stiffener plate column and cross sectional area of stiffener respectively
$A_{L,ef} = \varrho_n A_L$	effective cross sectional area of a stiffener plate column
A_f	flange area
a	cross frame spacing
α	imperfection factor for column
B	width of compressed flange betwween webs (Fig. 1)
b	distance of longitudinal stiffeners
$e = r_2^2/H$	end excentricity of loading
E	youngs modulus = 210 000 Nmm^{-2}
f, f_o	transverse deflection of column and initial deflection respectively
r	radius of gyration of full plate-stiffener unit
R_d, R_y	design ultimate stress, stress at yield respectively
t_f	plate thickness
z_{L1}, z_{L2}	distance from centroid cross-section to stiffener flange and to mid-thickness of skin plate respectively
z_1	depth from neutral axis of box girder to skin plate mid-thickness (Fig. 1)
$\omega = a/b$	
$\delta = A_{st}/b.t$	
σ_r	residual compressive direct stress in stiffener flan
φ	column buckling factor
$\lambda = a/r$	slanderness ratio
$\bar{\lambda} = (\lambda/93)\ (R_d/210)^{1/2}$	
$\lambda_e = b/t$	
ϱ_n	coefficient which denotes the effect of the local performance of the plate

1. Introduction

Some years, our departement was asked to elaborate a simplified approach, which would be adopted for a design stiffened compressed plate flanges of railway bridges. A few methods were published at that time for highway bridges but their utilisation was questionable. Railway bridges have some specifications in arrangement of their cross section. The total width of flange between webs and number of longitudinal stiffeners is smaller and their arrangement over the cross section is, in a few cases, irregular. The designing procedure, which was accepted by the Czechoslovak Railways [8], respected all specifications for railway bridges. From that time the following research has been carried out in our departement in this field, the method [8] was successfully improved and their modification was included into the new standard for checking railway bridges [4].

2. Design approach

The check recomended in [8] was based on the bar simulation analogy.

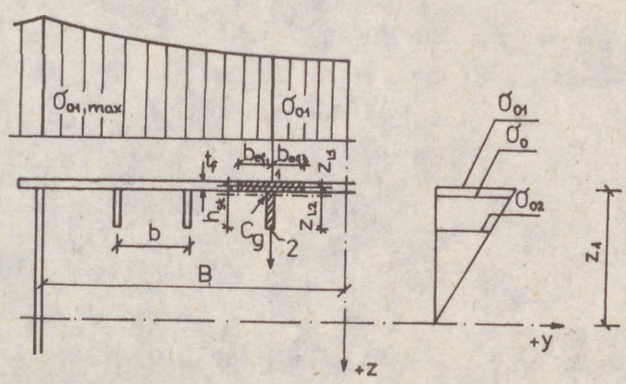

Fig. 1

The design approach recommended in [8] was similar to [1] with respect to the real imperfections of bridges in Czechoslovakia and the specifications of railway bridges. A local performance of the plate was expressed by the reduction of the design ultimate stress using the reduction coefficient ρ_n. This coefficient was estimated from the theory of large deflections. The value of the compressive residual stress $\sigma_r = 0{,}1\ R_y$ and

the initial bow of plate-panel b/200 were taken into account. ϱ_n was later accepted for [4] as an effective with the coeficient b_{ef} of the panel (Fig. 1)

$$b_{ef} = \varrho_n \, b \qquad (1)$$

The flange was investigated as a set of the compressed pin--ended initialy curred columns (Fig. 1) calculated by the theory of the II.-nd order.

The transverse initial deflection of the column can be taken from the measurement by checking old bridges. For design of new bridges f_o = + a/500, - a/750 and in places of welded erection joints $f_o = \pm$ a/300 were recommended. Those values were accepted on the basic of statistical evaluations of measured imperfections [3] .

To elaborate the standard [4] carried out recently in our departement it was necessary to continue in the research work concerning stabily problems of railways bridges.

Some interesting results of this research have been presented here.

3. Evaluation of the buckling factor of the compressed column with nonsymetric cross section

Behaviour of the compressed column with a nonsymetrical cross--section (Fig. 1) is influanced by the direction of deflection. The bending stressed by buckling depend on the distance from the neutral axis. As $z_{L1} << z_{L2}$, the sensitivity to negative imperfections is much greater than to positive ones.

As the variation of z_{L1}/i is in a relatively narrow interval ($z_{L1}/i \in \langle 0.45, 0.7 \rangle$) it was possible to derive φ_{D1} using elasto-plastic approach [5] in which the following was recommended.

Tab. 1

$\bar{\lambda}$	0,2	0,4	0,6	0,8	1	1,2
φ_{D1}	1	0,92	0,81	0,74	0,63	0,5
φ_D	0,98	0,91	0,78	0,62	0,45	0,35

In Tab. 1 φ_D is the buckling factor by [9] .

(5)

For a negative direction of the column the initial deflection $z_{L2}/i \in \langle 2,7 \rangle$ is valid. Simultaneously, as the disperion of measured imperfections [3] is great and as the influence of the residual stresses from welding is negligeable, it was recommeded for [4] to accept the check by [8] .

$$\varphi_{D2} = c - \sqrt{c^2 - 1/\bar{\lambda}^2} \qquad (2)$$

where $c = 0,5\ (1 + \mathfrak{X} + 1/\bar{\lambda}^2)$,

$$\bar{\lambda} = (\lambda/93)\ (R_d/210)^{1/2}$$

The influence of imperfections is expressed by

$$\mathfrak{X} = 8636\ (f/a)\ (z_{L2}/a)\ (210/R_d) \qquad (3)$$

To verify this approach the large experimental investigations have been carried out in which 4 series of T specimens examined and the computer program for numerical solution of the inelastic column problem was made up. The results of the elasto-plastic analysis of the tested spacimens were compared with the experimental results and with the recommended curre φ_{D1}. This comparison for one of the investigated serie is shown in Fig. 2.

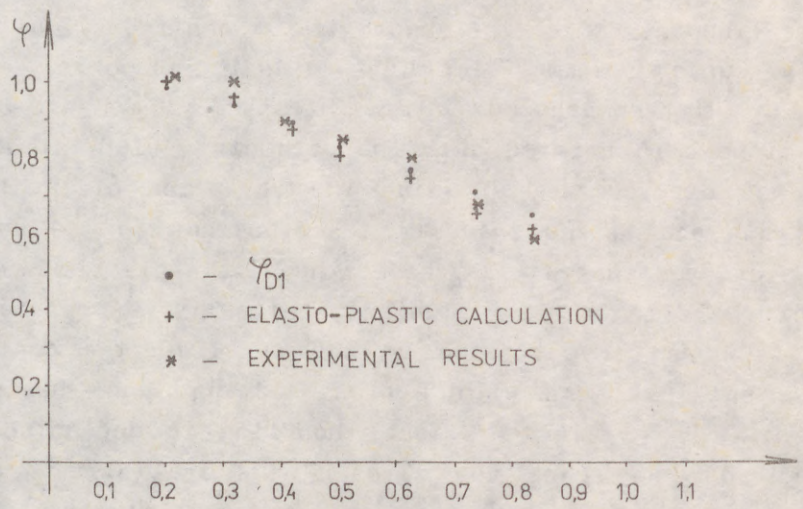

Fig. 2

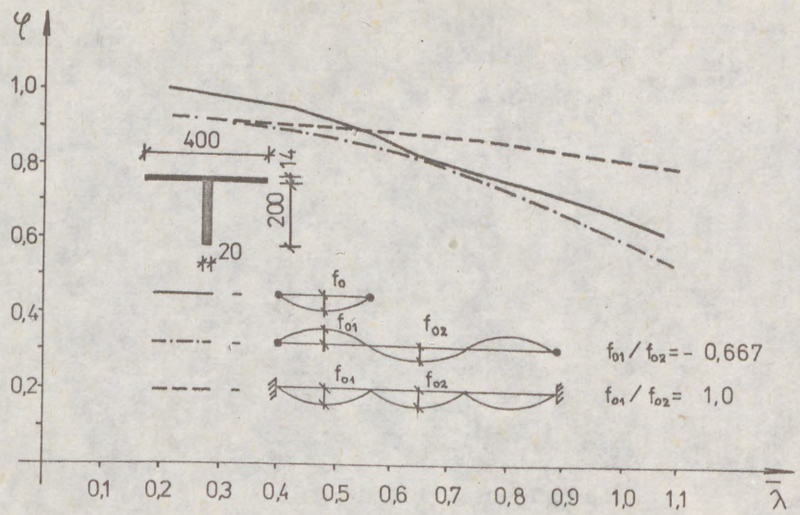

Fig. 3

4. Influence of longitudinal stiffeners continuity over the cross-frames

The mathematical model of the stiffener-plate column for investigation of this influence is a continuos multi-span initialy curved column seated at elastic supports, axially loaded by the compressed force. Elastic and elasto-plastic calculations were carried out. The parametric study in elastic region was carried out in which the variation of an initial bow, axial loading and shape of imperfections in the adjacent spans were investigated [7] . Later the elasto-plastic numerical study of the effect of longitudinal continuity was carried out. This effect was investigated on the model of the continuous stiffener -plate column with T cross-section spans having low b/t (b/t = 28 - effect of local buckling is neglected). The influence of the shape and size of the initial bow of the stiffener on the load-carrying capacity was investigated. The positive initial bow in the middle span was constant at f_{o2} = = + L/500, the negative one had the values f_{o1} = - L/750, and + L/500, this range of out-of-straightness being typical of practical constructions. The results of numerical study are

shown in Fig. 3 together with the corresponding results for a pin-ended stiffener-plate column. The most striking aspect to the results of Fig.3 is the negative effect of continuity as compared with the pin-ended column for the case of the shape of the initial bow with $f_{o1}/f_{o2} = - 0,667$. For the case with the value $f_{o1}/f_{o2} = + 1,0$ the effect of continuity is expressively positive for column slenderness $\bar{\lambda} > 0,5$, for cases of column slenderness $\bar{\lambda} \leqslant 0,5$ the effect of continuity is negative again. The analysis of numerical results has shown that the effect of continuity is negative in those cases, when the collapse of the continuous column is due to the stiffener failure (a compressive yield in the stiffener flange at the midpoint of the first span or at the middle support). It is more striking noticeable at low b/t where the stiffener-plate column is more prone to stiffener failure because z_{L2}/i is high.

5. Mutual collaboration of the single stiffeners by the overal buckling

In narrow railway bridges the influence of the supporting along the longitudinal adges of the plate over the web is great and must be taken into account. Many investigations have been carried out using a large deflection theory of plates. It was found that the influence of redistribution of stresses (overall buckling) in railway bridges is not great and it must be taken into account only in the case of large slendernesses of stiffeners ($\lambda > 60$). In generall, real slendernesses have $\lambda < 60$.
Much greater is the influence of the bending rigitidy of a plate in cross direction in narrow bridges which decreases deflections. This effect can be taken into account when modifying matimatical model as a continuous beam on the elastic foundation.

Conclusions

The simplified approach to the stiffened plates checking recommended for [4] has been presented. The modified bar simulation analogy where the influence of out of straightness, deformations continuity in longitudinal and cross direction and shear lag taken into account, is a suitable to estimate load carrying capacity and redistribution of stresses over the compressed stiffened flange.

(8)

The comparision of the recommended curve φ_{D1} with the results of elasto-plastic calculations and experimental results has proved it to be suitable for practical calculations.

The results of the numerical study of longitudinal continuity of stiffeners indicate a tendency of increasing the load-carrying capacity when a failure occurs in the plate, and of weakening when it occurs in the stiffener.

References

[1] British Standards Institution: 1979, BS 5400: Steel, Concrete and Composite Bridges

[2] Dwight, J.B.-Little, G.H.: 1976, Stiffened steel compresion flanges - a simpler approach. The Structural Engineer, Volume 54, pp. 111-127

[3] Kárniková, I.-Škaloud, M.: 1980, Initial Imperfections of Bottom Flanges of Czechoslovac Brodges. Stavebnícky časopis, n. 8, pp. 235-240

[4] Ministry of Transport and Communications: 1989, ON 73 6232 Checking of Steel Railway Bridges and calculation of their Load Carrying Capacity (In Czech)

[5] Nguyen Tran Thuat-Šertler, H.: 1988, parametric study of the compressed column on the elastic fondation (In Czech). Inženýrské stavby 36 No 6, pp. 299-303

[6] Šertler, H.: 1987, Basic models for calculation of the compressed stiffened flanges of Railway Bridges of an International conference on Traffic effects on Structures, Czechoslovakia, The High Tatras pp. 99-104

[7] Šertler, H.-Nguyen, T.T.: 1985, Parametric study of the stiffeners continuity on the load carrying capacity of the compressed flanges. Inženýrské stavby No 7 Vol. 33, pp. 82-88

[8] Šertler, H. and col.: 1980, Design of compressed flanges of railway bridges (In Czech). Internal publication of the ministry of Transport and Communications Praha No 214

[9] Standards Institutions: 1985, ČSN 73 1401: Design of Steel Bridges

(1)
ŠKALOUD, Miroslav (1)
ZÖRNEROVÁ, Marie (2)

TWO APPROACHES TO THE INTERACTION OF SHEAR LAG WITH PLATE BUCKLING IN LONGITUDINALLY STIFFENED COMPRESSION FLANGES

INTERNATIONAL COLLOQUIUM
STABILITY OF STEEL STRUCTURES
BUDAPEST, HUNGARY, 1990
PRELIMINARY REPORT

Summary: The (i) British and (ii) Liège-Prague approaches to the problem of interaction between shear lag and plate buckling in the longitudinally stiffened compression flanges of steel box girder bridges and similar structures are briefly discussed and their impact on design analysed via a parametric study. The resulting ultimate loods are compared with each other, for a variety of flange geometries, in Figs 5 and 6, and some conclusions for practical design are then drawn.

1. Introduction

The design of the longitudinally stiffened compression flanges of steel box girder bridges and similar structures is governed by the interaction that in such flanges usually occurs between shear lag and flange buckling. The ECCS Technical Working Group "Plated Structures" put forward in /TWG 8/3, 1988/ the following two approaches for the analysis of the problem:

(i) the British approach,
(ii) the Liège-Prague one.

The objective of this contribution is to analyse both approaches, compare them with each other and look into their impact on practical design.

2. The British Approach

This approach, based on a thorough study of the problem carried out recently at the Imperial College of Science and

(1) Head of Department,
(2) Principal Scientific Officer,
Institute of Theoretical and Applied Mechanics, Czechoslovak Academy of Sciences, Prague

(2)
Technology, London, is very simple. It consists in multiplying the flange ultimate loads, $\bar{\sigma}_{ult}$, determined with due regard to flange buckling but regardless of shear lag, by a factor ψ of shear lag effect, which (i) may be taken as unity for $b/L \leq 0.2$ (when L is the girder span in the case of simply supported girders or the distance between points of contraflexure for continuous spans and b is the overal flange width), and (ii) for $b/L > 0.2$ is given by the following equation

$$\psi = \rho_s^{(b/2L)}. \qquad (1)$$

There, ρ_s is the elastic shear lag effective width ratio, which in the British approach is given by another simple formula

$$\rho_s = e^{-\frac{b}{L}(1+\phi\sqrt{\delta})}, \qquad (2)$$

where

$$\delta = \frac{mA_s}{bt}$$

and

$$\phi = 0.6(3.4 - \frac{b}{L}),$$

with A_s being the cross-sectional area of one stiffener without effective width of sheet and m the number of stiffeners.

3. The Liège-Prague Approach

This approach, based on a solution via the theory of large deflections, is more complex. In its context, the analysis is divided into two stages: in the first one, the interaction between global flange buckling and shear lag is dealt with, while in the other stage the solution is modified so as to take also account of local flange sheet buckling between longitudinal ribs. The whole procedure is described in detail in /Jetteur, Maquoi, Škaloud and Zörnerová, 1984 and 1985/ and /Škaloud, Zörnerová, 1984/.

Three definitions of the ultimate limit state are presented in the above papers, each of them reflecting a various degree of plastification of the flange, so that the analysis can then be employed both for ultimate limit state and serviceability limit state considerations. Given the fact that the space available for this contribution is very limited, we can deal here in detail only with one of the definitions, and it is useful for the purpose of our comparative study to choose the strictest among them, in whose context the flange limit state is defined by the following three criteria:

(a) onset of membrane yielding in the flange sheet at the longitudinal edges of the flange,
(b) onset of membrane yielding in the flange sheet in the middle of the flange,
(c_1) onset of yielding at the centroid of the central longitudinel stiffener (i. e., of its stiffening element proper - without any cooperation of the flange sheet).

(3)

It is obvious that the application of criterion (c_1) involves the occurrence of some plastic deformations, at least in part of the most loaded longitudinal rib (and sometimes, even though to a lesser extent, in the neighbouring ribs); therefore, this definition of the limit state is called "quasi-elastic".

The results of the study, summed up in a number of charts, are given (in this paper, only for flanges made of Mild Steel 37, whose yield stress R_y = 240 MPa) in Figs 2 and 3, which can serve as a basis for design. As for the notations used in the figures, R_d is the design strength of the flange material (for Mild Steel 37 : R_d = 210 MPa), σ_{cr} the critical stress of the flange, ϱ_s again the elastic shear lag effective width ratio, and the remaining symbols are defined in Fig. 1.

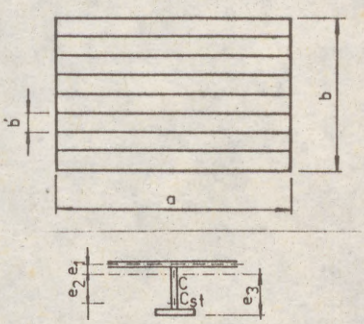

Fig. 1

The quantity $\bar{\sigma}_{ult,s}$, measured on the vertical axis for the corresponding limit state criterion (of course, relevant for design is only the lowest of the values obtained), gives the ultimate load of the compression flange for the case of interaction between global flange buckling and shear lag (i. e., for the first stage of solution), which equals the true flange ultimate load on the condition that the geometry of the flange is such that local sheet buckling between longitudinal stiffeners is no problem. In the event of partial flange sheet panels being more slender and consequently liable to buckle, the above quantity is corrected (in the second stage of solution) so as to allow for the effect of the local sheet buckling. This is achieved by means of introducing the effective widths of the partial sheet panels into the analysis, and the procedure involved is thoroughly described in the aforementioned papers by Jetteur, Maquoi and the authors. However, given the fact that the calculation of the influence of local sheet buckling is in principle the same for both the British and Liège-Prague approaches, we need not include it into our comparative study (this being also necessitated by the very limited scope of this paper) and will focus only on the interaction of global flange buckling with shear lag. The influence of local sheet buckling is included in the second stage of our comparative study, which is currently under way and whose conclusions will be presented in another paper.

4. Parametric Study

In order to be able to numerically compare both approaches with each other and to ascertain their impact on the design of longitudinally stiffened compression flanges, the writers analysed - using both approaches - the limit state of a number of longitudinally stiffened flange panels (see Table 1 and Fig. 4, the panels are assumed to be fabricated from Mild Steel

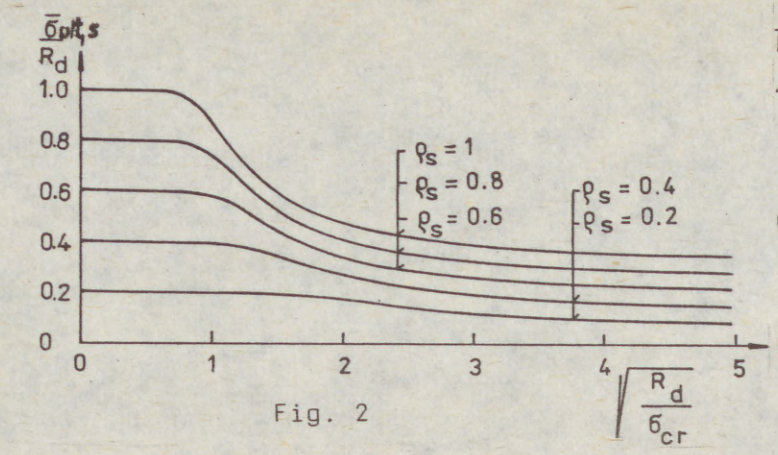

Fig. 2

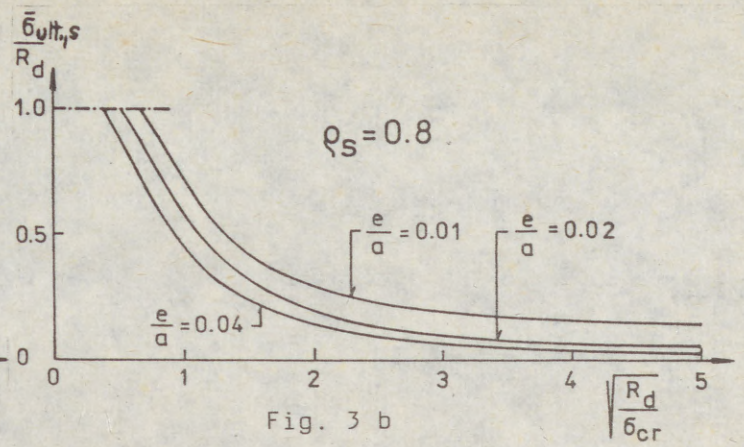

Fig. 3 b

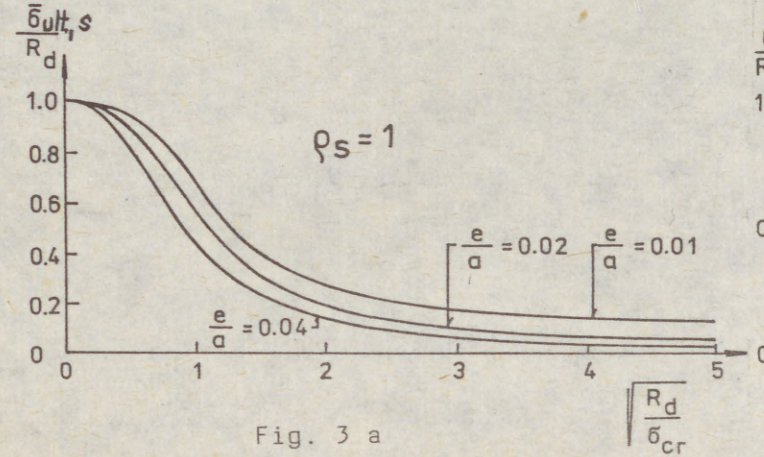

Fig. 3 a

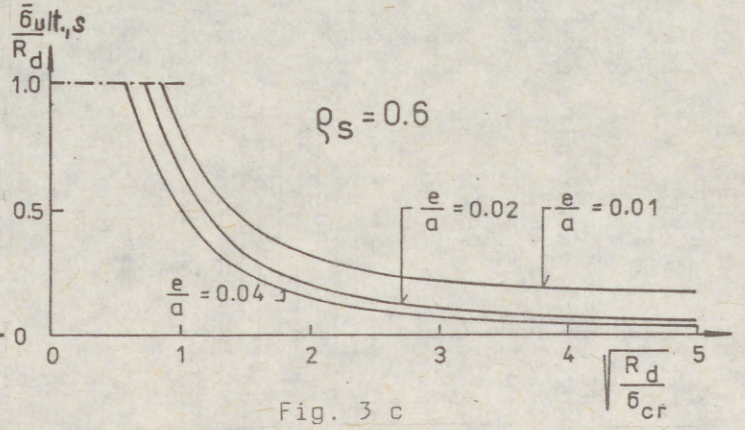

Fig. 3 c

(5)

Table 1

Stiffener cross-section		t = 10 mm				t = 15 mm			
		α = 0.5		α = 1		α = 0.5		α = 1	
		8 ribs	4 ribs	8 ribs	4 ribs	8 ribs	4 ribs	8 ribs	4 ribs
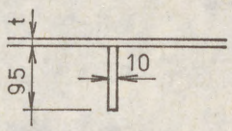	σ	3.67	6.62	3.68 •	6.62	1.09	1.96	1.09 •	1.96
	σ^*	9.94	5.54	39.69	21.91	9.63	5.34	38.42	21.02
	$\frac{\sigma}{\sigma^*}$	0.37	1.2	0.09	0.30	0.11	0.36	0.03	0.09
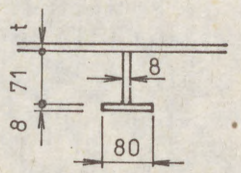	σ	5.37	9.67	5.37 •	9.67	1.59	2.87	1.59 •	2.87
	σ^*	10.21	5.66	40.72	22.48	9.80	5.43	39.11	21.58
	$\frac{\sigma}{\sigma^*}$	0.53	1.71	0.13	0.43	0.16	0.53	0.04	0.13
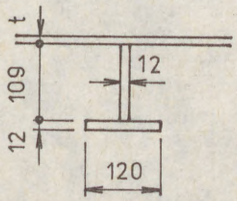	σ	21.27 •	38.28 •	21.27	38.28 •	6.30 •	11.34 •	6.30	11.34
	σ^*	11.74	6.51	46.88	25.91	10.82	6.00	43.22	23.87
	$\frac{\sigma}{\sigma^*}$	1.81	5.87	0.45	1.47	0.58	1.89	0.15	0.48
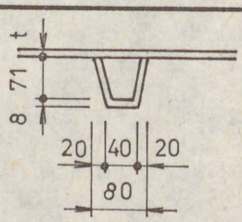	σ	4.65	8.36	4.65 •	8.36	1.38	2.48	1.38 •	2.48
	σ^*	10.45	5.80	41.71	23.03	9.96	5.53	39.77	21.95
	$\frac{\sigma}{\sigma^*}$	0.46	1.44	0.11	0.36	0.14	0.45	0.03	0.11
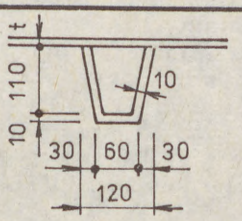	σ	17.35 •	31.24 •	17.35 •	31.24	5.14	9.26 •	5.14	9.26
	σ^*	11.79	6.54	47.09	26.02	10.86	6.02	43.35	23.94
	$\frac{\sigma}{\sigma^*}$	1.47	4.77	0.37	1.2	0.47	1.54	0.12	0.39

(6)

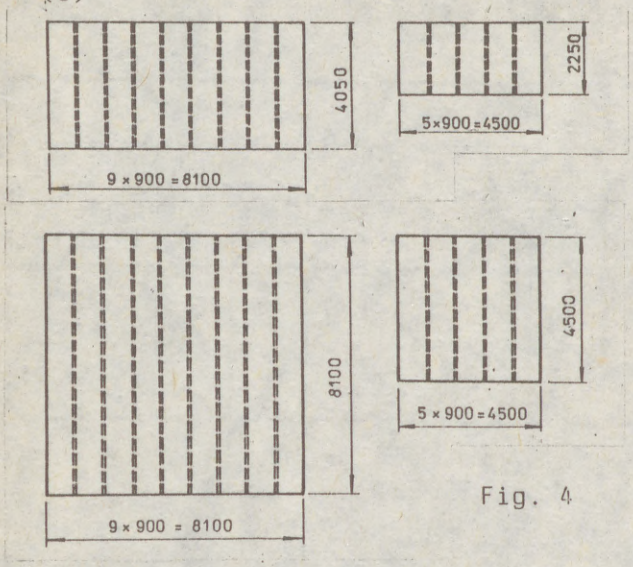

Fig. 4

37 with R_d = 210 MPa), varying in the study the aspect ratio of the flange panel investigated, the thickness of the flange sheet, and the number, configuration and size of the longitudinal stiffeners. With the view to give the reader an idea about the rigidity (or flexibility) of the respective longitudinal stiffening, the authors also indicated in Table 1 the ratio of the flexural rigidity γ of the steffeners concerned to their linear buckling theory optimum rigidity γ^*, calculated by means of the results obtained in /Škaloud, Zörnerová, 1977 /.

As the principal aim of the comparative study was to show how, in the context of either approach, shear lag influenced flange ultimate load and how the effect of shear lag was incorporated into the analysis of the flange ultimate state, the same values /viz., those given by criterion (c_1) of the Liëge-Prague approach) of $\bar{\sigma}_{ult}$ (i. e., of flange ultimate loads calculated with due allowance to flange buckling, but regardless of shear lag) were deliberately used in the calculations for both approaches. That is, the distinction in the calculation of the basic quantity $\bar{\sigma}_{ult}$ in each approach (which is, however, quite straightforward) is not in the scope of this study (but also this aspect of the comparison is under way and the results will soon be published in another paper).

Some comments regarding the consideration of the shear lag effective width ratio ς_s is also needed here. As in the context of the British approach not only ς_s but also the shear lag factor ψ depend on b/L, we should need to work with families of curves, each of them applying for one b/L- ratio. With the view to avoid this, the authors related, through formula (2) and for the geometry of the flange panel investigated, each value of ς_s on the horizontal axis to a particular b/L - ratio (i. e., to a particular girder span - composed of the corresponding multiple of the flange panel lengths under consideration) and then also evaluated for it the flange ultimate load. This means that the horizontal axis is also implicitely calibrated in b/L.

The writers also tried other formulae and tables for the determination of ς_s, but this did not much change the situation.

Some of the results of the whole analysis are plotted in

(7)
Figs 5 and 6; all other charts and conclusions will be published in another paper.

An examination of the plots shown in Figs 5 and 6 indicates that while for the British approach we have merely one curve (which for $b/L \leq 0.2$ goes over into a straight line parallel with the horizontal axis, which means that for such flange geometries in the light of the British approach the influence of shear lag is nil), the Liège-Prague approach yields two distinct limit state curves. One of them reflects the limit state criterion connected with the onset of plasticity at the longitudinal edges of the flange panel /see the above criterion (a)/ and the other applies for the limit state considerations in the central portion of the flange /see the above criteria (b) and (c_1); but, of the two, almost always is it (c_1) that is decisive./

So, in our comparison, we should first show how the simple and single curve of the British approach compares with the two-curve character of the Liège-Prague limit state considerations. Second, and more importantly, we should give a reply to the question of with what degree of plastification of the compression flange both approaches, for the individual flange geometries studied, are connected.

5. Conclusions of the Parametric Study

If we examine all (i. e., not only those which the restricted scope of this paper has permitted us to include into Figs 5 and 6) results obtained via our parametric study, we can draw the following conclusions:

a) For a greater part of the cases investigated with $b/L > 0.2$, the British limit state curve lies under those related to the Liège-Prague approach (see Figs 5 a and 6a). This means that for such flange geometries the British approach is "more elastic" than the quasi-elastic version of the Liège-Prague approach defined above. And in some cases the difference is quite significant, thus testifying to a more comservative character of the British approach in these instances.

b) On the other hand, for a lesser part of the cases studied (in Table 1, they are marked by full circles), the British curve lies above the Liège-Prague curves (see Figs 5b and 6b), which means that in such cases the British design procedure is linked with a larger degree of flange plasticization that the Liège-Prague quasi-elastic limit state criteria. In particular, given the fact that it is always the left-hand Liège-Prague curve, related to the onset of membrane plastification at the longitudinal flange boundaries, which is exceeded by the British curve, this means that in these cases significantly larger plastified areas develop along the longitudinal flange edges if the British design formula is used.

It should be mentioned at this juncture, however, that it can be seen in the figures (and the same can be observed in the charts that cannot be included in this short contribution) that the British curve never rises above the parallel passing through the curve points at $\varrho_s = 1$, which correspond to the

(8)

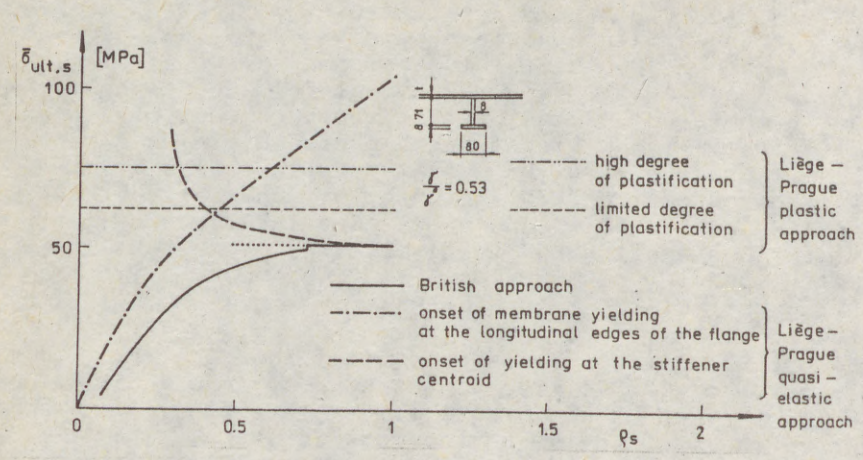

Fig. 5

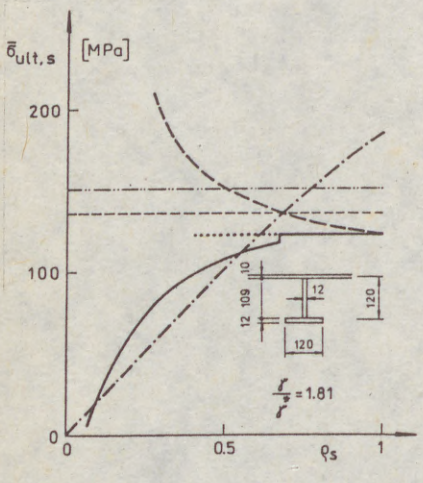

Fig. 5b

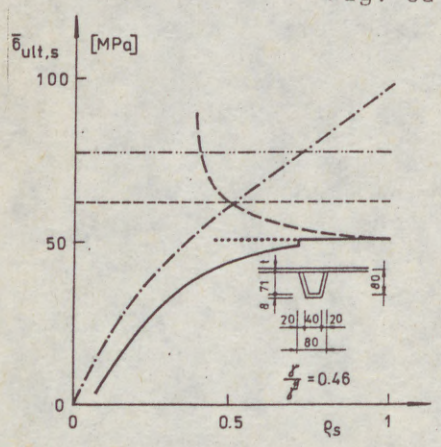

Fig. 6a

Fig. 6b

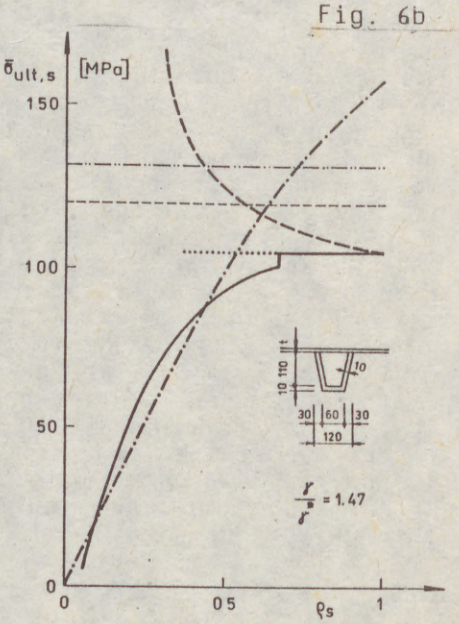

(9)

case where the quasi-elastic ultimate limit state is governed by flange buckling only while there is no shear lag.

And, as seen in Figs 5 and 6, even less does the British curve reach (let alone rise above) flange ultimate loads resulting from the plastic version of the Liège-Prague approach (and also this version of the interaction between shear lag and flange buckling is profoundly studied in the aforementioned publications by Jetteur, Maquoi and the authors), whether in its context the ultimate limit state be defined by (i) the plastification of longitudinal stiffeners over the whole flange panel (a high level of plasticity in the flange) or (ii) the plastification of longitudinal stiffeners only at the most loaded transverse section of the flange panel (a lower level of plasticity in the flange).

In regard to these plastically defined flange ultimate loads, it should also be mentioned here that one of the conclusions drawn by Jetteur, Maquoi and the writers is that when such a plastic definition of the ultimate limit state is applied, the effect of shear lag can be entirely neglected in flange design. Incidentally, the British approach does exactly so for $b/L \leq 0.2$.

Consequently, for this lesser part of the cases studied above, the British curve corresponds to states of flange plastification which are between (i) the quasi-elastic state and (ii) the plastic state. And this situation is acceptable on the condition that, additionally to an ultimate limit state check, also the limit state of serviceability - sufficiently controlling the onset of flange plasticization under working loads, which could have a detrimental influence on the fatique behaviour of the structure - is checked.

c) For $b/L \leq 0.2$, (and this situation is frequent in ordinary steel bridgework), the effect of shear lag in the light of the British approach is nil. With the Liège-Prague approach, the situation is a little more complicated, since in its context the shear lag effect depends on b/L through the factor ϱ_s only, which however very fast converges to unity with $b/L \to 0$.

Again, a serviceability check - safeguarding against plastification under working loads - is desirable.

d) Such a check of serviceability limit state can easily be accomplished via the "fully elastic" version of the Liège-Prague approach, which keeps criteria (a) and (b) given above in sec. 3, but replaces (c_1) by the following stricter criterion:

(c_1^*) onset of yielding at the extreme fibres of the outstand of the central longitudinal stiffener.

Then the charts given in Figs 2 and 3 can again be used; but when checking criterion (c_2^*), the distance e_3 of the extreme stiffener outstand fibres from the centroidal axis of the system sheet + stiffeners (see Fig. 1) is introduced for e.

6. Quasi-Rigid Longitudinal Stiffeners

Another point of compression flange design deserves our attention here.

(10)

The analysis of longitudinally stiffened compression flanges becomes much simpler and less time-consuming if longitudinal ribs can be regarded as quasi-rigid. Then there is no global flange buckling and the flange can buckle only in the sheet between the ribs, which can easily be taken into account by calculating the effective widths of the individual sheet panels. Therefore, it is of some importance to find out what size (or rigidity) the flange stiffeners need to posses so that the above situation can be achieved.

This was also one of the objectives of the experimental research /Škaloud, Kárníková, 1985/ conducted in Prague several years ago. By way of testing 12 large-size steel girders with longitudinally stiffened compression flanges, Kárníková and the first author came to the conclusion that longitudinal ribs on such flanges could be considered as rigid (i. e., their deflection could be disregarded) if their flexural rigidity $\geq 4\gamma^*$, with γ^* being their linear buckling theory optimum rigidity (which can be taken from /Škaloud,Zörnerová, 1977/).

However, for practical design, it is not of such importance to know for what dimensions stiffeners are geometrically rigid and remaining straight during the whole "life" of the girder; it is more useful to know that minimum size of the stiffeners for which the impact of stiffener flexure on flange ultimate state is negligible. And this was another goal of the authors´ parametric study, the Liège-Prague approach being again employed in the calculations.

An analysis of the results obtained reveals that the influence of stiffener flexure (i. e., the effect of global flange buckling) can be fully disregarded (with an error inferior to 2%) if the slenderness ratio of the longitudinal ribs (taken as struts and whose cross-sections consist of the stiffening elements proper and the effective portions of the adjacent sheet panels) is less than 50.

References

/1/ Jetteur, P., Maquoi, R., Škaloud, M. and Zörnerová, M., 1984: Interaction of shear lag with plate buckling in longitudinally stiffened compression flanges. Acta technica ČSAV, No. 3, pp. 376 - 397.

/2/ Jetteur, P., Maquoi, R., Škaloud, M. et Zörnerová, M., 1985: Interaction entre voilement et traînage de cisaillement dans les semelles comprimées raidies longitudinalement. Construction Métallique, No. I, pp. 13 - 30.

/3/ Stiffened compression flanges of box girders. Document prepared by ECCS TWG 8/3: Plated Structures, 1988, pp. 1 - 9.

/4/ Škaloud, M., Zörnerová, M., 1977: Linear-buckling-theory optimum rigidity of the longitudinal stiffeners of the compression flanges of steel box girder bridges. Acta technica ČSAV, No. 1, pp. 33 - 51.

/5/ Škaloud, M., Zörnerová, M., 1984: The role of larger initial curvatures and of local sheet buckling in the interaction of shear lag with buckling in longitudinally stiffened

(11)
compression flanges. Acta technica ČSAV, No. 5, pp. 623 - 647.

/6/ Škaloud, M., Kárníková, I., 1985: Experimental research on the limit state of the plate elements of steel bridges. Transactions of the Czechoslovak Academy of Sciences, Series of Techn. Sciences, Vol. 95, No. 1, Academia, Prague, pp. 1 - 141.

(1)
Usami, Tsutomu(1)

A Simplified Analysis of the Strength of Stiffened Box Members in Compression and Bending

INTERNATIONAL COLLOQUIUM
STABILITY OF STEEL STRUCTURES
BUDAPEST, HUNGARY, 1990
PRELIMINARY REPORT

SUMMARY: A simple, yet accurate method is presented for computing the ultimate strength of stiffened box members in combined compression and bending as an extension of a previously proposed algorithm for unstiffened box sections (Usami, 1982). The method is based on the strut approach (Dubas and Gehri, 1986) that is widely used for a strength analysis of stiffened plate panel in compression. The computed results for simply supported stiffened plates in compression and bending compare well with available solutions obtained from a more sophisticated FEM analysis (Nara, 1986). The results are furthermore discussed in various aspects.

INTRODUCTION

There exists a variety of methods for computing the ultimate strength of stiffened steel plates in pure compression as summarized by Dubas and Gehri (1986) and by Galambos (1988). Among others, the so-called strut approach is recognized to be the simplest, yet reasonably accurate method. The present state-of-the-art, however, shows that the application of the method is restricted to stiffened plates in pure compression. The present paper is aimed to extend the application of the strut approach to an ultimate strength analysis of stiffened box members under combined compression and bending (see Fig. 1). The box member is provided with a number of flexible longitudinal stiffeners of flat type and with stiff diaphragms at the member's ends. The length is assumed to be relatively short so that the overall member instability would not occur. The member is thought of a part of main towers of suspension bridges or cable stayed bridges.

COMPUTATIONAL PROCEDURES

Strut approach.-The strut approach adopted in this study is based on the method, developed by Komatsu and Kitada (1980), for analysing stiffened plates in compression. To apply the strut approach, both an effective width formula of the plate panel and a strength formula of a stiffener-plate column

(1) Professor of Civil Engineering, Nagoya University, Nagoya, Japan

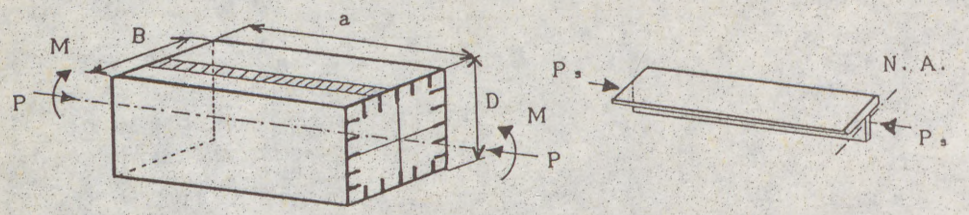

(a) Stiffened Box Member (b) Stiffener-Plate Column (Strut)

Fig. 1 Stiffened Box Member in Compression and Bending

(strut, see Fig.1b) must be defined a priori.

Effective width formula of a plate panel.-The effective width formulas proposed previously by the present author (Usami, 1982; Usami and Fukumoto, 1984) are slightly modified and used in the present study. The formulas are written as follows (see Fig. 2):

When $\sigma_1, \sigma_2 \geqq 0$

$$b_{e1}/b = 0.35\sqrt{\sigma_{cr}/\sigma_1} \qquad b_{e2}/b = (1+\xi\,\phi)\,b_{e1}/b \qquad (1),(2)$$

$$b_{e1} + b_{e2} \leqq b \qquad (3)$$

When $\sigma_1 \geqq 0$ and $\sigma_2 \leqq 0$

$$b_{e1}/b = \text{Eq.(1)} \qquad b_{e2}/b = (1+\xi)\,b_{e1}/b \qquad (4)$$

$$b_{e1} + b_{e2} \leqq b - b_{e3} \qquad (5)$$

The quantities ξ and ϕ in the above expressions are given by

$$\xi = 1.3 \ (\text{for } 0.0 \leqq \phi \leqq 1.5) \qquad \xi = 1.4\phi - 0.8 \ (\text{for } 1.5 \leqq \phi \leqq 2.0) \qquad (6)$$

$$\phi = (\sigma_1 - \sigma_2)/\sigma_1 \qquad (7)$$

In the above equations, σ_1 and σ_2 are, respectively, the maximum and minimum compressive stresses at the edges and σ_{cr} is the linear buckling stress of simply supported plate in compression (buckling coefficient k=4.0). The quantity ξ, which was assumed to be 0.44 in the previous studies (Usami, 1982; Usami and Fukumoto, 1984), has been modified by referring to a recent theoretical study (Nara, 1986) on the ultimate strength of plate elements in compression and bending.

Column strength formula.-In order to include the magnitude of initial out-of straightness of a stiffener-plate column in its strength formula, the

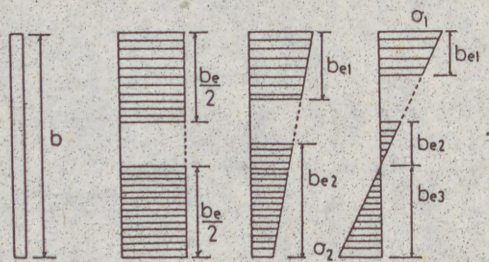

(a) $\sigma_1 = \sigma_2$ (b) $\sigma_1, \sigma_2 > 0$ (c) $\sigma_1 > 0, \sigma_2 < 0$

Fig. 2 Effective Widths

(3)

following Perry-Robertson formula has been adopted:

$$\sigma_u/\sigma_y = [1/(2\bar{\lambda}^2)][1+\eta+\bar{\lambda}^2 - \sqrt{(1+\eta+\bar{\lambda}^2)^2 - 4\bar{\lambda}^2}] \quad (8)$$

$$\eta = 364(\bar{\lambda} - 0.2)(\delta_o/a + 3.43\times10^{-4}) \quad (9)$$

$$\bar{\lambda} = (a/r)(1/\pi)\sqrt{\sigma_y/E} \quad (10)$$

where σ_u is column strength, σ_y yield stress, δ_o maximum initial column deflection, a column length, r radius of gyration of column cross-section about the principal axis parallel to the plate panel and E Young's modulus. When δ_o/a = 1/1000, the above formula reduces to the ECCS multiple column curve c (ECCS, 1983), which is applicable to a structural Tee section column. And, when δ_o/a = 0.0, the formula becomes identical to the ECCS column curve a_o, which is similar (in the range of $\bar{\lambda}$ less than 1.0) to the CRC basic column strength curve (Galambos, 1988) without any initial out-of-straightness.

Computational procedure.-In the strut approach, a stiffened plate panel is replaced by a series of disconnected, centrally loaded struts consisting of a stiffener and an associated plate width (see Fig. 1b). The following basic assumptions are made in the analysis: (1) The strut is simply supported at its ends and is subjected to a centrally loaded axial compression. (2) Shift of the neutral axis of the strut due to plate local buckling is ignored. (3)The strut is compact; i.e. no torsional buckling would occur. (4) The effect of stress gradient over the stiffener outstand (Little, 1976) is neglected. (5) The material properties of the plate panel and the stiffeners are the same in each component plate.

The compressive force P and banding moment M acting to the box member(Fig. 1a) are replaced by an eccentric compressive force P with an eccentricity

$$e_o = M/P \quad (11)$$

Figures 3 show the assumed states of direct stress at the ultimate state of the member. The upper flange (i.e., most compressed flange) is assumed to be always in the ultimate state of the stiffened plate. The stress blocks at the two corners of the upper flange reach the yield stress of the flange plate σ^f_y, while the magnitudes of the other stress blocks in the upper flange,

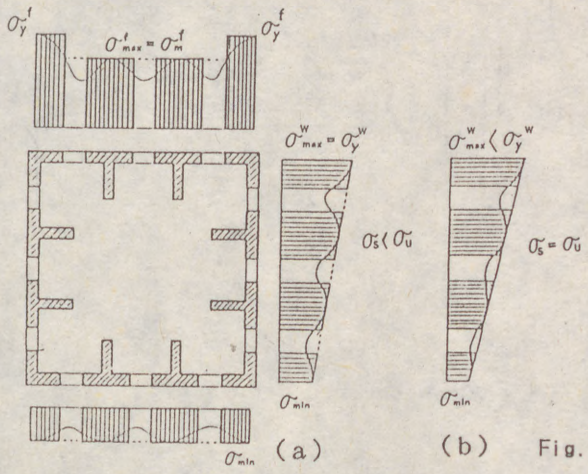

Fig. 3 Assumed Ultimate States

(4)

$\sigma_{f}max$, are determined from the strut approach as shown later. Two different cases of the ultimate states may be considered in the web plates as shown in Figs. 3. In the case of (a), the stress of the top stiffener of the webs, σ_s, is less than its ultimate strength, σ_u, obtained from the strut model. Therefore, the top edge stress in the webs, $\sigma_{w}max$, reaches the yield stress of the webs, $\sigma_{w}y$, and the top plate panel in the webs is considered to be in the ultimate state as in the upper flange. On the other hand, in the case of (b), the top stiffener stress σ_s reaches its ultimate strength, σ_u, so that stresses at the top panel in the webs remain less than the yield stress $\sigma_{w}y$. The above two collapse states are hereafter designated as follows:

Case (a) collapse mode = upper flange collapse mode (or top panel collapse mode in the case of isolated stiffened plate),

Case (b) collapse mode = top rib collapse mode.

It should be noted that even in "top rib collapse mode" the upper flange has already been in the ultimate state.

The basic computational procedures are shown in Fig. 4 as a flow chart. Some of the procedures are explained in more detail below:

Steps 2-4: These are to compute the state of stress in the upper flange. Since the effective width is dependent on the stress, iteration is necessary. The effective width of the panels adjacent to the stiffeners is computed from Eq. (1) with $\sigma_1 = \sigma_{f}max$, while the effective width of the two corners(i.e., flange-

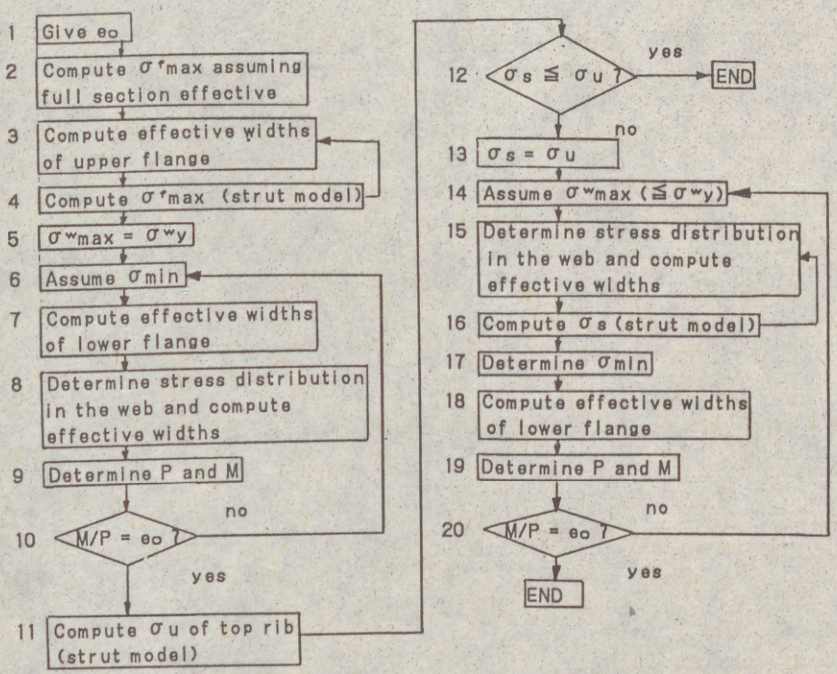

Fig. 4 Flow Chart of Computational Procedures

web junctions) with $\sigma_1 = \sigma_y$ (Komatsu and Kitada, 1980).

Steps 5-12: These are to compute the state of stress in the webs and the lower flange under "upper flange collapse mode". A linear stress distribution is assumed in step 8 and the effective width of each subpanel is computed using Eqs.(1) to (7).

Steps 13-20: These steps are for "top rib collapse mode".

When an isolated stiffened plate is analysed, steps 2,3,4 and 18 may be omitted. The Newton-Raphson method is employed for the iteration schemes of steps 6 to 10 and of steps 14 to 20.

NUMERICAL RESULTS AND DISCUSSION

Comparison with FEM solutions of stiffened plate.- The numerical results are first compared with more rigorous solutions obtained by Nara (1986) for simply supported stiffened plates in combined compression and bending (see Fig. 5). Nara computed the ultimate strength of equally spaced stiffened plates with initial imperfections by using an elastic-plastic large displacement FEM analysis. The unloaded edges are free to pull in and linearly varying edge displacements are applied along the loaded edges so that the stress resultants, P and M, along the same edges satisfy $e_o = M/P$. The initial imperfections assumed by Nara are as follows: initial out-of-straightness of the stiffeners $\delta_o/a = 1/1000$ (in the direction of stiffener outstand), initial out-of-flatness of plate panels = b/150 (b is widths between stiffeners), maximum compressive residual stresses = 0.3 σ_y (plate panels) and 0.2 σ_y (stiffeners). The notation in the figure is: N=number of stiffeners, $m = \gamma / \gamma^*$, γ =relative flexural rigidity of one stiffener, γ^* = optimum value of γ obtained from linear buckling theory (DIN 4114, 1953), α = a/B, B = total plate width. The ordinate and the abscissa are:

$$\frac{\sigma_{ult}}{\sigma_y} = \frac{Pu}{Py} + \frac{Pu \cdot e_o}{My} \qquad (11)$$

$$\bar{\lambda}_p = (B/t)\sqrt{(\sigma_y/E)12(1-\nu^2)/(\pi^2 k)} \qquad (12)$$

$$k = 8.4/(\psi + 1.1) \quad (\text{for } 0 \leqq \psi \leqq 1), \qquad k = 10\psi^2 - 6.27\psi + 7.63 \quad (\text{for } -1 \leqq \psi \leqq 0)$$

$$\psi = 1 - \phi/(N+1) \qquad (13),(14)$$

where Pu is axial compression at the ultimate state, Py squash load, My yield moment, ν =0.3 Poisson's ratio and t plate thickness. In the figure, the computed results are classified depending on the collapse mode. It is seen from the figure that the agreement between the computed results and Nara 's results is quite satisfactory. Almost all the cases, except for ϕ = 2.0 (pure bending), the plates are terminated due to the attainment of the ultimate state of the top ribs (i.e., top rib collapse mode) instead of the top panels. As a reference, the ultimate strength curve for pure compression calculated using the BS5400 (1982) method is also plotted in the graph.

Effect of stiffener rigidity (stiffened plates).- Figs.6 show the effect of stiffener rigidity on the ultimate strength of simply supported plates with four stiffeners. The assumed initial out-of-straightness of the stiffeners is $\delta_o/a = 0.470 \times 10^{-3}$, which is the average value of initial stiffener imperfections measured in actual steel bridges (Fukumoto, 1988). In the case of pure compression (ϕ =0), the increase in the ultimate strength with the

(6)

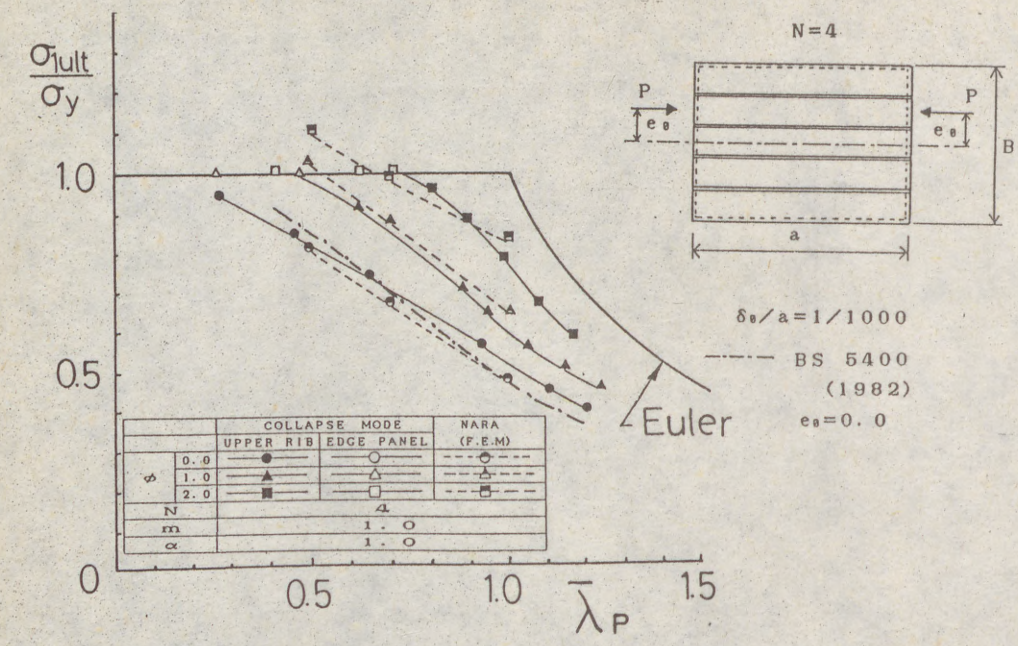

Fig. 5 Comparison of Computed Results and Nara's FEM Solutions

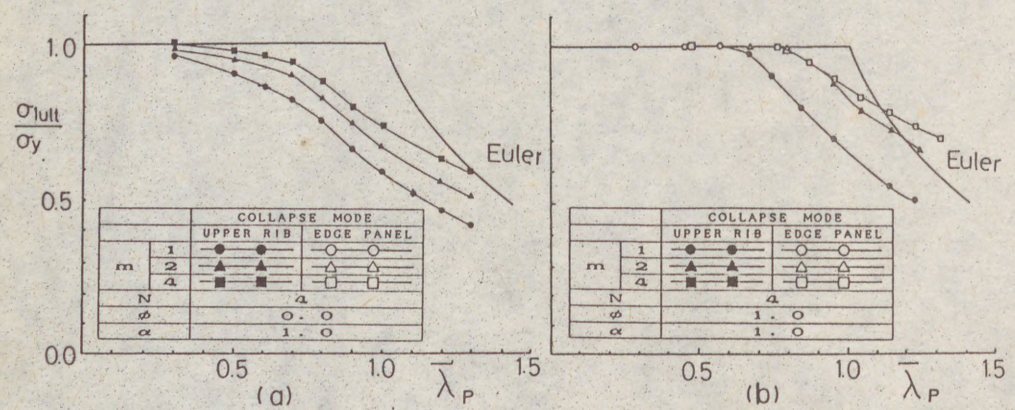

Fig. 6 Effect of Stiffener Rigidity (δ_o/a = 0.00047)

(7)

relative stiffener rigidity is seen to be always large. However, in the case of compression and bending (ϕ =1.0), the increase in the strength becomes less significant beyond a certain value of γ because the collapse mode shifts from "top rib collapse mode" to "edge panel collapse mode" and, therefore, increase of stiffener rigidity is meaningless.

Square box member in compression and bending.- Square box members having four equally spaced stiffeners (m= γ / γ *=1.0) in each component plate are analysed. The assumed stiffener initial out-of-straightness δ_0/a is again 0.470×10^{-3}. The four component plates are identical and the material properties are the same. The results are shown in Fig.7 as a form of interaction curves. The straight lines in the figure represent the following linear interaction equation proposed previously by the present author (Usami and Fukumoto, 1989):

$$\frac{P}{QPy} + \frac{M}{Q_B My} = 1.0 \tag{15}$$

$$Q = [1/(2\bar{\lambda}_p^2)][1+\eta+\bar{\lambda}_p^2 - \sqrt{(1+\eta+\bar{\lambda}_p^2)^2 - 4\bar{\lambda}_p^2}\,] \tag{16}$$

$$\eta = 0.332(\bar{\lambda}_p - 0.2) \tag{17}$$

$$Q_B = 1-[\{9\bar{A}+1+N(N-1)\delta/(N+1)\}](1-Q)/[4\bar{A}\{3\bar{A}+1+N(N-1)\delta\}/(N+1)] \tag{18}$$

$$\bar{A} = 1 + N\delta \tag{19}$$

where δ is relative extensional rigidity of one stiffener. The quantity Q represents the reduction in the ultimate compressive strength due to local buckling and has been obtained from the curve for m= γ / γ *=1.0 in Fig.5. Equation (18) is a special form of expression (square box member composed of identical plates) of the more general formula that provides the expression for the ultimate bending moment of box members with buckling of the compression flange being taken into consideration. The following is observed from the figure: when the plate width-thickness is relatively small (i.e., $\bar{\lambda}_p \leqq 0.7$) and when "upper flange collapse mode" occurs, the linear interaction equation (15) is reasonably good. However, as the plate becomes thinner, the collapse mode shifts to "top rib collapse mode" and the linear interaction

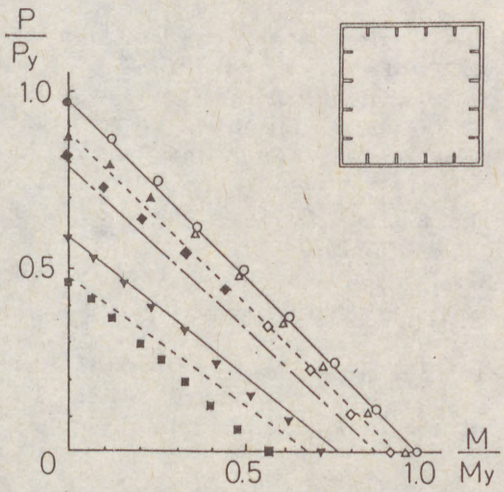

		COLLAPSE MODE		Eq.15
		UPPER RIB	UPPER FLANGE	
$\bar{\lambda}_p$	0.3	●	○	———
	0.5	▲	△	- - - - -
	0.7	◆	◇	— - —
	1.0	▼	▽	———
	1.2	■	□	- - - - -
N		4		
m		1.0		
α		1.0		

$\delta_0/a = 0.00047$

Fig. 7 Computed Results for Box Member

(8)

formula becomes less satisfactory. A modification to the formula (15) is needed in which buckling of the top stiffeners in the webs is taken into account.

SUMMARY AND CONCLUSIONS

A simple method has been presented for computing the ultimate strength of stiffened box members in combined compression and bending. The method is based on the strut approach which is widely used for predicting the ultimate strength of stiffened plate panel in compression. In spite of a rather crude treatment, the computed results compare fairly well with the solutions obtained from a more sophisticated, expensive FEM analysis. The developed algorithm is now being utilized to study an optimum proportioning of compression members and rigid frames stiffened by longitudinal stiffeners and diaphragms (Usami, 1989)

REFERENCES

British Standards Institute (1982): BS5400; Steel, Concrete and Composite Bridges, Part 3, Code of Practice for Design of Steel Bridges.

DIN 4114 (1953): Blatt 2, Stahlbau, Stabilitätsfälle (Knicken, Kippung, Beulung), Berechnungsgrundlagen, Richtlinien.

ECCS (1983): EUROCODE 3, Common Unified Code of Practice for Steel Structures, Draft.

Dubas, P. and Gehri, F.(1986): Behavior and Design of Steel Plated Structures, ECCS Publication No. 44.

Fukumoto, Y. ed. (1988): Guidelines for Stability Design of Steel Structures, Steel Structure Series 2, Japan Society of Civil Engineers (JSCE).

Galambos, T.V. ed.(1988): Guide to Stability Design Criteria for Metal Structures, 4th. ed. John-Wiley & Sons.

Komatsu, S. and Kitada, T.(1980): Practical Method of Calculation for the Ultimate Strength of Stiffened Plates under Compression, Proc. JSCE, No. 302, pp.1-13.

Little, G.H. (1976): Stiffened Steel Compression Panel-Theoretical Failure Analysis, The Structural Engineering, No. 12, Vol. 54, pp. 489-500.

Nara, S. (1986): Study on the Ultimate Strength of Unstiffened and Stiffened Plates under In-Plane Loadings, D. Eng. Dissertation, Osaka University.

Usami, T. (1982):Post-Buckling of Plates in Compression and Bending, J. of Struct. Div., Proc. ASCE, Vol. 108, No. ST3, pp. 591-609.

Usami, T. and Fukumoto, Y. (1984): Welded Box Compression Members, J. of Struct. Eng., ASCE, Vol. 110, No. 10, pp.2457- 2470.

Usami, T. and Fukumoto, Y.(1989): Deformation Analysis of Locally Buckled Steel Compression Members, J. Construct. Steel Research, Vol. 13, pp. 111-134.

Usami, T.(1989): Optimum Design of Locally Buckled Steel Compression Members, Proc. Fourth Int. Colloquium on Structural Stability, Asian Session (ICSSAS' 89), Tsinghua University, Beijing, People's Republic of China.

(1)
VAYAS, Ioannis (1)

TORSIONAL RIGIDITIES OF OPEN STIFFENERS TO COMPRESSION FLANGES

INTERNATIONAL COLLOQUIUM
STABILITY OF STEEL STRUCTURES
BUDAPEST, HUNGARY, 1990
PRELIMINARY REPORT

Summary: A critical review of Code provisions and other proposals concerning the requirements for torsional rigidities of flat stiffeners to compression flanges is made. The relevant rules are investigated by means of 65 tests on compressed, stiffened plates with various loading and supporting conditions. A new design rule for the determination of the dimensions of flat stiffeners, based on their ultimate stress and the ultimate stress of the stiffened plate, is proposed and relevant design charts are given.

1. INTRODUCTION

Theoretical and experimental research on axially loaded plates, stiffened one-sided by open stiffeners have shown, that two modes of failure are possible (Fig.1):

- -plate failure, caused by plate buckling, where the deformations at failure consist of a global, overall deflection towards the stiffener and local buckles of the plate (Fig.1a) and
- -stiffener failure, caused by lateral torsional buckling of the stiffeners, where the deformations at failure consist of a global, overall deflection towards the plate and local buckles of the stiffeners (Fig.1b).

The load carrying behaviour of these plates depends largely on the failure mechanism as experimental (Barbré et al 1982, Scheer, Vayas 1983) and theoretical research (Vayas 1981) have shown. Plates with stiffenerfailure behave almost linear up to failure, since only second order effects are relevant, whereas their load-carrying capacity is rapidly decreasing after failure (Fig.1b). Plates with plate-failure behave before failure largely non-linear because of plastic stress-redistributions and second order effects and they posess a high load-carrying capacity after failure (Fig.1a).

---

(1) Lecturer of Civil Engineering, National Technical University of Athens.

(2)

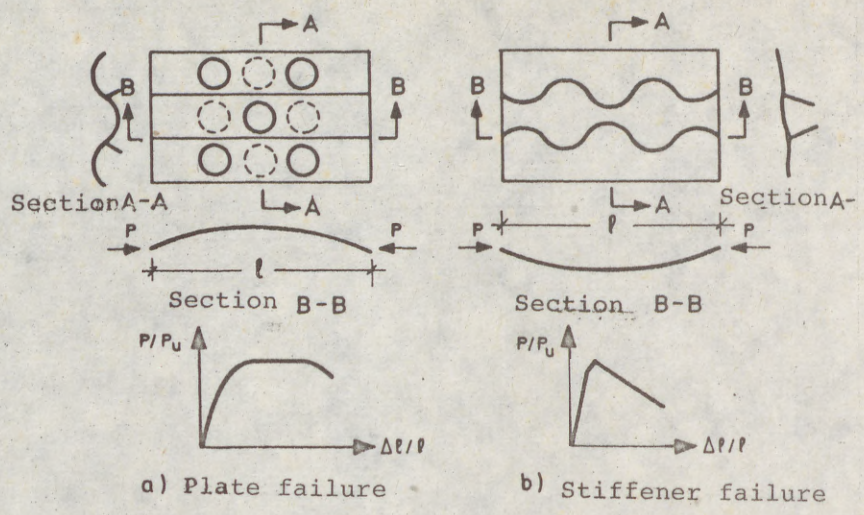

Fig 1:Failure modes of axially compressed,Stiffened plates

It is therefore wishfull and several Codes do it, to prescribe minimum torsional rigidities of the stiffeners in order to avoid lateral torsional buckling and consequently a stiffener mode of failure for the plate. In the present work the provisions for flat stiffeners of the Draft Code DIN 18800, Part 3 1983, the Code BS 5400, part 3 1982 and previous proposals of the author Vayas 1989 are examined through test results on compressed stiffened plates and new rules that fit best to the tests are proposed.

2.REQUIREMENTS FOR FLAT STIFFENERS

In a uniformly compressed, stiffened plate the stress distribution in the cross section is initially constant (Fig.2a). This remains so as long as the stiffnesses of the plate between the stiffeners and of the stiffeners are equal. At larger stresses (or strains) the stiffness of one of the two components is decreasing (in Fig.2b the stiffness of the plate). This results in a downwards or upwards (as in Fig.2) movement of the centroid S, so that the stiffened plate is compressed no more centrically but excentrically. Because of the excentrical compression the stiffened plate is deflecting towards the stiffener or the plate and it fails by plate or stiffener failure. The different Code provisions and proposals for torsional rigidition are derived from this background.

The provisions of the Draft Code DIN 18800, part 3 1989 have been based on the assumption that the stiffness reduction of the plate or the stiffener are starting when the corresponding critical buckling stresses σ_{pi} and σ_{si} are reached. Taking into account the relevant safety factors against plate and column buckling of 1,5 and 1,7 respectively is leading to the following condition

(3)

$$\sigma_{si} \leq \frac{1,5}{1,7}\,\sigma_{pi} \qquad (1)$$

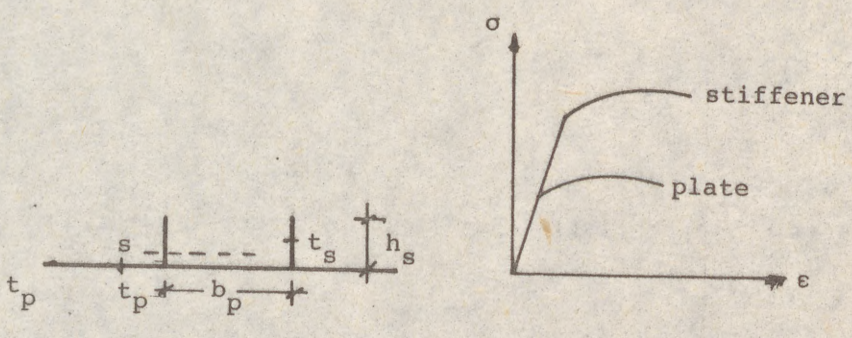

Fig 2: Notation, behaviour of stiffened plates

The proportions of the stiffeners with the notation of Fig.2 should then be such that (Fig.3)

$$\frac{h_s}{t_s} \leq \frac{1}{1,3}\,\frac{b_p}{t_p} \qquad (2)$$

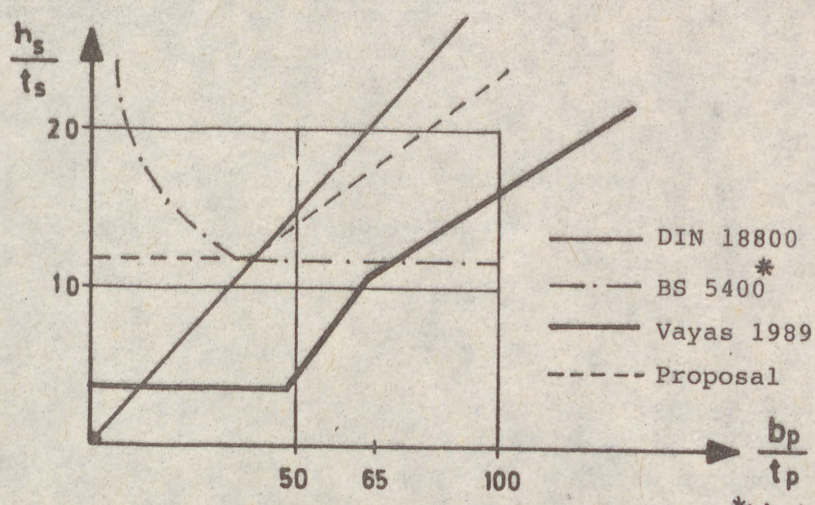

$$* \quad \frac{b_p t_p}{t_s^2}\sqrt{\frac{\sigma_{ys}}{355}} = 20$$

Fig 3: Provisions for flat stiffeners (σ_y=240 MPa)

(4)
The provisions of the Code BS 5400, part 3 1982 have been derived from the requirement that the slenderness of the stiffener $\bar{\lambda}_s = \frac{\sigma_{ys}}{\sigma_{si}}$ is limited to 0,673, so that for the considered buckling curve

$$\rho_s = \frac{1}{\bar{\lambda}_s} - \frac{0,22}{\bar{\lambda}_s^2} \qquad (3)$$

the ultimate stress σ_{us} is not reduced due to buckling, where

$$\sigma_{us} = \rho\sigma_{ys} \qquad (4) \quad (\sigma_{ys} = \text{yield stress of the stiffener})$$

The proportions of the stiffeners should be such that (Fig.3)

$$\frac{h_s}{t_s}\frac{\sigma_{ys}}{355} \leq 10 \qquad (5) \quad (\sigma_{ys} \text{ in } MP_a)$$

For small values of the slenderness of the plate b_p/t_p the slenderness of the stiffeners can be increased due to certain clamping effect of the plate as shown in Fig.3.
The provisions of the two Codes are clearly contradicting. DIN 18800 permits larger stiffener slenderness for larger plate slenderness due to the possible plate failure, whereas BS 5400 permits larger stiffener slenderness for smaller plate slenderness due to the clamping effects.
In a recent proposal the author, Vayas 1989, derives stiffener proportions from the requirement that the ultimate stress of the stiffener σ_{us} is at least equal to the ultimate stress of the plate σ_{up}. The relevant condition is

$$\sigma_{us} = \rho_s\sigma_{ys} \leq \sigma_{up} = \rho_p\sigma_{yp} \qquad (6), \quad (\sigma_{yp} = \text{yield stress of the plate})$$

where the reduction factor ρ_s is determined from the European column buckling curve c and the reduction factor ρ_p from the buckling curve

$$\rho_p = 1,13\left(\frac{1}{\bar{\lambda}_p} - \frac{0,22}{\bar{\lambda}_p^2}\right) \qquad (7)$$

The relevant requirement for the proportions of the stiffeners is shown in Fig.3.
In the present paper the stiffener proportions are proposed to be derived from eq.(6) using as reduction factors for the stiffeners the Winter curve for simply supported plates on 3 edges

$$\rho_s = \frac{0,7}{\bar{\lambda}_s} \qquad (8),$$

and for the plate the Winter curve for a plate supported on 4 edges (eq.(3) but ρ_p, $\bar{\lambda}_p$ instead of ρ_s, $\bar{\lambda}_s$).
The above requirements lead approximate to the following condition for the proportions of the stiffeners (Fig.3):

(5)

$$\frac{h_s}{t_s}\,\frac{\sigma_{yp}}{\sigma_{ys}} \leq \frac{1}{4,6}\,\frac{b_p}{t_p} + 4,0 \leq 12,9\,\frac{\sigma_{ys}}{\sigma_{yp}} \qquad (9).$$

3. TESTS AND TEST EVALUATION

In order to examine the different rules discussed in the previous section the results of 65 tests on stiffened plates performed in the Institute of Steel Structures at the Technical University of Braunschweig, reported by Barbré, Schmidt, Riemann 1982 and Scheer, Vayas 1983 are used.

Ser.	Loading conditions	1/i / b/t	A,D 20	A,D 70	A,D 100	B,E 20	B,E 70	B,E 100	C 20	C 70	C 100
II	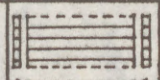	25	x	x	x	x	x	x	x	x	x
		50	x	x	x	x	x	x	x	x	x
		75	x	x	x	x	x	x	x	x	x
III		50		x							
		75		x	x		x	x			
IV		50		x							
		75		x	x		x	x			

Table 1. Test programme

The test programme is shown in Table 1. All plates were 7mm thick (nominally) and were stiffened by 4, equally spaced bulb stiffeners. The parameters of the tests were the plate slenderness b_p/t_p, the beam thickness 1/i, the supporting conditions, the stress distribution and the imperfections. The A-models were perfect, the B-and D-models had geometrical imperfections that lead to plate failure (B without, D with residual stresses due to welding), and the C and E models had geometrical imperfections that lead to stiffener failure (C without, E with residual stresses due to welding). In analogy to the deformations at failure the imperfections consisted of a global deflection towards the plate (C and E) or the stiffener (B and D) and local stiffener (C,E) or plate (B,D) buckles. They all were 4 times larger than those prescribed by the Merrison rules.

All the test evaluations described in the following are based on the actual properties of the specimens (widths, thicknesses, yield strengths, imperfections etc), The bulb stiffeners have been considered as equivalent plates having the same critical stresses σ_{si}. In Fig.4 the provisions of DIN 18800, part 3 are compared with the results of the tests. For each test equivalent $(h_s/t_s)e$ and $(b_p/t_p)e$ ratios have been determined according to the following procedure. Due to the overall imperfection

of the stiffened plate the initial stress distribution at the stiffeners is not uniform. For the actual stress distribution the critical stress σ_{si} has been determined and equated to the critical stress of a uniform compressed plate , simply supported on 3 edges having a slenderness of $(h_s/t_s)e$. The same procedure has been applied in order to determine $(b_p/t_p)e$ for test series IV were the stress distribution of the plate was not uniform.

In Fig.4 a plate failure is expected to occur below the straight line and a stiffener failure above it. The test results show that in 12 tests in total the predicted mode of failure is incorrect. In 8 tests the provisions of the Draft Code give conservative results, whereas in 4 tests with perfect models the rules for the stiffeners are not adequate.

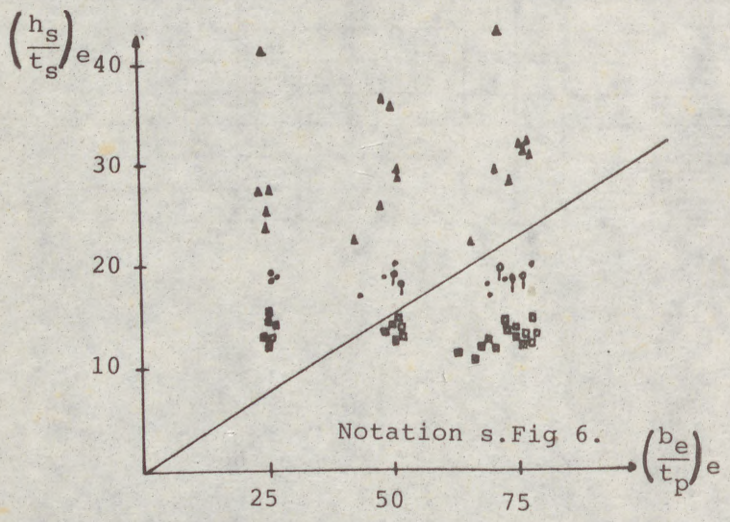

Fig 4: Comparison of the provisions of EDIN 18800,part3 with the test results

In Fig.5 the provisions of BS 5400, part 3 are compared with the results of the tests. The evaluation of the equivalent width to thickness ratios has been done according to the same procedure described before. The test results show that in 21 tests in total the predicted mode of failure is incorrect, as stiffener failure is predicted whereas plate failure is actually taking place. In Fig.6 the proposal of Vayas 1989 is compared with the results of the tests. The stiffeners are considered as excentrically compressed bars fixed at the plate that fail under lateral torsional buckling. An equivalent slenderness λ_u is determined accordingly and the European buckling curve c is used for the evaluation of the ultimate stress σ_{us}. The test results show that in 22 tests the proposal is conservative and in 1 the dimensions of the

(7)

Stiffeners are not adequate.

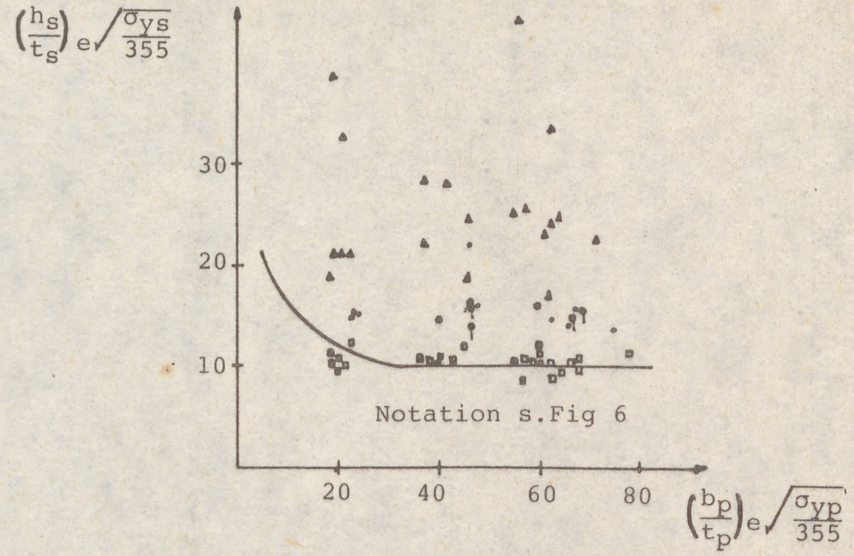

Fig 5: Comparison of the Provisions of BS 5400, part3 with the test results

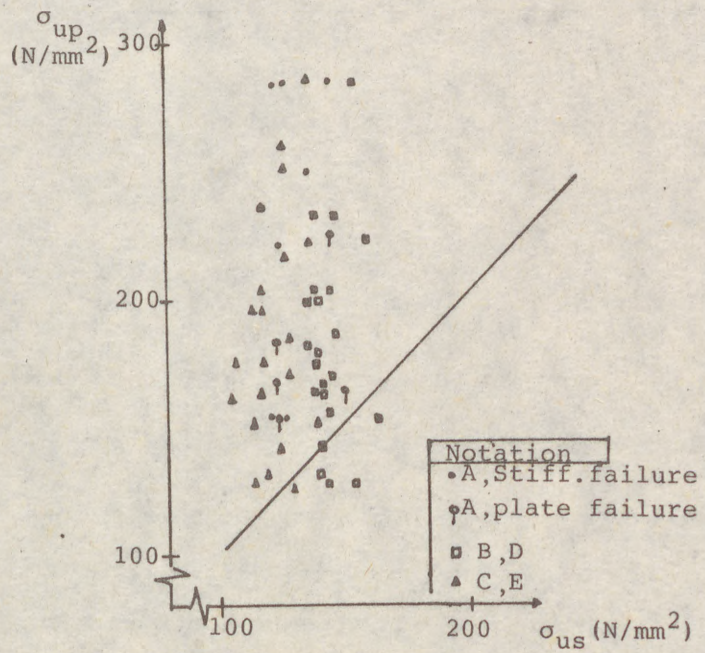

Fig 6:Comparison of Vayas,1989 proposal with the test results

(8)
In Fig.7 the current proposal is compared with the results of the tests. In 11 tests in total the predicted mode of failure is incorrect and in 2 tests with perfect models the dimensions of the stiffeners are not adequate.

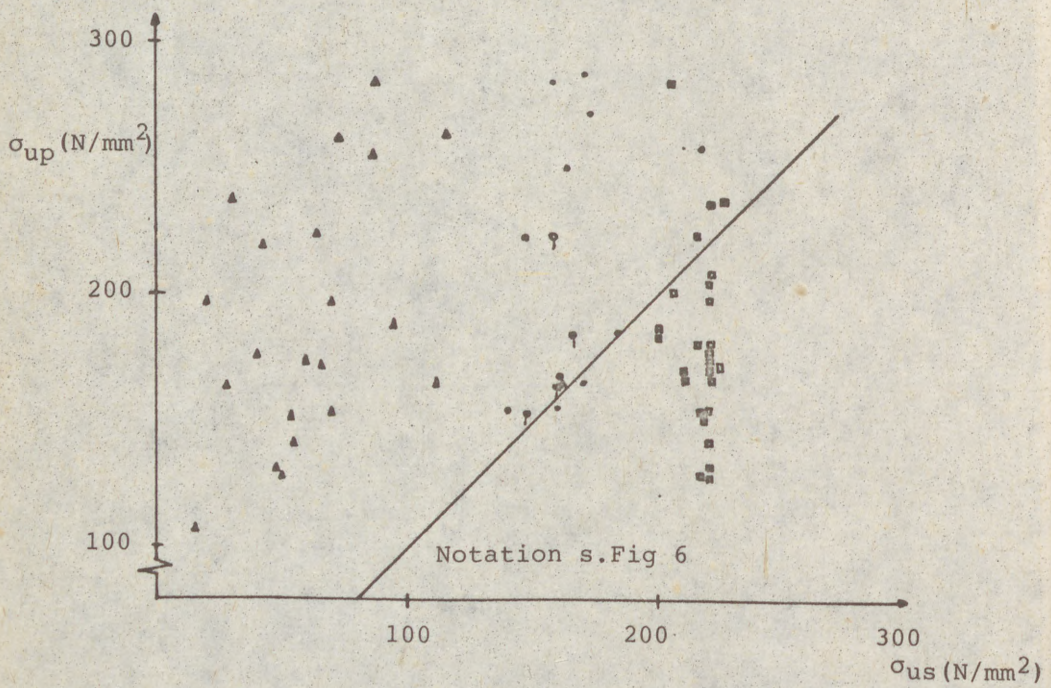

Fig 7: Comparison of the present proposal with the test results

4.CONCLUSIONS

From the comparison of the considered 65 test results with the examined provisions for flat stiffeners to compressed plates the following conclusions can be drawn:

1.The test evaluation takes into account, as described before, only the global imperfections and not the local ones. The latter were so large (4 times those of the Merrison rules), that they are not covered by any buckling curves. That explains the fact that the failure mechanism of so many tests is predicted incorrectly by the examined provisions.

2.The proposal of Vayas 1989 is overconservative for this type of stiffeners, as it does not take into account their post-buckling strength.

3.The provisions of BS 5400, part 3 are to conservative for large plate slendernesses, whereas those of DIN 18800, part 3 are too conservative for small plate slendernesses but not safe enough for large ones.

4.The present proposal seems to fit best to the results. It leads in only 2 tests to unconservative results both of which are very

(9)

near to the stated criteria. It must be however stated that for larger slendernesses, a non-linear behaviour of the stiffener is possible, that according to the design method of BS 5400 should be excluded.

5.The comparison indicates that for small plate slenderness it is possible to take into account a certain clamping effect of the stiffeners to the plate, allowing thus even larger stiffeners slendernesses than proposed, but the number of tests considered does not allow for conclusive evidence.

6.For bulb stiffeners it is possible to use the same rules as far the flat stiffeners by determining an equivalent $(\frac{h_s}{t_s})_e$ ratio as described in section 3.

7.Other types of open stiffeners are not expected to develop postbuckling strength so that the proposals of Vayas 1989 can be used, which takes into account the benefically effects of warping.

REFERENCES

Barbré R., Schmidt H., Riemann S., 1982, Der Stahlbau, Traglastversuche an längsgestauchten durch Wulstflachstähle versteiften Blechen mit freien Längsrändern, 51, 321-332.

British standard BS 5400, part 3, 1982 Code of Practice for Design of Steel Bridges.

DIN 18800, Teil 3, Entwurf 1987, Stahlbauten, Stabilitätsfälle, Plattenbeulen.

Scheer J., Vayas I., 1983, Der Stahlbau, Traglastversuche an längsgestauchten, versteiften Rechteckplatten mit allseitiger Lagerung, 52, 78-84.

Vayas I., 1981, Dissertation Braunschweig, Traglastberechnungen für Konstruktionen aus plattenartigen Bauteilen.

Vayas I., 1989, Der Stahlbau, Mindeststeifigkeiten und Bemessung von offenen Steifen versteifter, gedrückter Platten.

SESSION 7

FRAMES

(1)
ANDERSON, David (1)
BENTERKIA, Zoubir (2)

ANALYSIS OF SEMI-RIGID STEEL FRAMES AND CRITERIA FOR DESIGN

INTERNATIONAL COLLOQUIUM
STABILITY OF STEEL STRUCTURES
BUDAPEST, HUNGARY, 1990
PRELIMINARY REPORT

Summary: The paper reports studies on unbraced semi-rigid steel frames, carried out to determine criteria for design. The analyses of the frames were performed by a computer program which uses a secant stiffness approach to allow for the effect of semi-rigid connections on frame behaviour. A parameter entitled "Degree of Flexibility" is introduced as a measure of the effect of semi-rigid joints on the stiffness of the frame. Within the limits of the study, it is demonstrated that second-order effects will not be significant if the semi-rigid elastic critical load exceeds ten times the design load, and the degree of flexibility is less than 50%. This last requirement was satisfied by extended end-plate beam-to-column connections. It has also been found that under combined loading the serviceability limit on sway is likely to control design, rather than ultimate strength.

Introduction

In analysis and design of steel frames, it is customary to represent joint behaviour by an idealised model, either as a rigid-joint or as a pinned-joint. The definitions of these models are well known.

Experiments have shown that the behaviour of bolted connections is neither rigid nor pinned; rather, they possess some degree of rotational restraint which depends on the type of connection used. The term "semi-rigid" is used to describe such connections.

The behaviour of connections is represented by the moment-rotation relationship "M-φ" which must be included in the analysis and design of semi-rigid structures. Most common forms of beam-to-column connection have non-linear moment-rotation curves for the entire range of rotation. A review of techniques for modelling joint behaviour is provided by Anderson et al (1987).

Using computers, extensive studies have been carried out to investigate the main features of the behaviour of semi-rigid frames. It was found that the connection flexibility not only affects the behaviour of individual beams and columns but also the overall strength and stability of the structure. This paper addresses two considerations relevant to the design of unbraced semi-rigid frames:

---

(1) Senior Lecturer in Engineering, Warwick University, UK
(2) Research Student, Warwick University, UK

(2)

(a) whether first-order analysis can be used at the ultimate limit state (ULS);
(b) the significance of the serviceability limit on sway as a design criterion.

The investigations have been made using an elastic analysis procedure which is described first. A review of previous methods of analysis is given by Anderson et al (1987).

Method of analysis

The program described herein derives from one due to Majid and Anderson (1968), based on the matrix displacement method of analysis. It requires solution of the load-deflection equations:

$$\underline{F} = \underline{K}\,\underline{X} \qquad (1)$$

where $\underline{F}$ is the load vector, $\underline{K}$ is the stiffness matrix and $\underline{X}$ is the vector of unknown joint displacements. Iteration is used to allow for the influence of deformation on the equilibrium of the frame.

The program has been extended to include semi-rigid connections, treating them as elastic hinges. The non-linear $M-\varphi$ curve is idealised as a piece-wise linear variation. Successive estimates are made of the secant stiffness of each connection as the iteration proceeds.

Overall stiffness matrix

Consider a member i-j of a structure with semi-rigid connections at both ends as shown in Fig.1. Joints i and j are respectively the first end and the second end of the member i-j. This is indicated by the direction of the arrow on the member. The clockwise end moments acting on the member are considered positive. The effect of such moments will be to cause a deformed shape with reverse curvature as shown in the figure.

As a result of the semi-rigid connection at end i, the rotation of the member at i becomes the sum of the joint rotation θ_i without a hinge and the additional rotation φ_i due to deformation of the connection. Therefore a semi-rigid connection gives the frame an extra degree of freedom φ. As the external load vector $\underline{F}$ is equivalent to the joint displacement vector $\underline{X}$, there is a corresponding element in $\underline{F}$, denoted by M_h.

As a result of the deformation of the connections, the member shown in Fig.1 will tend to 'relax' and straighten out. Thus the rotations of the connections will be anticlockwise. It follows that the relationship between the bending moment M_h at a semi-rigid connection and the rotation is:

$$M_h = -K\varphi \qquad (2)$$

where K is the appropriate value of secant stiffness of the connection. Thus for the semi-rigid connections at i and j:

$$M_{hi} = -K_i\varphi_i \;;\; M_{hj} = -K_j\varphi_j \qquad (3)$$

It follows that for an assumed value of the secant stiffness, each semi-rigid connection contributes one additional unknown, φ, and one additional equation to the overall load-deflection equations for the structure (eqn. (1)).

Stability functions are used to take second-order effects into account (Livesley (1956)). The stability functions are calculated from axial forces given by the previous iteration's analysis.

Program procedure

The procedure iterates about both the secant stiffness of the joints and the axial forces in the columns. The solution is taken to have converged when firstly the secant stiffnesses and secondly the axial forces differ by less than 0.1% between successive iterations.

At each iteration, the program solves the overall stiffness equations for the unknown displacements, calculates member end forces and moments, and re-calculates K for each semi-rigid connection using current values of M_h and φ, and the connection's "$M-\varphi$" relationship. The recalculated value is denoted K_1. The tolerance test is then applied to successive values of K for each semi-rigid connection.

If the tolerance test on secant stiffness is not satisfied then the new value K_1 is compared with that obtained two iterations before (K_3). If both K_1 and K_3 for a particular joint satisfy the tolerance test then the stiffnesses are oscillating. In this case the new secant stiffness for the subsequent iteration is taken not as K_1 but as the average for the two previous iterations.

Throughout the analysis, the stability of the frame is checked by calculating the determinant of the overall stiffness matrix. If first-order analysis is required, the stability functions are set to unity to avoid reductions in member stiffness due to compressive axial force.

The success of the procedure in terms of speed of analysis and size of frame that can be dealt with owes much to the use of a compact form of the stiffness matrix due to Jennings (1966).

Criterion for first order analysis

For rigid frames, if the elastic critical load λ_{cr} is greater or equal to ten times the design load, the second order effects are assumed to be negligible and first order analysis can be used (ECCS (1984)). The adequacy of this criterion for semi-rigid frames has been investigated using the program described above. For this task, the elastic critical load has been determined by applying vertical loads as point loads at the heads of the columns and a small disturbing force of about 1% of the vertical load as an horizontal force at the top of the frame. The analysis was repeated at increasing levels of loading, a modified Southwell plot being used to determine the critical load. As this load relates to a bifurcation-type buckling problem, each semi-rigid connection was represented by its initial stiffness.

Fourteen different frames were studied with various beam-to-column connections. Frames E1-E9 employed extended end plates, without column stiffeners. The $M-\varphi$ data for Frames E1-E2 was derived by Tschemmernegg and Humer (1988) for frames specified by Zandonini (1986) as part of an ECCS study. Frame E1 is shown in Fig. 2, with a typical connection given in Fig. 3(a) Frames E3-E9 were designed during studies on the wind-connection method (Anderson et al (1987)), the connection stiffness being obtained from the proposals of Frye and Morris (1975).

The descriptions of the frames are summarised in Table 1. The range of sections used within each frame is given and the ratio of total vertical load to total horizontal load (V/H) is stated. The thickness of the end plates in Frames E3-E9 varied from 6 mm to 28 mm, dependent mainly on the bending moment due to wind loading that had to be transmitted by the connection.

The remaining five frames, designated H1-H5, were similar to Frame E1 except that header plate connections (Fig. 3(b)) were used to obtain very flexible frames, devised to extend the range of the study. Again Frye and Morris's work (1975) was used to determine the connection rotation. The depth of the end plate varied from 240 mm to 180 mm, and the thickness of the end plate from 12 mm to 8 mm.

The results of the study are summarised in Table 2. To measure the stiffness of the semi-rigid structure, the term 'degree of flexiblity' is defined as:

$$\left[\left[\lambda_{cr\ rigid} - \lambda_{cr\ semi\text{-}rigid} \right] / \lambda_{cr\ rigid} \right] \times 100\%$$

where $\lambda_{cr\ rigid}$ is the elastic critical load with all joints taken as rigid; $\lambda_{cr\ semi\text{-}rigid}$ is the elastic critical load taking account of the initial stiffness of all semi-rigid connections.

ϵ_1 and ϵ_2 represent the maximum difference between first-order and second-order analysis for sway and bending moment respectively, expressed as a percentage of the second-order result. It should be noted that ϵ_2 is calculated for those moments that would be critical for design.

The procedure followed to obtain these results will be explained by reference to Frame E1 (Fig. 2). The results for this frame are given at the top of Table 2. The

(4)

loading shown in Fig. 2 was regarded as corresponding to a load level λ of unity. The elastic critical load level λ_{cr} was then calculated in the manner previously described. The value of 11.4 given for Frame E1 in Table 2 indicates that the critical load level is 11.4 times the level of loading shown in Fig. 2. To determine the 'degree of flexibility' of the semi-rigid frame, it was also necessary to calculate the elastic critical load of the same frame but with rigid joints. The value for Frame E1 with rigid joints was found to be 16.7 times the level of loading given in Fig. 2.

To investigate the criterion for neglect of second-order effects, the semi-rigid frame was then analysed at a load level corresponding to one-tenth of the critical load for the frame - in the case of Frame E1, at loads 1.14 times those shown in Fig. 2. Both first-order and second-order analyses were performed and the results compared. The differences were expressed in terms of ϵ_1 and ϵ_2 defined above. For the semi-rigid Frame E1, it is seen that at one-tenth of the critical load the neglect of second-order effects underestimates the bending moments by no more than 8% and sway deflection by 12%.

For Frame E2, λ = 1.0 corresponds to the loads specified by Zandonini (1986).

Frames E3-E9 were designed in "Universal" I- and H- sections (Steel Construction Institute (1987)) using realistic 'characteristic' values of loading for the United Kingdom (British Standards Institution (1972, 1984)). When dead, imposed and wind loading are combined, British practice is to ensure that the structure can withstand 'design' loads equal to 1.2 times the characteristic loads (British Standards Institution (1985)). The load level denoted λ = 1.0 in this report corresponded to these 'design' loads.

Frames H1-H5 were derived from Frame E1, and therefore for these also the load level λ = 1.0 corresponds to the loads shown in Fig. 2.

The general trend in Frames E3-E9 observed from Table 1 and Table 2 is for the critical load to increase as the ratio V/H falls (compare for example Frames E5 and E7). Frames designed to withstand relatively high horizontal forces had greater lateral stiffness, which in turn gave higher values for the critical load. For Frames E4 and E7, it was not possible to analyse at one-tenth of the semi-rigid critical load. This was because this load level was far above that for which the frame had been designed and one or more connections were incapable of withstanding the higher loading. For this reason, it was decided to also analyse Frames E1-E9 at the load level λ = 1.0. It will be recalled that for Frames E3-E9 this corresponds to the 'design' load for the ultimate limit state under combined loading.

Difficulties similar to those encountered in Frames E4 and E7 also arose in some other of the frames H1-H5. These frames had been devised without design calculations and possessed very flexible semi-rigid connections. The manner in which Frames H1-H5 were devised causes the load level λ = 1.0 to be without significance and results are not therefore presented for this situation.

From the results in Table 2 it is apparent that when the elastic critical for semi-rigidly connected frames is greater than or equal to ten times the design load the second order effects are not significant. Except for frames in which the degree of flexibility is greater than 50% the maximum error in neglecting the second order effects is 12% for both sway and bending moment.

Governing design criterion for semi-rigid unbraced frames

For Frames E1-E9 the ultimate collapse load λ_f has been calculated by Ohta (1988). These frames were in mild steel (Grade Fe E 235 or similar). Account was taken of second-order effects, and loss of stiffness due to semi-rigid joint action and the development of plasticity in the members. The results are given in Table 3. The load level at which the second-order overall sway index equalled 1/300 has also been calculated by the authors assuming elastic behaviour. This is termed the 'h/300 load' (Table 3). By comparing λ_f and the 'h/300' load an insight can be gained into the likelihood of sway controlling design.

(5)

In design to EC3 (1989) the partial safety factor on combined load for the ultimate limit state may be taken as 1.35 whilst the limiting sway index of 1/300 only applies to unfactored loads. Thus those frames for which the collapse load exceeded 1.35 times the 'h/300' load would be governed by deflection. It can be seen from Table 3 that this is the case for all the frames studied in this way, except for Frame E8. This four-bay frame was subjected to very light wind loading, as indicated by V/H in Table 1.

Conclusions

A well-established computer program for second-order frame analysis has been extended to frames with semi-rigid connections. Successive estimates are made of the secant stiffness of these connections, to represent their effect on frame behaviour.

A parameter entitled 'degree of flexibility' has been introduced as a measure of the effect of semi-rigid joints on the stiffness of a frame.

It has been demonstrated that the errors in sway deflection and bending moment arising from neglect of second-order effects are unlikely to be significant if the semi-rigid elastic critical load exceeds ten times the design load and the degree of flexibility is less than 50%.

Even for frames with low degrees of flexibility it is likely that under combined loading the serviceability limit on sway will control design rather than ultimate strength.

References

1. Anderson, D., Bijlaard, F.S.K., Nethercot, D.A. and Zandonini, R., 1987, "Analysis and Design of Steel Frames with Semi-Rigid Connections", IABSE Surveys, S-39/87.
2. British Standards Institution, 1972. CP3 Code of Basic Data for Design of Buildings : Chapter V Loading : Part 2 Wind Loads.
3. British Standards Institution, 1984. BS6399 Design loading for buildings : Part 1 : Code of Practice for Dead and Imposed Loads.
4. British Standards Institution, 1985. BS5950 Structural Use of Steelwork in Building : Part 1 : Code of Practice for Design in Simple and Continuous Construction : Hot Rolled Sections.
5. European Convention for Constructional Steelwork, 1984. Ultimate Limit State Calculation of Sway Frames with Rigid Joints, Publication No. 33.
6. Eurocode No. 3, 1989. Design of Steel Structures : Part 1 : General Rules and Rules for Buildings, Commission of the European Communities, February.
7. Frye, M.J. and Morris, G.A., 1975, "Analysis of Flexibly-connected Steel Frames", Canadian Journal of Civil Engineering No.2, May.
8. Jennings, A., 1966, "A Compact Storage Scheme for the Solution of Symmetric Linear Simultaneous Equations", The Computer Journal, Vol.9, No.3, November.
9. Livesley, R.K., 1956, "The Application of an Electronic Digital Computer to some problems of Structural Analysis", Structural Engineer, Vol. 34, No.1, January.
10. Majid, K.I. and Anderson, D., 1968, "The Computer Analysis of Large Multi-storey Framed Structures", Structural Engineer, Vol. 46, No. 11, November, 357-365.
11. Ohta, O., 1988, "Analysis of Steel Frames with Semi-rigid Connections using One-dimensional Finite Elements", University of Warwick Civil Engineering Research Report CE25.
12. Steel Construction Institute, 1987. Dimensions and Properties of Structural Steel Sections.
13. Tschemmernegg, F. and Humer, C., 1988, "The Design of Structural Steel Frames under Consideration of the Nonlinear Behaviour of Joints", Journal of Constructional Steel Research, Vol. 11, 73-103.
14. Zandonini, R., 1986, Private Communication, March.

Ref. No.	Frame	Bay width (m)	Storey height (m)	$\frac{V}{H}$	Top storey			Bottom Storey		
					Beam	Ext Column	Int. Column	Beam	Ext Column	Int. Column
E1	3 storey 1 bay	5.0	4.0	18.6	IPE300	HE200B	-	IPE300	HE200B	
E2	2 storey 3 bay	5.0	4.0	85.7	IPE300	HE160A	HE160A	IPE300	HE160A	HE160A
E3	3 storey 1 bay	5.0	4.0	20.0	305x165x46 UB	203x203x46 UC	-	305x165x46 UB	203x203x46 UC	
E4	4 storey 1 bay	5.0	3.75	3.6	254x102x28 UB	203x203x46 UC	-	457x152x52 UB	254x254x73 UC	
E5	4 storey 1 bay	7.5	3.75	44.8	305x165x54 UB	152x152x30 UC	-	457x152x74 UB	203x203x46 UC	
E6	4 storey 1 bay	5.0	3.75	7.1	254x102x28 UB	152x152x37 UC	-	457x152x67 UB	203x203x60 UC	
E7	4 storey 1 bay	7.5	3.75	10.6	305x165x54 UB	203x203x46 UC	-	610x229x125 UB	203x203x86 UC	
E8	4 storey 4 bay	7.5	3.75	209	305x165x54 UB	152x152x30 UC	203x203x46 UC	457x152x74 UB	203x203x46 UC	203x203x60 UC
E9	7 storey 2 storey	5.0	3.75	6.6	254x102x28 UB	152x152x37 UC	203x203x46 UC	406x178x60 UB	254x254x89 UC	254x254x132 UC

Table 1 Summary of Frames E1-E9

Frame Ref. No.	Semi-rigid λ_{cr}	Rigid λ_{cr}	Degree of Flexibility	Semi-rigid frames				
				$\lambda = \lambda_{cr}/10$			$\lambda = 1.0$	
				λ	ϵ_1	ϵ_2	ϵ_1	ϵ_2
E1	11.4	16.7	32%	1.14	12%	8%	9%	6%
E2	5.86	6.66	12%	0.59	9.1%	8%	18%	20%
E3	6.88	9.24	26%	0.69	9%	6%	15%	12%
E4	17.2	25.2	32%	1.72	-	-	9.1%	8.5%
E5	6.22	8.44	26%	0.62	9.5%	4.5%	16%	7%
E6	14.8	17.5	15%	1.48	9.6%	8.5%	7%	7%
E7	19.5	22.6	14%	1.95	-	-	5%	4%
E8	4.50	6.40	30%	0.45	9.5%	9%	23%	25%
E9	9.48	12.2	23%	0.95	10%	11.5%	11%	12%
H1	8.32	16.7	50%	0.83	13%	4.4%		
H2	7.12	16.7	57%	0.71	10.8%	7.8%		
H3	5.96	16.7	64%	0.60	13.5%	10%		
H4	5.18	16.7	69%	0.52	-	-		
H5	4.13	16.7	75%	0.41	-	-		

Table 2 Results of elastic analyses

Frame Ref. No.	Collapse Load λ_f	Load level at h/300	Controlling design criterion
E1	1.70	0.85	Sway deflection
E2	1.55	0.85	
E3	1.57	0.52	
E4	1.16	0.26	
E5	1.44	1.00	
E6	1.37	0.45	
E7	1.72	0.80	
E8	1.24	> 1.24	Strength
E9	1.08	0.35	Sway deflection

Table 3 Governing design criterion

(8)

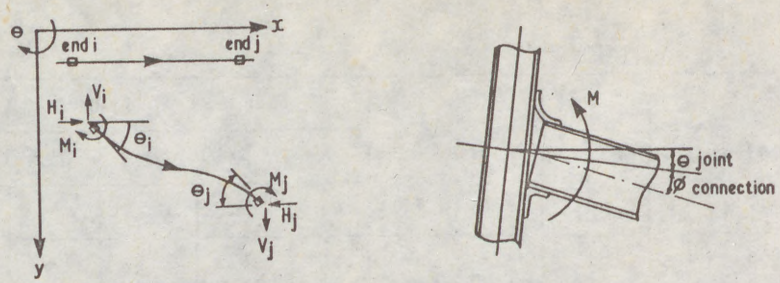

Fig. 1 Member with semi-rigid end connections

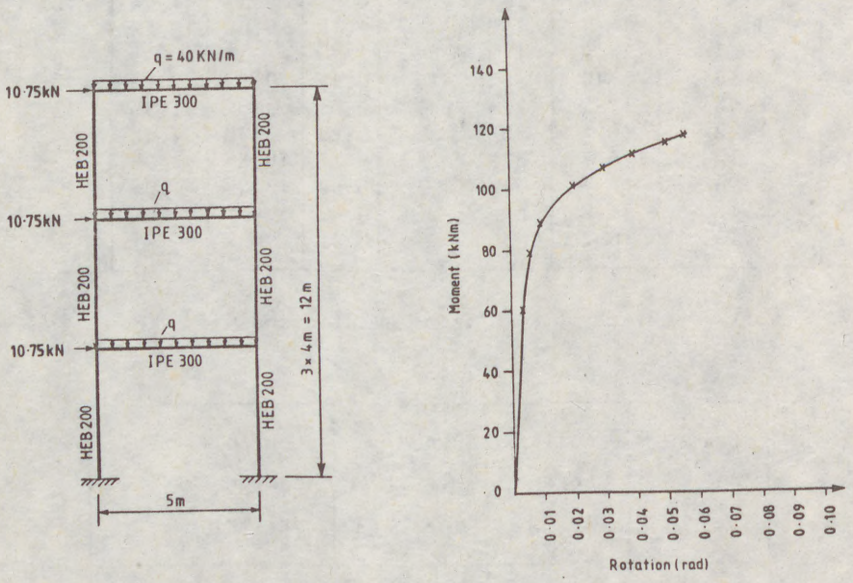

Fig. 2 Frame E1 and Connection "M-Ø"

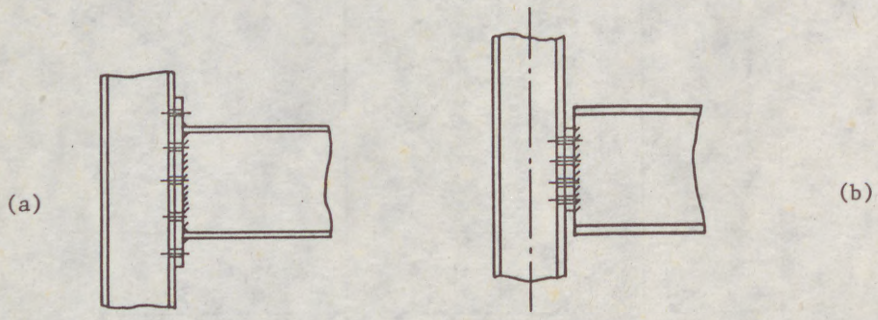

Fig. 3 Beam-to-column connections

COLSON , André (*)

THEORETICAL MODELING OF SEMI-RIGID CONNECTIONS BEHAVIOR .

INTERNATIONAL COLLOQUIUM
STABILITY OF STEEL STRUCTURES
BUDAPEST, HUNGARY, 1990
PRELIMINARY REPORT

Summary : The semi-rigid ,and non linear , behavior of the connections in the civil engineering structures is now well recognized . Nevertheless it is accepted and codified in the steel structures only . Therefore it is necessary to dispose of mathematical models in order to allow exact frame analysis with computer programs . The proposed model of this paper is based on physical parameters and verifies -a priori- the thermodynamics principles . The energy dissipation , associated to the non linearity , is considered as the main phenomenon .
The model is established in the unidimensional case - moment & rotation - which is the most usual and the most interesting in view of a cheaper design . The extension to the more general case (six degrees of freedom) is introduced with the same concepts The predictable feature of this model is emphasized in comparison with other curve-fitting techniques .

1 - INTRODUCTION .

All the civil engineering structures involve connections between the structural components .These connections are at the origin of geometrical and mechanical discontinuities that must be observed and handled with care from the manufacturer point of view but also studied in a rigourous way from the structural engineer point of view .
Depending on the materials that are used to build the structure the joints are made with different fasteners :

. Bolts,welds and secondary components like angles , plates, gussets in steel structures and composite stuctures .

. Nails,bolts,wood-screws,connectors ,sometimes along with steel parts , in timber stuctures .

(*) Professor of civil engineering ,Laboratoire de Mécanique et Technologie .Ecole Normale Supérieure de Cachan/CNRS/Paris 6 .

(2)

. Reinforcements and cast on site concrete in case of pre-cast concrete structures .

All these fasteners introduce local effects , stress concentrations for example ,and associated imperfections that induce the global, non linear behavior and the partial rigidity.That means that all the frame analysis methods must be based on the same concepts and the same philosophy . Nevertheless ,at the moment ,the steel structures are the only ones to be susceptible of such investigations ,probably due to the very high complexity of the others' stuctural materials .

Otherwise the semi-rigid (and non linear) effects are now regulated in Eurocode 3 . In this code it is specified that it is possible to use simplified models or more refined models depending on the complexity of the structure .Anyhow ,in order to propose simplified models it is of first necessity to have refined models.

In this paper is proposed a theoretical model which tries to be both the most general and mathematically simple .

2 - PHYSICAL BASES OF THE MODELIZATION .

The example used in all this paper is the beam-to-column connection .The moment M is the actual moment at the considered node (intersection of the neutral axis).The rotation Φ is the angle variation of the tangents to the neutral axis of the beam and the column (figure 1) In fact ,due to the geometrical complexity of the joint, it could be dicussed on the validity of such a definition . Perhaps the moment must be defined at the actual beginning of the beam (i.e at the end of the connection)? but what moment must be taken for the column calculation ? . Moreover the deformation is not uniform inside the connection. These two questions raise theoretical problems , which are not in the field of this paper and which should be examined in the framework of a new beam theory .We will satisfy ourself with the first assertion which fits with the classical engineer hypothesis .

From the tests results that have been obtained through the world the main features of the behavior are shown in figure 2 .For a monotonic loading (Part AB of the curve) the response is smooth . We suppose that for a very large deflection (Part BC of the curve) there exists an asymptotic value of the moment called M_u (In fact , actually ,due to the fracture it is not possible to reach such a value ,but is has been demonstrated experimentally that the fracture value is not in the range of utilization of the connection ,so for the modelization purpose it is convenient to put forward the hypothesis of ultimate moment M_u).At the beginning of the loading the behavior is characterized by the initial stiffness K . For the cyclic loading ,at each loading reversal , the initial stiffness is restored (Part BD on the diagram) and it is remarkable that the unloading is also non linear as soon as the loading reverses. This last characteristic is of first importance for the following modelization because the energy dissipation during a half cycle is less than that of a linear unloading .

(3)

The two main physical parameters are then the initial stiffness K and the ultimate moment M_u . The pincipal interest of this choice is that they are computable in a predictable way , for practical utilization ,from the geometrical (size , length ,...) and mechanical (Young modulus ,yield strength) properties of the connection components .(Colson ,1984 ; Kishi ,1987) .
The other interest of the initial stiffness is to allow the definition of the elastic part of the connection deflection at any level of loading in order to define the free energy (figure 3) . This corresponds to the partition hypothesis:

$$\Phi = \Phi^e + \Phi^{un} \quad \ldots\ldots\ldots\ldots\ldots (1)$$

with : Φ = total deflection of the connection.
Φ^e = elastic part of the deflection.
Φ^{un} = unelastic part of the deflection.

The unelastic part of the deflection is associated to the non linear behavior which is generated by the imperfections and the local effects (stress concentration for example) .All these effects will be taken into account with only one parameter in the framework of a thermodynamics format .

3 . THERMODYNAMICS FORMAT - ENERGY DISSIPATION . (Colson , 1984)

The free energy (which is the recoverable energy) at any point of the loading is indicated by the streaked area in figure 4 .
It is the sum of two terms :

$$\Psi(\Phi^e,\alpha) = \Psi_1(\Phi^e) + \Psi_2(\alpha) \quad \ldots\ldots\ldots (2)$$

with : $\Psi_1(\Phi^e)$ = free energy in case of elastic unloading (linear)
$\Psi_2(\alpha)$ = supplementary free energy due to the non linear unloading .α is an energy and a characteristic of a given connection .Ψ_2 is a dimensionless function.

For calculation simplicity we have to define the associated variables to Ψ^e and α which are M (moment) and "a" ,according to the well known table:

	Computable variable	Internal variable	Associated variable
Elastic deflection	(Φ^e). . .	. . . . .	. . M
Imperfections		α . . .	. .a

(4)

The whole connection is considered as an isolated thermodynamic system subjected only to slow mechanical effects (the moment applied by the column and the beam) .In such a case :

.The kinetical energy is negligible.
.The evolution is adiabatic. ($dQ = 0$)
.There are no temperature effects. ($dT = 0$)

With these hypotheses the internal energy variation ($\dot{E}$)equals the power of the external forces (P_e).

$$\dot{E} = P_e = M\dot{\Phi} \quad \ldots\ldots\ldots\ldots\ldots (3)$$

The second thermodynamics principle " $TdS \geq dQ$ " (S :entropy) is

$$TdS \geq 0 \quad \ldots\ldots\ldots\ldots\ldots (4)$$

The free energy (recoverable energy) is given by: $\Psi = E - TS$ then :

$\dot{\Psi} = \dot{E} - TdS/dt - SdT/dt$ (the dot means derivative with respect to the time) .

$\dot{E} - \dot{\Psi} = TdS/dt$ that means $\dot{E} - \dot{\Psi} \geq 0$ or:

$$\phi = M\dot{\Phi} - \dot{\Psi} \geq 0 \quad \ldots\ldots\ldots\ldots\ldots (5)$$

This is the CLAUSIUS-DUHEM inegality written for the whole system. (ϕ is the dissipated power) .The choice of the variables for the free energy Ψ allows to calculate this dissipation ϕ .

$$\phi = M\dot{\Phi} - \dot{\Psi} = M(\dot{\Phi}^e - \dot{\Phi}^{un}) - \frac{\partial \Psi}{\partial \Phi^e}(\dot{\Phi}^e) - \frac{\partial \Psi}{\partial \alpha}(\dot{\alpha})$$

$$\phi = \left[M - \frac{\partial \Psi}{\partial \Phi^e} \right] \dot{\Phi}^e + M\dot{\Phi}^{un} - \frac{\partial \Psi}{\partial \alpha}\dot{\alpha}$$

There is no dissipation from the elastic part of the deflection so

$$\left[M - \frac{\partial \Psi}{\partial \Phi^e} \right] = 0 \text{ or } M = \frac{\partial \Psi}{\partial \Phi^e} \quad \ldots\ldots\ldots\ldots\ldots (6)$$

and $\phi = M\dot{\Phi}^{un} - \frac{\partial \Psi}{\partial \alpha}\dot{\alpha}$

Considering the general form of the dissipation { $\phi = M\dot{\Phi}^{un} + a\dot{\alpha}$ }

then $$a = -\frac{\partial \Psi}{\partial \alpha} \quad \ldots\ldots\ldots\ldots\ldots (7)$$

It is more convenient for calculation purposes to use a " force approach " rather than a " kinematical approach " . So we use the LEGENDRE-FENSCHEL transformation of Ψ which is noted Ψ^* (Germain 1973)

$$\Psi^* = \Psi^*(M,a) = \Psi_1^*(M) + \Psi_2^*(a) \quad \ldots\ldots\ldots\ldots\ldots (8)$$

The state equations (6) and (7) become :

(5)

$$\Phi^{e} = \frac{\partial \Psi^{*}}{\partial M} \quad \ldots\ldots\ldots\ldots\ldots\ldots \quad (9)$$

and $$\alpha = -\frac{\partial \Psi^{*}}{\partial a} \quad \ldots\ldots\ldots\ldots\ldots\ldots \quad (10)$$

Choice of the free energy potential.

We propose the following expression :

$$\Psi^{*} = \frac{1}{2}\left[\, m^{2} - \beta\left(a^{2} - a_{o}^{2} \right) \right] \frac{M_{u}^{2}}{K} \quad \ldots\ldots\ldots\ldots \quad (11)$$

where $m = M/M_u$ and β a constant that will be determined with consideration of asymptotic behavior . a_o is the initial value (on the virgin connection) of the internal variable a . It has been established that the value of a is depending on the connection type (bolted , welded , end-plate ,angles) and on the connection size (a given imperfection has not the same effect in a small or in a large connection) .The elastic part of the deflection is known from equation (11) using relation (9) .

Choice of the unelastic part of the deflection.

The unelastic behavior of the connection is associated to the imperfections that are introduced by the parameter a :

$$\Phi^{un} = M_u \left(\sum_{1}^{\infty} m^{na+1} \right)/K \quad , \; n = 1,2,\ldots\infty$$

This particular expression has been chosen from analogical considerations on the perfect plastic behavior of individual mechanisms inside the connection .

4 . CONSTITUTIVE EQUATION .

The constitutive equation is obtained from relation (1) :

$$\Phi = \Phi^{e} + \Phi^{un} = M_u m/K + M_u(\sum m^{na+1})/K = M_u m(1+\ldots+m^{na})/K = M/K(1-m^{a})$$

or $$\boxed{\Phi = \frac{M}{K}\,\frac{1}{1-m^{a}}} \quad \ldots\ldots\ldots\ldots \quad (12)$$

Otherwise the first term of equation (12) gives the elastic part of the deflection and the second term is an amplification factor associated to the imperfections and giving the non linearity .In figure 5 one can see the influence of the a_o value .For a high value of a_o (6 or 7 for example) the curve is close to the perfect elastic-plastic behavior ,that means that the connection contains

(6)

few imperfections or little imperfections . For a lower value (1 or 1.5 for example) the curve takes away rapidly from the perfect behavior that means that the amplification factor is large and that the connection contains a lot of imperfections .
From the identification of a large number of test results the current values of a_o are approximately :

$a_o \neq 1.5$:fully welded connections (imperfections due to residual stresses of welding).

$a_o \neq 2.5$ or 3 :bolted connections without any particular manufacturing care .

$a_o \neq 4$ or 5 :bolted connections manufactured with care .

For practical utilization these numerical values can be used and they give ,already, a very good approximation .Of course an identification from a test result on a given connection will give a more refined value but it is not always possible to make a test. Also , it is convenient to keep "a" as a constant for the industrial utilization (i.e $a=a_o$) It was demonstrated that the evolution of the variable "a" is very slow .This may be established from the unloading behavior coupled with the cyclic behavior and the calculation of β (equation (11)) .

Cyclic behavior.

From the first monotonic loading the MASING rule is used to define the following cycles .The expression of the MASING rule is :

" If during the first loading (until M_1) the constitutive equation is $\Phi=f(M)$,during the first unloading (until M_2) the curve is given by $\Phi = \Phi_1 - 2f([M_1-M]/2)$ and during the first reloading by $\Phi = \Phi_2 + 2f([M-M_2]/2)$.(figure 6) and so on ".

From the calculation of the recoverable energy during the first unloading with the MASING rule on one hand and with the equation (11) on the other hand the value of β is calculated and the evolution law of "a" is obtained :

$$a^2 = a_o^2 - 14.678(a_o^2-1) \sum_{1}^{\infty} \frac{1}{na+2} [M/2M_u]^{na+2} \quad \ldots\ldots\ldots (13)$$

This implicit equation may be solved by a numerical procedure . In fact the accuracy is good with the first four terms of the serial .

5 . GENERALIZATION TO THE TRIDIMENSIONAL CASE .

From a theoretical point of view a structural connection has necessarily a three dimensional feature ,and even if for the engineer a mono-dimensional description is adequate , it is interesting to dispose of general description , more especially in order to explain some inter-action between the solicitations . In

particular this is the case of the column footing connections where the normal force stands along with the bending moment . The same solicitation type exists in large tubular structures. Looking to the buckling conditions of the bars it is necessary to evaluate the end restrained effect for both the weak and the strong axis combined with the normal force . Thus , it is interesting to explain the behavior from a tridimensional description .
Some experimental results show that the connections behave in a non linear way whichever the solicitation type . So we propose to use the same concepts for the tridimensional modelization . The kinematical description must be precised in the following way :

The overall connection is replaced by a macro-element (figure 8) which contains all the components like bolts , welds , plates , angles , etc. The constitutive equation will give the displacement {D} of one terminal cross section with respect to the other . Each terminal cross section is supposed to remain plane during the loading , so classical beam theory is always applicable to all of the bars that connected to the considered node (Bernoulli hypothesis) . The constitutive equation establishes a relation between the displacement vector $\{D\} = \{ u_i , \Phi_j \}$ and the force vector $\{F\} = \{ N_i , M_j \}$. i,j=1,2,3 .

u_i : translation

Φ_j : rotation

N_i : force (normal or shear)

M_j : moment (bending or torque)

The initial stiffness is now a matrix [R] such as :

$$\{D^e\} = [R]^{-1} \{F\} \quad . \quad . \quad . \quad . \quad . \quad . \quad . \quad . \quad . \quad . \quad (14)$$

where $\{D^e\}$ is the elastic part of the total displacement {D} .

The ultimate strength is expressed by the ultimate vector $\{F_u\}$ for which each component is the ultimate force in the concerned direction .The end of this vector determines the ultimate limit surface (U.L.S) in the forces space . The shape of the U.L S is able to take into account the inter-action between the solicitations .(figure 9).Of course without inter-action the U.L.S is a "cube" .

For the non linearity we choose to use always a scalar parameter "a" .In a certain way this means that the effects of the imperfections are the same whichever are the solicitations .In other words the imperfections are "isotropic" .

The level of loading is defined by λ such as $\lambda = \{F\}/\{F_u\}$. This implies that the loading must be radial (proportional) .
All the equations (2) to (10) may be rewritten replacing M by {F} and Φ by {D} .The new expression of the free energy (11) is :

(8)

$$\Psi^{*} = \frac{1}{2} \left[\lambda^{2} - \beta(a^{2}-a_{o}^{2}) \right] \{F_u\}^{T} [R]^{-1} \{F_u\} \quad \ldots\ldots\ldots\ldots (15)$$

The unelastic part of the displacement is :

$$\{D^{un}\} = [R]^{-1} \{F_u\} \sum_{i}^{\infty} \lambda^{na+1} \quad \ldots\ldots\ldots\ldots\ldots\ldots (16)$$

and finally the constitutive equation is :

$$\{D\} = [R]^{-1} \{F\} \frac{1}{1-\lambda^{a}} \quad \ldots\ldots\ldots\ldots\ldots\ldots (17)$$

The main interest of this modelization is the mathematical simplicity The shape of the U.L.S has been precised in the case of column footing connections (Colson ,1988) .

6 . CONCLUDING REMARKS .

A lot of models that have been gathered recently (Bijlaard et al 1989) are based on curve fitting techniques for which it is necessary to use a great number of parameters.Morever ,sometimes these parameters have no physical signification or physical bases. The proposed modelization is based on two main parameters , the initial stiffness and the ultimate solicitation ,that are now common in the engineering practise , and above all are calculable in a predictable way since the geometrical properties of the connection are known .This is of first interest in a design process avoiding thus experimental data for each connection size .The third parameter "a" is ,of course ,less common ;nevertheless it remains quite simple and its justification from the thermodynamics background warrants a physical meaning .

7 . REFERENCES .

Bijlaard,F.S.K , Nethercot,D.A. , Stark,J.W.B. , Tschemmernegg,F. Zoetemeyer,P. (1989) "Structural properties of semi-rigid joints in steel frames" I.A B S E Periodica 2/1989 .

Colson,A. (1984) "Modelisation des conditions aux limites de liaisons et d'assemblages en mécanique des structures metalliques" Thèse de doctorat d'état .Université Paris 6 .

Colson,A. , Penserini,P. (1988) "Three-dimensional physical and mathematical modeling of the column base connections" Structural Stability Research Council meeting proceedings .Minneapolis. April 1988 pp 301-308 .

Germain,P. (1973) "Cours de mécanique des milieux continus" MASSON Editions. Paris .

Kishi,N. , Chen,W.F. , Matsuoka K.G. , Nomachi S.G. (1987) "Moment rotation relation of top and seat angle with double web angle connections" Proceedings of the Cachan workshop.Connections in steel structures -Behavior,strength and design- Elsevier applied science .(Edited by Bjorhovde,R. , Brozzetti,J. , Colson,A.)

(10)

Figure 6

Figure 5

Figure 8

Figure 7

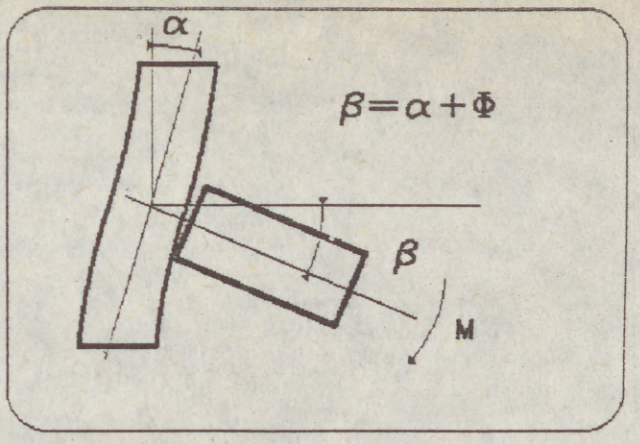

Figure 1

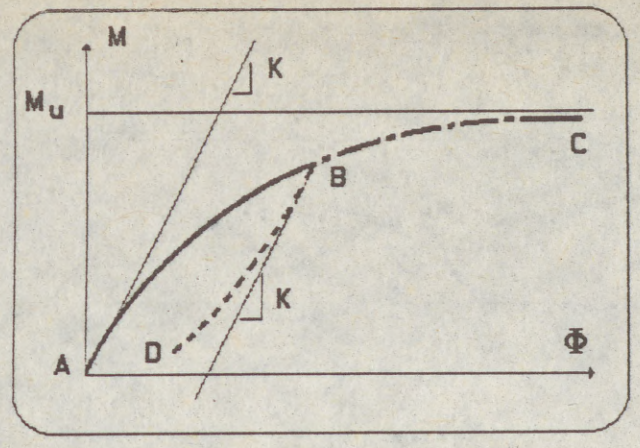

Figure 2

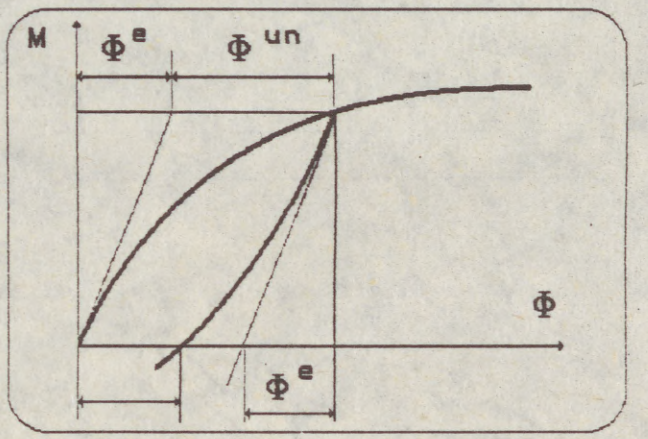

Figure 3

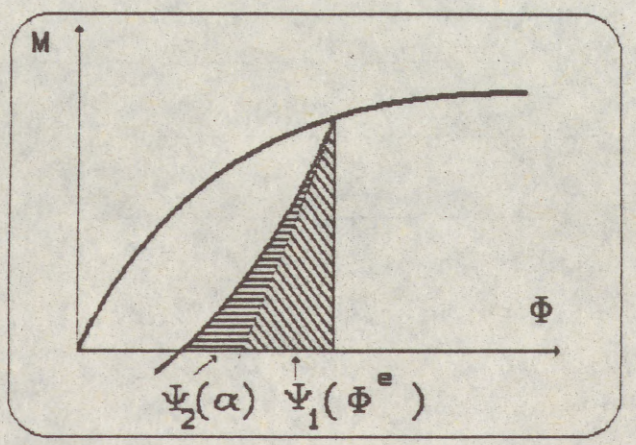

Figure 4

(1)
GALATENKO, W.A. (1)
ZAIDENBERG, A.I. (2)

THE STABILITY ANALYSIS OF THE FRAMES WITH VARIABLE SECTION ELEMENTS BY THE PRINCIPLE OF VIRTUAL WORK

INTERNATIONAL COLLOQUIUM
STABILITY OF STEEL STRUCTURES
BUDAPEST, HUNGARY, 1990
PRELIMINARY REPORT

We propose a difining procedure of the upper stability boundary for the frames of flange variable section in their plane. All elements of the frame are compressed to center or stretched with the forces, which increase proportionally with one parameter The stresses in the frame elements don't exceed the proportional limit. The frame elements with the following constructional features are considered: - flanges along the element axis have a constant width; - web height varies in a linear fashion; webs of all frame element lie in the same plane.

For a flange beam with the linearily variing web (fig.1) the moment of inertia of arbitrary section in the principal plane of web inertia takes the form:

$$EJ(x) = A_o\left[1+(1-\alpha)\frac{x}{\ell}\right]^2 + B_o\left[1-(1-\alpha)\frac{x}{\ell}\right]^3, \qquad (1)$$

where
$$\left.\begin{aligned} A_o &= EA_f h_o^2/2 \qquad (A_f \text{ - flange area}),\\ B_o &= E\delta_{cr} h_o^3/12. \end{aligned}\right\} \qquad (2)$$

---

(1) Design Chief Engineer, C.Sc. The Central Research, Design and Technological Institute of Light Metalworks
(2) Assistant Professor, C.Sc. Novosibirsk Civil Engineering Institute

(2)

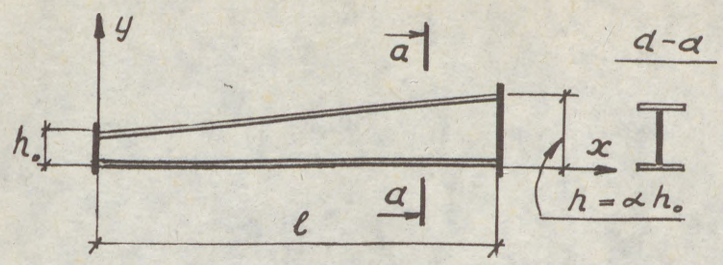

Fig. 1. Frame element

The bending equation of a separately taken beam:

$$EJ(x)\cdot\frac{d^2y}{dx^2} + Ny = M(x) \qquad (3)$$

Introduce a new variable $u = 1-(1-\alpha)\frac{x}{\ell}$. (4)

Later on denote the deriwatives of deflections with respect to variable "u" by

$$y^{(n)} = \frac{d^{(n)}y}{du^n}. \qquad (5)$$

In view of (4) and (5) equation (3) takes the form:

$$(u^2+\beta_0 u^3)y'' + \bar{N}y = \bar{M}(u). \qquad (6)$$

In equation (6):

$$\beta_0 = A_{0cr}/6A_f \qquad (A_{0cr} - \text{web area at } x = 0), \qquad (7)$$

$$\bar{N} = N\ell^2/A_0(1-\alpha)^2;\quad \bar{M} = M\ell^2/A_0(1-\alpha)^2 \qquad (8)$$

We have a general solution of a homogeneous part of equation (6) as a Taylor power series expansion at the point u = 1:

$$y(u) = y_0 + \sum_{n=1}^{\infty} y_0^{(n)}\frac{(u-1)^n}{n!}. \qquad (9)$$

Realize two functions: Φ_1 (u) for which the initial conditions have the form $y_0 = 1$, $y_0' = 0$; Φ_2 (u), for which $y_0 = 0$, $y_0' = 1$.

Define the expansion components (9) as C_n(u). The first three expansion components are determined with expressions:

$$C_0 = y_0;\quad C_1 = y_0'(u-1);\quad C_2 = -\bar{N}y_0/2(1+\beta_0) \qquad (10)$$

C_0 and the following series members (9) are defined by the homogeneous part of the equation (6) and its subsequent differentiation:

(3)

$$C_n(u) = -\left(\frac{2+3\beta_0}{1+\beta_0}\right)\left(\frac{n-2}{n}\right)(u-1)\,C_{n-1}(u) -$$
$$- \frac{\bar{N}+(n-2)(n-3)(1+3\beta_0)}{n(n-1)(1+\beta_0)}(u-1)^2 C_{n-2}(u) -$$
$$- \left(\frac{\beta_0}{1+\beta_0}\right)\cdot\frac{(n-3)(n-4)}{n(n-1)}(u-1)^3 C_{n-3}(u) \qquad (11)$$

Designate

$$\Phi_3(u) = \Phi_1'(u)\cdot(\alpha-1); \quad \Phi_4(u) = \Phi_2'(u)(\alpha-1). \qquad (12)$$

A general solution of the homogeneous differential equation by means of the initial parameters method takes the form:

$$\left.\begin{aligned}
&y = \bar{y}_0\Phi_1(u) + \varphi_0\Phi_2(u) + \bar{M}_0(1-\Phi_1(u)) + \bar{Q}_0\left(\frac{u-1}{\alpha-1} - \Phi_2(u)\right),\\
&\frac{dy}{dx} = \bar{y}_0\Phi_3(u) + \varphi_0\Phi_4(u) - \bar{M}_0\Phi_3(u) + \bar{Q}_0(1-\Phi_4(u)),\\
&\bar{M} = -\bar{y}_0\Phi_1(u) - \varphi_0\Phi_2(u) + \bar{M}_0\Phi_1(u) + \bar{Q}_0\Phi_2(u),\\
&\bar{Q} = -\bar{y}_0\Phi_3(u) - \varphi_0\Phi_4(u) + \bar{M}_0\Phi_3(u) + \bar{Q}_0\Phi_4(u).
\end{aligned}\right\} \qquad (13)$$

In the expressions (13) beam non-dimensional parameters take the form:

$$\bar{y} = y/\ell; \quad \bar{M} = M/N\ell; \quad \bar{Q} = Q/N. \qquad (14)$$

For $\beta_0 = 0$ the solution of the homogeneous part equation (6) has been obtained by A.N. Dynnik in a closed form /1/. In this case the fundamental functions $\Phi_i(u)$ take the form:

$$\left.\begin{aligned}
&\Phi_1(u) = \sqrt{u}\left(\cos z - \frac{\sin z}{2\beta}\right); \quad \Phi_2(u) = \frac{\sqrt{u}\sin z}{\beta(\alpha-1)};\\
&\Phi_3(u) = \frac{\delta N\ell^2}{EJ_0}\cdot\frac{\sin z}{(1-\alpha)\beta\sqrt{u}}; \quad \Phi_4(u) = \frac{1}{\sqrt{u}}\left(\cos z + \frac{\sin z}{2\beta}\right),
\end{aligned}\right\} \qquad (15)$$

where
$$z = \beta\ln u; \quad \beta = \sqrt{\frac{\delta N\ell^2}{A_0(1-\alpha)^2} - 1/4}. \qquad (16)$$

The expansion (9) converges always till $/u-1/ < 1$, ($u = 1$ for a constant section bar). The origin of coordinates can be always chosen in such way that $u_{max} \leq 1$. But this is not always convenient in the frame analysis by the principle of virtual work. Because of this we present the values of functions $\Phi_1(u)$ and $\Phi_2(u)$ determined through theirs inverse values:

$$\left.\begin{aligned}
&\Phi_1(u) = \left[\Phi_2'(1/\alpha)\cdot\Phi_1(u/\alpha) - \Phi_1'(1/\alpha)\cdot\Phi_2(u/\alpha)\right]/D_0,\\
&\Phi_2(u) = \left[\Phi_1(1/\alpha)\cdot\Phi_2(u/\alpha) - \Phi_2(1/\alpha)\cdot\Phi_1(u/\alpha)\right]/D_0(\alpha-1)
\end{aligned}\right\} \qquad (17)$$

(4)
where $D_o = \Phi_1(1/\alpha) \cdot \Phi_2'(1/\alpha) - \Phi_1'(1/\alpha) \cdot \Phi_2(1/\alpha)$

Φ_3 (u) and Φ_4 (u) are defined as the corresponding derivatives Φ_1' (u) and Φ_2' (u).

For determination of reactions from the unit values of angular and linear displacements of the variable section element end sections solve four types of problems at the following boundary conditions:

$$\left.\begin{aligned}
&1)\ y(x=0) = \frac{dy}{dx}(x=0) = y(x=\ell) = 0;\ \frac{dy}{dx}(x=\ell) = 1;\\
&2)\ y(x=0) = \frac{d^2y}{dx^2}(x=0) = y(x=\ell) = 0;\ \frac{dy}{dx}(x=\ell) = 1;\\
&3)\ y(x=0) = \frac{dy}{dx}(x=0) = \frac{dy}{dx}(x=\ell) = 0;\ y(x=\ell) = 1;\\
&4)\ y(x=0) = \frac{d^2y}{dx^2}(x=0) = \frac{dy}{dx}(x=\ell) = 0;\ y(x=\ell) = 1.
\end{aligned}\right\} \quad (18)$$

By realizing the condition (18) we find from the equations (13) the required unit reactions of the principle of virtual work (table 1). In the table 1 the functions of parameter α are expressed in terms of the fundamental function Φ_i (u):

$$\begin{aligned}
&\cdot\ A_1 = \nu^2\Phi_2/(\Phi_2 - \Phi_4);\quad A_2 = \nu^2\Phi_4/(\Phi_2 - \Phi_4);\\
&\cdot\ A_3 = -\nu^2\Phi_3/D;\ A_4 = \nu^2(1-\Phi_4)/D;\ A_5 = \nu^2(\Phi_2 - \Phi_4)/D; \qquad (19)\\
&\cdot\ A_6 = \nu^2(1-\Phi_2)/D;\quad A_7 = \nu^2(1-\Phi_1)/D,
\end{aligned}$$

where $D = 2 + \Phi_3 - \Phi_1 - \Phi_4$, $\nu = N\ell^2/EJ_o$,

i_o (stiffness per unit length) $= EJ_o/\ell$

The above-stated procedure is presented on example of the frame (fig. 2).

Table 2

Mumber of element	l (m)	N (TM)	EI_{A_2} (TM^2)	EI_{B_2} (TM^2)
1	6,93	10	10/10,5	100/117
2	3	5	100/117	100/117

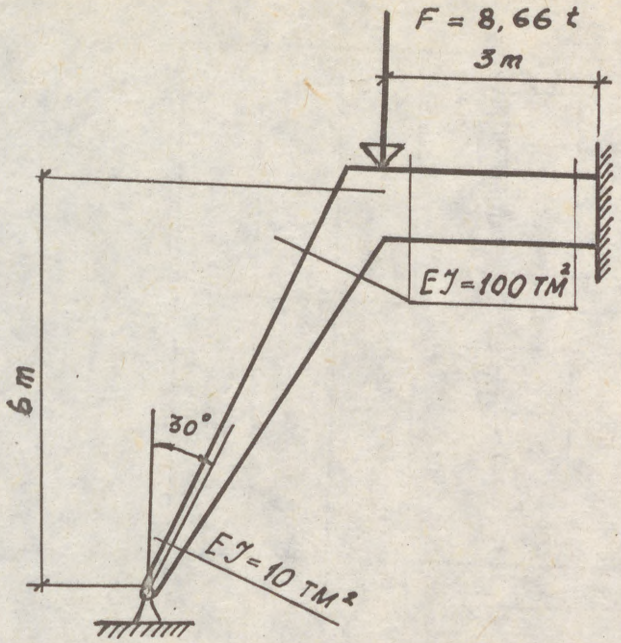

Fig. 2. The analysis diagram of the frame.

The web thickness of both frame elements is 10 mm. The web height of the first element varies from 32 mm. to 100 mm. The web height of the second element is constant and equal to 100 mm. The flanges section area is constant and equals for both elements 50 sm^2. The initial data of two elements are tabulated in the table 2.

Bending stiffnesses are presented having regard to the flange beam web work (denominator) and without it (numerator).

In result of the frame analysis without regard to the web work the stability margin is defined by the value 1,329 (the critical load equals $F_{kp.}$ = 1,329 x 8,66 = = 11,51 t).

The frame stability margin having regard to the web work is defined by the value 1,52 (the critical load equals $F_{kp.}$ = 1,52 x 8,66 = 13,16 t).

The mentined procedure in distinction to the agreed-upon one (the change of a variable section bar for a bar with a step constant section) enables to reduce a body of calculations at the expense of reduction of the matrix order which defines the frame stability.

(6)

Table 1

Analysis diagram	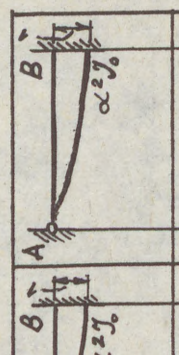	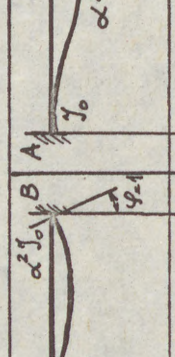	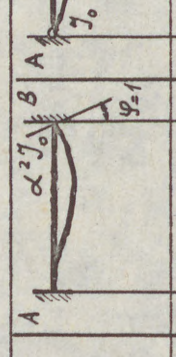	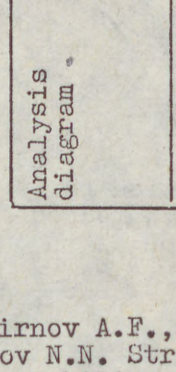
Bending moment curve				
Reactions M_A	$i_0 A_6$	—	$i_0 A_7/\ell$	—
Reactions M_B	$i_0 A_5$	$i_0 A_1$	$i_0 A_4/\ell$	$i_0 A_1/\ell$
Reactions $Q_A = Q_B$	$i_0 A_7/\ell$	$i_0 A_1/\ell$	$i_0 A_3/\ell^2$	$i_0 A_2/\ell^2$

Literature:

1. Smirnov A.F., Alexandrov A.V., Lashchenirov B.G., Shaposhnirov N.N. Structural mechanics. The structure dynamics and stability.
Moscow, Stroyizdat, 1984, 250 p.

[1]

GIBBONS, C. (1)
KIRBY, P.A. (2)
NETHERCOT, D.A. (3)

EXPERIMENTAL BEHAVIOUR OF 3-D COLUMN SUBASSEMBLAGES WITH SEMI-RIGID JOINTS

INTERNATIONAL COLLOQUIUM
STABILITY OF STEEL STRUCTURES
BUDAPEST, HUNGARY, 1990
PRELIMINARY REPORT

Summary

Preliminary results are presented for a series of full scale subassemblage tests designed to illustrate the beneficial effects of semi-rigid joint action on the 3-dimensional response of non-sway steel columns. The experimental arrangement, including the specially devised instrumentation systems, is described, the generally observed behaviour discussed and the use of the tests to verify a parallel theoretical study is cited.

Introduction

It is now widely accepted that steel beam-to-column connections function as

(1) Research Assistant, University of Sheffield, England.
(2) Lecturer in Civil and Struct. Eng., University of Sheffield, England.
(3) Professor of Civil Engineering, University of Nottingham, England.
(formerly Reader, University of Sheffield)

partial strength, semi-rigid joints, with the idealised cases of 'pinned' and 'rigid' being the two extremes of the range of possible behaviour. In recent years, numerous studies have been undertaken to improve understanding of the effects of semi-rigid joint action on the performance of individual members and complete frames (8,9). This work has, however, been almost entirely restricted to considerations of the two-dimensional in-plane behaviour.

Analytical capabilities are now being extended (10) to incorporate the 3-dimensional response which requires a knowledge of the out-of-plane joint characteristics (2). To date, it has not been possible to verify these analytical procedures because of a lack of suitable test results.

This paper reports on a study (5) in which ten large-scale, fully instrumented 3-dimensional column subassemblages, incorporating a variety of joint types, have been tested. Only the basic experimental method and the main results are presented herein; detailed study of the full test histories, comparisons with numerical simulations and appraisals of the full significance of the findings are still in progress (5).

Development of the experimental set-up.

Figure 1 shows the two basic subassemblage configurations considered. Each subassemblage effectively represents an isolated subframe forming part of a more extensive multi-storey structure. That subassemblage containing three beams represents an edge column arrangement, whilst that with just two beams represents a corner column.

Before deciding upon the test arrangement a sophisticated finite element computer program, developed specifically for analysing the three-dimensional response of restrained columns (10), was used to carry out a detailed investigation of the predicted subassemblage behaviour. Using the program, a basic subassemblage configuration was developed which would fail at manageable loads and which incorporated boundary conditions least sensitive to potential experimental errors. One significant outcome of this initial analytical study was the inclusion of a fixed (or near fixed) support condition at the base of all subassemblage specimens; the studies having shown that unlike a simulated pinned support condition, in which the influence of the small inherent rotational stiffness can be quite appreciable, small variations in the rotational stiffness of a stiff base support had a negligible effect on column behaviour.

All the subassemblages in the study comprised a 6.0m long 152x152x23UC column section with up to three 1.5m long 254x102x22UB beam sections. At this length the column slenderness, L/r_{yy}, was 164, however, due to the fixed base condition and the restraint from the beams, the effective slenderness Le/r_{yy} is significantly less. The section sizes used were similar to those in other recent studies of flexibly connected steel structures (2,8), and thus permitted close comparisons between various aspects of the experimental performance. The support condition at the remote ends of the beams permitted displacement in a direction parallel to the axis of the column, but prevented in-plane beam rotation. The centreline through the support therefore represented an axis of symmetry with each beam behaving similar to a beam of twice the actual length spanning 3.0m between adjacent columns in a frame.

The subassemblages were tested in a purpose built self-straining rig constructed from 7 tonnes of 305 x 102 RSC sections connected using over 300 20mm High Strength Friction Grip Bolts. Due to the restricted headroom available in the test area, all the specimens were tested with the column in a horizontal position. Although it is expected that in this orientation the self weight of the column will have a small influence on column behaviour, its effect can be taken into account in subsequent detailed analytical modelling of the tests. Figure 2 shows a subassemblage specimen installed in the test rig. A single point load was applied to each beam using up to three 250kN capacity hydraulic jacks acting at distances of between 400mm and 800mm from the column centreline. The jacks were load controlled and could therefore apply a constant beam load to the subassemblage despite the resulting member deformations. A 500kN capacity screw jack applied load to the head of the column. This jack was displacement controlled and enabled the subframe to be deformed beyond the failure load in a safe and controlled manner.

Subassemblage Instrumentation

It was important that the displacements and rotations resulting from three-dimensional deformation could be accurately monitored at specific points on the specimen. At the time of these experiments, there were no single proprietary instrumentation devices capable of performing such measurements. As a result, the authors developed a measurement system (6) consisting of up to seven Linear Voltage Displacement Transducers (L.V.D.T.) which was capable of accurately monitoring all six degrees of movement resulting from three-dimensional deformation.

[4]

The member forces which were of particular interest were those resulting from longitudinal strains, i.e. axial load (P), major axis moment (M_{xx}), minor axis moment (M_{yy}) and warping bi-moment (B). The strains were measured using adhesive fixed foil strain gauges with a gauge length of 10mm. In the elastic range, it would be possible to determine these four force components from the readings of just four gauges. However, at measurement locations on the column 10 strain gauges were used, four on each of the flanges and two on the web. The readings from the additional 'redundant' gauges were processed by a computer program which used a least square error approximation to generate the three-dimensional strain profile in both the elastic and the elastic-plastic ranges (7).

The force and displacement components which were measured during a test are summarised on the plan and elevation of the subassemblage shown in figure 3. A total of 154 logging channels was required, 108 for strain gauges (54 recording, 54 energising), 42 for L.V.D.T. monitoring, 3 monitoring the pressure in the hydraulic beam rams and a single channel for the load cell beneath the column head jack.

Subassemblage test procedure.

The aim of the test programme was to investigate the influence of the four basic connection types on subassemblage behaviour for different column orientations, under a series of different loading arrangements. The series of subassemblage tests are outlined in table 1.

Before commencing a test, the physical properties of the beam and column sections were determined. This included measurement of the geometric properties and the material properties from tests on coupons and stub columns. In each case, the procedures in current technical guidelines were followed.

An initial curvature was induced into the column to produce initial deflections at the column centre in the range of L/1000 to L/500. This had the advantage of predetermining the direction of failure, and thus enabled the L.V.D.T. displacement measuring systems to be used most effectively, and also ensured that the specimens failed in a controlled manner. In one instance however, test S6, an almost perfectly straight column was tested to investigate the ability of the analytical modelling techniques to predict the more dramatic bifurcation type failure mode.

During each test, the beam loads were applied first in a minimum of ten equal increments up to a predetermined limiting value which was then held constant. At the end of the beam loading phase, the column head jack was advanced, applying load to the column head until excessive deformation was observed, typically an 80mm minor axis deflection at the column centre. Load was applied at a rate corresponding to an increase in column stress of approximately 5 to 7 N/mm^2/minute. This compares with the 10 N/mm^2/minute loading rate recommended for stub column tests (3).

The data recording channels were scanned using an Orion Solatron Data Logging System with the raw experimental data stored on an IBM compatible computer. Scans were taken at every increment of beam loading, and at every 20kN increment during the subsequent column head loading phase. The complex nature of the displacement and force measurement systems meant that the raw experimental data had to be 'post-processed' on a Prime mainframe computer after completion of the test.

Results and Discussion

Table 2 shows the initial column deflection for each of the seven tests carried out to-date. Table 3 shows the beam load arrangements used in the tests and the resulting ultimate load capacities. The squash loads, derived from the stub column tests, are also presented for comparison purposes.

Although in certain circumstances beam loading arrangements were selected to induce large major axis moments, all the columns tested to-date have failed as a result of excessive minor axis deflection. The difficulties of inducing major axis failure in steel 'H' columns has been reported by Birnstiel (1). Figures 4a and 4b show the experimentally observed deflections and twists at the centre of column test S2, together with the analytically predicted values. Although large amounts of twist were eventually induced in all columns, in each case the amount of twist which occurred before incipient failure was surprisingly small. The implications of this apparent lack of interaction between the major and minor axes deformations is currently being investigated.

Figures 5a and 5b show the major and minor axis bending moments at the centre of column S2, whilst figures 6a and 6b show the major and minor axis moments at the top of column S4. The linear nature of the second phase of both the major axis moment diagrams again illustrates the lack of major-minor axis interaction. In the case of the top of column S4, the major axis moment is

[6]

approximately constant, equal to the applied beam moment, until just before failure when the column loses stiffness. The plot of minor axis moment at the top of column S4 illustrates the concept of moment reversal previously observed in model subassemblage tests (4). In the initial beam phase of loading, the beam is applying a disturbing moment to the column. As the column approaches failure, the applied moment reduces to zero and then becomes a negative restoring moment. This effect has been observed in all the column tests, the extent of restraint being dependent on the type of connection employed. It is evident from the above plots that the analytically predicted column behaviour using the finite element model (10), is very close to that observed in the experiments. Studies are presently continuing to validate the model for the full range of tests which have been conducted.

Conclusions

The test apparatus and instrumentation systems developed to conduct a series of large-scale restrained column tests have been described. The results obtained provide full test histories against which numerical simulations and/or design approaches may be verified. Particular features observed in the tests were the virtual absence of twisting and the occurrence of moment shedding as the column maximum loads were approached. The test results have yet to receive a full appraisal.

Acknowledgements

The experimental study carried out at the University of Sheffield and described in this paper has been supported by the Science and Engineering Research Council, the Building Research Establishment and the Steel Construction Institute.

References

1. Birnstiel, C. "Experiments on H-columns under biaxial bending" Journal of the Structural Division, A.S.C.E., No. ST10, October 1968, pp. 2429-2449.

[7]

2. Celikag, M. and Kirby P.A., "Out of plane moment rotation response for common joints", International Colloquium on Bolted and Special Structural Connections, Moscow, May 1989, Vol.2, pp.136-142.

3. Galambos, T.V., "Guide to stability design criteria for metal structures", Structural Stability Research Council, 4th Edition, Wiley Interscience 1988.

4. Gent, A.R and Milner H.R. "The ultimate load capacity of elastically restrained H-columns under biaxial bending", Proc. Institution of Civil Engineers, Vol. 41, December 1968, pp. 685-704

5. Gibbons, C., P.A. Kirby and Nethercot D.A., "Experimental assessment of the elastic-plastic response of thin-walled structural steel sections" (in preparation).

6. Gibbons C., "The behaviour of biaxially loaded beam-columns in flexibly connected subframes", Ph.D. Thesis, University of Sheffield, England. (in preparation)

7. Gibbons, C., P.A. Kirby and Nethercot D.A., "The development of a device for measuring the 3-dimensional deformation of steel columns." (in preparation).

8. Kirby, P.A., Davison, J.B. and Nethercot, D.A., "Large scale tests on column subassemblages and frames". Connections in steel structures: Behaviour Strength and Design, ed. R. Bjorhovde, J. Brozzetti and A. Colson, Elsevier Applied Science Publishers, 1988, pp. 291-299.

9. Nethercot, D.A., Kirby P.A. and Rifai, A.M., "Columns in partially restrained construction: Analytical studies", Canadian Journal of Civil Engineering, Vol. 14, 1987, pp. 485-497.

10. Wang Y.C. and Nethercot D.A., "Ultimate strength analysis of three-dimensional column subassemblages with flexible connections", Journ. Const. Steel Res., No. 9, 1988, pp. 235-264.

[8]

Subframe Test	Beam to Column Connection Type	Column * Orientation	Number of Beams
S1	Web Cleats	A	3
S2	Flange Cleats	A	3
S3	Web and Seat Cleats	A	3
S4	Flush End Plate	A	2
S5	Web Cleats	B	3
S6	Flange Cleats	B	3
S7	Web and Seat Cleats	B	3
S8	Web Cleat	A	3
S9	Flange Cleat	A	3
S10	Web and Seat Cleat (B1 & B3) Flush End Plate (B2)	A	3

* Column Orientations shown in section

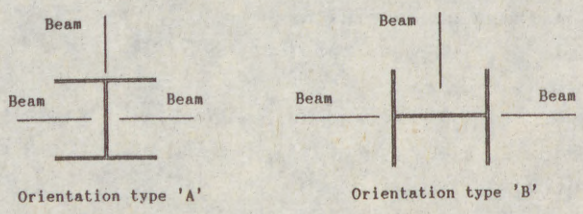

Table 1: Details of subassemblage tests

Subframe Test	Column head load eccentricity (mm)		Initial deformations at mid column (mm)	
	Major	Minor	Major	Minor
S1	+7.0	-7.0	+1.0	+6.0
S2	+6.5	-9.5	-1.5	+9.0
S3	+7.5	-7.5	+3.0	+9.0
S4	+8.0	-9.0	+1.0	+7.5
S5	-10.0	0.0	+4.0	+9.0
S6	-12.0	-2.0	+1.5	+0.5
S7	-6.5	-1.0	+6.5	+5.0

Table 2: Initial column deformations and applied load eccentricity

Subframe Test	Beam load offset (mm)			Nominal Maximum Beam Load (kN)			Total Failure Load (kN) Pult	Squash Load (kN) Psq
	B1	B2	B3	B1	B2	B3		
S1	400	400	400	5	50	50	467.4	913.1
S2	630	700	633	50	50	50	503.0	892.0
S3	630	700	633	50	50	50	542.4	982.1
S4	-	695	625	-	50	50	494.5	934.7
S5	617	708	637	30	30	60	479.0	938.5
S6	615	713	635	30	30	60	614.0	941.5
S7	845	709	830	45	45	90	490.0	959.7

Table 3: Beam load arrangements and ultimate column capacities

[9]

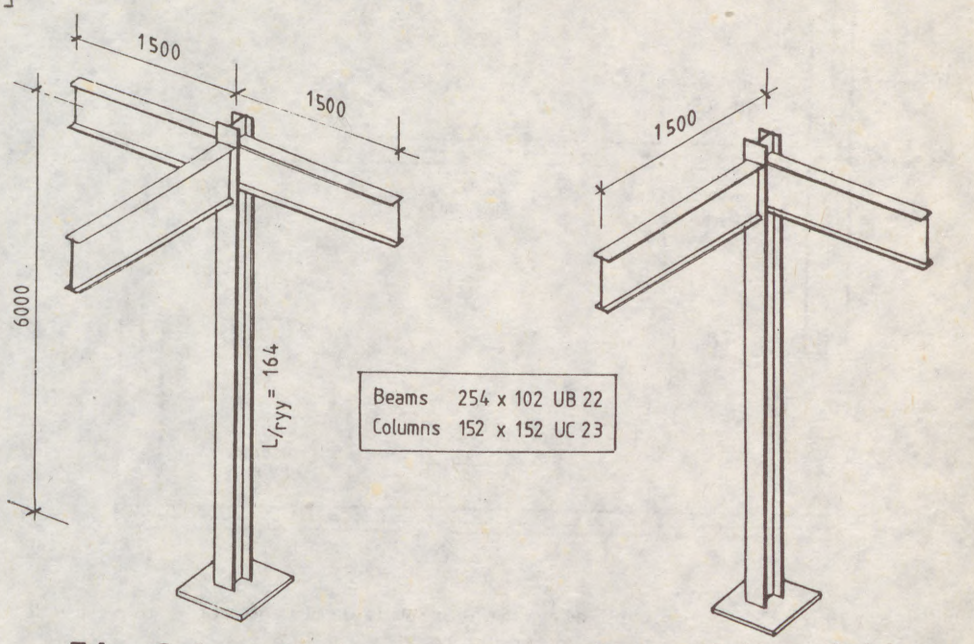

Figure 1: Basic subassemblage configurations

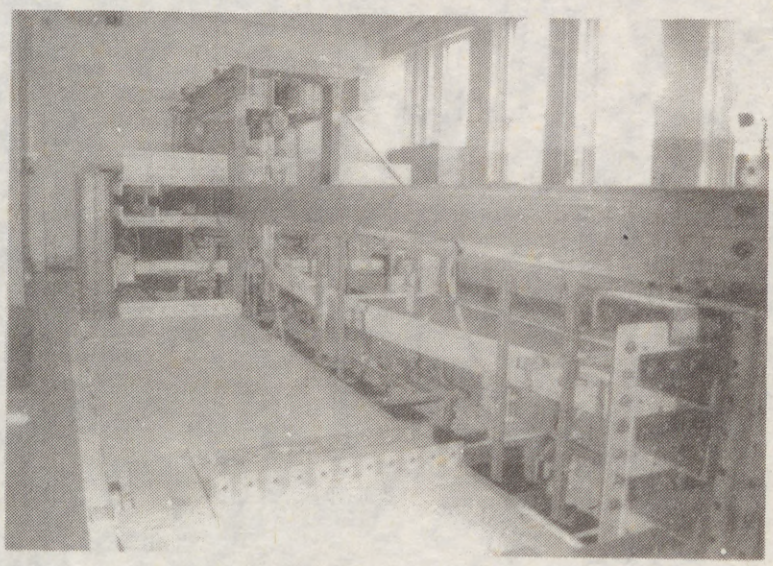

Figure 2: Photograph of a failed subassemblage in the testing rig

[10]

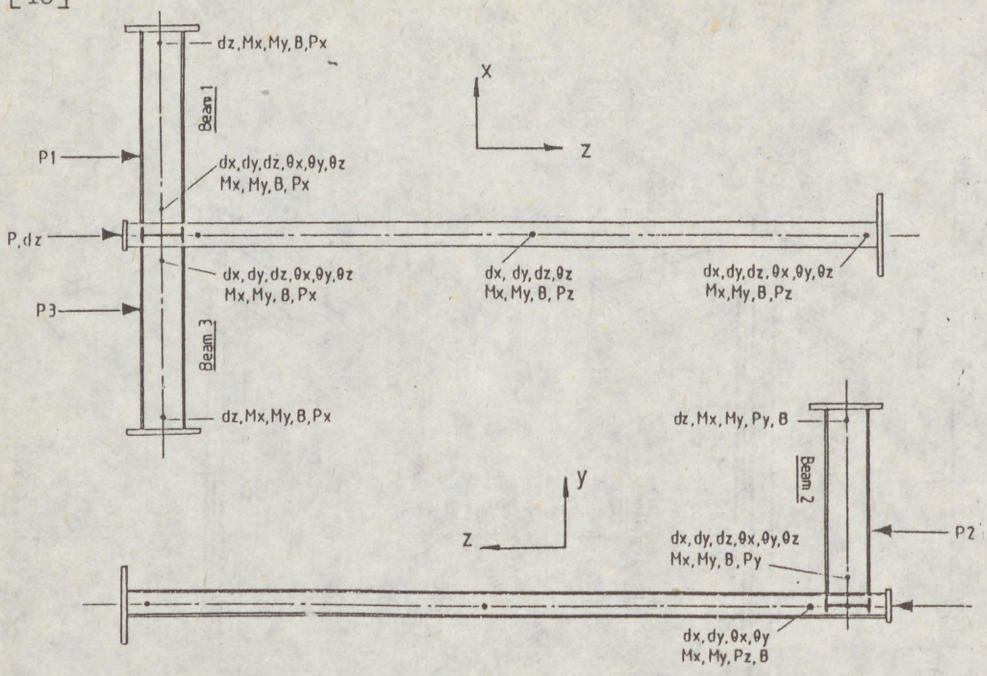

Figure 3: Plan and elevation of subassemblage showing parameters monitored during a test

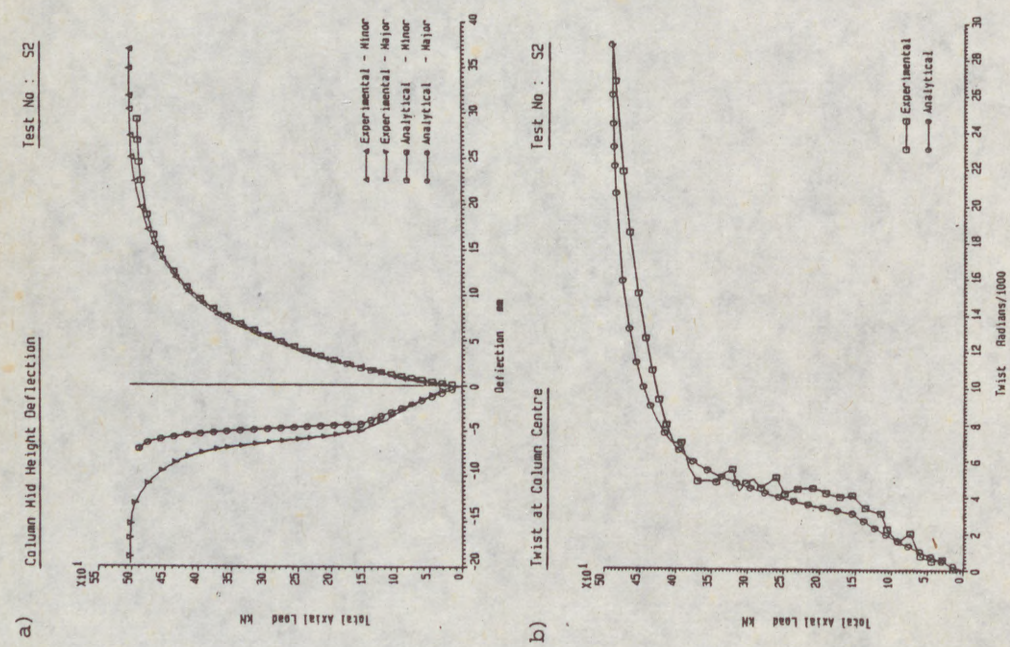

Figure 4

Figure 4

a) Bending Moments at Column Centre — Test No : S2

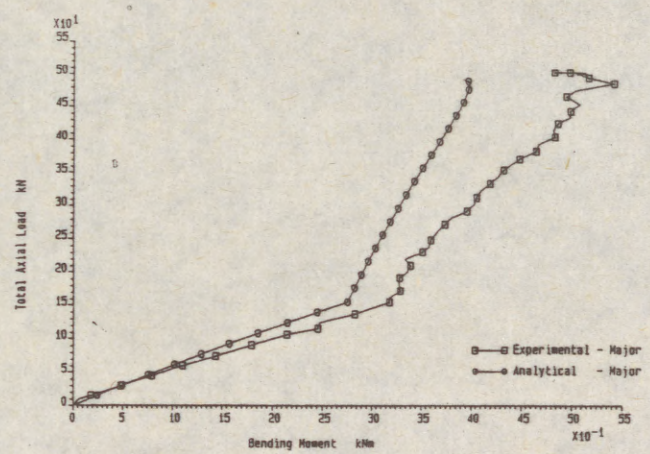

b) Bending Moments at Column Centre — Test No : S2

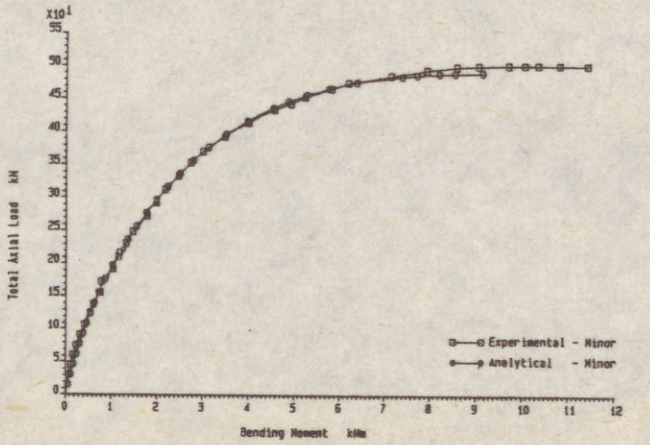

Figure 5

a) Bending Moments at Column Top — Test No : S4

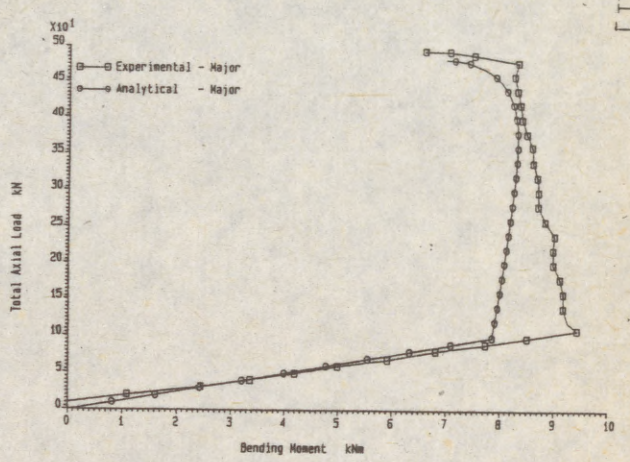

b) Bending Moment at Column Top — Test No : S4

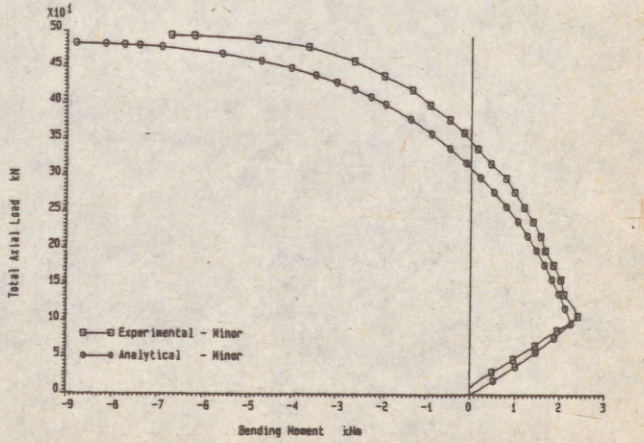

Figure 6

(1)
GIZEJOWSKI, Marian (1)
MZILIKAZI, Pearson (2)

IN-PLANE ELASTIC STABILITY OF SEMI-RIGID FRAMEWORKS

INTERNATIONAL COLLOQUIUM
STABILITY OF STEEL STRUCTURES
BUDAPEST, HUNGARY, 1990
PRELIMINARY REPORT

Summary: The in-plane stability analysis of elastic semi-rigid frameworks is presented. The behaviour of flexible joint connections is represented by assumming an immovable spring with initial stiffness constant. The external boundary conditions are modeled by employing linear springs, both translational and rotational. The matrix finite element formulation is presented using non-conventional shape function vector derived herein. The solution of eigenvalue and eigenvector problem is demonstrated through several examples considering a portal frame with different boundary conditions.

1. INTRODUCTION

The classical stability analysis of steel framed structures assumes that the beam-to-column connections satisfy the requirements of pinned joints or rigid joints. Pinned joints maintain only continuity for linear displacements while the rigid joints maintain continuity resulting in the same angle between connected members during deformations. A number of experimental results on different types of steel, particularly bolted joints have shown that beam-to-column connections are flexible and have to be classified as semi-rigid joints with the degree of flexibility being dependent upon the particular arrangement of the joint. In the past, the behaviour of structural connections was investigated extensively, while progressively efforts were directed to explain the influence of connection flexibility upon member and subassemblage

---

(1) Senior Lecturer, Civil Engineering Department, University of Zimbabwe.
(2) Research Student, Civil Engineering Department, University of Zimbabwe

perfomances, and finally to account for the effect of flexible connections in complete frame analysis, [1], [2] ,[3], [4]. The up-to-date experimental and theoretical investigations have proved that connection flexibility has significant effect on frame strength, determination of which requires more accurate analyses accounted for both material and geometrical nonlinearities. In the paper the refined finite element analysis is presented for stability of elastic semi-rigid frames. Developed model may also be used for the nonlinear analysis of semi-rigid frames by finite element method.

2. SHAPE FUNCTION VECTOR FOR SEMI-RIGID LINE FINITE ELEMENT

The connection flexibility may be fully described by providing its so-called moment rotation characteristic (see Fig. 1).

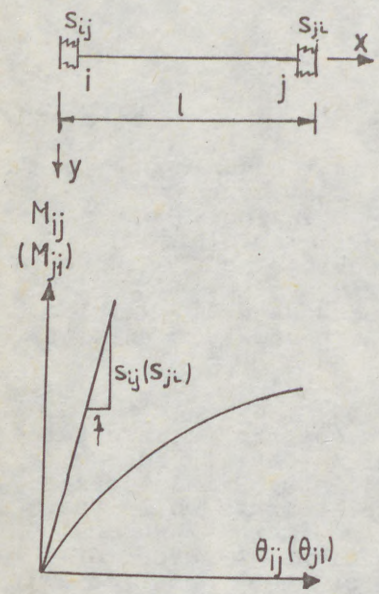

Fig. 1

The slope of the curve taken for moment of zero value is usually referred to as the initial rotational stiffness s_{ij} (s_{ji}), while $f_{ij} = 1/s_{ij}$ ($f_{ji} = 1/s_{ji}$) indicates its initial rotational flexibility. Since frames are under joint loads, giving primarily axial compressive (tensile) forces, only the initial spring constants are needed for stability analysis. Considering the prismatic line element (ij) elastically connected at joints (i,j), its deflected shape may be expressed in matrix form as

$$u_0(X) = X_u^T C_u, \qquad v_0(X) = X_v^T C_v, \tag{1}$$

where $X_u^T = \langle 1, X \rangle$, $C_u^T = \langle C_1, C_4 \rangle$,

$X_v^T = \langle 1, X, X^2, X^3 \rangle$,

$C_v^T = \langle C_2, C_3, C_5, C_6 \rangle$

and $X = (2x/l)-1$ is nondimensional co-ordinate.

The relationship between the vectors of integral constants; C_u, C_v and the vectors of element nodal displacements; $q_u^{(1)}$, q_v may be obtained by including the member kinematic and static boundary conditions

$$u_0(-1) = q_1, \quad u_0(1) = q_4, \quad v_0(-1) = q_2, \quad v_0(1) = q_5,$$

$$EIv_0''(-1) = s_{ij}[q_3 - v_0'(-1)]l, \quad EIv_0''(1) = s_{ji}[q_6 - v_0'(1)]l, \tag{2}$$

where q_1, q_4 are member longitudinal displacements at joints

(3)
(i,j), respectively; q_2, q_5 are member transverse displacements and q_3, q_6 are rotational displacements at joints (i,j), respectively. Using matrix notation it follows that

$$C_u = L_u\, q_u^{(1)}, \quad C_v = L_v\, q_v^{(1)} . \tag{3}$$

Solving equations (3) for unknown integral constants and substituting for equations (1), the following is obtained

$$u_0(X) = F_u^T\, q_u^{(1)}, \quad v_0(X) = F_v^T\, q_v^{(1)}, \tag{4}$$

where F_u is the standard linear shape function vector

$$F_u^T = \langle -0.5(X-1),\ 0.5(X+1) \rangle$$

and F_v is the cubic shape function vector for semi-rigid line finite element given by

$$F_v^T = X_v^T\, (L_v)^{-1} = \langle f_1,\ f_2,\ f_3,\ f_4 \rangle,$$

where $f_1=\{(ef-dg+ag-bf+f+g)+(ag-bf)X-gX^2+fX^3\}/(ef-dg)$,

$f_2=l\{(ef-dg-2fb-bd+2ag+ae+2f+d+2g+e)+(ef-dg-2fb-bd+2ag+ae)X$

$-(2g+e)X^2+(2f+d)X^3\}/\{2(ef-dg)\}$,

$f_3=\{(bf-ag-f-g)+(bf-ag)X+gX^2-fX^3\}/(ef-dg)$,

$f_4=l\{(bd-ae-d-e)+(bd-ae)X+eX^2-dX^3\}/\{2(ef-dg)\}$

and $a=4EI/(ls_{ij}) - 2$, $b=-12EI/(ls_{ij}) + 3$, $d=8EI/(ls_{ij}) - 4$,

$e=-24EI/(ls_{ij}) + 4$, $f=4EI/(ls_{ji})-4EI/(ls_{ij}) + 4$,

$g=12EI/(ls_{ij})+12EI/(ls_{ji})$.

3. SECOND-ORDER EQUILIBRIUM EQUATIONS

The following assumptions are used to formulate the basic equilibrium equations for frame analysis

(1) The member is straight, prismatic and symmetric about the plane of frame (the member(x,y) plane). All member x-axes are laying in the plane of the frame (the structure (X,Y) plane). The member reference axis is passing through the point O on the cross section which coincides with the centroid of the cross section. Thus the cross sectional axes (y,z) are principal axes.
(2) Loads are conservative forces applied in the plane of the frame only at the ends of the element.
(3) Only in-plane deformations occur and Euler-Bernoulli hypothesis is recognized.
(4) Nonlinear kinematic relations are derived on the basis of small rotational displacements of the elemental length, dl(=dx) of line element.

(4)

The above assumptions permit the axial displacement $u=u(x)$ and transverse displacement $v=v(x)$ of an arbitrary point on an element cross-section to be expressed in terms of the displacements of the reference axis; $u_0=u_0(x)$ and $v_0=v_0(x)$. Thus the only one non-zero component of the strain tensor associated with normal stresses σ_x may be expressed as

$$\varepsilon_x = u' + 0.5\,[\,(u')^2 + (v')^2\,], \tag{5}$$

where $u' = u_0' - y\,v_0''$, $v' = v_0'$.

In the following the symbol $(\,)'$ will be used to denote x-derivatives.

Involving the principle of virtual displacements, the element eqilibrium equation takes the form

$$INT - EXT = 0, \tag{6}$$

where INT is the external virtual work

$$INT = \int_V \sigma_x\,\delta\varepsilon_x\,dV$$

and EXT is the external work done

$$EXT = \delta q^{(1)T}\,Q^{(1)},$$

where V is the element volume, and work done by body forces and surface tructions is excluded. The vectors $Q(1)$ and $q(1)$ are vectors of nodal forces and displacements, respectively

$$Q^{(1)T} = < N_{ij}, N_{ji}, T_{ij}, M_{ij}, T_{ji}, M_{ji} >,$$

$$q^{(1)T} = <u_0(-1), u_0(1), v_0(-1), v_0'(-1), v_0(1), v_0'(1)>. \tag{7}$$

Perfoming variation of the normal strain component given by equation (5), substituting this into equation (6), integrating over the area A of cross section and defining the stress resultants as

$$n = \int_A \sigma_x\,dA,\quad m = \int_A \sigma_x\,y\,dA,\quad m^* = \int_A \sigma_x\,y2\,dA \tag{8}$$

yields

$$\int_1 [n\,\delta u_0' - m\,\delta v_0'' + n(u_0'\,\delta u_0' + v_0'\,\delta v_0') + m^* v_0''\,\delta v_0'']\,dl - \delta q^{(1)T}\,Q^{(1)} = 0. \tag{9}$$

Taking linear elastic response (Hooke's Law)

$$\sigma_x = E\,\varepsilon_x \tag{10}$$

and assuming only axial uniform stress state for elements, the stress resultants can be expressed in terms of displacement and rigidity resultants as

(5)

$$n = \int_A E\ \varepsilon_x^{(1)}\ dA = EA\ u_0',$$

$$m = \int_A E\ \varepsilon_x^{(1)}\ y\ dA = -EI\ v_0'', \qquad (11)$$

in which EA and EI are the axial and flexural rigidities

$$EA = \int_A E\ dA, \quad EI = \int_A E\ y^2\ dA.$$

To derive equations (11) only the linear part of the normal strain component is assumed to be contributed

$$\varepsilon_x^{(1)} = u' = u_0' - y\ v_0''. \qquad (12)$$

To form the second-order element equilibrium equation the third stress resultant is expressed in the form

$$m^* = \int_A \sigma_x\ y^2\ dA = (n/A) \int_A y^2\ dA = n\ r^2, \qquad (13)$$

where r is the radius of gyration of the cross section ($=\sqrt{I/A}$). It yields

$$EI \int_l (r^{-2}\ u_0'\ \delta u_0' + v_0''\ \delta v_0'')\,dl +$$

$$n \int_l (u_0'\ \delta u_0' + v_0'\ \delta v_0' + r^2 v_0''\ \delta v_0'')\,dl - \delta q^{(1)T}\ Q^{(1)} = 0. \qquad (14)$$

To derive the finite element matrices we use equations (4) to perform the approximate deflected shape of the line element. Recognizing that dl = dx = (1/2) dX, substituting equations (4) and their derivatives into equation (14) yields

$$EI(1/2) \int_{-1}^{1} [r^{-2}\ \delta q_u^{(1)T} T_{F_u}' T_{F_u}'\ q_u^{(1)} + \delta q_v^{(1)T} T_{F_v}'' T_{F_v}''\ q_v^{(1)}]\,dX +$$

$$n(1/2) \int_{-1}^{1} [\ \delta q_u^{(1)T} T_{F_u}' T_{F_u}'\ q_u^{(1)} + \delta q_v^{(1)T} T_{F_v}' T_{F_v}'\ q_v^{(1)} +$$

$$r^2\ \delta q_v^{(1)T} T_{F_v}'' T_{F_v}''\ q_v^{(1)}]\,dX = \delta q^{(1)T}\ Q^{(1)}. \qquad (15)$$

Carrying out integration, recognising the arbitrary nature of $\delta q(1)$, the second order equilibrium equation may be written in matrix form as

$$k_s^{(1)}\ q^{(1)} = Q^{(1)}, \qquad (16)$$

where $k_s^{(1)} = k^{(1)} + k_g^{(1)}$ is the so-called element secantial stiffness matrix which is subdivided into the element elastic stiffness matrix, $k^{(1)}$ and the geometric stiffness matrix, $k_g^{(1)}$. These again may be expressed as sum of two components

$$k^{(1)} = k_u^{(1)} + k_v^{(1)}, \qquad (17)$$

$$k_g^{(1)} = k_{gu}^{(1)} + k_{gv}^{(1)}, \qquad (18)$$

where $k_u^{(1)}$ and $k_v^{(1)}$ are the axial and flexural components of the elastic stiffness matrix, respectively

(6)

$$\mathbf{k}_u^{(1)} = EI/(l\, r^2)\left[\begin{array}{c|c} \underline{\mathbf{k}}_u^{(1)} & \mathbf{0} \\ \hline \mathbf{0}^T & 0 \end{array}\right], \quad \underline{\mathbf{k}}_u^{(1)} = \left[\begin{array}{c|c} 1 & -1 \\ \hline -1 & 1 \end{array}\right],$$

$$\mathbf{k}_v^{(1)} = EI/\, l \left[\begin{array}{c|c} \mathbf{0} & \mathbf{0} \\ \hline \mathbf{0}^T & \underline{\mathbf{k}}_v^{(1)} \end{array}\right]$$

and $\mathbf{k}_{gu}^{(1)}$ and $\mathbf{k}_{gv}^{(1)}$ are the similar components of the geometric stiffness matrix

$$\mathbf{k}_{gu}^{(1)} = n/l \left[\begin{array}{c|cccc} \underline{\mathbf{k}}_{gu}^{(1)} & \multicolumn{4}{c}{\mathbf{0}} \\ \hline & 1 & 0 & -1 & 0 \\ & & 0 & 0 & 0 \\ \text{symm.} & & & 1 & 0 \\ & & & & 0 \end{array}\right], \quad \mathbf{k}_{gv}^{(1)} = n/l \left[\begin{array}{c|c} \mathbf{0} & \mathbf{0} \\ \hline \mathbf{0} & \underline{\mathbf{k}}_{gv}^{(1)} \end{array}\right].$$

The finite element matrices $\mathbf{k}_v^{(1)}$ and $\mathbf{k}_{gv}^{(1)}$ are given by

$$\underline{\mathbf{k}}_v^{(1)} = \begin{bmatrix} A_{S2} & A_{S3} & A_{S4} & A_{S5} \\ & A_{S6} & A_{S7} & A_{S8} \\ \text{symm.} & & A_{S9} & A_{S10} \\ & & & A_{S11} \end{bmatrix}, \quad \underline{\mathbf{k}}_{gv}^{(1)} = \begin{bmatrix} A_{C2} & A_{C3} & A_{C4} & A_{C5} \\ & A_{C6} & A_{C7} & A_{C8} \\ \text{symm.} & & A_{C9} & A_{C10} \\ & & & A_{C11} \end{bmatrix},$$

where $A_{S2}=64(3f^2+g^2)/\{l^2(ef-dg)^2\}$, $A_{S9}=A_{S2}$, $A_{S4}=-A_{S2}$,

$A_{S3}=32\{3f(2f+d)+g(2g+e)\}/\{l(ef-dg)^2\}$, $A_{S7}=-A_{S3}$,

$A_{S5}=-32(3fd+eg)/\{l(ef-dg)^2\}$, $A_{S10}=-A_{S5}$,

$A_{S6}=16\{3(2f+d)^2+(2g+e)^2\}/(ef-dg)^2$,

$A_{S8}=-16\{3d(2f+d)+e(2g+e)\}/(ef-dg)^2$, $A_{S11}=16(3d^2+e^2)/(ef-dg)^2$,

$A_{C2}=\{64(3f^2+g^2)/z^2+2(2x^2+4xf+8g^2/3+18f^2/5)-(ef-dg)^2\}/(ef-dg)^2$,

$A_{C3}=l\{32(3f(2f+d)+g(2g+e))/z^2+2(xy+xw+4gv/3+fy+9fw/5)\}$
$/(ef-dg)^2$,

$A_{C5}=l\{-32(3fd+eg)/z^2+2(ux-dx-4ge/3+fu-9fd/5)\}/(ef-dg)^2$,

$A_{C6}=l^2\{16(3(2f+d)^2+(2g+e)^2)/z^2+2(y^2/2+yw+2v^2/3+9w^2/10)\}$
$/(ef-dg)^2$, $A_{C4}=-A_{C2}$, $A_{C7}=-A_{C3}$,

$A_{C8}=l^2\{-16(3d(2f+d)+e(2g+e))/z^2+2(uy/2-dy/2-2ev/3+wu/2-9wd/10)\}$
$/(ef-dg)^2$, $A_{C4}=-A_{C2}$, $A_{C7}=-A_{C3}$, $A_{C9}=A_{C2}$, $A_{C10}=-A_{C5}$,

$A_{C11}=l^2\{16(3d^2+e^2)/z^2+2(u^2/2-ud+2e^2/3+9d^2/10)\}/(ef-dg)^2$,

(7)

and $x=ag-bf$,
$y=ef-dg-2fb-bd+2ag+ae$,
$u=bd-ae$,
$v=2g+e$,
$w=2f+d$

and z is the element slenderness ratio (=l/r) and other variables are as assigned before.

For the element rigidily connected at both ends, the matrices $k^{(1)}$ and $k_g^{(1)}$ reduce to the classical elastic slope deflection matrix and the classical component of geometric stiffness matrix extended to account for the effect of slenderness ratio. In this case we can simply use the static condensation scheme to allow the matrices $k_v^{(1)}$ and $k_{gv}^{(1)}$ for member boundary conditions. For element hinged at both ends these matrices become zero-matrices.

Applying the standard finite element procedure, the element matrices can be transformed from the local member co-ordinate system to the global structure co-ordinate system and then assembled to obtain the structure matrices. Thus, for member axial forces being known from the first-order analysis, we obtain the total structure stability equilibrium equation as

$$(K_s + \Lambda K_g) r = 0, \qquad (19)$$

where Λ is an unknown load parameter.
Equation (19) corresponds to the linear eigenvalue and eigenvector problem. The lowest load parameter which satisfies equation (19) gives the load level corresponding to the critical state of the structure.

4. NUMERICAL EXAMPLES

The compter program **SASERF** (Stability Analysis of SEmi-Rigid Frames) is developed for the numerical studies. The program is written in Fortran IV and implemented on IBM-PC compatible computers. The dynamic reservation scheme for the core memory is adopted and Ryan McFarland Fortran Compiler (version 2.42) is used to compile the program. The stability problem is solved iteratively for the lowest eigenvalue and corresponding eigenvector. As a convergence criterion for the iteration process the Euclidean norm for the eigenvector is used.

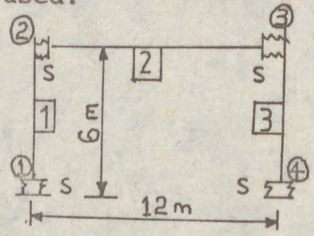

Fig. 2

Fig.2 shows the frame under consideration, elastically supported at joint 1 and 4. Element 2, connected at joint 2 and 3, is treated as semi rigid element. Fistly the critical loads were calculated assuming classical finite element matrices for rigidly connected line element and static condensation scheme where appropriate to allow for member boundary conditions. Next, using computer program **SASERF** the critical loads where calculated for different boundary conditions to display the effect of

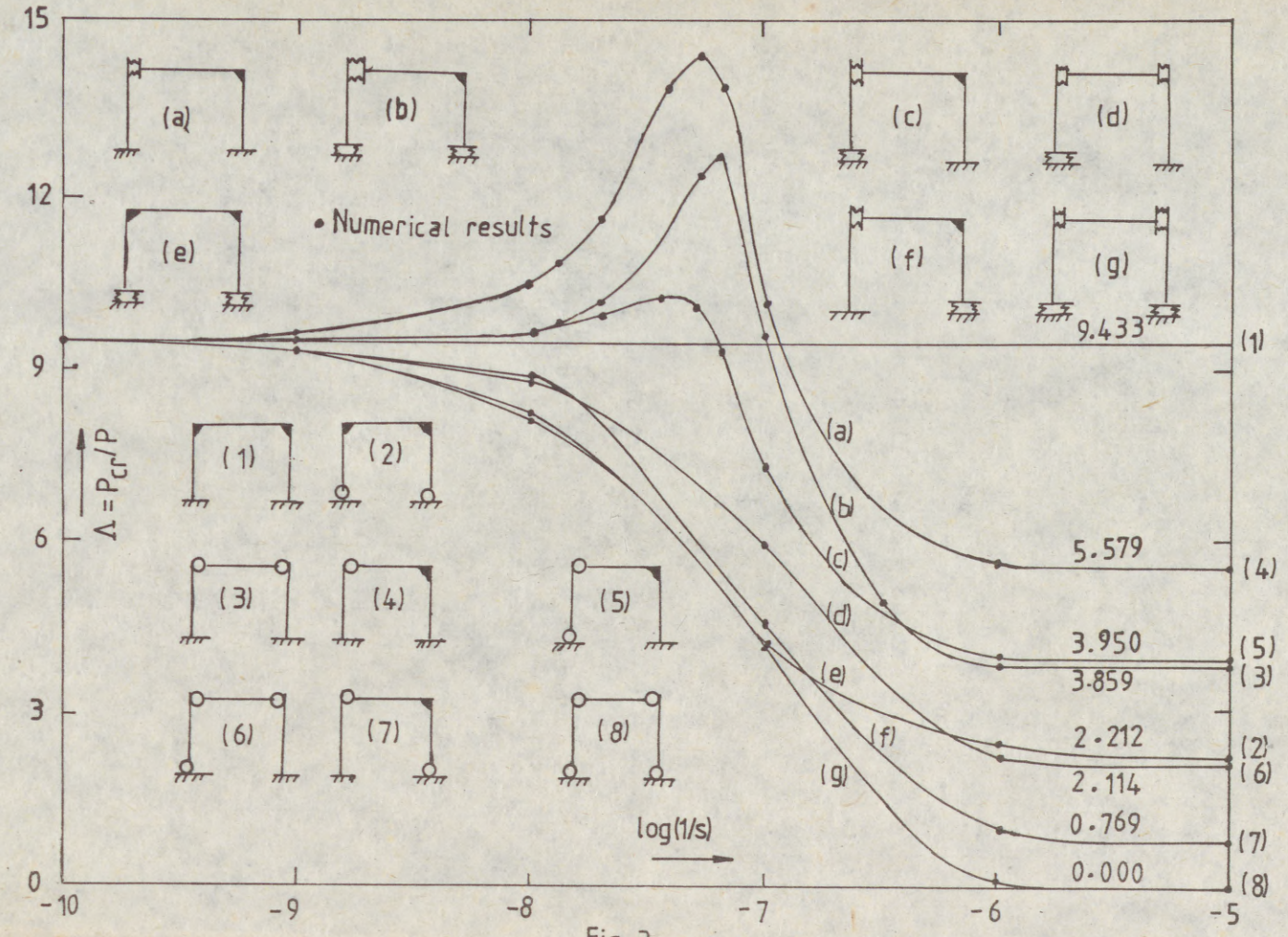

Fig. 3

(8)

(9) se cr in To we re sm jo

5. fr th in

REF

[1]

[2]

[3]

[4]

[5]

semi-rigid connections and elastically supported joints on critical load. All considered cases and the results are plotted in Fig.3. For all cases a relative error of 10^{-4} is assumed. To solve each frame for critical load parameter four iterations were needed as an average . The results presented here and reported in [5] show that the critical load for each case smoothly approaches the solution obtained for ideal hinges if joint spring flexibilities increase.

5. REMARKS

A method of the stability analysis of elastic semi-rigid frames has been presented. The problem is formulated within the concept of finite element analysis. The numerical examples indicate that efficiency of the method is satisfactory.

REFERENCES

[1] Bijlaard F.S.K. ,Zoetemeijer P., Influence of Joint Characteristics on the Structural Response of Frames. Steel Structures, Recent Research Advances and their Applications to Design. Ed. M.N.Pavlovic, Elsevier Applied Science Publishers, London-New York, 1986 (109-133).

[2] Nethercot D.A., The Behaviour of Steel Frame Structures Allowing for Semi-Rigid Joint Action. Steel Structures, Recent Research Advances and their Applications to Design. Ed. M.N.Pavlovic, Elsevier Applied Science Publishers, London-New York, 1986 (135-151).

[3] Simitses G.J. ,Vlahinos A.S., Elastic Stability of Rigidly and Semi-Rigidly Connected Unbraced Frames. Steel Framed Structures, Stability and Strength. Ed. R.Narayanan, Elsevier Applied Science Publishers, London-New York, 1985 (115-152).

[4] Gerstle K.H., Flexibly Connected Steel Frames. Steel Frame Structures. Stability and Strength. Ed. R.Narayanan, Elsevier Applied Science Publishers, London-New York, 1985 (205-239).

[5] Mzilikazi P., Stability of Semi-Rigid Frames. Lab. Project, University of Zimbabwe, Department of Civil Engineering, 1989 (manuscript).

Fig. 3

HEGEDŰS, László (1)

INTERACTION BETWEEN THE LOADING CONDITIONS AND STRUCTURAL RESPONSE IN STABILITY TESTS OF FRAMES

INTERNATIONAL COLLOQUIUM
STABILITY OF STEEL STRUCTURES
BUDAPEST, HUNGARY, 1990
PRELIMINARY REPORT

Summary: The paper deals with some special questions of the experimental research being important when tests of frames are carried out and the load bearing capacity of the structure is lost because of any instability phenomenon. An example is presented to illustrate the difference between the real and "virtual" structural behaviour, which is depending on the character of the loading and to show that in certain conditions a structure, which became unstable because of the instability of its element, is able to turn again to a stable state before complete loss of its load bearing capacity.

Introduction

When the mathematical analyses of structures are carried out, a number of approximations and suppositions has to be done to simplify the difficulties of getting a solution and to increase the possibility of handling the complexity of the problem under investigation. These are the reasons why the mathematical model of a structure is always different (usually simplified) from the real one and the behaviour of the mathematical model of course will differ from that of the real structure.

An other possibility is to carry out the investigations on physical models. Physical models are able to follow the real behaviour on a more accurate level because the necessity of simplifications is lower. That's why physical models can give a real solution to a certain problem or a possibility for checking the results of an analysis carried out on the mathematical model.

If a structure can be examined on a prototype, the correspondence between the real structural behaviour and the measured one can be closer. Even in this case the structure under investigation is "cut out" from the

(1) Research worker
Department of Steel Structures
Technical Universitiy of Budapest, Hungary

(2)

structural system, first of all its supporting conditions and connections to the other parts of the system are only worse or better imitations of the real ones. All of these differences between the structure and the structural model will cause a modified behaviour of the model.

The tested model gets into contact with the external loads which are usually again models of the real ones.

Types of loading in experimental research

Real load carrying structures are affected mainly by meteorological (as snow and wind) or dead loads, e.g. by self-weights of the vehicles in case of bridges or that of the cranes and loads lifted in industrial buildings, etc.

The common characteristic of these kinds of loads is that the intensitiy of the load is independent from the properties of the structure. When a load of this type is applied to the structure, it's on the structure, how to respond to it.

As usually in the practice we suppose that the structural behaviour can be characterized and followed by the connection between one pair of the characteristric deformations and the external loads (Fig. 1).

Load is independent from deflection

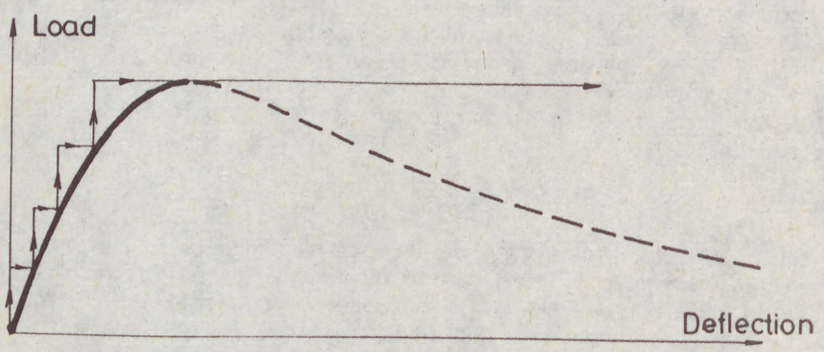

Self-weight load

Fig. 1

A self-weight-type-load can be represented in this case with horizontal lines in the figure, as the intensity of the load is independent from the properties of the structure, so after application of the load the structure will find its position in which the equilibrium of the external and internal forces can take place. But the possibility of the equilibrium is given only till the moment while the intensity of the external load is exactly lower than the limit of the load bearing capacity of the structure.

It can be noticed here that by applying self-weight-type-loading to the structure only the increasing part of the load-deflection diagram can be

(3)
followed (when the slope of the curve or which is equal to it, the rigidity of the structure is higher than zero). This is the main disadvantage of self-weight-type-loads beside the handling of relatively heavy weights.

Researchers are always interested in knowledge of the whole structural behaviour because different safety factors are declared in the standards against failure depending on the form of the descending path in the diagram (HEGEDÜS-IVÁNYI (1986)). That's why other types of loads are more often preferred in the experimental research.

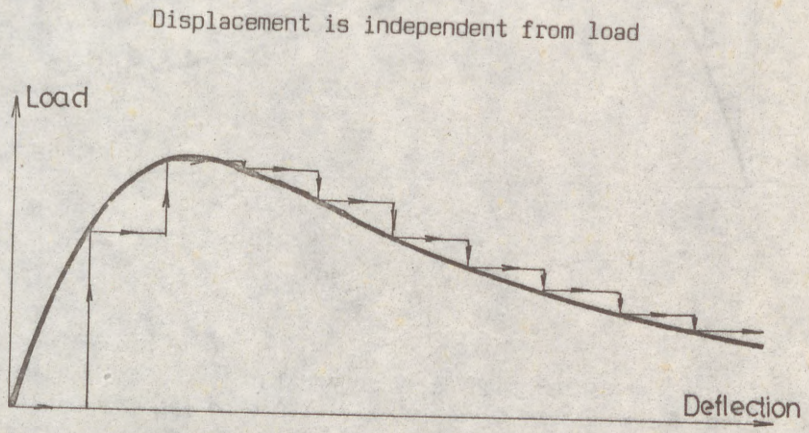

Kinematic load

Fig. 2

For this purpose those types of loads are chosen which have a deflection dependent intensity as the so-called kinematic (Fig. 2) and "spring-type" (Fig. 3) loads. In the first case a deflection or a system of deflections are applied to the structure and depending on the rigidity characteristics of the structure the intensity of the load(s) will be determined by the structural response. This kind of loading is realized usually by the testing machines. Hydraulic jacks are the typical examples for the "spring-type" loading, when by injection of oil its volume and preasure in the jack is increased. Because of the deflection increases of the structure the preasure and therefor the external loads are changing in a structure-dependent way.

Loading and structure, as a system

An other, very important aspect is that the loading and the structure together form a closed system, because the loading system and the structure are connected to each other and both to a fixed basis. Therefor the behaviour of one component in the system is depending on and modified by the behaviour of the other, that is an equilibrium state can be achieved by interaction of the two subsystems.

Load and displacement is in interaction with the structure

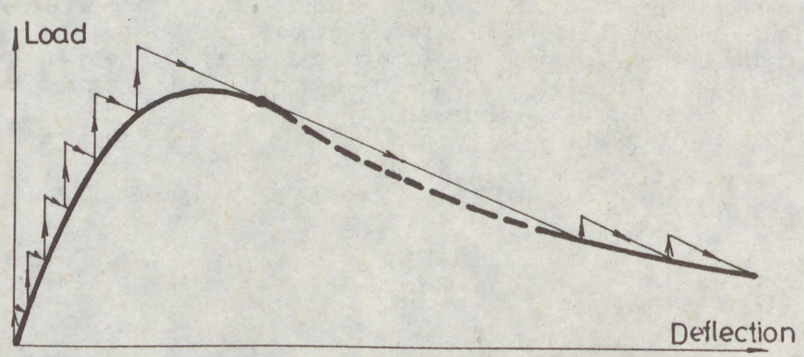

Spring load

Fig. 3

If the subsystem of the loading is an absolutely rigid one (which is the case of the kinematic load) its character can be represented by vertical lines in the load-deflection diagrams, while "spring-type" loads give of negative (descending) slope in the figure.

In the latter case the real value of the slope is depending on the properties of the system, that is on the actual rigidity of the structure and the loading subsystem.

From this point of view the "spring-type" loading can be considered as a general one and its specific cases are the

- self-weight-type-loads, when the rigidity of the loading subsystem is equal to zero or its elasticity is infinite, and its opposite is the
- kinematic loading, when the rigidity of the loading subsystem is infinite or its elasticity is equal to zero.

Some of the specific aspects of these questions are analysed by IVÁNYI (1979), SZATMÁRI (1986) and ESZE (1986).

Following from the facts which were discussed above the analysis of the loading process should be carried out on the system containing the structure and the loading subsystem. This system is in a stable state while its rigidity is greater than zero that is the rigidity of the structure should be greater than the minus one times the rigidity of the loading subsystem. All those states of the behaviour can be analysed by a step-by-step loading method which fulfill the condition of the stability of the system. It means that unstable states of the structure can be analysed, too, while the system is stable.

At the first sight the kinematic load can be considered as the most suitable one, because in the longest part of the structural behaviour can be followed by it. But even in this case there is the possibility of the instability, when at the same displacement state but at several and different load levels can the equilibrium conditions be fulfilled.

Illustrative example

A computer simulation program has been developed to analyse the influence of the structural properties of a simple frame, which can cause a temporary unstable state before reaching the maximum of the load bearing capacity.

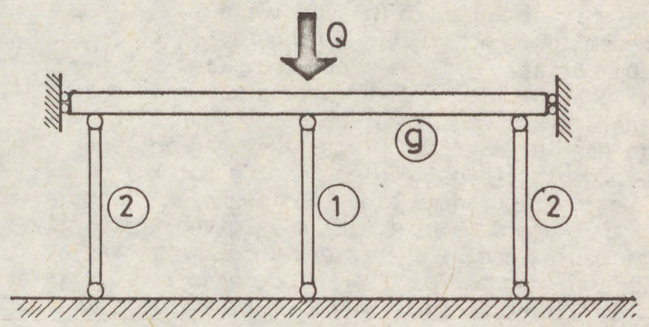

Simulation model

Fig. 4

The model of the structure shown in Fig. 4 is simple enough to be handled. The individual behaviour of the columns and the beam are approximated by simple mathematical functions simulating the theoretical

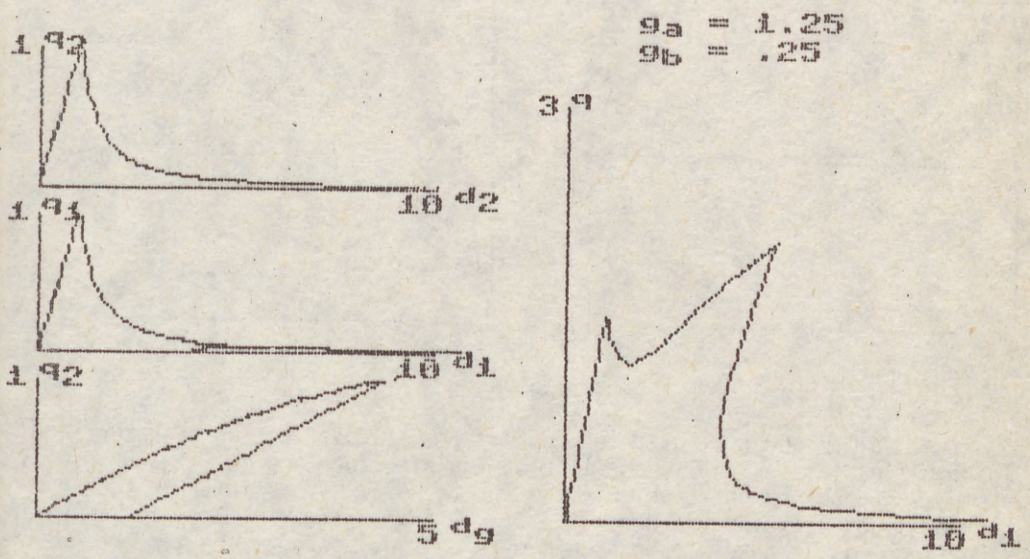

Fig. 5

and experimental results with a good correspondence. The distribution of

(6)

the external load among the three columns was determined by the compatibility of the displacements, that is the sum of the vertical displacements of the upper end of the side columns and the deflection of the beam is equal with the vertical displacement of the upper end of the middle column.

The same model was analysed by ESZE (1986) in his research diploma work experimentally. His results inspired the author to develop the computer simulation program for demonstration purposes.

Choosing appropriate ratios for the load-bearing and deformation properties of the columns and the beam a strange load-deflection diagram can be determined for the model as shown in Fig. 5.

On the left-hand side of the figure the load-deflection diagrams of the individual components (side columns, medium column, beam in order) can be found, while on the right-hand side the function of the external load and the deflection in the middle of the beam is given, respectively.

This diagram has a special character, local maxima either in the load or in the deflection can be found and these specific points are signes of a possible unstable state supposing any kind of loading.

This diagram doesn't include the influence of the loading yet.

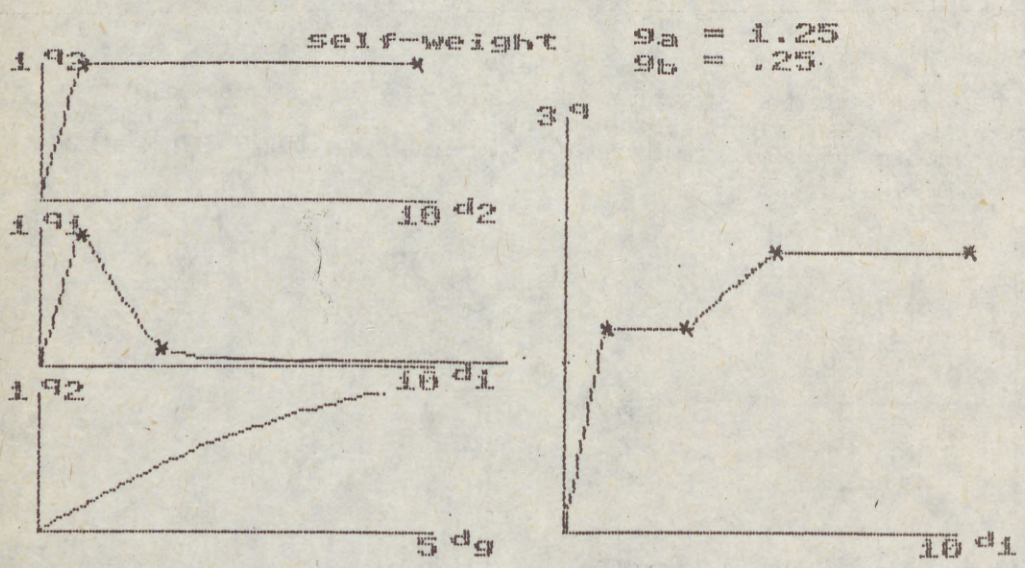

Fig. 6

Figs. 6, 7 and 8 illustrate the the virtual modification effect of the loading to the overall behaviour of the structure and to its individual elements supposing self-weight-type (Fig. 6), kinematic (Fig. 7) and "spring-type" (Fig. 8) cases.

Portions of the diagrams signed by a pair of stars at the two ends are the unstable states of the behaviour of an element of the model or the total model itself.

In these states the individual behaviour of a member or the structure and the character of the loading together don't allow to fulfill the requirements of the equilibrium.

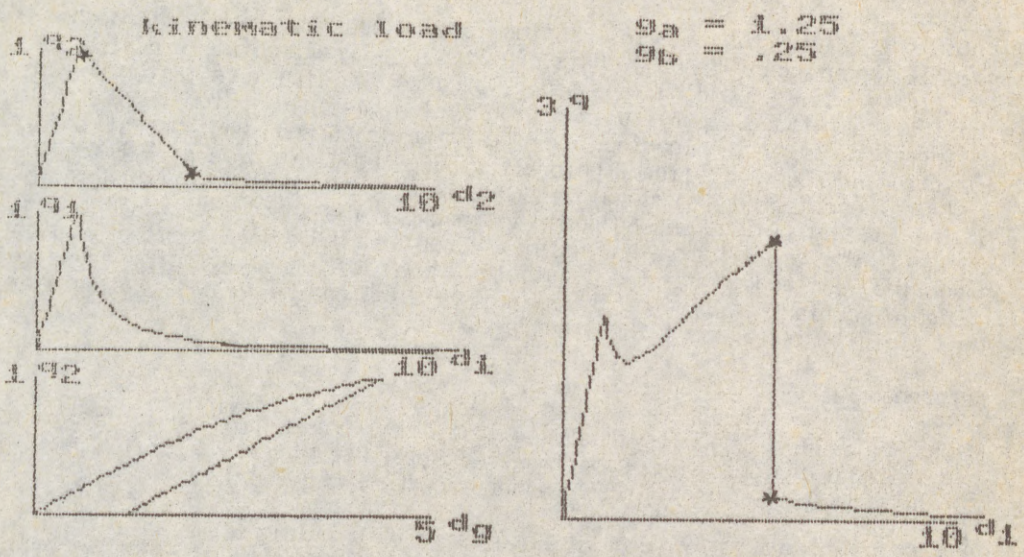

Fig. 7

The situation for the side columns is always a specific one because their loads are transferred by the beam and the elasticity of the beam causes a certain kind of "spring-type" loading for them.

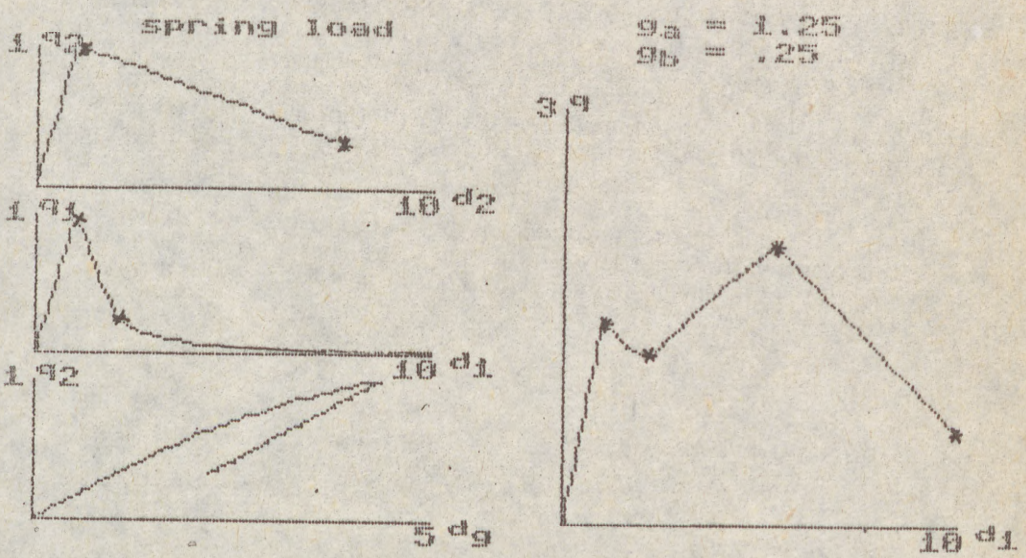

Fig. 8

(8)

Conclusions

In the paper two special topics are discussed. The first one has a special importance for researchers dealing with experimental investigation. As it is shown, during a loading process the structure tested and its loading apparatus are parts of a closed system. As this system is stable in a larger range of the loading than the structure alone, unstable states of the structure can be followed before reaching the limit of stability of the system. The detected structural response is effected by the characteristics of the loading. In the second part of the paper the phenomenon of "temporal instability" is illustrated using a computer simulation program. In this case the influence of the unstable state of one element can cause an unstable period in life of the structure which can be turned to stable by the rigidity reserves of the other elements.

References

ESZE, Gy. (1986): Stability analysis of elastic frames (in Hungarian). Research diploma work. Department of Steel Structures. Technical University. Budapest. p.82. (Supervised by the author)

HEGEDŰS, L. - IVÁNYI, M. (1986): Load tests of building structures. Final Report. Second Regional Colloquium on Stability of Steel Structures. Hungary. p.161-162.

HEGEDŰS, L. (1987): Model analysis of frames with unstable elements. (in Hungarian). 5th Hungarian Conference on Mechanics. Miskolc. Hungary. p.55.

HEGEDŰS, L. (1988): Model analysis of frames with unstable elements. Oral presentation for T.V.Galambos visiting the Department of Steel Structures. Technical University. Budapest. Hungary.

IVÁNYI, M. (1979): Experimental analysis of structures (in Hungarian) Guide to the laboratory lessons in Steel Structures. Tankönyvkiadó. p.145-159.

SZATMÁRI, I. (1986): Numerical method for investigation of 2D bar structures with optional material or joint characteristics. Final Report. Second Regional Colloquium on Stability of Steel Structures. Hungary. p.171-179.

IVÁNYI Miklós,(1)

FAILURE LOAD OF STEEL FRAMEWORKS. A SIMPLE APPROXIMATE METHOD

INTERNATIONAL COLLOQUIUM
STABILITY OF STEEL STRUCTURES
BUDAPEST, HUNGARY, 1990
PRELIMINARY REPORT

Summary
A simple approximate method applying the Mechanism Curve Method has been presented to investigate frame structures.
Procedures have been developed to study the plasticity of steel structures that retain the known, traditional steps of investigation incorporating however, instead of the traditional plastic hinge, the model of the interactive hinges as well.
[IVÁNYI 1985]

1. Introduction

Numerous approximate engineering methods are introduced in the literature [HORNE, MORRIS 1981] from which as one of the possibilites we are going to deal with the extension of the Mechanism Curve Method. The Mechanism Curve Method - above the determination of the plastic load bearing capacity - can be applied to take the effect of finite deformations and strain hardening of steel into consideration.

2. Mechanism Curve Method

(1) Plastic collapse loads are idealizations of the failure loads of elastic-plastic structures. In these idealizations the collapse load refers to infinitely small differences from the undeformed states with infinitely small plastic hinge rotations.

(1) Professor of Structural Engineering
Department of Steel Structures
Technical University of Budapest, Hungary

(2)

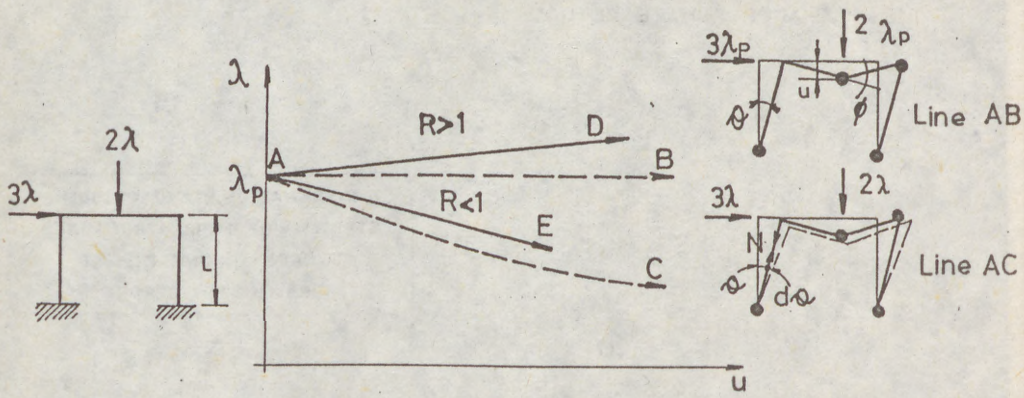

Fig.1.

Based on previous consideration an adequate yield mechanism (pattern of plastic hinges) is to be chosen (Fig.1.). Denoting the displacements of the external forces in the yield mechanism by u_i and the hinge rotations by θ_j (Fig.1.), the virtual work equation furnishes:

$$\lambda \sum_i Q_i u_i = \sum_j M_p \theta_j \qquad (1)$$

This gives the collapse mechanism load factor λ_p.(Fig.1.)

(ii) In order to determine the rigid-plastic mechanism line it is necessary to follow the variation in the load factor λ at increasing finite values of the rotation ϕ. At finite deformations, the mechanism itself becomes non-linear, and consideration of the exact geometry changes becomes laborious. HORNE (1960) has shown that a simple treatment gives a value for λ which is correct up to the first power of ϕ. The work equation for the incremental deformation may be written as:

$$\lambda \sum_i Q_i du_i + \sum_k N_k L_k \phi_k d\phi_k = \sum_j M_{pj} d\theta_j \qquad (2)$$

The second term of the equation is due to the additional external work arising from finite deformations.

The axial thrusts N_k may be obtained with sufficient accuracy by proportion from the values they have in the simple collapse state. The axial thrusts are $\lambda(N_{kp}/\lambda_p)$. A further approximation is that the total and incremental rotations and displacements are all in the same proportion as those for the same mechanism during an infinitely small deformation from the undeformed state. Hence

(3)

$$\frac{du_i}{u_i} = \frac{d\phi_k}{\phi_k} = \frac{d\theta_j}{\theta_j} \qquad (3)$$

and Equ(2) becomes

$$\lambda \left[\sum_i Q_i u_i + \sum \frac{N_{kp}}{\lambda_p} L_k \phi_k^2 \right] = \sum_j M_{pj} \theta_j \qquad (4)$$

This gives the relationship AC shown in Fig.1.

(iii) HORNE (1960) proposed the use of the simple rigid-plastic-rigid relationship in order to take into account the effect of strain-hardening on the collapse load of a structure.
Change of geometry due to elastic-plastic deformations tends to decrease the ultimate load bearing capacity of steel frames in comparison with the plastic collapse load. This tendency is counteracted by the strain-hardening properties of steel. The rigid-plastic-rigid theory of structural behaviour is found to be an adequate mean to assess the stiffness of a structure immediately on the formation of the last hinge in a plastic hinge mechanism.
Different strain-hardening theories can be used during the analysis: (Fig.2)

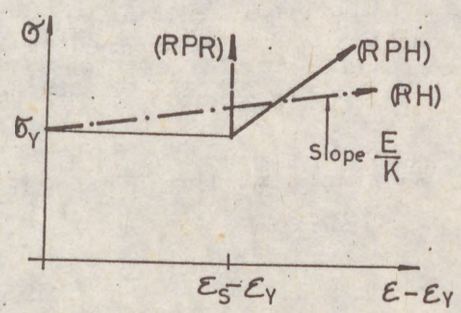

Fig.2.

-rigid-plastic-rigid (RPR) model:[HORNE 1960]
-rigid-plastic-hardening (RPH) model:[HORNE, MEDLAND 1988]
-rigid-hardening (RH) model.

This treatement uses the rigid-hardening (RH) hinge model.
Hinge model determines the end moments of cantilevers of the length h and the depth b, the shape factor f of symmetrical I-section, the end moment comes out to be (M_p+m) (Fig.3.)

(4)

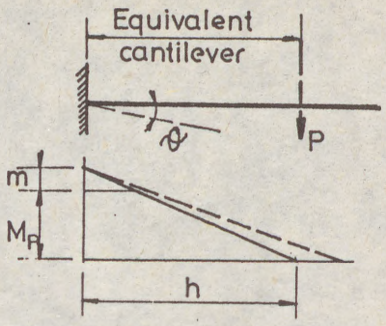

Fig. 3.

$$m = M_p \sqrt{\left(\frac{b}{fh}\right) \frac{E}{K\sigma_y}\,\theta} \qquad (5)$$

The summations (2) and (5) could both be included in the rigid-plastic work equation, which then becomes

$$\lambda \left(\sum_i Q_i u_i + \sum_k N_k L_k \phi_k^2 \right) = \sum_j \left(M_{pj} + m_j \right) \theta_j \qquad (6)$$

The slope of the approximately linear relationship between λ and u which as a result of equation (6) depends on the relative values of the two extra terms containing the deformations, namely $\lambda \sum \frac{N}{\lambda_p} L\phi^2$ and $\sum m\,\theta$. It follows that strain-hardening will predominate over the tendency to instability and the rigid-plastic collapse mechanism will be stable if the "stability ratio" R is greater than unit where

$$R = \frac{\sum_j m_j \theta_j}{\lambda_p \sum_k N_k L_k \phi_k^2} \qquad (7)$$

This, if R>1 the rigid-plastic load/deflection relationship is raised from AC to AD in Fig.1. If, however R<1, the relationship drops, as shown by AE.

3. Approximate Engineering method to take the effect of plate buckling into consideration [IVÁNYI 1983]

In the field of the plastic design of steel structures the effect of plate buckling can be taken into consideration by the so called indirect method. During analysis it should be determined that the ratio of plate elements dimensions of the section should be less than the ratio given in the specification; in this case buckling

(5)
of plate elements do not occur until mechanism formation. Such kind of direct method can be applied to eliminate the disturbing effect of plate buckling, but not to analyse - at least only to predict - the effect of plate buckling in regard with a given structure. We extend the category of hardening plastic hinges by taking the effect of plate buckling into consideration. Such hinge model can be the basis of an approximate engineering method, that - without analysing the full load history -, with simple methods can directly take the effect of plate buckling into consideration.

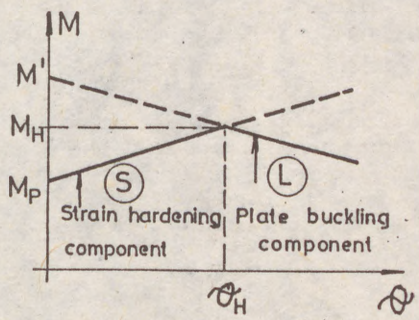

Fig. 4.

Figure 4. shows the linear interaction of moment-rotation of interactive hinge that contains the effects of strain hardening and plate buckling. The essence of approximate engineering method is that the two effects are separated and the interactive hinge of the structure is put together from two separate components: (Fig. 5.)

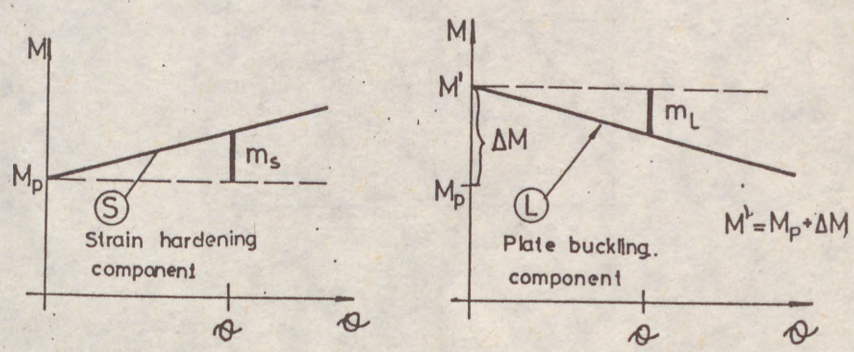

Fig. 5.

(1) Strain hardening component: (S)
(2) Plate buckling component: (L).

(6)

With the assumed two hinge components the values of the load parameter for the chosen mechanism of the framework can be determined as a function of finite deformations.
The expression for (1) hardening component is:

$$\lambda_{(S)}\left[\sum Q\,u + \sum N\,L\,\phi^2\right] = \sum M_p\theta + \sum m_S\theta$$

$$\lambda_{(S)} = \frac{\sum M_p\theta + \sum m_S\theta}{\sum Q\,u + \sum N\,L\,\phi^2} \qquad (8)$$

To write down the expression for the (2) plate buckling component it should be assumed that the interactive hinge characteristic curve contains rigid plate buckling effects, so rigid behaviour goes up to the value of $M' = M_p + \Delta M$ first , then a linearly decreasing change is taken into consideration due to the effect of plate buckling. Because of the shape of the characteristic curve belonging to the (2) plate buckling component, external and internal capacities and works are written similarly to the (1) hardening component - except the sign of the increment $m\,d\theta$.

$$\lambda_{(L)}\left[\sum Q\,u + \sum N\,L\,\phi^2\right] = \sum M'\theta - \sum m_L\theta$$

$$\lambda_{(L)} = \frac{\sum M'\theta - \sum m_L\theta}{\sum Q\,u + \sum N\,L\,\phi^2} \qquad (9)$$

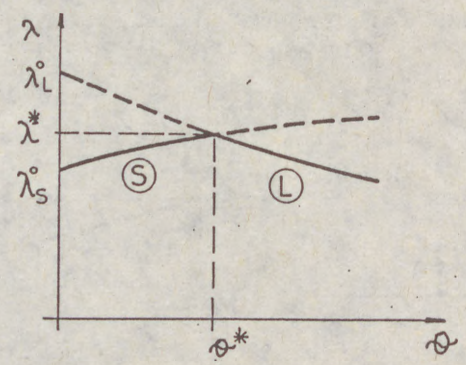

Fig. 6.

Load parameter $\lambda_{(S)}$ takes the effect of strain hardening into consideration, whiles load parameter $\lambda_{(L)}$ that of plate buckling.
From the displacement given by the intersection of the two curves ; the reduction-like change of state is due to the effect of plate buckling (Figure 6.). In connection with the results it should be

(7)

analysis - the expression - taking the two separate components into consideration - assumes the structure motionless till the moments M_p and M' in the hinges form.

We assume that axial forces in bars are proportional to the external loading. Equivalent cantilever length h for the interactive hinge can be determined by the moment diagram from plastic load bearing capacity analysis.

4. Application of approximate engineering method

In the past decade numerous tests were carried out in connection with load bearing capacity of frames at the Department of Steel

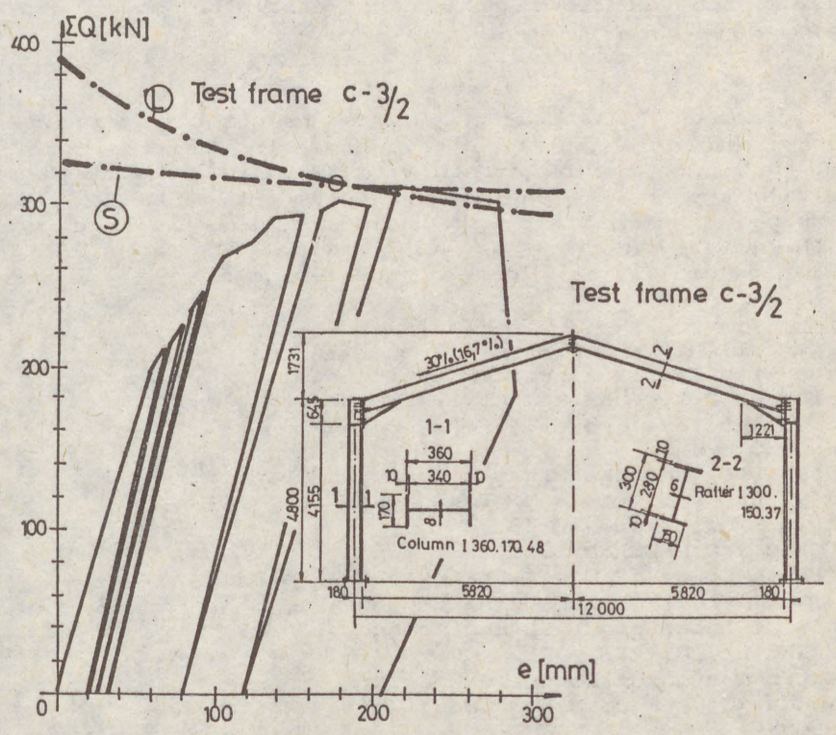

Fig. 7.

Structures of the Technical University, Budapest CHALÁSZ, IVÁNYI 1979). The approximate engineering method is presented on test frame C3/2 .Column base of test frame was supported by the foundation, but did not act as fix end, so plastic load bearing capacity of column base was determined by experiments; these values were used in the calculations.

(8)

Approximate engineering method described in Section 3. is suitable for analysis of the strain hardening and the effect of plate buckling. The most important steps of the analysis of frame C3/2 given in Figure 7 are as followes:

(i) Plastic load bearing capacity analysis: by mechanism chosen by test results.

(ii) Analysis of effects of finite deformations with the help of the chosen mechanism

(iii) Effect of strain hardening: moment-rotation relationship of inelastic zones can be replaced by straight lines, therefore rigid-hardening model can be applied to determine m_s .

(iv) Effect of plate buckling: characteristic curves of interactive hinges can be replaced by straight lines too, therefore the rigid-hardening model can be applied to determine M' and m_L .

5. Summary

Figure 7. compares test result and the results of approximate engineering method taking the strain hardening of steel and the effect of the plate buckling into consideration. The comparison shows that the approximate engineering method gives a satisfactory result for the maximum loads and the instable equilibrium state path of the whole structure as well; and at the same time the analysis can be done at the "desk of the designer".

6. References

HALÁSZ O. and IVÁNYI M. 1979
Tests with Simple Elastic-Plastic Frames
Periodica Polytechnica; Civil Engineering
Vol. 23 No. 3-4. pp. 151-182.

M. R. HORNE 1960
Instability and the Plastic Theory of Structures
Transactions of the Eng. Inst. Canada.
Vol. 4. No. 2. pp. 31-43.

M. R. HORNE and J. C. MEDLAND 1966
Collapse Loads of Steel Frameworks Allowing
for the Effect of Strain-Hardening
Proc. of Inst. of Civil Engineers, Vol. 33. pp. 381-402.

M. R. HORNE and L. J. MORRIS 1981
Plastic Design of Low-Rise Frames
Granada, Constrado Monographs

M. IVÁNYI 1983
"Interaction of Stability and Strength Phenomena
in the Load Carrying Capacity of Steel Structures.
Role of Plate Buckling" (In Hungarian)
Thesis of Doctor of Sciences, Hung. Ac. Sc., Budapest.

M. IVÁNYI 1985
The Model of the "Interactive Plastic Hinge"
Periodica Polytechnica, Civil Engineering
Vol. 29., Nos 3-4 pp. 123-146.

JASPART, Jean-Pierre (1)
MAQUOI, René (2)

GUIDELINES FOR THE DESIGN OF BRACED FRAMES WITH SEMI-RIGID CONNECTIONS.

INTERNATIONAL COLLOQUIUM
STABILITY OF STEEL STRUCTURES
BUDAPEST, HUNGARY, 1990
PRELIMINARY REPORT

Summary : This paper describes the mode of application of the two usual design philosophies - elastic and plastic - to the braced frames with semi-rigid connections.
The attention of the designer is particularly drawn on the influence of the second-order effects on the frame stability. Practical recommendations which allow to define the collapse load of the frame in the most convenient way are proposed. Examples illustrate the stated design principles.

1. INTRODUCTION

The cost of a building steel frame is considerably influenced by the nature of the choosen beam-to-column connections and particularly by their degree of stiffening. A substantial economy may be easily achieved by using bolted connections without stiffeners, the fabrication in workshop and the easy assembling on site of which ensure a minimum cost.

The use of this kind of connections for the design of steel frames compels however to account for their semi-rigid and partial strength character. The actual behaviour of bolted connections is indeed intermediate between the two idealized cases : the perfect hinge which transfers no bending moment and possesses an infinite rotation capacity, and the rigid connection which ensures full rotational continuity between the connected members at each bending moment level.
This so-called semi-rigid behaviour of the connections is governed by a non-linear relationship between the connection moment M and the associated relative rotation ϕ between the connected members (Fig. 1).

---

(1) Assistant, University of Liège, Belgium.
(2) Professor of Civil Engineering, University of Liège, Belgium.

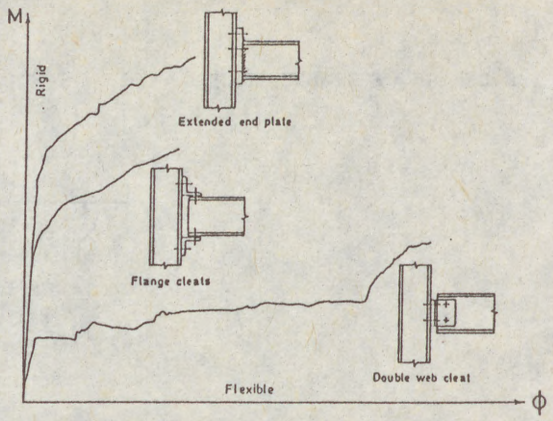

Figure 1 - M - ϕ curves for semi-rigid joints.

The recent development of numerical programs for structural analysis [1] capable of integrating all the material and geometrical non-linearities, and particularly the actual behaviour of connections, enables presently the simulation, until collapse, of the response of the frames. However this does not prevent us from the necessity of proposing to designers simple but nevertheless accurate design methods more appropriate to daily practice. Present paper devoted to the study of braced frames falls within this field.

The non-linear behaviour of connections can obviously not be taken into consideration for practical design and the associated M - ϕ curves must be schematized. The maximum bending moment M_v assumed to be carried over by the connections is represented on figure 2. This pseudo-plastic moment is physically linked up to an ultimate limit state that generally corresponds to the yielding of a connection part.
The connection constant stiffness considered in the stability calculation of frames is the secant stiffness (Fig. 2).
Hand calculation methods for the assessment of the pseudo-plastic moment and of the secant stiffness are available for usual connections [2, 3]. BIJLAARD and ZOETEMEIJER assert in [4] that this bi-linear representation of the semi-rigid and partial strength connection behaviour constitutes a safe approximation for the stability calculation of steel frames.

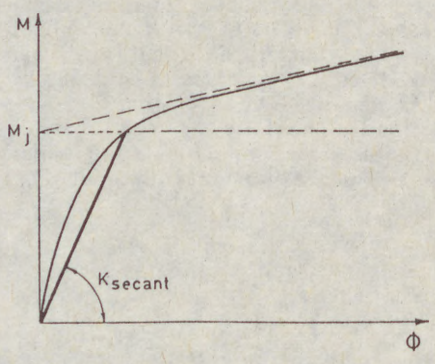

Figure 2 - Modelisation of the connection behaviour.

2. ELASTIC DESIGN OF BRACED FRAMES.

2.1. Design principles.

The elastic design of a braced frame requires a first order elastic linear analysis in order to determine the internal forces.
The extending to the analysis of frames with semi-rigid connections of classical elastic linear methods such as the slope-deflection method and the moment-distribution method has been introduced in 1942 by JOHNSTON and MOUNT [5].
The design in itself is achieved according to a "weak column-strong beam" criterion [6, 7] which consists to design beams and connections in such a way that their collapse never precedes that of the columns. The stability check of the whole frame is then reduced to the individual check of columns by means of usual interaction formulae for in plane or space loaded columns [8].

The buckling length of an isolated column, useful to its stability check, may safely be choosen equal to the column height, commonly termed "system length" [9]. As columns form however part of the frame, a more accurate estimation of their carrying capacity is obtained by considering a buckling length, termed effective length [9], smaller than the system length. This reduction results from the presence of end restraints due to the rest of the structure and particularly to the surrounding beams and connections, whose elastic behaviour until frame collapse provides restraints with a constant character.

2.2. Buckling length of linearly end-restrained columns.

The formulae for the stability check of bent and compressed columns apply to assumed isolated columns. Their application to actual columns in braced frames needs the definition of an equivalent isolated and restrained column (Fig. 3). The effect of restraints is revealed by the presence, at the column ends, of flexural springs, the rigidity of which is defined in such a way that it equals that of the rest of the structure.
The determination of the effective buckling length of actual columns will result from the study of corresponding isolated and restrained columns.
The main problem lies obviously in the evaluation of the flexural characteristic of springs.

BJORHOVDE [10] limits the influence of the structure on the studied column to the beams (and the corresponding connections) ending at the considered extremity (Fig. 4). He proposes the following expression for the stiffness of the equivalent flexural spring at each column extremity :

$$R = \frac{2EI_g}{L_g}\left[\frac{1}{1+\frac{2EI_g}{CL_g}}\right] \qquad (1)$$

where : E = YOUNG modulus ;
I_g = stiffness of the beam(s) ending at the considered extremity ;
L_g = length of the beam(s) ending at the considered extremity ;
C_g = secant stiffness of connection(s) between beam(s) and column.

This equation assumes that the beams of the substructure are bent in single curvature with equal and opposite end rotations. It may be easily modified according to the actual beam end conditions.

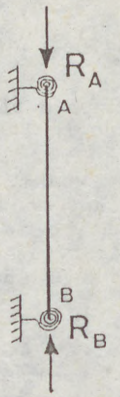

Figure 3 - Isolated column

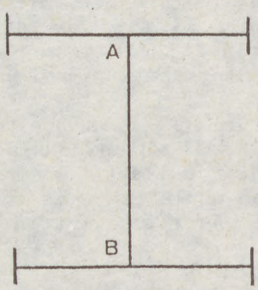

Figure 4 - Substructure

The practical assessment of the effective buckling length of isolated and linearly end-restrained columns may be achieved by means of simplified formulae resulting from a study of elastic linear stability or from the use of buckling curves for end-restrained columns.
A survey of the main existing approaches, as well as an original buckling length evaluation method for columns with different restraints at the ends are proposed in [11].

2.3. Second-order effects.

SNIJDER, BILAARD and STARK [9] have highlighted the possible importance of second-order effects on the behaviour of braced frames. Indeed the compression axial forces acting in the columns produce a decrease in flexural stiffness ; this so-called "ϵ effect" has an influence on the bending moment diagram and may cause the premature collapse of beams and/or connections, what results, for the columns, in a reduction of the amount of restraint at their ends and in a modification of their loading.
According to BIJLAARD and SNIJDER, the influence of these second-order effects could be neglected when :
- the beam span to column height ratio is larger than 1.0 ;
- the moment capacity of the beam is larger than that of the column.

However, studies performed in Liège [12, 13] have not allowed to confirm these conclusions.
As long as more reliable criteria are not available, it is suggested :
- to design the frame according to the principles expressed here above by referring to the first order elastic linear analysis of the whole frame ;
- then to check that the second-order moments in the frame at collapse do not exceed the plastic moment M_{pb} of the section in the beams and the pseudo plastic moment M_v in the connections. It must be noted that the second-order elastic linear analysis of a braced frame may be achieved in a simple, accurate and non iterative way by means of the modified slope-deflection method developed by VANDEPITTE [14].

2.4. Examples of application.

The described approach has been applied (Table 1) to the planar frame of figure 5 in two different cases (HE140B and HE100B beam) and the computed collapse load multipliers have been compared with those resulting from a

numerical simulation of the frame behaviour by means of the finite element program FINELG [1] which accounts for all the material and geometrical non linearities.

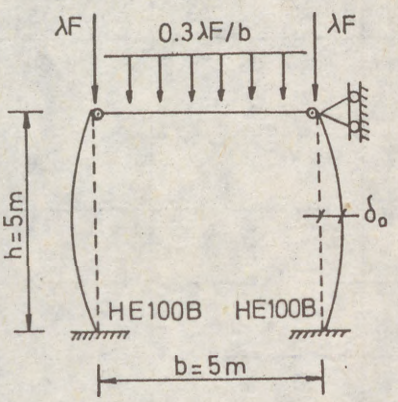

- beams and columns bent about strong axis ;
- F = 100 kN ;
- λ = 1 corresponds to the service loads ;
- δ_o/h = 1/1000 (sinusoidal initial deformation) ;
- elastic-perfectly plastic stress-strain diagram of steel (f_y = 235 MPa) ;
- non-dimensional characteristic curves of the beam-to-column connections (end plate): see figure 6.

Figure 5 - Frame for application

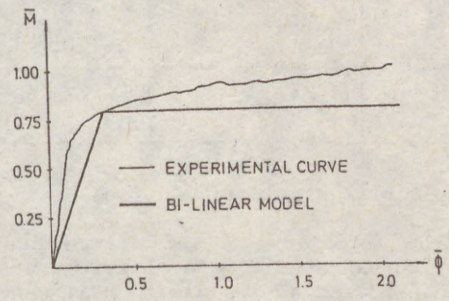

- $\bar{M} = \frac{M_c}{M_{pb}}$

  with M_c = moment in the connection
  M_{pb} = plastic moment of the beam

- $\bar{\phi} = \frac{\phi_c}{\phi_p}$

  with ϕ_c = connection relative rotation

  $\phi_p = \frac{M_{pb}}{\frac{EI_p}{5h_b}}$ where I_p = beam inertia
  h_b = beam depth

Figure 6 - Connection non-dimensional M-ϕ curves

From the first order analysis of the frame, it may be stated in both cases that the buckling of the column precedes the yielding of the beams and of the connections and determines consequently the collapse of the frame.

The second-order elastic linear analysis allows however to point out the non negligible influence of the axial loads in the columns on the maximum bending moment in the beam and in the connections.
In the frame with a HE140B beam, the "ϵ effect" is not sufficient to give rise to plastic hinges in the beam at mid-span. The assessment of the collapse load multiplier based on the first order analysis may be considered as a valuable appraisal of the actual frame collapse multiplier (see table 1) despite the modification of the column loading due to the second-order effects. The situation is quite different for what regards the frame with a HE100B beam, where the premature development of a plastic

hinge in the beam during the loading sequence reduces the ultimate strength of the frame.

Type of analysis	Results	HE140B beam : M_{pb} = 57,8 kNm Connections: M_v = 46,2 kNm	HE100B beam : M_{pb} = 24,4 kNm Connections: M_v = 19.5 kNm
First order elastic linear analysis	Collapse load multiplier for beams and/or connections	4.05	2.30
	Collapse load multiplier for columns	3.02	2.29
	Frame collapse load multiplier	3.02	2.29
	Moment in the beam at mid-span(kNm)at collapse	$43.1 < M_{pb}$	$24.3 < M_{pb}$
	Moment in the connections (kNm) at collapse	$13.5 < M_v$	$18.7 < M_v$
Second-order elastic linear analysis	Moment in the beam at mid-span (kNm) at "first order" collapse	$49.7 < M_{pb}$	$35.7 > M_{pb}$
	Moment in the connections (kNm)at "first order" collapse	$6.9 < M_v$	$7.3 < M_v$
Non-linear analysis FINELG	Frame collapse load multiplier	3.1	2.06

Table 1 - Collapse load multipliers (elastic design).

The load multiplier associated to the formation of this hinge has been evaluated in [12] (λ = 1.7); it constitutes the ultimate elastic resistance of the frame and has to be normally considered as its design resistance.
A less safe estimation of the collapse load may however be calculated by dtermining the buckling resistance of the column assumed to be hinged at its upper extremity and subjected to the first order internal forces.
This approach leads to a value of the frame collapse load multiplier λ equal to 2.16; this slightly unsafe result (the actual collapse multiplier equals 2.06 - see table 1) is principally linked up to the degree of accuracy of the stability check formula. However, it must be noted that the formation of a hinge in the beam at mid-span for λ = 1.7 deletes actually the restraint at the upper column extremity in the particular frame studied (figure 7); this will be rarely encountered in practical cases so that this approach may be generally considered as a safe one.

Figure 7 - Reduction to zero of the beam stiffness after the formation of a hinge at mid-span.

3. PLASTIC DESIGN OF BRACED FRAMES.

The plastic design is achieved according to a "strong column-weak beam" criterion [6, 7], in which the frame collapse is associated to the formation of beam plastic mechanisms. The check of the column is performed, in a similar way to that described here above, in the structure submitted to collapse loads, a part of which remains elastic.
The problem of the rotation capacity and of the required minimum stiffness of connections for a plastic design is dealt with, among other things, in [15].

The plastic design approach has been applied to the frame defined in figure 5 constituted in this case of HE200B columns and of a HE140B beam.
The collapse load multipliers are reported in table 2. The plastic collapse of the beam precedes that corresponding to the column instability and determines therefore the frame collapse. The column collapse multiplier has been evaluated by assuming hinge conditions at upper extremity of the columns which are each subjected there to an increasing axial load and to a concentrated constant bending moment equal to the plastic moment of the connection (M_v) or to that of the beam (M_{pb}), according to which is lesser. The agreement between the hand computed collapse multiplier and that resulting from a numerical simulation by means of the FINELG program is seen to be excellent.

Type of analysis	Results	HE140B beam: M_{pb} = 57,8 kNm Connections: M_v^{pb} = 46,2 kNm
First order plastic analysis	Collapse load multiplier for the beam	5.01
	Collapse load multiplier for the columns	6.18
	Frame collapse load multiplier	5.01
Non-linear analysis FINELG	Frame collapse load multiplier	5.1

Table 2 - Collapse load multipliers (plastic design).

4. CONCLUDING REMARK

The supplementary calculation in Liège of a great deal of different structures through the FINELG and the described design methods will enable to define with more precision the range of validity and also the general degree of accuracy of the proposed methods.

5. REFERENCES.

1. JASPART, J.P. and de VILLE de GOYET, V., "Etude expérimentale et numérique du comportement des structures composées de poutres à assemblages semi-rigides", Construction Métallique, n° 2, 1988.

2. "Steinfenlose Stahlskeletttragwerke und dunnwandige Vollwandträger, Berechnung und Konstruktion", Europäishe Konvention für Stahlbau, 1977.

3. ZOETEMEIJER, P., "Samenvatting van het onderzoek op geboute balkkolom verbindingen", Report 6-85-7, Delft University of Technology, Stevin Laboratory, 1983.

4. BIJLAARD, F.S.K. and ZOETEMEIJER, P., "Influence of joint characteristics on the structural response of frames", presented at the International Conference "Steel Structures, Recent Advances and their Application to Design", Budva, Yugoslavia, 29 Sept. - 1 Oct. 1986.

5. JOHNSTON, B. and MOUNT, E.H., "Analysis of building frames with semi-rigid connections", American Society of Civil Engineers, Transactions, 1942, 107, pp. 993 - 1019.

6. VINNAKOTA, S., "Design of columns in planar frames. A few comments", presented at the National Conference on Tall Buildings, held at New-Delhi, 1973.

7. VINNAKOTA, S., "Design of columns as part of frames - Some remarks", paper submitted to TG 3 : SSRC, 1983.

8. EUROCODE 3, "Common unified rules for steel structures". Directorate General for Internal Market and Industrial Affairs. Commission of the European Communities, 1984.

9. SNIJDER, H.H., BIJLAARD, F.S.K. and STARK, J.W.B., "Use of the elastic effective length for stability checks of columns and consequences for checks on beams in braced frames", Proceedings of the Michael R. HORNE Conference, edited by L.J. MORRIS, London, Granada, 1983.

10. BJORHOVDE, R., "Effect of end restraint on column strength - Practical applications", Engineering Jl. A.I.S.C., to be published.

11. MAQUOI, R. and JASPART, J.P., "Contribution to the design of braced frames with semi-rigid connections", Proceedings of the Fourth International Colloquium on Stability of Metal Structures, North American Session, New-York City, 17-19 April, 1989.

12. ELSEN, Ph., "Méthodes manuelles de prédimensionnement des ossatures métalliques contreventées à assemblages semi-rigides", Diploma Work, MSM Department, University of Liège, 1989.

13. AMOUR, A., "Contribution à l'étude de la capacité portante des colonnes de structures contreventées à noeuds semi-rigides", Maîtrise en Sciences Appliquées, Service MSM, Université de Liège, 1988.

14. VANDEPITTE, D., "Non-iterative analysis of frames including the P-Δ effect". Journal of Constructional Steel Research, 2 (1982), pp. 3 - 10.

15. STARK, J.W.B. and BIJLAARD, F.S.K., "Monograph on beam-to-column connections. Ch. 17:Design rules for beam-to-column connections in Europe" Inst.TNO for Buildg.Struct. and Buildg.Materials,Delft,Holland, 1984.

(1)
KAZACHOK, Vladimir (1)
BYKOVSKII, Sergei (2)
SHER, Mark (3)
SHILOV, Alexander (4)

THE DEVELOPMENT OF THE EFFECTIVE-COLUMN-LENGTH-DESIGN-PROCEDURE IN INDUSTRIAL BUILDINGS

INTERNATIONAL COLLOQUIUM
STABILITY OF STEEL STRUCTURES
BUDAPEST, HUNGARY, 1990
PRELIMINARY REPORT

Summary: The problem of effective column length definition has been formulated as a problem of determination of increesing/decreesing coefficient on real column length. The technique for quantitative and qualitative estimation of single-storey industrial building parameter influence on the effective column length has been developed. The technique is based on the frame stability design. It has been shown that the effective length coefficient is influenced with the length, stiffeness, normal forces ratios of stepped column parts. The formulae for the effective length coefficient for upper and lower stepped column parts with and without taking into account the normal forces ratio have been developed. It has been proposed to consider each column as a part of a building frame. Some numerical results have been presented.

---

(1) Associated professor, Cand.techn.Sci., Byelorussian Polytechnic Institute
(2) Associated professor, Cand.techn.Sci., Byelorussian Polytechnic Institute
(3) Research engineer, Byelorussian Polytechnic Institute
(4) Research engineer, Byelorussian Polytechnic Institute

(2)

An accuracy of definition of effective column lengths is one of important factors determining design economy on building frames. However design codes of different countries are essentially different.

So the USSR design codes for metal structures /2/ consider a column not having a top support if it is a part of a single-span frame, and having a non-moving horizontal support if a frame has two or more spans. An effective length is approximately defined by tables taking into account the ratio of upper to lower column parts and the ratio of their normal forces.

The GDR design codes for concrete structures/3/ and the guides developing the codes/2/ contain more precise recommendations. The USA codes/4/ define the effective column length depending on full stiffness of frame members neighbouring the column.

The USSR codes for concrete structures/1/ recommend to define the effective length of an unaxially compressed frame member taking into account its deformed axis resulting from a mostly strong load combination, non-elastic material deformations and cracking. But there are not any practical recommendations. Moreover for single-storey production building columns the code/1/ recommend approximate effective length values independent from building dimensions and loads.

The technique for quantitative and qualitative estimation of the single-storey industrial building parameter influence on the effective column length was developed in the Byelorussian Polytechnic Institute. It is based on the frame stability design. In accordance with the adopted approach the column having weak design parameters becomes unstable and the rest columns are considered to be a support for the first one. So the column is considered to have a rigid lower support and elastically compliant upper one (Fig. 1). The upper support stiffness is defined as a sum of the "rest" column reactions due to virtual deflection of their tops. Each reaction depends on normal force, dimensions and materials of a column. The "rest" column number the character of buckling depend on the load type. For example, a framework is considered to be a plane frame under the wind load and it is looked at as a space frame under a crane load. In this case it is possible to determine internal section forces (taking into account the effective lengths and increasing coefficients) resulting from separate loads. Then the forces can be summed for each section.

$$M_j = \sum^{i} M_{ji} \times \delta_{ji} \times (l_{oi}) \qquad (1)$$

where M_j - the internal moment in j-th section resulting from load combination;

δ_{ji} - the coefficient increasing the j-th section internal moment resulting from i-th load;

l_{oi} - the effective length of column part taking into account the all normal forces resulting from the load combination.

M_{ji} - the bending moment in j-th section resulting from

(3)
a static calculation of a frame under the i-th load;

The computer program "PAMA" was developed for definition length coefficient K for stepped columns with hinged upper supports. More then 2 000 calculations covering the entire range of real industrial building columns were made by the program. The ratios of lengths ($m=l_1/l_2$), rigidities ($i=I_1/I_2$) and normal forces

$$\rho = \frac{N_1}{N_1+N_2}$$

for upper and lower column part were varied. A digital analysis resulted in formulas for definition of effective coefficients for upper (K_1) and lower (K_2) column parts:

$$K_1 = K_2 \frac{\sqrt{i}}{m\sqrt{\rho}} \qquad (2)$$

$$K_2 = (0{,}98 - 0{,}15\rho)\sqrt{\frac{(i+1{,}5m)(m+\rho)+0{,}22n+(m^2+1{,}1n(m+\rho))m\rho/\sqrt{n}}{0{,}4((n+m^2)+3i(m+1))}} \qquad (3)$$

The formulas allow to receive results according with accurate calculations for the entire range of the coefficient ρ from 0.05 to I.0(Fig. 2).

In some cases it is necessary to have formulae for the definition of the coefficient K without taking into account the normal forces ratio.

In the USSR the roofs of single-storey industrial buil-sings are usually made of reinforced concrete. So it is possible to consider the coefficient ρ ranging only from 0.6 to 1.0 and to propose the following formulae for K_1 and K_2 definition:

$$K_1 = K_2 \frac{(1{,}4-0{,}4m)\sqrt{i}}{m} \qquad (4)$$

$$K_2 = (1{,}225-0{,}125m)\sqrt{\frac{m^2(n+1{,}5)+0{,}22n+(m^2+1{,}1i)m/\sqrt{n}}{0{,}4((n+m^2)+3i(m+1))}} \qquad (5)$$

A number of calculations was made to investigate the influence of the "rest" columns number (K_n) on coefficients K_1 and K_2 values. The "rest" columns number was ranged from 0 15. To compare these the calculation for $K_n = \infty$ was also made. Figures 4 and 5 show a $K_2, K_1 - K_n$ diagram for column of 10.8m and 14.4m height as an example. A digital analysis resulted in a formula for calculation of effective column length coefficient (K_i) for a column with limited number of the "rest" columns on the basis of coefficient K_∞

(4) (5)

for a column with unlimited number of the "rest" columns:

$$K_2 = \frac{1{,}7\sqrt[3]{l_1/l_2 \times D_1/D_2}}{\sqrt[5]{K_n}} \times K_\infty \qquad (6)$$

The formula (6) gives good results for entire range of coefficients K_n, but to simplify the calculation it can be adopted that $K_i = K_\infty$ if $K_n = 6$.

The same investigation was made for reinforced concrete frame columns. It was determined that the bending moment in the plane of the frame with three and more spans should be defined when a value of coefficient K_2 was:in

$$0{,}7 \leq K_2 \leq 0{,}25 + 1{,}55/n \leq 1{,}55 \times i$$

If a traditional approach is used when considering the buckling effect it is recommended that the values of K_1 and K_2 derived from formulae (2,3,4,5) for one- and two-span buildings should be increased on 10 and 25 per cent respectively.

Bibliography

I. СНиП 2.03.01-84. Бетонные и железобетонные конструкции. Нормы проектирования./Госстрой СССР. - М.: ЦИТП Госстроя СССР, 1988. - 96 с.

2. СНиП II-23-81. Стальные конструкции/ Госстрой СССР. -- М.: ЦИТП Госстроя СССР, 1988. - 96 с.

3. T.G.L. 0-1045. Bauwerke/aus Stahlebeton. Projektierung und Ausführung. 1985.

4. Guide to Stability Design Criteria for Metal Structures. Third Edition. Structural Stability Research Council. Edited by Bruce G. Johnston. A Wiley-Interscience Publication. 615pp.

Stepped and frame column schemes

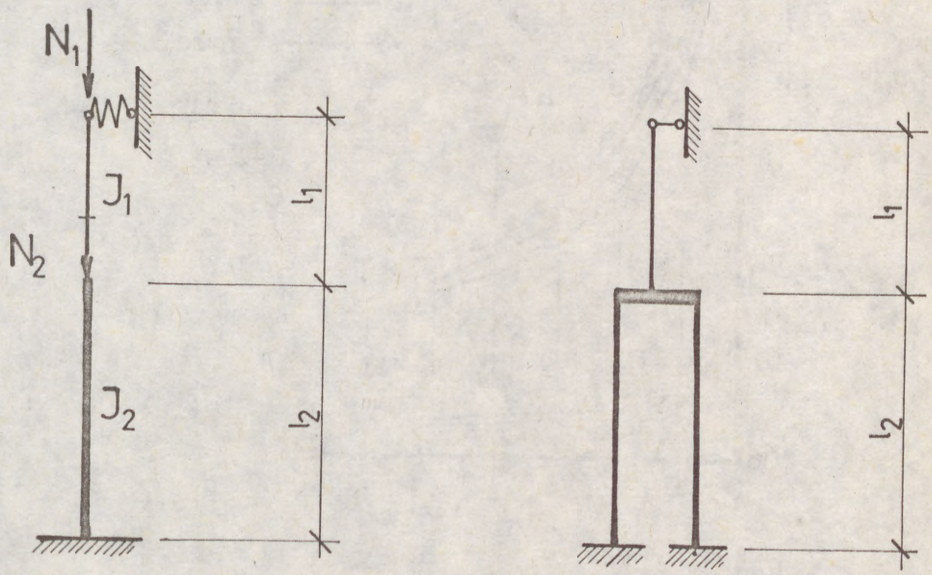

$$m = \frac{l_1}{l_2} \qquad \varrho = \frac{N_1}{N_1 + N_2}$$

$$i = \frac{J_1}{J_2} \qquad n = \frac{i}{m} = \frac{J_1 \cdot l_2}{l_1 \cdot J_2}$$

Fig. 1

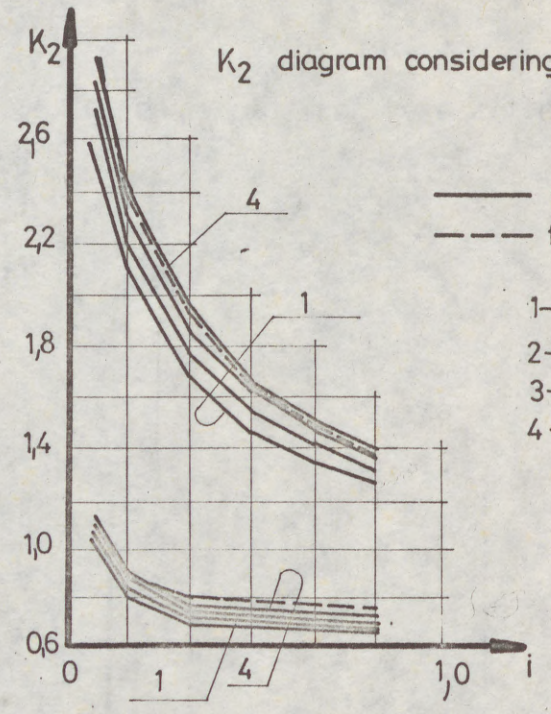
K_2
K_2 diagram considering (ϑ) ratio
2,6
2,2
1,8
1,4
1,0
0,6
0
1
4
1,0
i
exact
formula 3
1– ϑ = 1,0
2– ϑ = 0,9
3– ϑ = 0,8
4 – ϑ = 0,7

Fig. 2

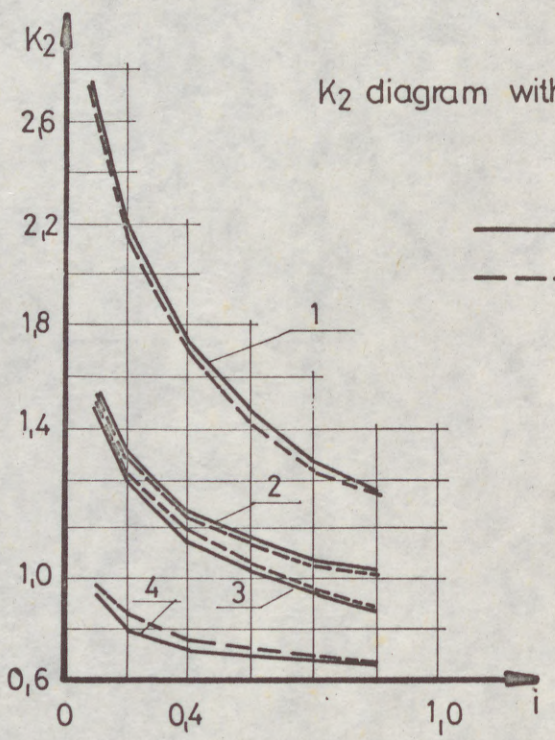
K_2
K_2 diagram without considering (ϑ) ratio
2,6
2,2
1,8
1,4
1,0
0,6
0
0,4
1,0
i
exact
formula 5
1– ϑ = 1,0; m = 1,0
2– ϑ = 0,05; m = 1,0
3– ϑ = 1,0; m = 0,4
4 – ϑ = 0,05; m = 0,4

Fig. 3

(7)

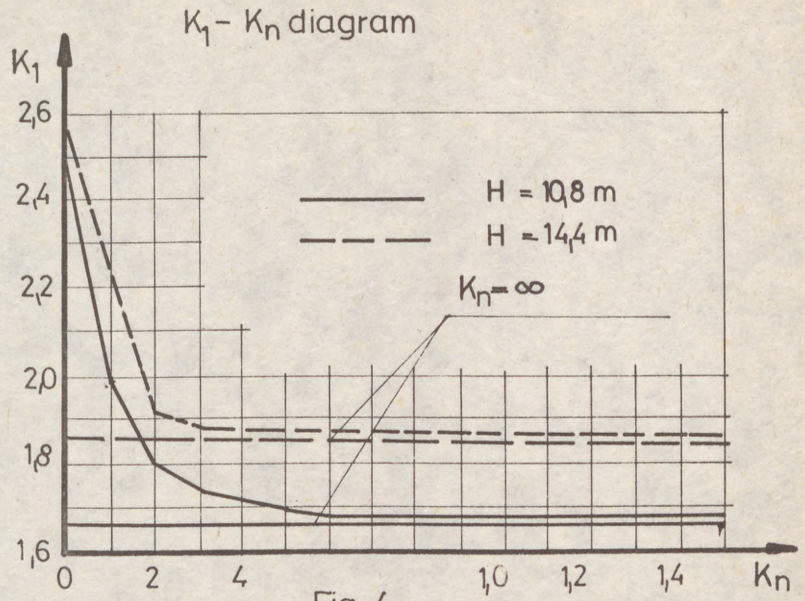
K1 - Kn diagram
K1
2,6
2,4
2,2
2,0
1,8
1,6
H = 10,8 m
H = 14,4 m
Kn = ∞
0
2
4
1,0
1,2
1,4
Kn

Fig. 4

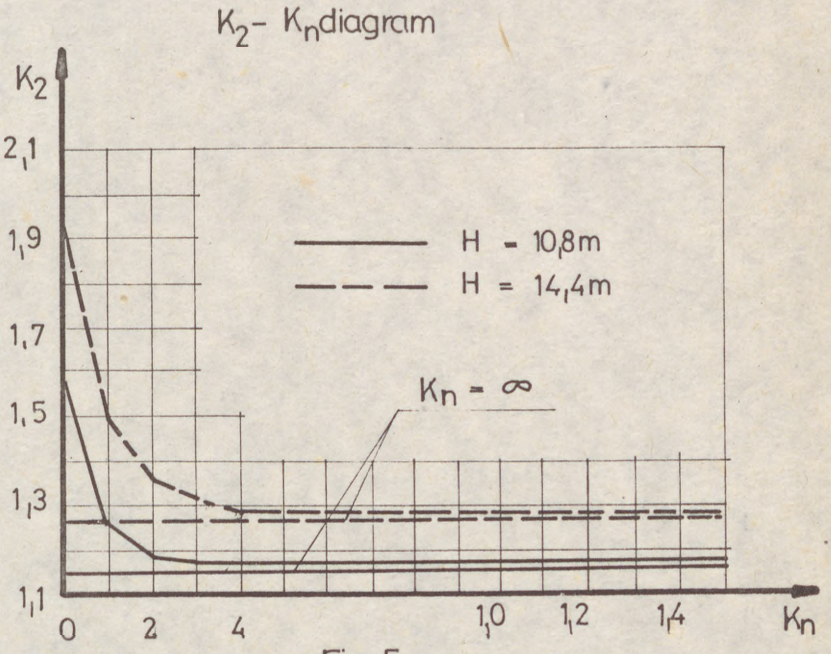
K2 - Kn diagram
K2
2,1
1,9
1,7
1,5
1,3
1,1
H = 10,8m
H = 14,4m
Kn = ∞
0
2
4
1,0
1,2
1,4
Kn

Fig. 5

(1)

N
FI

SUMMAR
of space f
equations
element wi
adopted.
where the
discretized
which allo

INTROD
Steel frame
use of high
and increa
The charac
assessing t
complicate
cases.

The b
extensively
studies are
1970, Atta
Bažant &
1987. Stud
& Murray
Except Eps
have used

(⋆) Helsin

(1)

Reijo Kouhia (⋆)

NONLINEAR FINITE ELEMENT ANALYSIS OF SPACE FRAMES WITH THIN-WALLED OPEN CROSS-SECTION

INTERNATIONAL COLLOQUIUM
STABILITY OF STEEL STRUCTURES
BUDAPEST, HUNGARY, 1990
PRELIMINARY REPORT

SUMMARY: A finite element method for geometrically nonlinear elasto-plastic analysis of space frames with thin-walled open cross-section is developed. The equilibrium equations are formulated using an updated incremental Lagrangian description. An element with linear shape functions for all displacement and rotation components is adopted. Torsional behaviour is modelled using two parametric deplanation model, where the angle of twist and its derivative have independent approximations. The discretized equilibrium equations are solved using the orthogonal trajectory method which allows the determination of the post buckling regime.

INTRODUCTION

Steel frames are common load carrying structures in engineering constructions. Effective use of high strength steel results in thin-walled members, and due to the slenderness and increased imperfection sensitivity the stability problems become more significant. The character of the load-deformation path in the post-buckling range is important in assessing the safety of the structure. Coupled geometrical and material nonlinearities complicate the structural analysis, and only numerical solutions are feasible in practical cases.

The behaviour of beams with thin-walled open cross-section has been studied extensively. Several finite element models have been published, although most of these studies are limited to the determination of buckling loads, eg. BARSOUM & GALLAGHER 1970, ATTARD 1986. Large deflection analyses of elastic members have been presented eg. BAŽANT & EL NIMEIRI 1973, EPSTEIN & MURRAY 1976, SEKULOVIĆ 1986 and ATTARD 1987. Studies with both geometrical and material nonlinearities are eg. RAJASEKARAN & MURRAY 1973, LEE et al. 1984, WUNDERLICH et al. 1986 and HASEGAWA et al. 1987b. Except EPSTEIN & MURRAY 1976 and SEKULOVIĆ 1986 all the other mentioned studies have used Vlasov's theory to model the torsional behaviour of a thin-walled beam.

(⋆) Helsinki University of Technology, Department of Structural Engineering

EQUILIBRIUM EQUATIONS

If the body- and inertia forces are neglected the principle of virtual work in the Lagrangian description is

$$\int_{{}^1V} {}^2S_{ij}\delta({}^2E_{ij})d^1V - \int_{{}^1A_t} {}^2t_i\delta u_i d^1A = 0, \tag{1}$$

where $\mathbf{S}$ is the 2^{nd} Piola-Kirchhoff stress tensor, $\mathbf{E}$ the Green-Lagrange strain tensor, $\mathbf{u}$ the displacement vector and $\mathbf{t}$ the surface traction vector. Left superscripts 1 and 2 refer to the known reference configuration and to the configuration which is looked for, respectively. The incremental form of equation (1) is

$$\begin{aligned}\int_{{}^1V} (\Delta S_{ij}\delta u_{i,j} + {}^1S_{ij}\Delta u_{k,i}\delta u_{k,j})d^1V - {}^2\lambda \int_{{}^1A_t} \frac{\partial^1 t_i}{\partial u_j}\Delta u_j \delta u_i d^1A = \\ {}^2\lambda \int_{{}^1A_t} {}^1t_i\delta u_i d^1A - \int_{{}^1V} {}^1S_{ij}\delta u_{i,j} d^1V,\end{aligned} \tag{2}$$

where ${}^2S_{ij} = {}^1S_{ij} + \Delta S_{ij}$ etc. The surface tractions are assumed to depend on a single parameter λ:

$${}^2t_i = {}^2\lambda t_i|_{{}^2u_k} = {}^2\lambda {}^2t_i \approx {}^2\lambda({}^1t_i + \frac{\partial^1 t_i}{\partial u_j}\Delta u_j). \tag{3}$$

The displacement vector $\mathbf{u}$ is interpolated within an element by shape functions $\mathbf{N}$ and nodal point displacement variables $\mathbf{q}$. The discretized incremental form of the equilibrium equation obtained from (2) is

$${}^1(\mathbf{K}_1 + \mathbf{K}_G - \mathbf{K}_L)\Delta\mathbf{q} = {}^2\mathbf{Q} - {}^1\mathbf{R}, \tag{4}$$

where $\mathbf{K}_G$ and $\mathbf{K}_L$ are the geometrical and load stiffness matrices, $\mathbf{Q}$ is the external force vector, $\mathbf{R}$ the vector of internal forces and $\Delta\mathbf{q} = {}^2\mathbf{q} - {}^1\mathbf{q}$ the incremental nodal point displacement vector between the current and the reference configuration. In the incremental Lagrangian formulation the matrix $\mathbf{K}_1$ depends also on the deformation between configuration 1 and 2. Configuration 2 is found by iteration using equilibrium configuration 1 as a reference state.

Incremental displacements for a three dimensional straight beam element, where the thin-walled open cross-section is composed of narrow rectangular parts, are assumed to be in a particular part

$$\begin{aligned}\Delta u(x,y,z) &= \Delta u_c(x) + z\Delta\phi_y(x) - y\Delta\phi_z(x) - \omega_s(s)\Delta\theta(x) - \omega_r(s,r)\Delta\phi_{x,x}(x),\\ \Delta v(x,y,z) &= \Delta v_c(x)\cos\alpha + \Delta w_c(x)\sin\alpha - e_r\Delta\phi_x(x),\\ \Delta w(x,y,z) &= \Delta w_c(x)\cos\alpha - \Delta v_c(x)\sin\alpha + e_s\Delta\phi_x(x),\end{aligned} \tag{5}$$

where u_c, v_c, w_c are the displacement components of the centroidal axis ϕ_x, ϕ_y, ϕ_z are the rotations with respect to x, y and z axes and θ is the twist. The abbreviations e_r and e_s are

$$e_r = z_c\cos\alpha - y_c\sin\alpha + r, \qquad e_s = z_c\sin\alpha + y_c\cos\alpha + s, \tag{6}$$

(3)

where y_c, z_c are the coordinates of the centroid of the cross-section part and α is the angle between the principal axes of the cross-section and the local axes of the part. The warping function is assumed to consist of two contributions

$$\omega_s(s) = h_s(s)s, \qquad \omega_r(s,r) = h_r(s)r, \tag{7}$$

where h_s and h_r are the components of the radius vector onto the normal r and tangential s directions of an arbitrary point of the cross-section.

The strain increments are evaluated using the general formulas

$$\begin{aligned} \Delta\varepsilon_x &= \Delta u_{,x} + \frac{1}{2}(\Delta u_{,x}^2 + \Delta v_{,x}^2 + \Delta w_{,x}^2), \\ \Delta\gamma_{xs} &= \Delta u_{,s} + \Delta v_{,x} + \Delta u_{,x}\Delta u_{,s} + \Delta v_{,x}\Delta v_{,s} + \Delta w_{,x}\Delta w_{,s}. \end{aligned} \tag{8}$$

The terms $\Delta u_{,x}^2$ and $\Delta u_{,x}\Delta u_{,s}$ are significantly smaller than the remaining ones in (8), so they can be dropped out from the equilibrium equations (4).

The matrix

$$\mathbf{K}_1 = \int_{{}^1V} \mathbf{B}^T \mathbf{C}_L \mathbf{B} d^1V, \tag{9}$$

where $\mathbf{C}_L$ contains the material parameters, and the discrete gradient operator matrix $\mathbf{B}$ is

$$\mathbf{B} = \begin{bmatrix} \mathbf{N}_{,x} & a_1\mathbf{N}_{,x} & a_2\mathbf{N}_{,x} & a_3\mathbf{N}_{,x} & z\mathbf{N}_{,x} & -y\mathbf{N}_{,x} & -\omega_s\mathbf{N}_{,x} \\ \mathbf{0} & b_1\mathbf{N}_{,x} & b_2\mathbf{N}_{,x} & b_3\mathbf{N}_{,x} + b_4\mathbf{N} & b_5\mathbf{N} & b_6\mathbf{N} & -\omega_{s,s}\mathbf{N} \end{bmatrix}, \tag{10}$$

in which

$$\begin{aligned} a_1 &= \Delta v_{c,x}^1 - (e_r\cos\alpha + e_s\sin\alpha)\Delta\phi_{x,x}^1, \qquad a_2 = \Delta w_{c,x}^1 + (e_s\cos\alpha - e_r\sin\alpha)\Delta\phi_{x,x}^1, \\ a_3 &= (y^2+z^2)\Delta\phi_{x,x}^1 - (e_r\cos\alpha + e_s\sin\alpha)\Delta v_{c,x}^1 + (e_s\cos\alpha - e_r\sin\alpha)\Delta w_{c,x}^1, \\ b_1 &= \cos\alpha - \sin\alpha\Delta\phi_x^1, \qquad b_2 = \sin\alpha + \cos\alpha\Delta\phi_x^1, \qquad b_3 = -\omega_{r,s} - e_r + e_s\Delta\phi_x^1, \\ b_4 &= \cos\alpha\Delta w_{c,x}^1 - \sin\alpha\Delta v_{c,x}^1 + e_s\Delta\phi_{x,x}^1, \qquad b_5 = \sin\alpha, \qquad b_6 = -\cos\alpha, \end{aligned}$$

and $\Delta v_{c,x}^1$ etc. means the incremental displacements prior the current iteration. The geometric stiffness has the form

$$\mathbf{K}_G = \begin{bmatrix} \mathbf{0} & \mathbf{0} & \mathbf{0} & \mathbf{0} & \mathbf{0} & \mathbf{0} & \mathbf{0} \\ & \mathbf{K}_{vv} & \mathbf{0} & \mathbf{K}_{v\phi x} & \mathbf{0} & \mathbf{0} & \mathbf{0} \\ & & \mathbf{K}_{ww} & \mathbf{K}_{w\phi x} & \mathbf{0} & \mathbf{0} & \mathbf{0} \\ & & & \mathbf{K}_{\phi x\phi x} & \mathbf{0} & \mathbf{0} & \mathbf{0} \\ & & & & \mathbf{0} & \mathbf{0} & \mathbf{0} \\ & & & & & \mathbf{0} & \mathbf{0} \\ & \text{s} & & \text{y} & \text{m} & \text{m.} & \mathbf{0} \end{bmatrix}, \tag{11}$$

(4)

where

$$\mathbf{K}_{vv} = \mathbf{K}_{ww} = \int_{{}^1V} {}^1S_x \mathbf{N}_{,x}^T \mathbf{N}_{,x} d^1V,$$

$$\mathbf{K}_{v\phi x} = -\int_{{}^1V} {}^1S_x (e_r \cos\alpha + e_s \sin\alpha) \mathbf{N}_{,x}^T \mathbf{N}_{,x} d^1V - \int_{{}^1V} {}^1S_{xs} \sin\alpha \mathbf{N}_{,x}^T \mathbf{N} d^1V,$$

$$\mathbf{K}_{w\phi x} = \int_{{}^1V} {}^1S_x (e_s \cos\alpha - e_r \sin\alpha) \mathbf{N}_{,x}^T \mathbf{N}_{,x} d^1V - \int_{{}^1V} {}^1S_{xs} \cos\alpha \mathbf{N}_{,x}^T \mathbf{N} d^1V,$$

$$\mathbf{K}_{\phi x \phi x} = \int_{{}^1V} {}^1S_x (y^2 + z^2) \mathbf{N}_{,x}^T \mathbf{N}_{,x} d^1V + \int_{{}^1V} {}^1S_{xs} e_s (\mathbf{N}_{,x}^T \mathbf{N} + \mathbf{N}^T \mathbf{N}_{,x}) d^1V.$$

The J_2 flow theory is adopted to model the plastic behaviour of the material, and the constitutive matrix $\mathbf{C}$, which relates the corotational Jaumann rate of Cauchy stress $\overset{*}{\boldsymbol{\sigma}}$ to the strain rate $\mathbf{D}$, can be written in the form

$$\mathbf{C} = \mathbf{C}^e - h^{-1} \mathbf{b} \mathbf{b}^T, \tag{12}$$

where $\mathbf{b} = \mathbf{C}^e \mathbf{a}, \mathbf{a} = \partial f / \partial \boldsymbol{\sigma}, h = \mathbf{a}^T \mathbf{b} + E_p, f = \sqrt{3J_2}$ and J_2 is the second invariant of the deviatoric Cauchy stress and $\mathbf{C}^e$ is the elastic constitutive matrix. The plastic hardening modulus E_p is obtained from the tangent modulus E_t and from the elastic modulus E. The matrix $\mathbf{C}_L$ is obtained from $\mathbf{C}$ using the relationship between the strain rate $\mathbf{D}$ and the rate of Green-Lagrange strain $\dot{\mathbf{E}}$.

The discretized form of the equilibrium equation can be briefly written as

$$\mathbf{F}(\mathbf{q}, \lambda) \equiv \lambda \mathbf{Q}(\mathbf{q}) - \mathbf{R}(\mathbf{q}) = \mathbf{0}. \tag{13}$$

The orthogonal trajectory method, FRIED 1984, is used to solve the nonlinear system (13). This method does not require a known equilibrium configuration to start the iterative process, in contrast to most other methods. This is a great advantage in computing the branch after bifurcation points. The iterative changes $\delta\mathbf{q}^i$ and $\delta\lambda^i$ can be solved from

$$\delta\lambda^i = -\frac{(\delta\mathbf{q}_Q^i)^T \mathbf{C}^u \delta\mathbf{q}_F^i}{(\delta\mathbf{q}_Q^i)^T \mathbf{C}^u \delta\mathbf{q}_Q^i + \alpha^2}, \quad \delta\mathbf{q}^i = \delta\lambda^i \delta\mathbf{q}_Q^i + \delta\mathbf{q}_F^i,$$
$$\delta\mathbf{q}_Q^i = (\mathbf{K}^{i-1})^{-1} \mathbf{Q}^{i-1}, \quad \delta\mathbf{q}_F^i = (\mathbf{K}^{i-1})^{-1} \mathbf{F}^{i-1}, \tag{14}$$

and where $\mathbf{C}^u$ is an updated weighting matrix and α^2 is a scaling factor, KOUHIA & MIKKOLA 1989.

NUMERICAL EXAMPLES

Elasto-plastic behaviour of simply supported and continuous steel I-beams have been studied. Computed results have been compared with experimental data KITIPORNCHAI & TRAHAIR 1975 (simply supported beams = S) and POOWANNACHAIKUL & TRAHAIR 1976 (continuous beams = C). Load-deflection curves and the FE discretizations used are shown in Figs. 1 and 3. For the continuous beam the interaction curve is in Fig. 2. Imperfection sensitivity seems to be clear explanation to the discrepancy between experimental results and theoretical predictions made by POOWANNACHAIKUL & TRAHAIR 1976. The imperfection sensitivity curves are shown in Fig. 4.

In Fig. 5 load-deflection curve for an elastic analysis of a space frame is shown.

(5)

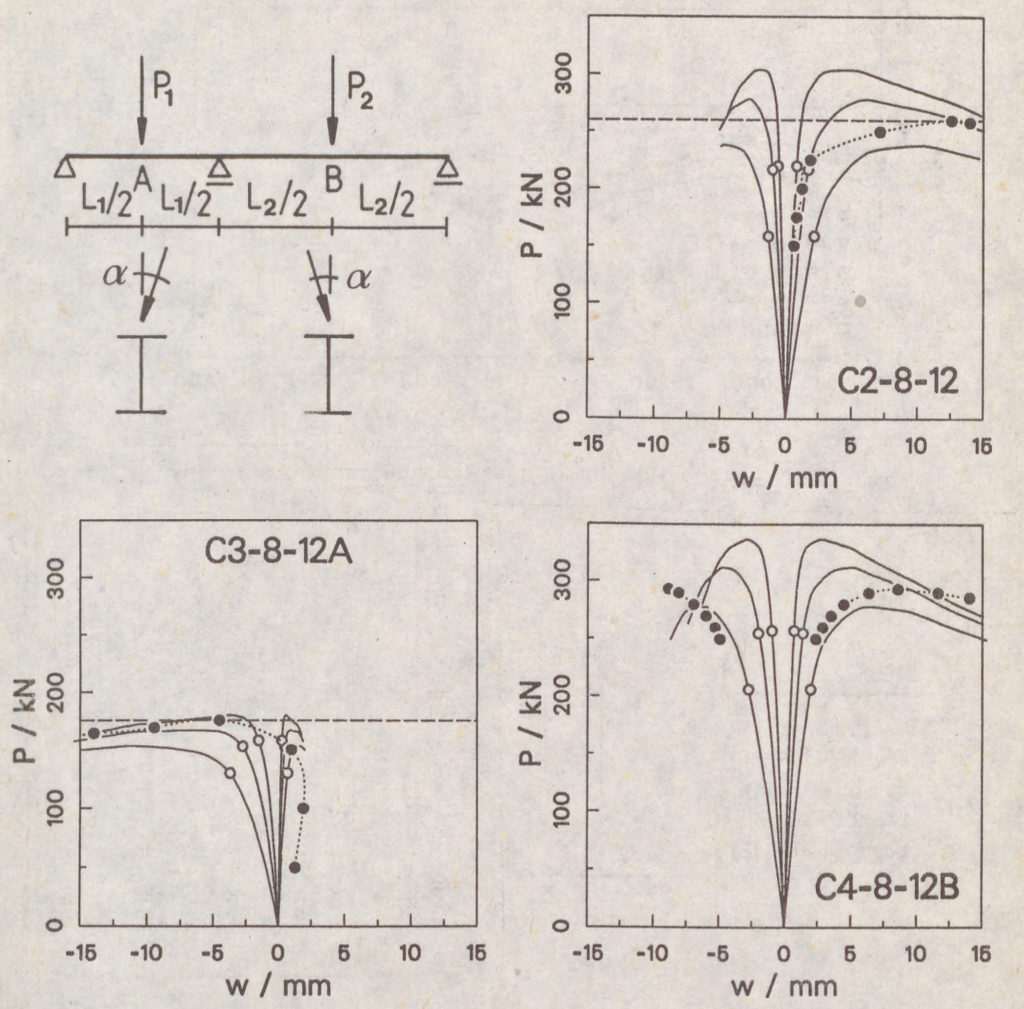

FIG. 1 Lateral deflections at the midpoints of the spans. The circular black markers connected with dotted line are the experimental results. Solid curves indicate the calculated results with different values of imperfection. All calculations with strain hardening material ($E_t = E/35, E = 203$ GPa, $\sigma_Y = 320$ MPa, $\nu = 0.3$). The blanked circle show the load level at which first yield was noticed. Imperfections in the FE computations: C2-8-12 ($P_1 = P, P_2 = 0$) $\alpha = 1°, 2°, 4°$; C3-8-12A ($P_1 = 0, P_2 = P$) and C4-8-12B ($P_1 = P, P_2 = 2/5P$) $\alpha = 0.5°, 1°, 2°$. For the cross-section data see Fig. 3, $L_1 = 2.44$ m, $L_2 = 3.66$ m. 24 elements have been used to model the beam including two small elements (length $\approx$ 100 mm) around points A, B and at the midsupport. Deflections at point A are positive and at B negative.

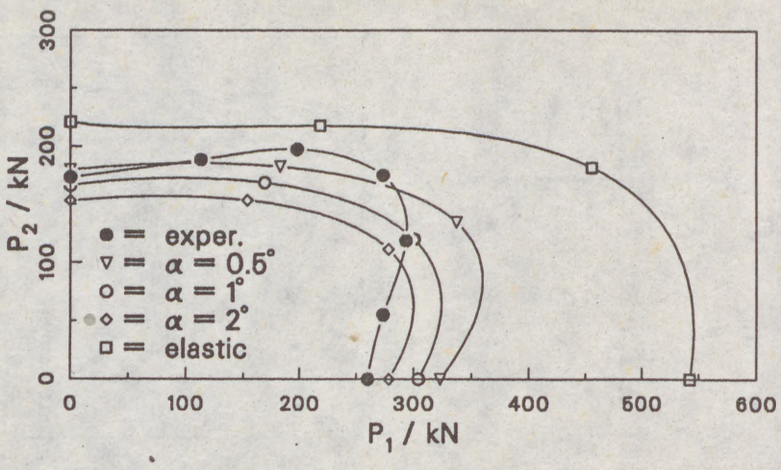

FIG. 2 Interaction diagram for the continuous beam.

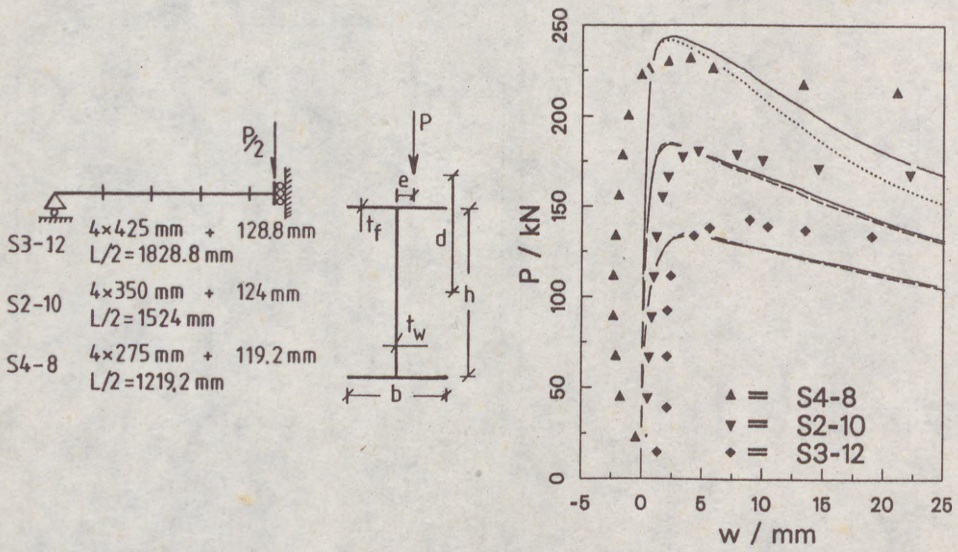

FIG. 3 Lateral midpoint deflections of the simply supported beams. Dashed lines indicates calculations without residual stresses and the dotted line (beam S4-8) is the case with no strain hardening ($E_t = 0$, in all other calculations $E_t = E/35, E = 203$ GPa, $\sigma_Y = 320$ MPa, $\nu = 0.3$). Solid lines are calculated curves with the same residual stress pattern (quartic polynomials) as in KITIPORNCHAI & TRAHAIR 1975 (Fig. 7, p. 1340). Black markers which are not connected are the experimental measurements. Imperfections in FE calculations: S4-8 $e = 4$ mm, S2-10 and S3-12 $e = 2$ mm. Cross-section 261 × 151 UB 43, $h = 248.7$ mm, $b = 151.5$ mm, $t_w = 7.67$ mm, $t_f = 12.3$ mm and $d = 219$ mm.

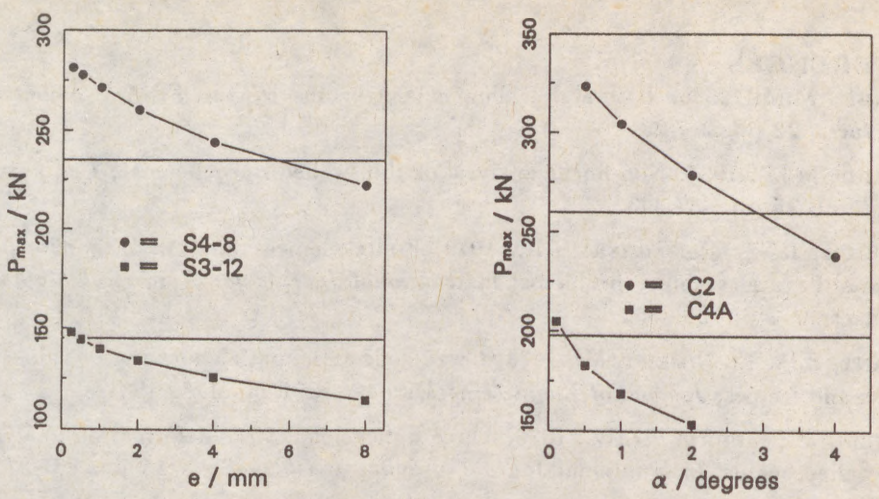

FIG. 4 Imperfection sensitivity of simply supported beams and continuous beams.

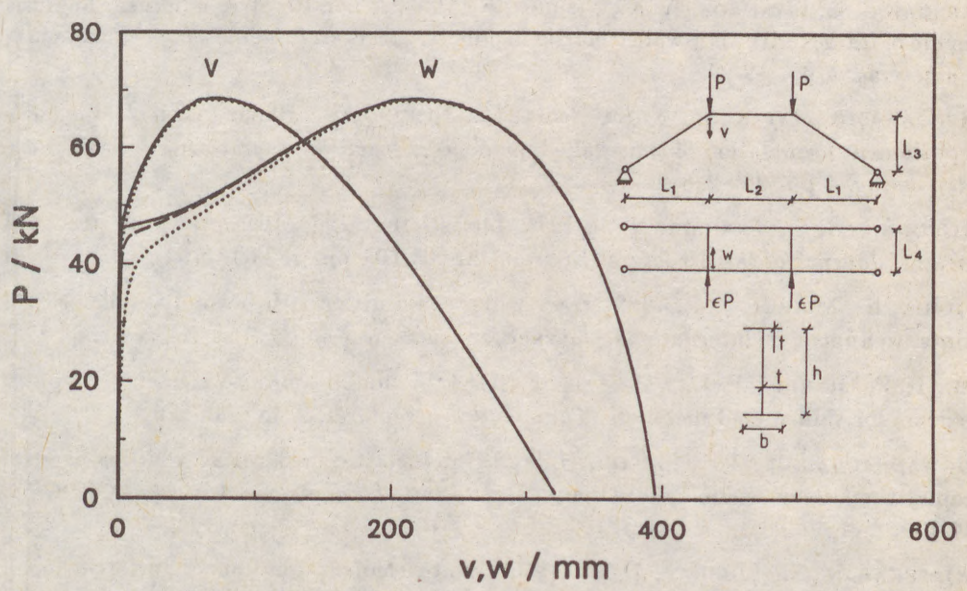

FIG. 5 Elastic space frame, HASEGAWA et al. 1987. Solid line $\epsilon = 0$, dashed line $\epsilon = 0.01$, dotted line $\epsilon = 0.1$, $L_1 = 692.8$ mm, $L_2 = 614.4$ mm, $L_3 = 400$ mm, $L_4 = 300$ mm, $h = 120$ mm, $b = 60$ mm, $t = 3.3$ mm, $E = 206$ GPa, $\nu = 0.3$, u, v, w displacements and rotation around member axis is prevented at the supports, 5 elements / member.

(8)

REFERENCES

ATTARD, M.M., 1986, Lateral buckling of the beams by the FEM, *Computers & Structures*, **23** pp. 217-231.

ATTARD, M.M., 1987, Non-linear analysis of thin-walled open beams , *Computers & Structures*, **25** pp. 437-443.

BARSOUM, R.S., GALLAGHER, R.H., 1970, Finite element analysis of torsional and torsional-flexural stability problems, *International Journal for Numerical Methods in Engineering*, **2** pp. 335-352.

BAŽANT, Z.P., EL NIMEIRI, M., 1973, Large deflection spatial buckling of thin-walled beams and frames, *Journal of Engineering Mechanics*, **99** pp. 1259-1281.

EPSTEIN, M., MURRAY, D.,W., 1976, Three dimensional large deformation analysis of thin-walled beams, *International Journal of Solids and Structures*, **12** pp. 867-876.

FRIED, I., 1984, Orthogonal trajectory accession to the equilibrium curve, *Computer Methods in Applied Mechanics and Engineering*, **47** pp. 283-297.

HASEGAWA, A., LIYANAGE, K.,K., NISHINO, F., 1987, A non-iterative nonlinear analysis scheme of frames with thin-walled elastic members, *Structural Engineering / Earthquake Engineering*, **4** pp. 19-29.

HASEGAWA, A., LIYANAGE, K.,K., NODA, M., NISHINO, F., 1987b, An inelastic finite displacement formulation of thin-walled members, *Structural Engineering / Earthquake Engineering*, **4** pp. 269-276.

KITIPORNCHAI, S., TRAHAIR, N.,S., 1975, Inelastic buckling of simply supported steel I-beams, *Journal of the Structural Division*, ASCE **101** pp. 1333-1347.

KOUHIA, R., MIKKOLA, M., 1989, Tracing the equilibrium path beyond simple critical points, to appear in *International Journal for Numerical Methods in Engineering*.

LEE, H.,P., HARRIS, P.,J., HSU, C-T.,T., 1984, A nonlinear finite element computer program for thin-walled members, *Thin-Walled Structures*, **2** pp. 355-376.

POOWANNACHAIKUL, T., TRAHAIR, N.,S., 1976, Inelastic buckling of continuous steel beams, *Civil Engineering Transactions, Institution of Engineers, Australia*, CE **8**, pp. 134-139.

RAJASEKARAN, S., MURRAY, D.W., 1973, Finite element solution of inelastic beam equations, *Journal of Engineering Mechanics*, **99** pp. 1025-1041.

SEKULOVIĆ, M., 1986, Geometrically nonlinear analysis of thin-walled members, Proceedings *'Steel Structures: Recent Research Advances and Their Applications to Design'*, Elsevier Applied Science Publishers Ltd. pp. 219-243.

WUNDERLICH, W., OBRECHT, H., SCHRÖDTER, V., 1986, Nonlinear analysis and elastic-plastic load-carrying behaviour of thin-walled spatial beams with warping constraints, *International Journal for Numerical Methods in Engineering*, **22** pp. 671-695.

(1)

MURZEWSKI, Janusz W. (1)

OVERALL INSTABILITY OF STEEL FRAMES WITH RANDOM IMPERFECTIONS

INTERNATIONAL COLLOQUIUM
STABILITY OF STEEL STRUCTURES
BUDAPEST, HUNGARY, 1990
PRELIMINARY REPORT

Summary: The equivalent sway θ_o of a frame is treated as a random variable which increases the variance of stresses μ_σ. The effect of random residual stress σ_o is taken into account by an increase of the coefficient of variation v_c of ultimate compression force of structural members. The imperfection parameters μ_σ and v_c are calibrated in a semi-empirical way. Elastic and plastic instability modes are treated as independent random events and their probabilities are multiplied. The probability-based formula for the characteristic buckling strength of columns is extended to framed systems. The frame slenderness ratio Λ is defined by means of conditional instability factors $\breve{\gamma}_{pl}$ and $\breve{\gamma}_{cr}$ relative to plastic and elastic failure modes. A rigid-plastic frame analysis and an elastic equilibrium analysis are needed for evaluation of carrying capacity of the frame. The coefficient of variation v_c of the carrying capacity is augmented for medium values of the frame slenderness ratio Λ in correspondence with experimental data. A partial safety index β_R is formulated as the safety measure. It is more adequate from the point of view of the constructor's responsability than the global safety index β which covers also field of responsability of the designer and the user of the structure.

---

(1) Professor of Civil Engineering, Politechnika Krakowska, Kraków, Poland

(2)

1. Introduction

Neither elastic stability nor plastic limit analysis can give realistic estimates of the carrying capacity of frames. Cumbersone nonlinear calculations do not help any more unless geometrical and structural imperfections are taken into account. Two kinds of imperfections are defined in the new European design recommendations: an initial sway θ_o of the frame system and a residual stress σ_o of structural members. The effect of sway is replaced by an equivalent horizontal force H_o and the effect of residual stress is replaced by an initial deflection y_o. The deflection y_o trans--forms any column problem in the beam-column problem and it reduces the buckling strength f_c in reference to both the plastic limit f_{pl} and the Euler's critical value f_{cr}. In the probabilistic approach, the sway θ_o and the residual stress σ_o are treated as random variables with zero mean values, $\overline{\theta}_o = 0$ and $\overline{\sigma}_o = 0$. So is the mean equivalent horizontal force, $\overline{H}_o = 0$, however its variance μ_H^2 is positive.

$$\mu_H^2 = \mu_\theta^2(\overline{P}^2 + \mu_p^2) \approx \mu_\theta^2 \overline{P}^2 \ , \tag{1}$$

where $\mu_\theta^2 > 0$ - variance of sway of the frame,

$\overline{P}$, μ_p^2 - the first and second moments of the gravitational loads,

The random residual stress σ_o and other structural imperfections reduce the median strength $\breve{f}_c$ of a sample of columns under compression, in reference to its upper bound,

$$\breve{f}_c(\lambda) \leq \min\left[\breve{f}_{pl}, \breve{f}_{cr}(\lambda)\right], \quad \lambda = L\sqrt{A/I} \ . \tag{2}$$

The reduction of strength $\breve{f}_c$ is extreme for medium values of the slenderness ratio λ, i.e. when plastic and critical strengths are equal ,

$$\breve{f}_{cr}(\lambda_k) = \breve{f}_{pl} \rightarrow \lambda_k = \pi\sqrt{\breve{E}/\breve{f}_{pl}} \ . \tag{3}$$

The Young's theoretical model, i.e. a column with an initial deflection $|y_o| > 0$ and without any other imperfections, helped to explain the reductions of f_c for $\lambda \approx \lambda_k$. It enabled to derive an analytical formula for the buckling coefficient $\chi(\lambda) = \breve{f}_c(\lambda)/\breve{f}_{pl}$, the Ayrton-Perry formula. If the initial deflection y_o was randomized, $\overline{y}_o = 0$, $\mu_y^2 > 0$, and equivalent standard deviations $\mu_y(\lambda)$ were derived from the conventional buckling coefficients $\chi(\lambda)$, the variance values $\mu_y^2(\lambda)$ would be not realistic. They would be much

(3)

higher than empirical values of variance.

The Euler's theoretical model, i.e. a straight column ($y_o = 0$) under compression $N = A\sigma$, may also explain the reductions of the carrying capacity Af_c for $\lambda \neq \lambda_k$ if the plastic and elastic instability modes are considered as independent random events. The median $\breve{f}_{cr}$ depends on λ according to the Euler's theory

$$\breve{f}_{cr} = \breve{f}_{pl}/\Lambda^2 , \tag{4}$$

where $\Lambda = \lambda/\lambda_k$ - relative slenderness ratio.

A probabilistic formula for the elastic-plastic buckling strength has been derived in a simple form [Murzewski 1973, 1989b],

$$\breve{f}_c = \breve{f}_{pl} / (1 + \Lambda^{2/\upsilon})^{\upsilon}, \tag{5}$$

where $\upsilon = \upsilon(\Lambda)$ - the Weibull coefficient of variation.

It was assummed that both random variables f_{pl} and f_{cr} follow the Weibull probability law,

$$W(f) = 1 - \exp\left(-\sqrt[\upsilon]{f/\breve{f}}\right), \quad f > 0 . \tag{6}$$

Either Weibull random variable f has two distribution parameters, $\breve{f}$ and υ. The logarithmic mean $\breve{f}$ and variance ν^2 are related with the Weibull parameters $\breve{f}$ and υ as follows

$$\ln \breve{f} = \int_0^\infty \ln f \, dW(f) = \ln \breve{f} - C\upsilon \rightarrow \breve{f} = \breve{f} e^{-0,45\upsilon} ,$$
$$\nu^2 = \int_0^\infty \ln^2(f/\breve{f}) \, dW(f) = \upsilon^2\pi^2/6 \rightarrow \nu = \upsilon\pi/\sqrt{6} . \tag{7}$$

where $C = 0,5772$ - the Euler's constant.

The formula (5) was derived with an additional assumption that the coefficients of variation are equal and dependent on the slenderness ratio Λ,

$$\nu_c(\Lambda) = \nu_{pl}(\Lambda) = \nu_{cr}(\Lambda) = 1,28\,\upsilon . \tag{8}$$

The Rankine-Merchant's formula is a case of (5) if $\upsilon = 1$ and $\nu_c = 1,28$. The theoretical values of the coefficient of variation $\nu_c(\Lambda)$ which have been derived from the conventional buckling coefficients $\chi(\Lambda)$ are realistic. They agree with empirical values [Gwóźdź 1977, Fukumoto and Itoh 1984].

2. Imperfection parameters

The initial sway θ_o is an equivalent parameter of frame imperfections. It cannot be directly taken from statistical measurements of the geometrical accuracy of columns. The conventional value θ_o recommended for the partial safety factor design [Eurocode No.3, 1984] is as follows

$$\theta_k = r_1 r_2 / 200 \,, \tag{9}$$

where $r_1 = \min\left(\sqrt{5/h}\,,\ 1\right)$, $h[m]$ - height of a storey,
$r_2 = (n + 1)/2n$, n - number of loaded columns.

The standard deviation μ_θ depends on the type and scope of inspection of the construction. Some calibrated values are given in Table 1.

Table 1. Standard deviation of equivalent sway

Inspection class	μ_θ for $h \leq 5$, $n = 1$
moderate	0,004
normal	0,003
stringent	0,002

The conventional reduction factors r_1, r_2 may be used unless some more sophisticated models are applied.

The Weibull coefficient of variation $v(\Lambda)$ of the column strength $f_c(\Lambda)$ is specified in a semi-empirical way. Multiple buckling curves a, b, c are taken from standard specifications (Fig.1) and their collocation at the point $\Lambda = 1$ with the new buckling curves gives equations from which the values $v(1)$ are derived for three classes of compression members a, b, c. An index $k_R = 2$ is taken for the characteristic value f_k,

$$f_k\,(1) = \breve{f}_c \exp(-2v_1) \,, \quad v_1 = v(1) \,, \tag{10}$$

where $\breve{f}_c = \breve{f}_y / 2^{v_1}$, $v_1 = (\sqrt{6}/\pi)\cdot v_c(1)$.

$\breve{f}_{pl}/f_k = 285/235 = 1{,}2$ for a structural carbon steel, $t = 16$ mm.

(5)

hence $\nu_1 = \begin{Bmatrix} 0,22 \\ 0,25 \\ 0,31 \end{Bmatrix}$ for the buckling curve $\begin{Bmatrix} a \\ b \\ c \end{Bmatrix}$.

The values ν_1 are considerably higher than the values $\nu_o = \nu(0)$ taken from experimental tests of yield limit of structural steel

$$\nu_o = \begin{Bmatrix} 0,087 \\ 0,079 \\ 0,087 \end{Bmatrix} \text{ for the carbon steel } \begin{Bmatrix} \text{effervescent} \\ \text{killed} \\ \text{manganese} \end{Bmatrix} .$$

The values ν_1 are also higher than a coefficient of variation $\nu_\infty = 8\%$ for very slender columns with semi-rigid connections. The values ν_1 may be reduced if there is no or little uncertainty about end restraints of the column. Attention must be paid that the relative slenderness ratio Λ introduced to Forms.(4) and (5) is different than the ratio $\bar{\lambda}$ defined in the Eurocode,

$$\bar{\lambda} = (\lambda/\pi)\sqrt{f_k/E} = \Lambda/\sqrt{1,2} \quad . \tag{11}$$

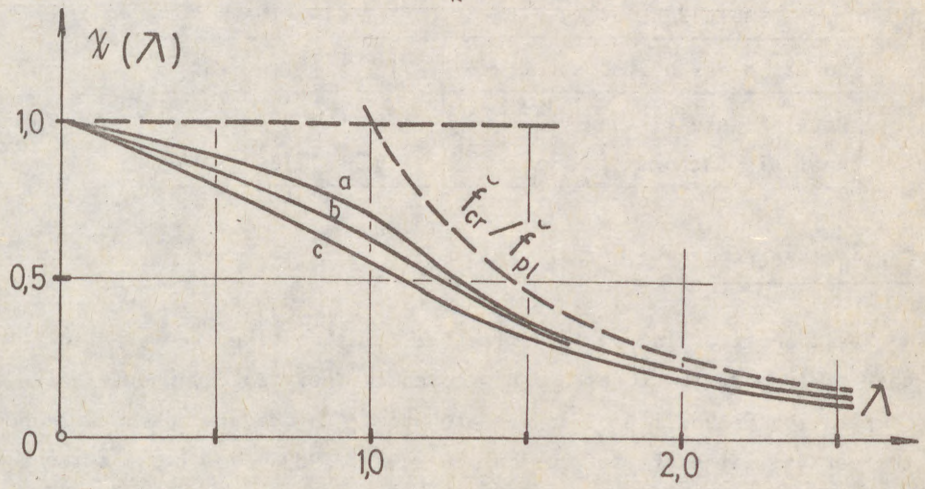

Fig.1. Multiple instability curves according to the probabilistic formula (5)

The function $\nu_c(\lambda)$ is defined according to an interpolation formula which corresponds with the experimental data. The values ν_c are augmented by addition of $\nu_A = 0,06$ due to random variability of dimensions of cross-sections

$$\nu_c(\Lambda) = \sqrt{(\nu_o^2 + 2\Lambda^2\Delta\nu^2 + \Lambda^4\nu_\infty^2)/(1 + \Lambda^4) + \nu_A^2} \quad , \tag{12}$$

(6)

where $\Delta\nu^2 = \nu_1^2 - \nu_A^2 - (\nu_o^2 + \nu_\infty^2)/2$ - increment of variance due to imperfections of a compression member,

$\Delta\nu = \begin{Bmatrix} 0,19 \\ 0,23 \\ 0,29 \end{Bmatrix}$ for the buckling curve $\begin{Bmatrix} a \\ b \\ c \end{Bmatrix}$.

A partial safety index β_R for a column under a design compression force N_d:

$$\beta_R = \ln[f_c(\Lambda)/\sigma_d]/v_c(\Lambda), \qquad (13)$$

where f_c as in (5) - median strength,

$\sigma_d = \gamma_d N_d/A$ - design stress,

$\gamma_d > 1$ - analysis factor.

The index β_R has to exceed a limit value β_R^* specified in Table 2. The analysis factors γ_d for each class of structural safety are calibrated under a supposition that random variations of designer's results are $v_d = 5\%$, and no gross errors are committed in the structural analysis.

Table 2. Safety elements of steel members

Safety class of the structure	1	2	3
Partial safety index β_R^*	1,4	2,0	2,8
Analysis factor γ_d	1,07	1,10	1,14

3. Frame slenderness ratio

The basic question is how to define the relative slenderness ratio Λ in the case of framed structures and how to check their safety when elastic and/or plastic instability modes are probable. A procedure has been proposed for the partial safety factor design [Murzewski 1989a]. Now it is extended to the level-2 probability-based design as follows:

a) The frame slenderness ratio Λ depends on the conditional median instability factors $\breve{\gamma}_{pl}$ and $\breve{\gamma}_{cr}$. The condition is that the failure occurs in effect of either rigid-plastic frame collapse (γ_{pl}) or the elastic equilibrium bifurcation(γ_{cr}),

$$\Lambda = \sqrt{\breve{\gamma}_{pl}/\breve{\gamma}_{cr}} \; . \qquad (14)$$

(7)

b) The conditional mean instability factor $\bar{\gamma}_{pl}$ is equal to the ratio of the mean power $\bar{D}_{pl}$ which is dissipated in plastic hinges of the frame in its limit state and a design value Φ_d of random power of applied loads at the moment when the frame begins to collapse under a most severe combination of actions,

$$\bar{\gamma}_{pl} = \bar{D}_{pl}/\Phi_d \approx \breve{\gamma}_{pl} \ . \tag{15}$$

c) The conditional median instability factor $\breve{\gamma}_{cr}$ is equal to the ratio of the design value $\gamma_d N_d$ of random axial force N of the most severely loaded column and the median value $\breve{N}_{cr}$ of critical force N_{cr} which is random mainly due to uncertain end restraints. The effective length $\breve{L}$ may be determined in a conventional way,

$$N_{cr} = \pi^2 EI/L^2 \ . \tag{16}$$

d) The load system F_j, $j = 1, 2, 3...$ applied to the frame is devided in two subsystems. One subsystem gives only axial forces N_i in the columns, another subsystem gives bending moments M_i.

e) The log-normal coefficient of variation $v_c(\Lambda)$ of the carrying capacity of the frame depends on its slenderness ratio Λ so as it does in the case of a single column, (12).

f) The structural safety is checked by comparison of the partial safety index β_R with a specified limit value β_R^* ,

$$\beta_R = -(\sqrt{6}/\pi)\ \ln\left(\sqrt[\upsilon]{1/\breve{\gamma}_{pl}} + \sqrt[\upsilon]{1/\breve{\gamma}_{cr}}\right) > \beta_R^* \ , \tag{17}$$

where $\upsilon = (\sqrt{6}/\pi) v_c(\Lambda)$,

β_R^* - value from Table 2.

This procedure is formulated under assumption that design values of action effects, N_d , M_d , have been given, no matter how. Preferably they should be determined also by means of the level-2 probability-based procedure with a specified partial safety factor β_S^*. Evaluation of a global safety index β is not necessary although it is recommended by many authors and it is sometimes considered as an "exact" method of safety verification. But there are separate responsability fields of the constructor and the user and the designer. Therefore the separate safety check is postulated for the first one [Murzewski 1970, 1989b].

(8)

4. Conclusions

The random sway θ_o is considered as the equivalent imperfection of the frame system. It does not change the mean stress calculated for a combination of expected actions but it augments the stress variance μ_σ^2 and the design stress σ_d. Its final value should be determined with an analysis factor γ_d

$$\sigma_d = \gamma_d(\overline{\sigma} + \beta_S^* \mu_\sigma) . \tag{18}$$

The structural failure is considered as a logical sum of plastic collapse and/or elastic instability. Median values of conditional stability factors $\breve{\gamma}_{pl}$ and $\breve{\gamma}_{cr}$ are taken to a definition of frame slenderness ratio Λ. The coefficient of variation v_c of the frame resistance depends on Λ. It is enhanced by random effects of residual stress and other imperfectiona of the structural member. The unconditional stability factor $\breve{\gamma}$ determines the partial safety index β_R.

$$\beta_R = \ln\breve{\gamma}/v_c . \tag{19}$$

The partial index β_R is a better safety measure than the global safety index β if the responsability field of the constructor is limited.

References

FUKUMOTO Y., ITOH Y., 1984: Exploitation do courbes multiples de flambemant par une approche à base de données experimentales, Construction Métallique, No.3, pp.3-22

GWÓŹDŹ M. 1977: Distribution parameters of axial and lateral buckling strengths (in Polish) XXIII Civil Engineering Conference - Krynica, Vol.2, pp.55-61

MURZEWSKI J., 1970; Safety of Building Structures (in Polish), Arkady Warsaw:1974 (in German) Verlag Bauwesen, Berlin

MURZEWSKI J., 1973: Stochastic stability of structural systems. Lecture Notes.Stokes Session, CISM Udine

MURZEWSKI J., 1989a: Failure mode interaction for multi-storey frame design (in Polish), VIII Intern. Conference Metal Structures, Gdańsk, Vol.3, pp.228-235

MURZEWSKI J., 1989b: Reliability of Civil Engineering Structures, (in Polish), Arkady,Warsaw

NESHEVA, Iskra G.

ON STABILITY OF ELASTOPLASTIC STEEL PLANE FRAMES

INTERNATIONAL COLLOQUIUM
STABILITY OF STEEL STRUCTURES
BUDAPEST, HUNGARY, 1990
PRELIMINARY REPORT

SUMMARY: A relatively accurate estimate of the critical value of the load which a given steel framework can carry might be achieved only when both geometric and material nonlinearity are taken into consideration. This requires the application of an efficient mathematical method ensuring fast convergence of the solution even when strongly expressed nonlinearity is available. In the search of an appropriate method the results of three similar in their approach methods are discussed. Also a precising of the critical load step value is suggested.

The main purpose of this study is the determination of the critical equilibrium of steel frames in a highly plastified state. This type of structures when increasing plastic deformations are available lose their carrying capacity mainly because of instability.

Nevertheless still in the design practice the stability of steel frames is analysed at the assumptions of a linearly elastic material, longitudinal non-deformability of the elements and relatively small displacements of the joints. As a critical load the Euler critical load is assumed. But the investigations done show that the so received critical load might turn to be significantly bigger than the actual, i.e. a mistake is made in the dangerous direction overestimating the load capacity of the system.

(1)Seniour Research Associate, CESSI, Sofia

Even when a nonlinear analysis is carried out most often the plastic hinge concept is applied for the different models and the considerable geometric nonlinearity occuring near the critical state cannot be taken into account.

The above statement and the investigations done show that the correct estimate of the critical value of the load which a given structure can carry is achieved only when both geometric and material nonlinearity are taken into consideration. This circumstance makes rather difficult obtaining numeric evaluations as it requires the application of an efficient mathematical method. This method should provide the possibility of solving the system for loads very near the critical,i.e. for strongly expressed nonlinearity and it should ensure fast convergence of the solution.

In this sense the best theoretic method still is the Newton-Raphson's one (NRM). For pity the necessity of assembly and inversion of the tangent stiffness matrix at every iteration makes it very labour- and computer time-consuming.

That is why a number of more easily applicable modified N-R methods have recently been introduced,such as the BFGS method or the method of M.Crisfield [1], etc. Though considerably more convenient than NRM, the NGFS method is still rather clumsy to use. The method of Crisfield is further simplified from an user's point of view.

In 1986 another MNRM was suggested by S.Simeonov [2], similar in approach to the Crisfield's one, but basicly different and with much faster convergence even in the cases of high nonlinearity. It was programmed and used as a basis for a research in our institute [3]. The material nonlinearity here is considered according the deformation theory of plasticity. The nonlinear relationship between the stress and the strain is introduced as input data by a realistic stress-strain diagram for building steel with two linear zones for the elastic and the yielding state and a curve line for the material strengthening zone. Unloading is treated as well.

The geometric nonlinearity is taken into account by a II order theory. The effect of N-forces is accounted for by correction factors called Livseley's stability functions [4] - depending on N/N_E, where N_E is the Euler critical load for a member.
The structural distortion is considered by the change of the angles between members in the process of the incremental loading and is calculated at each iteration.
The solution of the nonlinear equations is carried out by an accelerative method of successive approximations. So the iterative process arrives at the true solution of the nonlinear problem by means of a series of approximate linear solutions of the kind:

$$\delta^{\nu+1} = X^{\nu} - \alpha_{\nu} . B_o [A(X^{\nu}) . X^{\nu} - P] = X^{\nu} - \alpha_{\nu} . B_o . R^{\nu} \quad (1)$$

where:

B_o is the global stiffness matrix of a nonlinearly deformable system,

X is the nodal displacement vector,

P is the load vector,

$R = [r_1, r_2, r_3, \ldots, r_n]$ is the vector of unbalanced internal and externally applied forces when given displacements X_ν are reached,

α_ν is an accelerative factor and is calculated in the following way: $\alpha_\nu = \alpha_{\nu-1} . \bar{\alpha}_\nu$, $(\alpha_o = 1)$

$$\bar{\alpha}_\nu = \frac{(Bh_\nu, h_\nu)}{(AX^{\nu} - AX^{\nu+1}, h_\nu)} = \frac{(R_\nu, h_\nu)}{(R_\nu - R_{\nu+1}, h_\nu)} = \frac{R_\nu^T . (Z_\nu - Z_{\nu-1})}{(R_\nu - R_{\nu+1})^T . (Z_\nu - Z_{\nu-1})} \quad (2)$$

With the existing variety of methods the problem of numeric study of their efficiency arises. The efficiency depends mainly on the speed of convergence and on the number and complexity of the calculation operations.
The spheric norm of the unbalanced forces vector or the ratio of the norms of current to initial vector of unbalanced forces are assumed as a criterion for achieved convergence:

$$\| R \| = \sqrt{\sum_{I=1}^{N} R_I^2} \leq \delta_2 \quad \text{or} \quad \left\| \frac{R^{\nu}}{R^{o}} \right\| < \delta_2 \quad (3)$$

A comparitive analysis of three similar in their approach methods has been carried out by the author:

1.- a MNRM with an accelerative coefficient α_v - a constant number chosen in advance on the basis of numeric experiments;

2.- the here described SSM [2] [3] with a varying accelerative factor α_v calculated at each iteration as a function of the displacements' vectors of the structural joints and the unbalanced forces' vectors of two subsequent approximations;

3.- the MCM [1], where an improved iterative increase of the displacement's vector is expressed as a sum of the previous step's X increment multiplied by an appropriately chosen scalar number and the current X increment.

The results from the analysis of a portal steel frame are presented. For the first series of solutions a tolerance of 0.005 is chosen. On fig. 1. the number of iterations by the three methods for four load steps are presented graphicly. Apparently at this accuracy all the three methods show good convergence. On fig.2. the results of the second series of computations are represented . The analysis is carried out for a 10 times higher accuracy, but only the material nonlinearity is considered. The iteration process for the first method does not satisfy the set accuracy condition for the previously chosen maximum 30 iterations. And last, for the same assumed tolerance of 0.0005, but for both geometric and material nonlinearity considered both the first and the third method do not converge for the 30 iterations calculated. Only the second method remains covergible even when a strong nonlinearity has been developed.

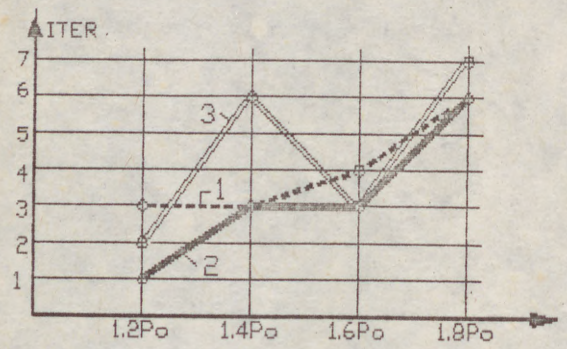

NLE δ=0.005	1.2Po	1.4Po	1.6Po	1.8Po
1- MNRM	3	3	4	6
2- SSM	1	3	3	6
3- MCM	2	6	3	7

Figure 1

Besides the accelerated iterative procedure SSM when systems with substantial nonlinearity are analysed, is two to three times faster than the modified Newton-Raphson method.

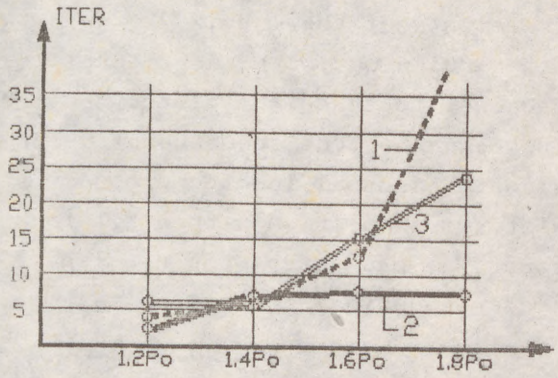

NLM δ=0.0005	1.2Po	1.4Po	1.6Po	1.8Po
1- MNRM	4	6	13	30
2- SSM	3	7	8	8
3- MCM	6	6	15	24

Figure 2

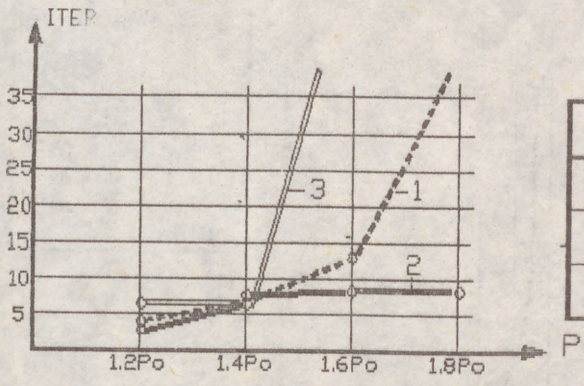

NL2 δ=0.0005	1.2Po	1.4Po	1.6Po	1.8Po
1-MNRM	4	6	13	30
2-SSM	3	7	8	8
3-MCM	6	6	30	30

Figure 3

Throughout the non-linear analysis of the frame a stability check is carried out by [3]. As a basic criterion for the critical state of the structure the annulation of the determinant of its tangent stiffness matrix has been assumed:

$$\det K_t = \prod_{ii=1}^{n} a_{ii} = 0, \qquad (4)$$

where: K_t is the global matrix updated with the currently calculated stiffnesses of the plastified cross sections and the current stability functions of the members,

a^{ii} are the diagonal elements of the matrix.

The check of the criterion is carried out with incremental load applied to the structure, because to trace the history of the process, it is necessary to trace the true sequence of deformation and stability states as the actual loading program is put through. This requires stepwise solution with small load increments, taking into account at each step the non-linear material properties and the corresponding correction factors.

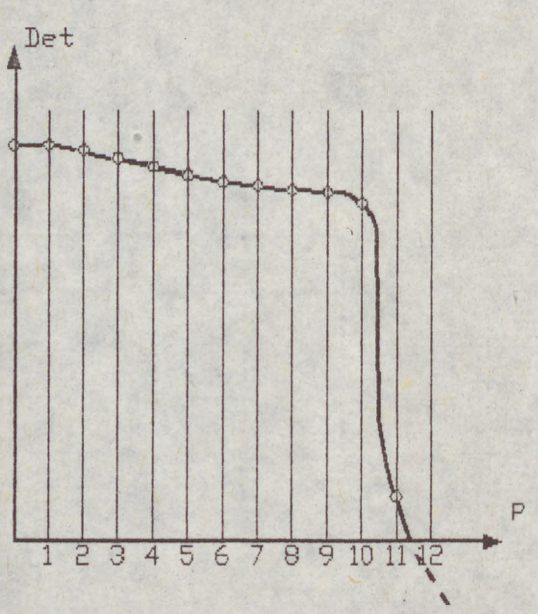

	Det
0	0.0375×10^{53}
1	0.0375×10^{53}
2	0.0770×10^{52}
3	0.0240×10^{51}
4	0.0964×10^{49}
5	0.0840×10^{48}
6	0.0127×10^{48}
7	0.0224×10^{47}
8	0.0126×10^{47}
9	0.0230×10^{46}
10	0.0043×10^{45}
11	0.0059×10^{44}
12	0

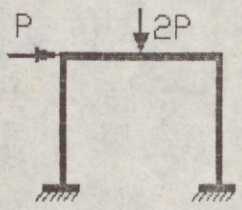

Figure 4.

On fig. 4. the change of the value of the determinant in the process of incremental loading of a portal frame is shown.

It has been proved that instability of the steel frame can be reached earlier before reaching the yield deformations or a rupture of the material.

It should be stated also that the graph 'Det - load' is influenced a lot by the availability and intensity of the plastic deformations. As Simeonov's method ensures convergence for values of the load near the critical one, the loading is increased stepwise till divergence of the process of subsequent solutions occurs. This enables us to study the behaviour of a non-linear frame near its collapse.

Let us assume that this happens at the (n+1) load step. Different approaches of precising the solution are possible. One plausible way is splitting the last load step in several smaller ones and repeating the solution. Another one is based on the property of the determinant of the tangent stiffness matrix rapidly to tend to zero value in the vicinity of the critical load. This gives the possibility of particularising the value of the critical load by interpolation and extrapolation:

$$\mu_{\kappa} = \frac{D_{i-1} \cdot \mu_{i-1} - D_i \cdot \mu_i}{D_{i-1} \cdot D_i} \qquad (5)$$

Here μ_i is the load parameter at the last load step for which the iterative process converges. D_i is the determinant of K_t for this loading step.

This study is a minor contribution to getting nearer the precise analysis of the actual behaviour of steel frameworks in the process of incremental loading. It is as well an attempt of a due response to the new higher requirements of practice for designing slender structures with improved aesthetics and at lower expenses.

REFERENCE:

1. Crisfield M., Incremental/ Iterative Solution Procedures for Non-linear Structural Analysis., Int. Conf. on Numer. M. for Nonlinear problems, Swansea,1980.

2. Симеонов С. В., Върху нелинейното статическо изследване на едномерните деформируеми системи.,"Теоретична и приложна механика", БАН, кн.1,1987, (Bulgarian Academy of Science - Simeonov S.V.)

3. Nesheva I.G., Nonlinear Elastoplastic Analysis of Steel Plane Frame Structures., Conference, "Transformation Models for Design of Steel Structures",CSSR, 1989.

4. Majid K.I., Matrix Methods of Analysis and Design by Computers Non-linear Structures, Wiley-Interscience, 1972.

(1)
PAPP. Ferenc (1)

OVERALL IMPERFECTION METHOD ON FRAMES FOR COMPUTER AIDED DESIGN

INTERNATIONAL COLLOQUIUM
STABILITY OF STEEL STRUCTURES
BUDAPEST, HUNGARY, 1990
PRELIMINARY REPORT

ABSTRACT

Geometrically nonlinear finite element method has important role in computer aided design of space frames with compact cross-sections. The design code formulations (including Hungarian Standard 1985) demand to check the strength limit state and simultaneously the stability limit states as overall buckling. The complete structure can be analyzed with 3-D FEM program for strength limit state but designer must divide the structures into parts to analyze them for overall buckling.

This paper develops an approximate method which neglects the stability analysis by using overall initial crookedness on the structural members. Recent study deals with steel I-sections and shows some examples.

NOTATION

C	Centroid of the cross-section
O	Torsional center of the cross-sections
u, θ	Nodal displacements
X,Y,Z	Global coordinate system
u,v,w	Local coordinate system of members
K	Stiffness matrix
σ	Normal stress
σ_H	Strength by Hungarian code
φ, φ_k	Reduction coefficients for buckling and l.t.buckling
λ	Modified slenderness ratio
Ry	Nominal strength by Hungarian code
σ_{cr}	Elastic critical stress
bo	Initial overall imperfection about the minor axis of I-section
E	Young's modulus of elasticity
G	Shear modulus of elasticity

(1) Senior Assistant Professor of Structural Engineering, Department for Steel Structures, TU Budapest

(2)

I	Inertia moment
ω	Sectorial coordinate of cross-section
A	Sectional area
F,P,f	External forces
F_H,P_H,f_H	External limit forces by Hungarian code

1. INTRODUCTION

The method is based on 3-D FEM program which uses thinwalled elements with 14 degrees of freedom (Fig. 1.). The equilibrium equation of the complete structure in the X,Y and Z global system can be written as

$$\{ [K_s] + [K_g] \} [u] = [F] \qquad (1)$$

where $[K_s]$ is the flexural stiffness matrix, $[K_g]$ is the geometrical stiffness matrix and [u] is the displacement vector on the [F] load vector. According to the Hungarian code the solution of the eq.(1) gives the base for the strength limit state

$$\sigma = \sigma_u + \sigma_v + \sigma_v + \sigma_\omega \leqq \sigma_H \qquad (2)$$

where σ_H denotes the limit stress.

Design formulation for limit state of overall buckling can be written as

$$\frac{\sigma_u}{\varphi \sigma_H} + \frac{\sigma_\omega}{\varphi_k \sigma_H} \leqq 1 \qquad (3)$$

where φ is the reduction coefficient for column bucking and φ_k is the reduction coefficient for beam buckling. Reduction factors can be determined by the code. According to the Hungarian code the elastic extrapolation formula can be used to calculate the modified slenderness ratios

$$\bar{\lambda} = (R_y/\sigma_{cr})^{0.5} \qquad (4)$$

where σ_{cr} elastic critical stress can be obtained from the reduced basic equation

$$\det \{ [K_s] + [K_g] \} = 0 \qquad (5)$$

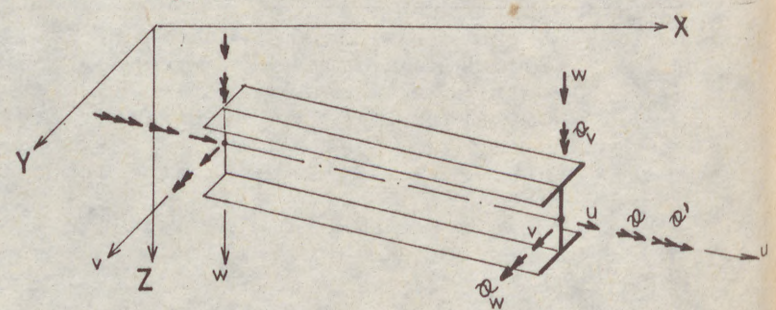

Figure 1.
Finite element with 14 degrees of freedom.

(3)

2. OVERALL IMPERFECTION ON SIMPLE SUPPORTED BEAM-COLUMN

Fig. 2. shows a simple supported beam-column with I-section. The member is loaded with initial crookedness about the minor axis. The governing equilibrium equations of the member are

$$EI_v\, v'' + F(v_o + v) + M_v\, \theta = 0$$

$$EI_v\, w'' + F(w_o + w) = -M_v$$

$$EI_\omega\, \theta''' + (GI_t + \bar{K})\theta' + M_v(v_o' + v') = 0 \qquad (6)$$

where $\bar{K}$ denotes the Wagner coefficient. Solving the eqs.(6) the maximum normal stress derived from the effect of v_o initial imperfection can be obtained

$$\sigma_o = b_o E \frac{\pi^2}{l^2} \frac{\frac{I_v}{W_v}\left[\left(\frac{P_t}{F} - 1\right) r_o^2 + \left(\frac{M_v}{F}\right)^2\right] + \omega \frac{M_v P_v}{F^2}}{\left(\frac{P_t}{F} - 1\right)\left(\frac{P_v}{F} - 1\right) r_o^2 - \left(\frac{M_v}{F}\right)^2} = b_o \alpha \qquad (7)$$

where $P_t = \frac{1}{r_o^2}\left(\frac{\pi^2 E I_\omega}{l^2} + GI_t\right)$, $P_v = \frac{\pi^2 E I_v}{l^2}$

and $r_o^2 = (I_v + I_w)/A$.

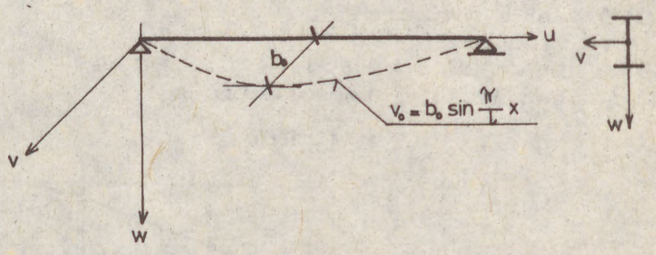

Figure 2.
Simple supported beam-column with initial imperfection.

Considering eq.(2) the stability requirements will be satisfied by the strength limit state which includes the effect of initial imperfection

$$\alpha\, b_o + \frac{F}{A} + \frac{M_v}{W_v} = \sigma_H \qquad (8)$$

(4)
F and Mv must satisfy the buckling formula (eq.3)

$$\frac{F}{\varphi \sigma_H A} + \frac{Mv}{Wv \varphi k \sigma_H} = 1 \qquad (9)$$

From the eqs. (8) and (9) we can get the overall initial imperfection

$$bo = \frac{1}{\alpha} \left[\sigma_H (1 - \varphi k) + \frac{F}{A} \left(\frac{\varphi k}{\varphi} - 1 \right) \right] \qquad (10)$$

The φ and φk coefficients are known directly from the code. Since

$$Mv = Wv \, \varphi k \left(\sigma_H - \frac{F}{A} \frac{\varphi k}{\varphi} \right) \qquad (11)$$

the bo initial imperfection depends on F normal force.

EXAMPLE 1.

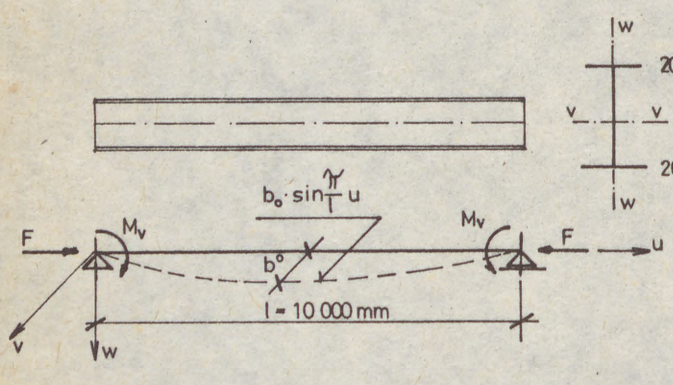

$R_y = 235$ N/mm²
$l = 10000$ mm
$I_v = 13200 * 10^4$ mm⁴
$I_v = 1600 * 10^4$ mm⁴
$W_v = 160 * 10^3$ mm³
$W_v = 846 * 10^3$ mm³
$I_\omega = 389400 * 10^6$ mm⁶
$I_t = 25.28 * 10^4$ mm⁴
$\omega = 15600$ mm²
$E = 206000$ N/mm²
$\sigma_H = 200$ N/mm²
$A = 8672$ mm²

$\bar{\lambda} = 2.196$ and $\varphi = 0.1668$
$\bar{\lambda}k = 1.514$ and $\varphi k = 0.416$
$P_t = 1263$ kN , $P_v = 325.3$ kN and $r_o^2 = 22182$ mm²
The calculated initial imperfections:

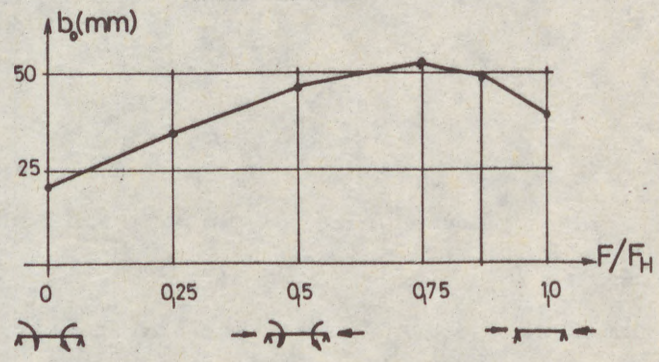

3. EXTENSION OF THE METHOD.

Practical usage of the imperfection method demands simple calculation process for bo. This means that the determination of bo must be independent of the restrictions of the

(5)

complete model and of the load distributions. In the first step we have extended the method to simple beam-columns assuming that bo can be derived from the simple supported model (Fig. 2.). Table 1. shows some of the results on EXAMPLE 1. Load parameters f_H and P_H mean the specified limits by the Hungarian code. The ratios of σ_{max}/σ_H denote the errors of the method.

Table 1. Extending the method to beam-columns.

model	initial imperfection		limit load by H. code	error of the imperfection method
	F/F_H	bo (mm)	f_H (N/m) P_H (N)	σ_{max}/σ_H
A1. 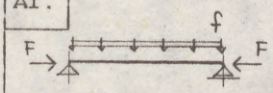	0	19.76	6836	1.009
	0.25	34.96	5065	0.963
	0.50	48.15	3534	1.039
	0.75	59.47	1947	1.061
	1.00	41.67	0	1.000
A2. 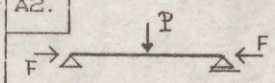	0	19.76	39878	1.090
	0.25	34.96	28986	0.990
	0.50	48.15	19192	0.994
	0.75	59.47	9399	0.979
A3. 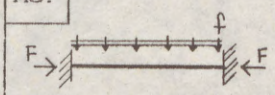	0	19.76	22160	1.104
	0.25	34.96	16464	0.921
	0.50	48.15	10849	0.926
	0.75	59.47	5970	1.155
	1.00	41.67	0	1.289
A4. 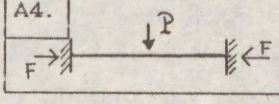	0	19.76	124865	1.068
	0.25	34.96	91817	1.070
	0.50	48.15	60536	1.117
	0.75	59.47	29719	1.132

EXAMPLE 2.

Figure 4. shows a simple frame in space. According to the code the reduction coefficients

for beam: $\varphi_k=0.712$

for column: $\varphi_k=0.674$ and $\varphi=0.588$

and the limit load parameter $P_H=22500$ N .

From the first order analysis the actual normal forces in the members can be obtained and we can calculate the initial imperfections

	F (N)	F/F_H	bo (mm)
in beam	27000	0.083	13.83
in column	123750	0.248	9.74

The second order analysis on the imperfect frame gives the maximum normal stress and the error ratio $\sigma_{max}/\sigma_H= 0.92$.

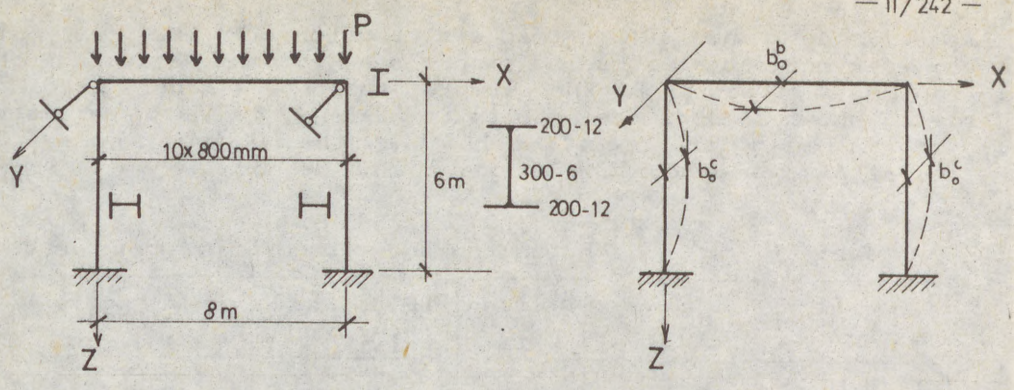

Figure 4.
Simple frame in space with initial imperfections.

REFERENCES

1 W. Chen, T. Atsuta: Theory of Beam-Columns, Volume 2. Space behaviour and design; page 551-564;

2 W. Duy: Festigkeitsnachweis biegebeanspruchter vorverformter Trager: Biegetorsion, Stahlbau 57 (1988), page 263-268

(1)
PAVLOV, Andrey (1)
BERDICHEVSKY, Stanislav (2)

DESIGN PROCEDURE OF THE SECOND ORDER AND STABILITY VERIFICATION OF FRAMES WITH SEMI-RIGID JOINTS

INTERNATIONAL COLLOQUIUM
STABILITY OF STEEL STRUCTURES
BUDAPEST, HUNGARY, 1990
PRELIMINARY REPORT

Summary: All steel constructions are semi-rigid but traditional design methods for frames in the USSR consider them as completely rigid or pinned ones. The paper shows the design procedure of the second order for frames with verification of buckling in frames with semi-rigid joints. During the elaboration of the design procedure the authors have constructed stiffness matrix using deflecltion method for the elements with semi-rigid connections subjected to longitudinal force for including in the finite elements library. This procedure could also be used in designs made manually.

Traditionally in the USSR the steel frames design is made assuming that joints in frames are either rigid or pinned. In reality all the joints possess some definite stiffness and should be considered as semi-rigid ones. Account of real stiffness of the connections during the frames design allows to choose effective low labour-consuming types of connectins, to distribute in correct way efforts in frames elements, to reduce weight of constructions and to decrease the quantity of structural elements.

Behavior of connections could be conveniently represented with the moment-rotation curves where the slope of the curve is rigidity of connection (Fig.1). Beam line gives limit point of the

---

(1) Cand.Sc.(Eng.), Head of Group "Investigations of Steel Frames in Multistorey Buildings", VNIPIPromstalconstruktsiya, Moscow, USSR
(2) Sc.Worker (Eng.), VNIPIPromstalconstruktsiya, Moscow, USSR.

(2)
curve M- φ for real elements of frames. The actual M- φ curve could be replaced by straight line with tangent slope K [1] in practical range of use up to the intersection with beam line. In frame design rigidity of connection is taken as constant value equal to K.

Modern design methods for frames with semi-rigid joints specify strength analysis with account to transverse-longitudinal bending (so called design of the second order) and verification of frame stability and also of every element stability taken separately. The theory of this design procedure has been worked out in the papers of W.-F. Chen, Y.Goto, D.A.Nethercot, R.Zandonini, P.A.Kirby, A.Colson, Y.Galéa and others [2-6].

Some years ago the programme of the first order static design for steel frame by finite elements method for personal computers has been worked out in the Scientific-Research Institute VNIPIPromstalconstructsiya and Moscow Institute of Civil Engineers.Later this programme was modified for the design of frames with account of transverce-longitudinal bending and verification of stability.

The design programme should be changed in the followig way:
- to construct stiffness matrix for the the element which has semi-rigid connections possessing rotational stiffnesses K1 and K2 and subjected to the action of longitudinal force N (Fig.2);
- to organize iteration process with comparison of longitudinal forces at every step of iteration.

For the construction of stiffness matrix of beam elements method of deflection has been chosen with generally used functions $\varphi_i(\nu)$ [7] ,which could be obtained solving differential equilibrium equation of transverse-longitudinal bending

$$y^{IV} + \frac{N}{EJ} \cdot y'' = 0 \qquad (1)$$

with corresponding boundary conditions. Analytical expression of functions and their expansion in a McLoren series are given in Table 1.
Notation in Table 1:

$$\nu = \sqrt{\frac{N}{EJ}} \cdot l \quad ; \qquad (2)$$

l - length of element;
EJ- bending rigidity of element;
N- longitudinal force.

At $|\nu| > 0.01$ it´s more convenient to calculate functions $\varphi_i(\nu)$ with their analytical expression; at $|\nu| < 0.01$ - by expansion of functions in a McLoren series.The first members of expansion give values $\varphi_i(0)$ equal to their coefficients of deflection method in the absenes of longitudinal forces.

(3)

Table 1.

Function	Analytical expression	Expansion in a McLoren series
	Compression (N < 0)	
$\varphi_1(\nu)$	$\frac{\nu^2 \cdot \sin\nu}{3(\sin\nu - \nu\cos\nu)}$	$1 - \frac{\nu^2}{15} - \frac{\nu^4}{525} - \frac{2\nu^6}{23625} - \ldots$
$\varphi_2(\nu)$	$\frac{\nu \cdot \sin\nu - \nu^2 \cdot \cos\nu}{4(2 - \nu\sin\nu - 2\cos\nu)}$	$1 - \frac{\nu^2}{30} - \frac{11\nu^4}{25200} - \frac{\nu^6}{108000} - \ldots$
$\varphi_3(\nu)$	$\frac{\nu^2 - \nu \cdot \sin\nu}{2(2 - \nu\sin\nu - 2\cos\nu)}$	$1 + \frac{\nu^2}{60} + \frac{13\nu^4}{25200} + \frac{11\nu^6}{756000} - \ldots$
$\varphi_4(\nu)$	$\frac{\nu^2 \sin\nu}{6(2\sin\nu - \nu\cos\nu - \nu)}$	$1 - \frac{\nu^2}{60} - \frac{\nu^4}{8400} - \frac{\nu^6}{756000} - \ldots$
$\varphi_5(\nu)$	$\frac{\nu}{4\,\mathrm{tg}\,\nu/4}$	$1 - \frac{\nu^2}{48} - \frac{\nu^4}{11520} - \frac{\nu^6}{1935360} - \ldots$
	Tension (N > 0)	
$\varphi_1(\nu)$	$\frac{\nu^2 \mathrm{sh}\,\nu}{3(\nu\mathrm{ch}\,\nu - \mathrm{sh}\,\nu)}$	$1 + \frac{\nu^2}{15} - \frac{\nu^4}{525} + \frac{2\nu^6}{23625} - \ldots$
$\varphi_2(\nu)$	$\frac{\nu^2 \mathrm{ch}\,\nu - \nu\,\mathrm{sh}\,\nu}{4(2 + \nu\,\mathrm{sh}\,\nu - 2\mathrm{ch}\,\nu)}$	$1 + \frac{\nu^2}{30} - \frac{11\nu^4}{25200} + \frac{\nu^6}{108000} - \ldots$
$\varphi_3(\nu)$	$\frac{\nu\,\mathrm{sh}\,\nu - \nu^2}{2(2 + \nu\,\mathrm{sh}\,\nu - 2\mathrm{ch}\,\nu)}$	$1 - \frac{\nu^2}{60} + \frac{13\nu^4}{25200} - \frac{11\nu^6}{756000} - \ldots$
$\varphi_4(\nu)$	$\frac{\nu^2 \mathrm{sh}\,\nu}{6(-2\mathrm{sh}\,\nu + \nu\mathrm{ch}\,\nu + \nu)}$	$1 + \frac{\nu^2}{60} - \frac{\nu^4}{8400} + \frac{\nu^6}{756000} - \ldots$
$\varphi_5(\nu)$	$\frac{\nu}{4\,\mathrm{th}\,\nu/4}$	$1 + \frac{\nu^2}{48} - \frac{\nu^4}{11520} + \frac{\nu^6}{1935360} - \ldots$

(4)

Forces calculation in restraint of element with semi-rigid connections per unit rotation of this restraint would show how it's possible to obtain elements of stiffness matrix. The main system of the deflection method and bending moments curve are given in Fig.3. Reactions in introduced restraints are equal to :

$$r_{11}' = 4i \cdot \varphi_2(\nu) + \kappa_1 \; ; \quad r_{12}' = r_{21}' = 2i \cdot \varphi_3(\nu) \; ;$$

$$r_{22}' = 4i \cdot \varphi_2(\nu) + \kappa_2 \; ; \quad R_{1p}' = -\kappa_1 \; ; \quad R_{2p}' = 0 .$$

During rotation of left real restraint per unit, the reactive action K1 appeares. In this case system of equations by deflection method is the following

$$\begin{cases} (4i \cdot \varphi_2 + \kappa_1) Z_1 + 2i\varphi_3 \cdot Z_3 - \kappa_1 = 0 \\ 2i\varphi_3 \cdot Z_1 + (4i\varphi_2 + C_2) \cdot Z_2 = 0 \end{cases} , \tag{3}$$

from which we obtain

$$Z_1 = \frac{\kappa_1 (4i\varphi_2 + \kappa_2)}{det} \; ; \tag{4}$$

$$Z_2 = \frac{-2\kappa_1 i \cdot \varphi_3}{det} , \tag{5}$$

where i =EJ/l - is the reduced stiffness of element;

det - determinant of the system (3).

$$\text{det} = 16i^2 \cdot \varphi_2^2 + 4i \cdot \varphi_2 \cdot \kappa_2 + 4i \cdot \varphi_2 \cdot \kappa_1 + \kappa_1 \kappa_2 - 4i^2 \cdot \varphi_3^2 . \tag{6}$$

Then the moment in the left semi-rigid connection per unit rotation of this connection is equal to

$$M_{11} = (1 - Z_1) \cdot \kappa_1 = \frac{(16i^2 \varphi_2^2 - 4i^2 \varphi_3^2 + 4i\varphi_2 \kappa_2) \cdot \kappa_1}{det} . \tag{7}$$

The moment in the rigth semi-rigid connection per unit rotation of the left one is equal to

$$M_{12} = Z_2 \cdot \kappa_2 = \frac{2i\varphi_3 \cdot \kappa_1 \kappa_2}{det} . \tag{8}$$

Lateral forces in the restraints could be determined from the condition of equilibrium

(5)

(5)

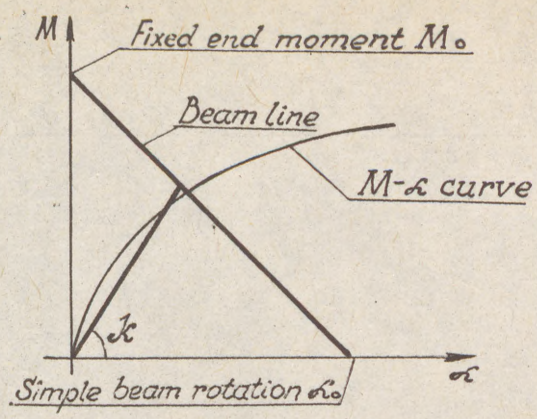

Fig.1.

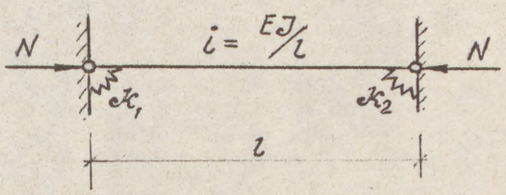

Fig.2.

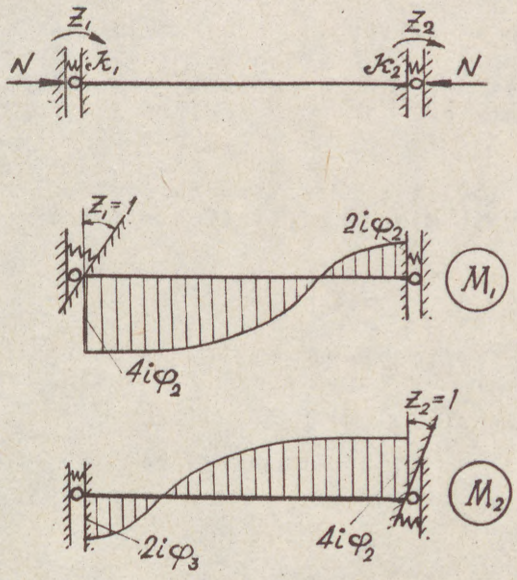

Fig.3.

(6)

$$H_{11} = -H_{12} = \frac{M_{11} + M_{12}}{l} =$$

$$\frac{(16i^2\varphi_2^2 - 4i^2\varphi_3^2 + 4i\varphi_2 k_2 + 2i\varphi_3 k_2)\cdot k_1}{l \cdot det} \quad (9)$$

Elements of stiffness matrix rotation per unit of another restraint and deflection per unit of supports could be found analogously.

Formulae to calculate single reactions in semi-rigid connections for the case of compressed longitudinal forces actions are given in Table 2.

As an example design formulae for the determination of the reactions in the main system from the most abundant loads-equally - distributed and concentrated forces in the middle of the span are given in Table 3.

The obtained stiffness matrix and the subroutine for function $\varphi_i(\nu)$ were included in the library of finite elements in design programme. After that the iterative process was organized for frame design of the second order. The process convergence was determined by the comparison of longitudinal forces values at each step of iterations.The process converges quickly because real constructions possess large rigidity of elements.

The subjected design procedure also allows to verify the stability of frames with semi-rigid joints and to determine critical parameter of load.

Verification for the stability is necessary because the design procedure of the second order determines only the set of equilibrium states,but it's impossible to evaluate the stability of these states. It could occur,that the obtained state is not stable.

To verify the stability it's necessary to costruct and to equate to zero the determinant of stiffness matrix of deflection method

$$det[r_{ij}] = 0, \quad (10)$$

where $r_{ij} = f(\nu_i)$ — elements of stiffness matrix, determined from Table 2. According to formula (2) for the i-rod

$$\nu_i = \sqrt{\frac{N_i}{EJ_i}} \cdot l_i .$$

Longitudinal force in i-rod could be represented as followes

$$N_i = \alpha_i \cdot N, \quad (11)$$

where N - parameter of load ;
α_i - coefficient of proportionality to this parameter of the longitudinal forces in i-rod.

Table 2.

Scheme	Design formulae for the determination of reactions per unit
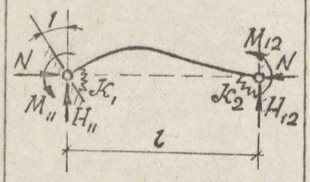	$M_{11} = \frac{(16i^2\varphi_2^2 - 4i^2\varphi_3^2 + 4i\varphi_2 k_2)\cdot k_1}{det}$ $M_{12} = \frac{2i\varphi_3 k_1 k_2}{det}$ $H_{11} = \frac{M_{11}+M_{12}}{l} = \frac{(16i^2\varphi_2^2 - 4i^2\varphi_3^2 + 4i\varphi_2 k_2 + 2i\varphi_3 k_2)k_1}{l\cdot det}$ $H_{12} = -H_{11}$
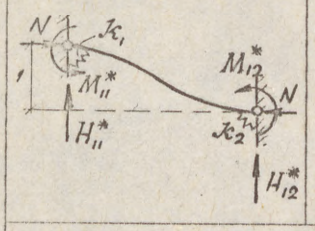	$M_{11}^* = \frac{6i\varphi_4 k_1(4i\varphi_2 + k_2 - 2i\varphi_3)}{l\cdot det} = H_{11}\ \left(i.e.\ \varphi_4 = \frac{1}{3}(2\varphi_2+\varphi_3)\right)$ $M_{12}^* = \frac{6i\varphi_4 k_2(4i\varphi_2 + k_1 - 2i\varphi_3)}{l\cdot det}$ $H_{11}^* = \frac{6i\varphi_3(4i\varphi_2 k_1 + 2k_1k_2 - 2i\varphi_3 k_1 + 4i\varphi_2 k_2 - 2i\varphi_3 k_2)}{l^2\cdot det} - \frac{\nu^2 i}{l^2}$ $H_{12}^* = -H_{11}$
Application. In the case of tensile longitudinal effort action, corresponding coefficients are included in the design formulae. Besides this for the determination of H the item must have sign "+".	

Table 3.

Scheme	Design formulae for the determination of reactions of loads in main system
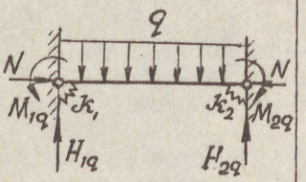	$M_{1q} = \frac{ql^2(6i\varphi_4 + k_2)k_1}{12\varphi_4\cdot det}$; $M_{2q} = \frac{ql^2(6i\varphi_4 + k_1)k_2}{12\varphi_4\cdot det}$ $H_{1q} = \frac{ql}{2} + \frac{qli(k_1-k_2)}{2\cdot det}$; $H_{2q} = \frac{ql}{2} - \frac{qli(k_1-k_2)}{2\cdot det}$
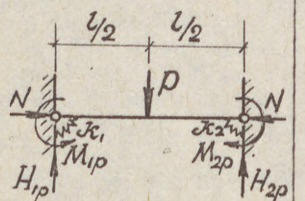	$M_{1p} = \frac{pl(6i\varphi_4 + k_2)k_1}{8\varphi_5\cdot det}$; $M_{2p} = \frac{pl(6i\varphi_4 + k_1)k_2}{8\varphi_5\cdot det}$ $H_{1p} = \frac{P}{2} + \frac{3i\varphi_4 P(k_1-k_2)}{4\varphi_5\cdot det}$; $H_{2p} = \frac{P}{2} - \frac{3i\varphi_4 P(k_1-k_2)}{4\varphi_5\cdot det}$

(8)

Coefficient of proportionnality α_i could be determined from the static design when there is no bending in columns.

From the solusion of transcendental equation

$$det\,[r_{ij}] = det\,[f(\alpha_i N)] = 0 \qquad (12)$$

by the method of secants, critical value of load parameter $N_{cr.}$ is determined.

To simplify the designs at the verification of stability it´s possible to accept for rods subjected to tension $\varphi_i = 1$. It increases margin of stability and leads to smaller values of critical forces.

CONCLUSION

The authors of the paper realize that there are numerous methods of exact designs for the transverse-longitudinal bending and stability with account of non-linear behavior of frame elements, their connections and so on. But they take into account that the suggested finite element,recieved by the deflection method is convenient for the addition to the finite elements library of already existing design programmes and also for design methods made manually.

REFERENCES

[1] J.-P. Jaspart, R.Maquoi : Simple Design Method for Sway Frames with Semi-Rigid Connections, International Colloquium,Bolted and Special Structural Connections, Moscow, 1989, Proceedings, Volume 3, pp. 72-79.

[2] Y.Goto,S.Suzuki,W.-F.Chen: Bifurcation and Limit Load Instability of Flexibly Jointed Frames,International Colloquium, Bolted and Special Structural Connections,Moscow 1989,Proceedings,Volume 3,pp. 80-89.

[3] Y.Galéa, A.Colson, P.Pilvin: Programme d´Analyse de Structures Planes à Barres avec Liaisons Semi-Rigides à Comportement non Linéare. Costruction Métallique, 1986, № 2, pp.3-16.

[4] D.Anderson, F.Bijlaard, D.A.Nethercot, R.Zandonini: Analysis and Design of Steel Frames with Semi-Rigid Connections,IABSE SURVEYS, S-39/87, pp.61-78.

[5] S.W.Jones, P.A.Kirby, D.A.Nethercot : The Analysis of Frames with Semi-Rigid Connections A-State-the-Art-Report, J.Construct. Steel Research, 3(2),1983, pp.1-13.

[6] Y.Goto, W.-F.Chen : On the Computer-Based Design Analysis for the Flexibly Jointed Frames,J.Construct. Steel Research ,8,1987, pp.203-231.

[7] Справочник проектировщика промышленных, жилых и общественных зданий и сооружений. Расчетно-теоретический. Под.ред. проф. А.А.Уманского, Книга 2, Издательство литературы по строительству, М., 1973, 415 с.

(1)
SCHEER, Joachim (1)
PASTERNAK, Hartmut (2)
SCHWEEN, Tobias (3)

TENSION BAND MODELS FOR THE ESTIMATION OF THE LOAD CAPACITY OF STIFFENED FRAMES WITH THIN WEBS - ONGOING RESEARCH

INTERNATIONAL COLLOQUIUM
STABILITY OF STEEL STRUCTURES
BUDAPEST, HUNGARY, 1990
PRELIMINARY REPORT

Summary: Current experimental and FEM-analyses of the overcritical behaviour of stiffened frames in Braunschweig will be introduced. The fundamental finding is that a tension band also in stiffened knee joints with thin webs can appear. The load capacity can clearly lie above its elastic buckling load.

1 Introduction

In the past three decades, various so-called tension field models have been developed. Its superposition with the shear field allows a prediction of the ultimate load capacity of transversely stiffened plate girders (Fig. 1a) with thin webs subjected to shear and bending loads (Gehri/Dubas,1986). In the meantime, some models for stiffened girders have been introduced in codes, e.g. in Swiss Code SIA 161 (1979), the projects of EUROCODE 3 (1984, 1988) and the German DASt-Ri015 (1988). Moreover, models for girder fields with web openings have been developed. Characteristics of continuous beams are currently being investigated at the Institute for Steel Structures at the Technical University of Braunschweig.

Recently, it was shown (Scheer/Pasternak, 1989) that tension field models are in themselves not consistent (e.g. they violate equilibrium conditions) and, therefore, cannot have any boundary properties; this does not make these models unworkable, but requires a comparison of experiment and calculation and,

---

(1) Professor for Steel Struct., (2) Dr.-Ing., (3) Dipl.-Ing., all Technical University Carolo-Wilhelmina, Braunschweig

(2)

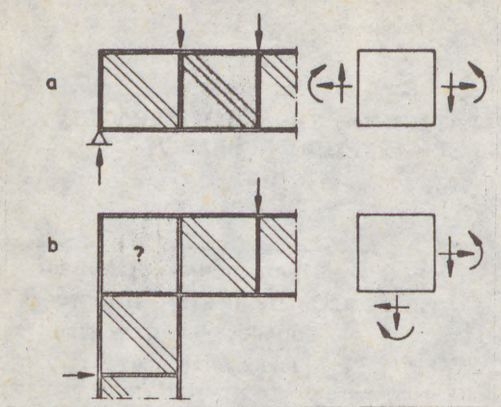

Fig.1 Girder and frame. Internal forces and tension bands

finally, a calibration of the calculation model. An analysis of 230 tests is given in the mentioned paper.

The ultimate load capacity of frame rafters and columns with thin-walled webs can also be calculated with the described model. A simple application of this model onto knee joints of frames is not possible e.g. due to the fundamentally different character of the load (Fig. 1b).

For the construction of modern singlestory steel buildings it is of great interest to know the real load capacity of the web plates in the area of the knee joints, since with their utilization a simplification of the web construction seems to be allowable in many cases. Warranted knowledge about the postbuckling states of knee joints are lacking thus far. Work towards a solution to this problem began in Braunschweig in 1988.

2 State of art

Practice by-passes this knowledge deficit with additional construction expense: it renounces a possibly sufficient, continuous web plate for the whole rafter and instead employs either thicker webs or additional bracing for the knee joint, and therewith remains within the domain of the classical buckling theory. According to Petersen, 1982, for thin-walled webs the buckling load can be evaluated with good approximation for a constant shear stress distribution across the knee joint and with omission of the normal stress.

3 Experiments

In order to gain insight into the postbuckling behaviour of a knee joint with a thin-walled web, tests in model (scale 1:3) and natural size were and will be performed. The configuration for tests in model size is shown in Fig.2.

The arms (1) and (2) are made of IPE 300. Arm (1) is tightly connected with the carrying construction below. The other arm (2) can easily be moved because it is layered on ball-bearings; friction can be neglected. Arm (2) is also supported from above

(3)
(see section A–A) in order to prevent its torsion and buckling under greater loads. It is possible to install a hydraulic cylinder between the two arms in different positions, to simulate different ratios moment/shear force and moment/normal force. This configuration allows rotation of the knee joint up to 23° depending on the model size and the position of the hydraulic cylinder.

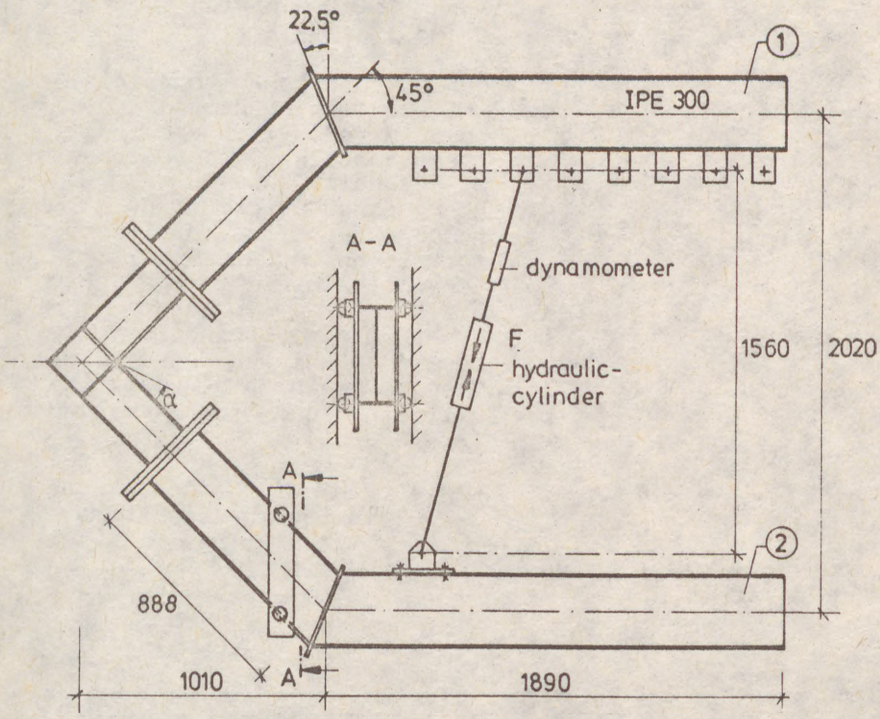

Fig.2 Testing frame with knee joint

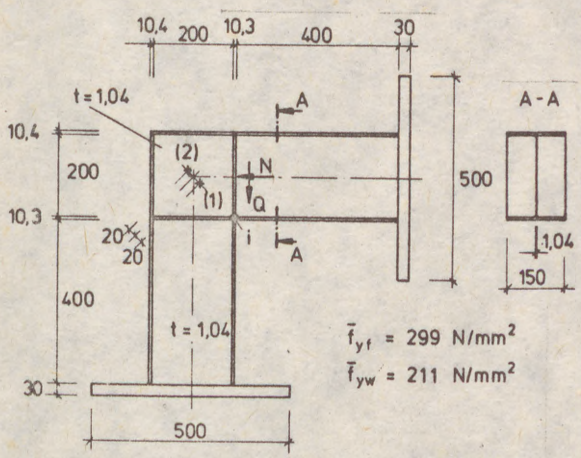

Fig.3 Test specimen

The experimental sequence is examplified by test specimen A-10-10-1 (see Fig.3). Large initial deformations of the web are typical for this model.

The applied loads are registered electronically with help of a dynamometer, while the rotations of the knee joint are registered by a protractor. The web deformations are measured by dial gauges at points (1) and (2) shown in Fig.3. During the test, the rotations were ap-

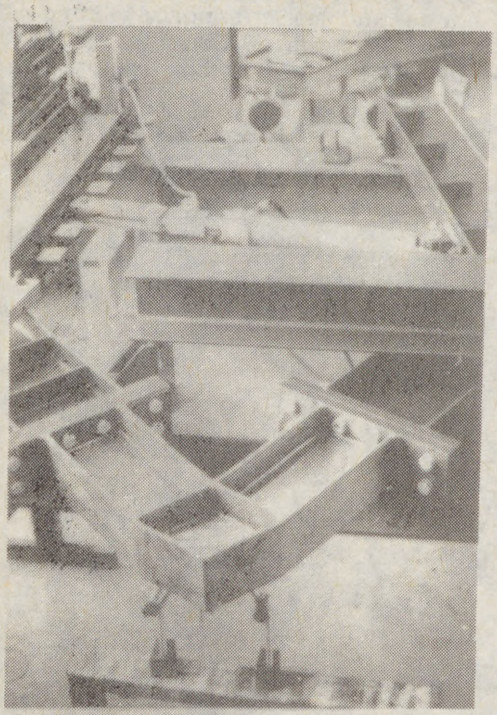

plied in steps of ca. 0.7°.

Fig.4 shows a view of the knee joint in the testing frame.

During this test no "classical buckling phenomena" could be observed. Fig.5 shows different phases of development of a tension band:
a – the web deformations already exceed the initial deformations substantially; a tension band is formed (F ≈ ≈ 2.5 kN),
b – the tension band is fully formed; plastic hinges in the flanges begin to develop; the ultimate load is achieved (F ≈ 3.3 kN).

Fig.4 View of the knee joint in the testing frame

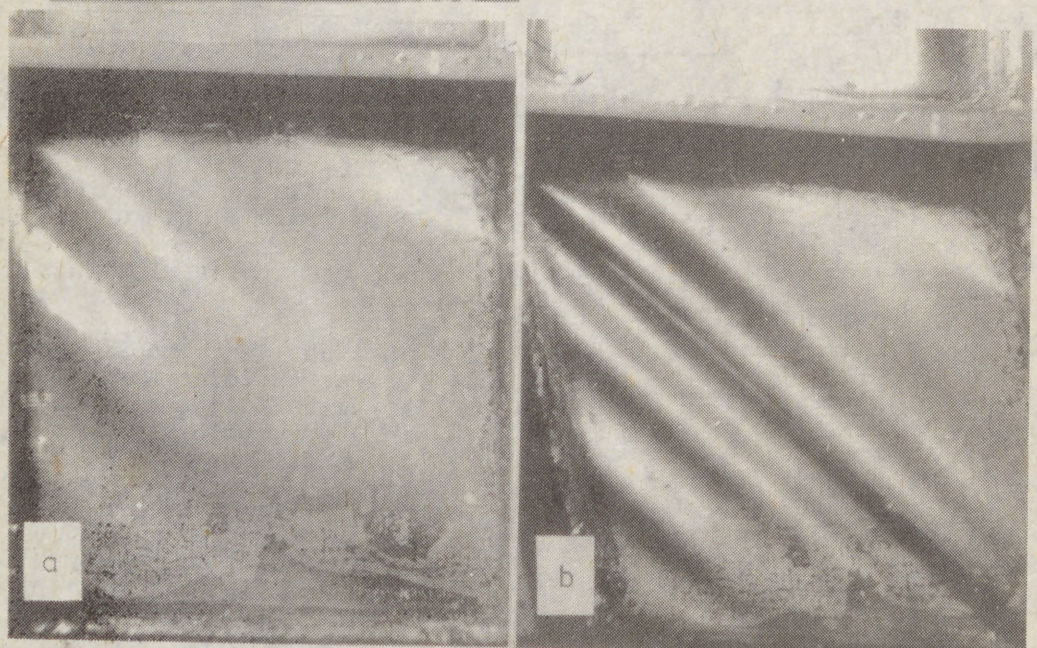

Fig.5 Development of the tension band for model A-10-10-1

(5)

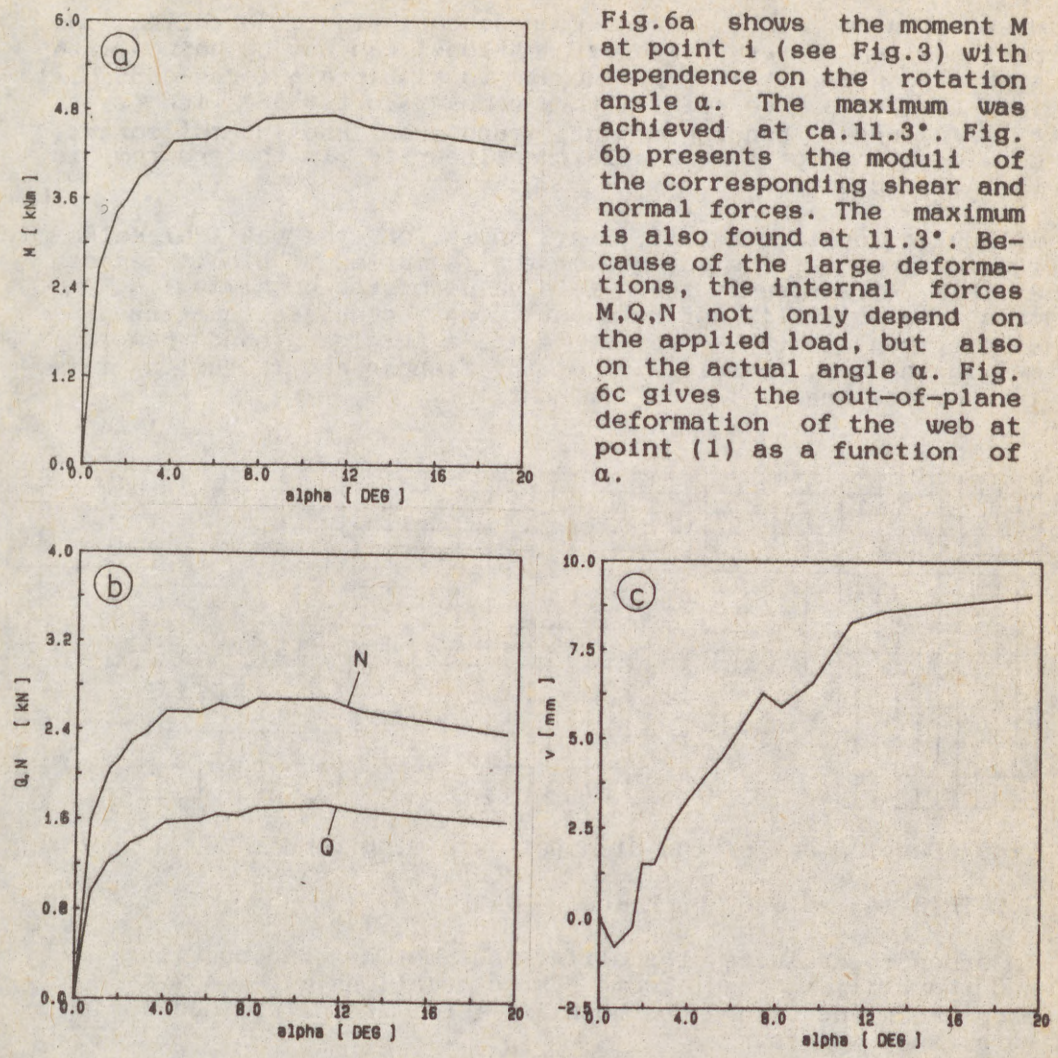

Fig.6a shows the moment M at point i (see Fig.3) with dependence on the rotation angle α. The maximum was achieved at ca.11.3°. Fig. 6b presents the moduli of the corresponding shear and normal forces. The maximum is also found at 11.3°. Because of the large deformations, the internal forces M,Q,N not only depend on the applied load, but also on the actual angle α. Fig. 6c gives the out-of-plane deformation of the web at point (1) as a function of α.

Fig.6 Internal forces in dependence on the rotation angle

4 FEM investigations

4.1 Compact web

In a primary stage of the project knowledge was gathered concerning the carrying behaviour of the knee joints with a FEM

(6)
disk program. Since information about elastic buckling and postbuckling states (large deformations) can not be gained with such a program, it was appropriate to simulate a force-controlled test of a knee joint with a compact (b/t ≈ 33) web ($\tau_{cr} > f_y/\sqrt{3}$) under bending moment, transversal and normal forces. Consideration of the material nonlinearity in the program is then sufficient.

Without going into detail, Fig.7 shows, on the basis of selected load ranges, the advance of the formation of plastic zones. At this, λ represents the n-fold value of the buckling load (in this case naturally not relevant). One recognizes that the plasticity begins at λ≈ 0.6; at λ≈ 1.2 a "yielding band" has formed in the web. Plasticizing of the flanges and therewith failure of the knee joint is imminent.

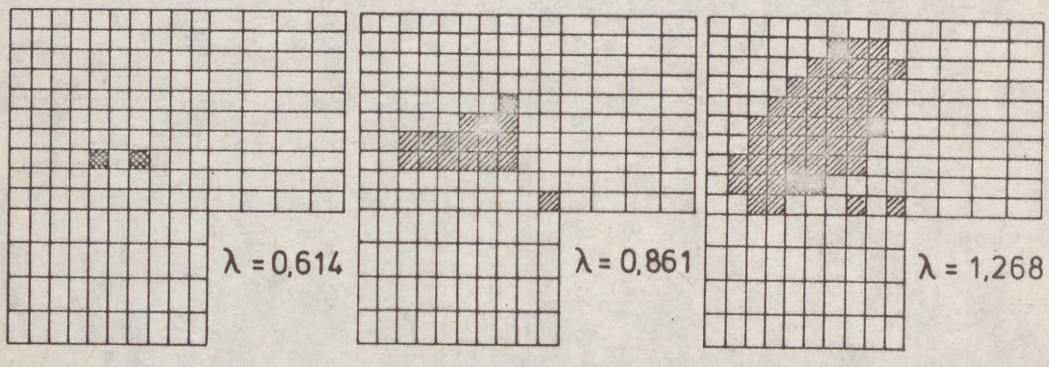

Fig.7 Development of the diagonal "yielding band"

4.2 Thin-walled web. Buckling

In order to evaluate the difference between the buckling load and the ultimate load, some FEM calculations with ANSYS were made. Buckling value and buckling form were determined for several knee joints.

As a result it was found, that the distribution of shear-stresses in knee joints with thin webs is nearly constant. This fact verifies the assumption for the calculation of classical buckling (Petersen, 1982). For the data in Fig. 3 buckling occurs at: M = -3.13 kNm, Q = 1.11 kN, N= -1.88 kN.

In this case, the lowest buckling value of the complete structure obtained by FEM was 64% higher than that of the simply supported and 4% higher than that of the fully clamped web (according to Petersen, 1982). The buckling load obtained by FEM is about two thirds of the ultimate load capacity from the test.

FEM investigations show, that, already with elastic buckling,

(7)
the horizontal deformations along a field diagonal are largest (Fig.8).

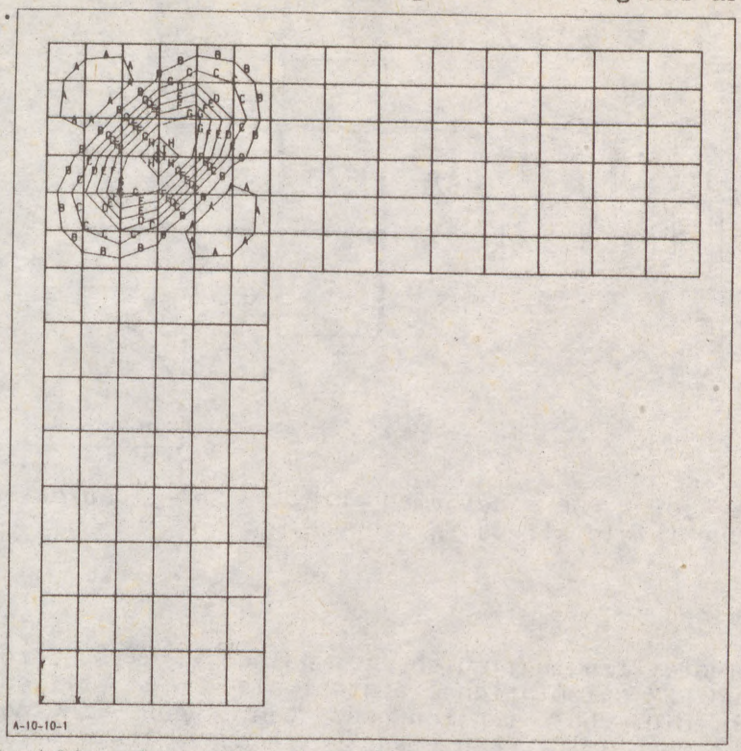

Fig.8 Buckling form of a knee joint

4.3 Thin-walled web. Overcritical behaviour

Actually, works on the calculation of the overcritical behaviour of knee joints are continuing.

In the used computer program BOX the displacement form of the FEM, the stationary Lagrangian description and the incremental formulation are used. A four-node, plane, rectangular element with 24 degrees of freedom (plate element with beam effect) is applied for digitizing. Large displacements, moderate rotations and small initial imperfections in geometry are taken into account. For the web plate of the knee joint (and the directly adjoining regions of column and rafter web) ideally elastic-plastic material behaviour is taken into account; the remaining regions of the web are modelled with ideally elastic material behaviour.

Here a tension band in the knee joint is also formed (Fig. 9a). The dependence of the out-of-plane deformation in the middle of the web plate of the knee joint on the applied load shows Fig. 9b (λ is the n-fold value of M = -31.5 kNm, Q = 66.3 kN, N = = -35.7kN); the initial out-of-plane deformation totals 2 mm.

(8)

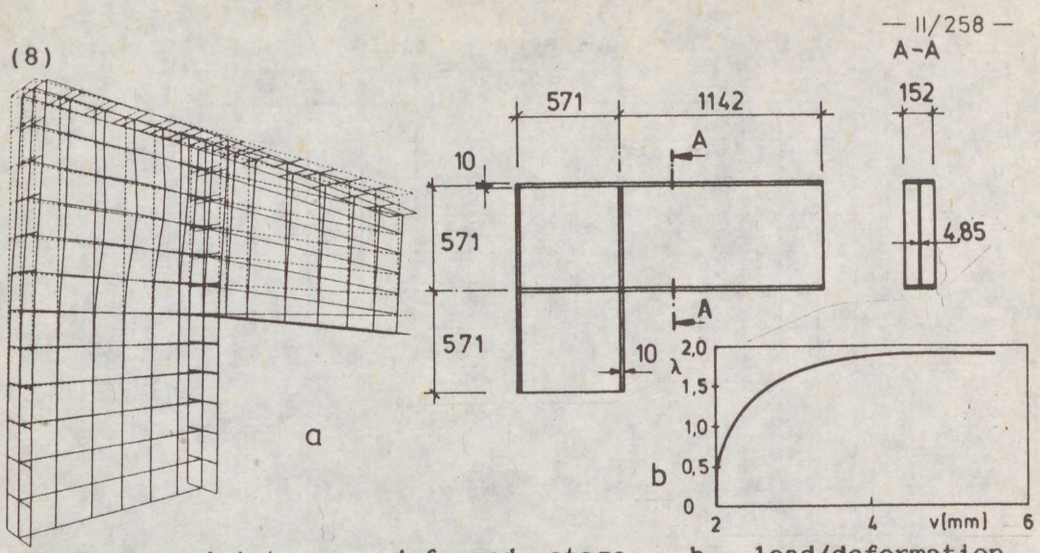

Fig.9 Knee joint. a - deformed stage, b - load/deformation curve (yield stress f_y = 252 N/mm²)

5. Conclusions

The fundamental finding, which was gained likewise from experiments and FEM calculations, states: also in a stiffened knee joint with thin webs a tension band can appear. The load capacity of the knee joint can clearly lie above its elastic buckling load.

For further investigations the following are planned:
- additional experiments (model and natural size) on welded knee joints,
- FEM calculations,
- elaboration and calibration of a simple calculation model,
- inclusion of bolted knee joints.

Acknowledgements

The authors thank Prof. R.Maquoi, Liège, and his co-workers for the fundamental discussion of the topic as well as Dr. J.Chróścielewski, Gdańsk, for the support of the indicated continuing FEM calculations in section 4.3. The German Science Foundation (DFG) is thanked for financial promotion of this project.

References

1. Dubas P., Gehri E., 1986: Behaviour and design of steel plated structures, ECCS publication n. 44, Zurich
2. Petersen Ch., 1982: Statik und Stabilität der Baukonstruktionen, F.Vieweg & Sohn, Braunschweig/Wiesbaden, pp.817-820
3. Scheer J., Pasternak H., 1989: Zum Nachweis von Vollwandträgern mit dünnen Stegen .... Bauingenieur Vol. 64, pp.121-133

Sydorovitch E.M.(1)
Kazachyok V.G.(2)
Korshun E.L.(3)

NUMERICAL INVESTIGATION OF PHYSICALLY AND GEOMETRICALLY NONLINEAR PLANE FRAMES UNDER DIFFERENT LOAD HISTORIES

INTERNATIONAL COLLOQUIUM
STABILITY OF STEEL STRUCTURES
BUDAPEST, HUNGARY, 1990
PRELIMINARY REPORT

Summary: To study the behaviour of metal and reinforced concrete bar systems through all stages of loading with the help of step-by-step procedure together with approximate estimation of tangent cross-section stiffness was used. A universal program enabling the investigation plane systems with semi-rigid connections was worked out on the computer. The comparison of the calculation results and experiments made in the USSR and the USA showed good agreement. Simple frames example helped to reveal the influence of loading history upon the stress-deformed condition up to instability.

(1) Assistant of Professor, Byelorussian Polytechnic Institute
(2) Assistant of Professor, Byelorussian Polytechnic Institute
(3) Researcher, Byelorussian Polytechnic Institute

To estimate the bar system behaviour a step method of successive loading developed by us for short-time loading of metal and reinforced concrete constructions was used. Those constructions are considered to ba phusically and geometrically nonlinear systems.

The step-by-step procedure gives the possibility to ignore the iterative processes at some stages of calculation but to calculate stress-deformed condition of the system with accumulation determining added stresses and displacements by supplement portion of load. It is convenient to use methods based on the proposals of W.F.Chen(1) for determination of the cross-section stiffness taking into consideration the physical nonlinearity of metal construction combining it with the step-by-step procedure considering the geometrical nonlinearity. The calculation is made depending on the type of the cross-section behaviour:

0 - elastic stage,
1 - appearance of one-side yield of cross-section,
2 - appearance of two-side yield of cross-section,
Pl- ulrimate elastic-plastic moment of cross-section.

Depending on the cross-section (I, ⊢, □, ▨), relative longitudinal force P and transversal force Q the limit value of relative moments M, and relative curvatures $\varphi_i = \varkappa/\varkappa_y$ where index i characterizes the type of cross-section behaviour (0;1;2;Pl) are found according to empirical formulas.

Depending on the degree of plastic deformation development in cross-section values of relative curvatures can be calculated according to the expressions given in the work(1). Formulas for determining the tangent stiffness on the given stage of cross-section loading necessary for step-by-step method were developed by derivation of the given expressions.

The plane system calculation is made by displacement method in the form of finite elements approach taking into consideration the influence of the compression tensile longitudinal forces on the finite relements stiffness coefficiants. The system is divided into finite number of straight elements. The calculation is made by an increment in load at every step:

(1)
$$R(X_{i-1}, N_{i-1})\Delta Z_i + \Delta P_i = 0 \qquad (1)$$

where i-is the number of the step, ΔP - is an increment of load, ΔZ - displacement(an increment of displacements) at the next step of loading, x - systems units coordinates at the previous step of loading, N - longitudinal forces at the previous step as well, R(x,N) - stiffness matrix made considering the geometry and logitudinal forces determined at the previous step.

After the system solution (1) the increments of the forces ΔM_i , ΔQ_i , ΔN_i , and then full forces

$$\begin{aligned} M_i &= M_{i-1} + \Delta M_i \\ Q_i &= Q_{i-1} + \Delta Q_i \\ N_i &= N_{i-1} + \Delta N_i \end{aligned} \qquad (2)$$

and full coordinates:

$$X_i = X_{i-1} + \Delta Z \qquad (3)$$

are found, i.e. a deformed scheme of the construction is produced. After that the stiffness matrix is made anew considering the deformed scheme and new longitudinal forces and the system calculation is repeated at the next step.

The system of linear algebraic equations is solved by Gauss method by choosing the leading element along the main diagonal.

The bar systems calculation with semi-rigid connections has its peculiarities. The elastic hinge is supposed to be linearly compliant in respect to angle deformations and absolutely incompliant in respect to longitudinal and transverse deformations.

The usage of basic system and basic unknowns of the mixed method gives the possibility to manipulate with absolutely undeformed joints as it requires assigning of zero compliants. This approach enables to consider the history loading not from the point of view of the history of changing sections stiffness but in the sense of consideration the bars geometry change. iwith the load growth. Along with this practical tasks of determination the real stress-deformed condition of the constructions appear to be solvable when their computational scheme can be changed under loading e.g. when reconstructed, reinforced, etc.

According to the above approach the double-T steel colu columns tested under unaxial stress (2) were calculated. All in all 14 bars were considered, 9 of the being with excentricity in the less rigid direction and 5 were with excentricity in the plane of higher stiffness. To study the quantity of finite elements influence on the designed bearing capacity the test specimens were arbitrarily dismembered to 4 and 10 sections with 5 and 11 cross-sections observed. In the process of designing the test specimens were loaded gradually making 1/10 and 1/100 per cent of the expected bearing capacity.which It makes possible to study the loading scheme influence on the designed bearing capacity of the unaxially loaded specimens.

The design results analyses of the steel double-T specimen and the comparison of the experimental and designed bearing capacities and deflections result in the following:

1. The amount of finite elements practically did not influence the deflecyions and bearing capacity at all stages of loading of short specimens (l = 1.33m; 2,43m).

2. In longer specimens the amount of finite elements influence the deformation on stages close to failure.

3. With decreasing of the value of the step of applied load i.e. increasing the amount of steps the deflection of middle cross-section of the specimens increases.

4. The deviation of the calculated ultimate load from experimental results does not exceed $\pm$ 20%.

Unaxially compressed columns of circular cross-section with accidental excentricity l = 0,001L (where L is the colu column length) and of different slanderness were designed according to the offered procedure as above-mentioned. The test results of them are given in paper(2). The comperison of experimental and calculated results showed that the design

error is not more than 5% (fig. 1).

Experiments made by Davison J. Buick(3) were studied. During these experiments frames of welded double-T's were tested and the evaluation of the stiffness of the column and beam connection was made. Look for the designed scheme and the P-f chart on fig. 2. The load was applied first of all to the right beam with the excentricity of 0,352m from the column axis upto 45 kN and then load was applied in the centre up to 576 kN and then the right bean was loaded up to 100 kN untill the bearing capacity of the frame exhausted itself.

The calculated bearing capacity of the frame with stiff joints is $\Sigma P = 761$kN and considering semi-rigid connections it is $\Sigma P = 759$kN. Thus in this frame the account of joint compliant have not influenced the value of destructive load anddeflection which proves the conclusions of paper (3) made with the help of approximate method of analysis.

The influence of the loading history on the bearing capacity of the frames was studied on the simple II-shaped frame with stiff joints(5).

Frame columns with the height h = 6m are made of rolled double-T's N40 and cross-bar I N50 with 12m span (ГОСТ 8239-72). The columns are loaded by equal longitudinal forces and the horizontal force P = N/4 was applied at the cross-bar level. Calculations made according to our program ware compared with the results of different variants of calculations of frames considered accounting the physical and geometrical nonlinearity using the technique given in the paper(5).

When calculating with assumption of the possibility of limited plastic deformations ε_{pl} = 0,2% using methods (5) ignoring geometric nonlinearity the boundary yeilding at the spots of embedding the columns in the foundation appears at P = 121.1kN (N=484.4kN)..

Several calculations of frames with different load succession according to the program offered were made remebering the physical and geometrical nonlinearity.

Columns and cross-bars were divided into 4 finite elements during every regime.

1. The first regime. Longitudinal forces are applied (full value N = 424.4kN at one time) and then step by step of 0.01 ofthe nominal load (P = 121.1kN) bring the frame to failure.

The chart of dependence of P-f is shown on fig. 3b. Concrete points on the chart in the form of some fractions carry the information about the presence and character of the yeilding in a definite finite element. Under the load of P = 96.9kN one-side yeild of the first and the twelfth finite elements (1/1; 12/1) was found. Under nominal loading P = 121.1kN the yeilding was seen in the upper and the lower quarter of each column.

When = 160kN (89% out of maximum) two-sided yeilding appears at the bottom of both columns. The the yeilding at the middle of the columns occurs and soon the instability at nearly horizontal dependence P-f when P_{max} = 179.23kN, f_n = 12.05mm takes place.

It is necessary to note that sharp nonlinearity of the f frame deformation under loads close to ultimate ones stands

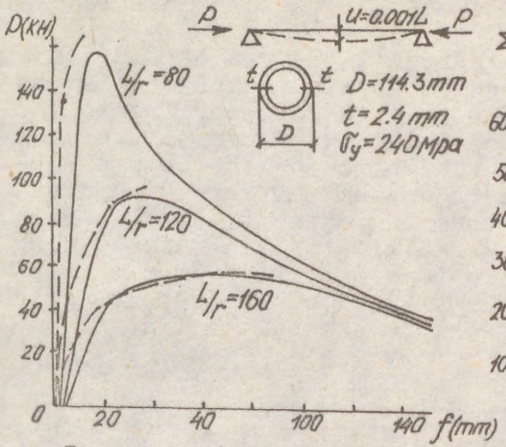

Fig.1. Axial load-deflection curves.
(–) Test, (---) present method.

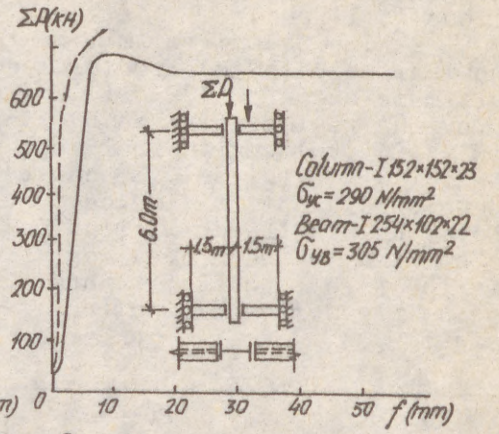

Fig.2. Total Load versus Central Deflection
(—) Test, (---) present method.

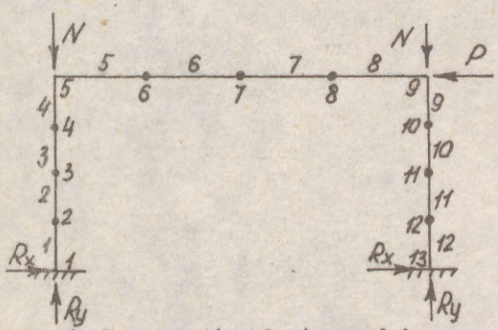

a) Computational scheme of frame.

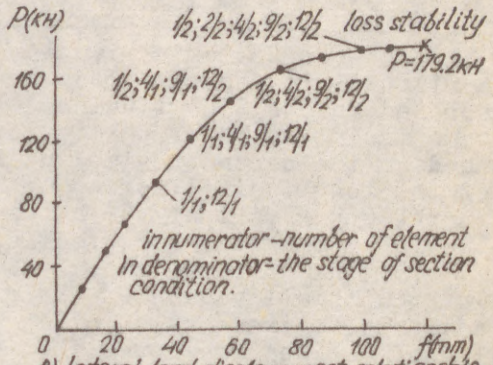

b) Lateral load-displacement relationship with constant axial loads (N=484.4KH).

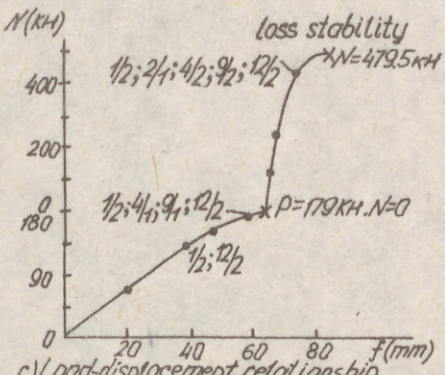

c) Load-displacement relationship with constant lateral load (P=179KH).

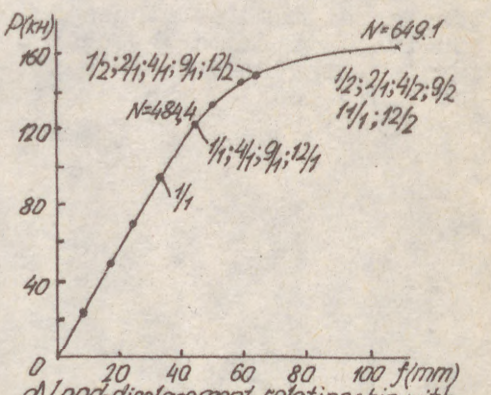

d) Load-displacement relationship with simultaneous loading P and N (P/N = 1/4).

Fig.3.

mostly for the physical than for geometrical nonlinearity as diagram M along the column length even at ultimate load are close to linear.

2. The second regime. Beginning with steps of 0.01 of the nominal load the horizontal load is applied which equals the ultimate ones P = 179kN (147 steps) reached according to the previous regime and then by steps of 0.01 of nominal value (N = 484.4kN)longitudinal load is applied on the columns up to failure (fig. 3c). It can be seen that different load succession did not influence the bearing capacity of the frame. Nevertheless the deflection under ultimate load when loading according to the second regime appeared to be 30% less than in the first one (8.53mm and 12.05mm), i.e. the superposition principle for determination of deformed condition is not right.

Table 1

Regime	P(kN)	N(kN)	f(mm)
1 (N = const)	179.23	484.4	12.02
2 (P = const)	178.017	479.5	8.53
3 N/P = 4	162.27	649,1	11.01

The comparison of two loading regimes under the same horizontal load showed that the presence of previously applied forces (longitudinal) brought to the increasing of moments in the upper part of columns up to 23%. On the other hand in the second regime under full lateral and increasing of the longitudinal forces up to ultimate ones the moments in the upper part of the columns increase by 12% whereas in the lower one they are practically unchanged.

3. The third regime. Loads N and P grow simulteneously up to ultimate values in the given ratio N/P = 4 (fig. 3d). Analysis of these calculation results shows that the character of the deformation with the increase of load is similar to the first regime with some little diferences.

All in all the data obtained confirm that the load history sometimes influences some parameters of stress-deformed condition of frames at characteristic stages of loading. In particular it was found out that the earlier the logitudinal loads are applied the more the deflection value at ultimate stage is.

B i b l i o g r a p h y

1. Chen, W.F. and Atsuta, T., 1977. "Theory of beam-columns, vol. 2. space behavior and design". McGraw-Hill, New York, 5 504-538.

2. Chen,W.F. and Sugimoto, H., 1987. "Analysis of tubular beam-columns and frames under reversed loading". Eng.Struct. vol. 9, October pp. 233-241.

3. Davison, J.Buick, Kirby Patrick A. and Nethercot David A., 1987. "Column behavior in PR construction: Experimental Behavoir. J.Struct.Eng. vol. 113,No 9, September pp 2032-2052.

4. Геммерлинг А.В., Климов А.И., 1986. Несущая способность центрально и внецентреннотсжатых стержней из стали марки нл2. Сборник ЦНИИПС (Исследования по специальным конструкциям) Москва, С. 699- 96.

5. Рекомендации по расчету перераспределения усилий в стальных конструкциях, вследствие физической и геометрической нелинейности при комбинациях нагрузок. ЦНИИПроектстальконструкция им. Мельникова, 1986.

(1)
SZABÓ, Bertalan (1)

LOCAL BUCKLING OF FRAME CORNERS WITH SEMI-RIGID CONNECTIONS

INTERNATIONAL COLLOQUIUM
STABILITY OF STEEL STRUCTURES
BUDAPEST, HUNGARY, 1990
PRELIMINARY REPORT

SUMMARY

This paper presents an experience about the behaviour of local buckling of frame corners obtained from the tests with semi-rigid frame structures and frame parts. The tests consist of among others, a comprehensive stress analysis of the connection parts under compression, the failure modes and the theoretical studies ot the haunching of the frame corners.

NOTATION

F - external applied load
F_o- specified nominal force of high strength (10.9) bolts in end-plates

P_u, N_u, T_u, M_u - force, normal force, shear force and bending moment at failure

M_{PL}, M_{PL1} - plastic moment capacity of the haunched beam and beam section in Fig.7.

b,h,m,m, - geometric properties in Figures 7. and 8.

Introduction

Research work on full-size structures has been carried out for more than a decade in the laboratory of the Department of Steel Structures, Technical University, Budapest. The above gained experience played a key role in the

---

(1) Senior assistant of Structural Engineering
Department for Steel Structures
Technical University, Budapest, Hungary

(2)

preparation of this work. The main aim of the study was the experimental analysis of the local buckling phenomena of semi-rigid frame structures connections and the corners of frame parts, with the consideration of the resulting connection stiffness caused by varying bolt prestressing and the geometrical dimensions of the beam haunching which both effected the resulting force actions.

Tests with frame structures and frame parts

The experimental tests started with the loading of full-size one-storey CONDER-IPARTERV frames [1] of the span of 12,0 m and a height of approximately 5,0 m. On this tests frame corners remained undamaged, local failure on columns occured at the beginning of the haunching and on the frame beams occured at the end of the haunching. For the purpose of further tests the undamaged column to beam connections were taken out from the frame structures or specimens of the same size (as those of frame corners) were manufactured and those were tested in different research works [2], [3], [4], [5]. The force distribution was observed from the manufacturing stage entiely to the failure. During the tests on the significant cross sections of the frame corner elongations were measured by means of electric resistance wire strain gauges and by mechanical PFENDER strain gauge instrument. Vertical and horizontal displacements opening of bolted end-plates and bolt forces were also measured. On the frame corners made from welded plates the welding residual stresses at several points reached the yield stresses. The dimensions of the tested frame to beam connections can be seen on Fig 1. The sections of frame column

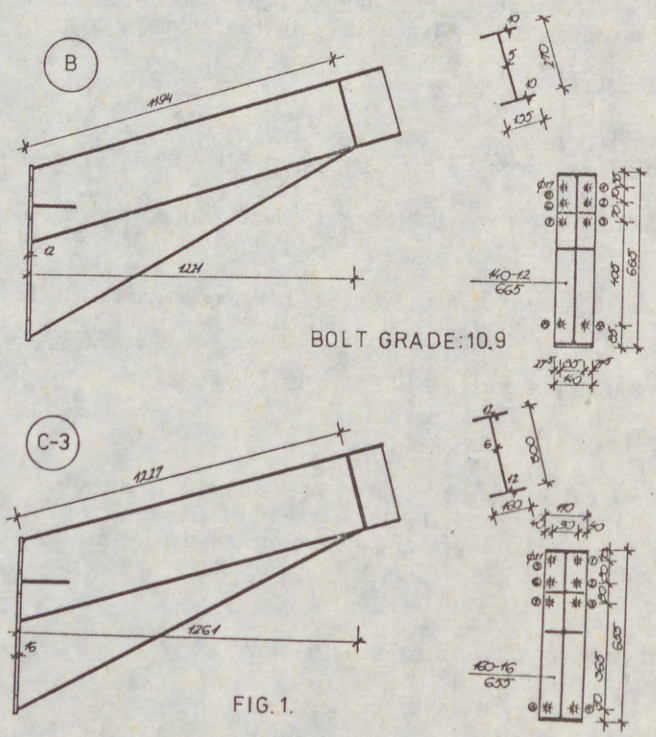

FIG. 1.

(3)
were made from H-I 360.170.48 and H-I 400. 180.58. welded sections.
Fig. 2a. and Fig.2b. show the normal stresses distribution on three loading stages on the flange and web of haunched beam and the flanges of the column respectively. Whilst significant stresses occured on the flanges of the column, on the hauched heam slight stresses were observed.

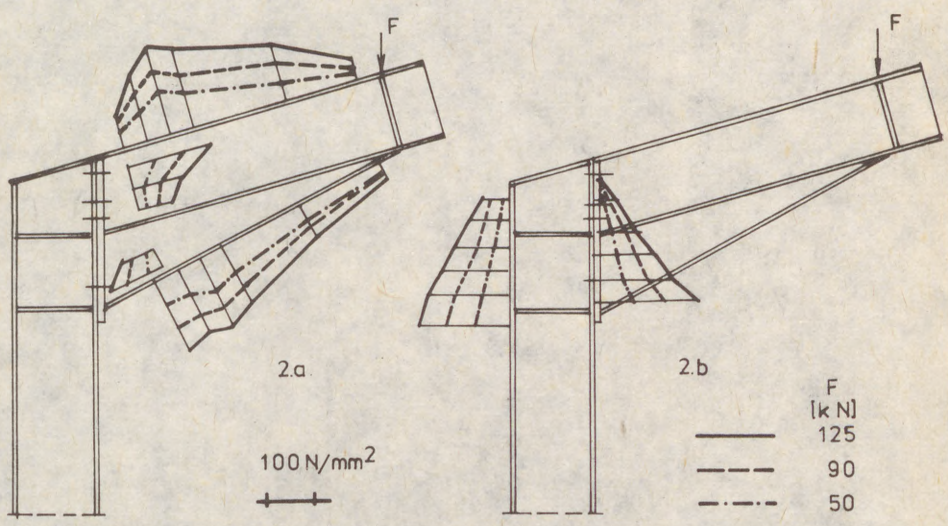

FIG.2.

This gives the explanation for failure mode of the 4 tested CONDER-IPARTERV column to beam connections which was the local buckling of the compressed flange column (Fig.3.)

Fig.3.

(4)
In [6] the column to beam connections ot the FÉM-TIP frame system were tested. In these tests the local buckling of the hauched beam caused the failure for all three tested specimens (Fig.4.)

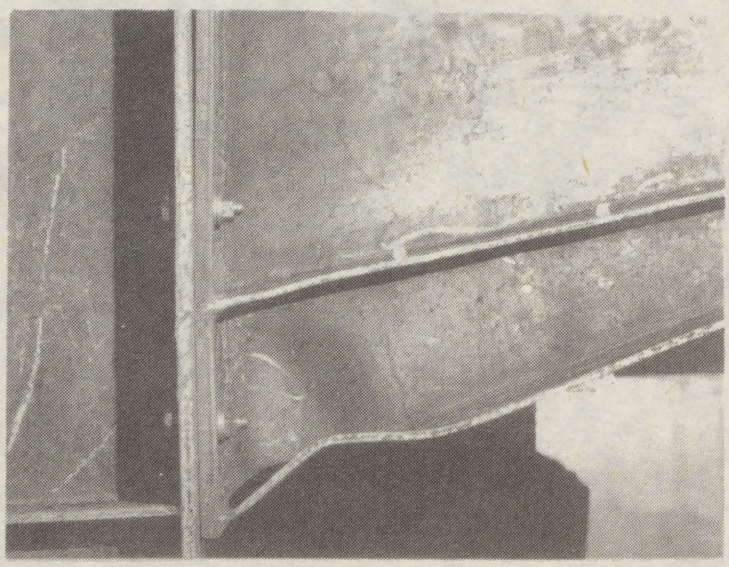

Fig.4.

In order to induce the failure of the hauched CONDER-IPARTERV frame system the column was replaced by an infinitely rigid test auxiliary appliance. This rendered the determination of some special cases of the force distibution on the compressed connection zone possible. The failure of the specimens (Fig. 1.) was due to: in case of low bolt prestressing force-bolt breaking, plastic deformation of the tensile zone of the end-plate and local buckling of the compressed zone (Table 1., Fig. 5.)

TABLE 1.

PROGRAM	SIGN OF TEST	F_o^e [kN]	N_u [kN]	T_u [kN]	M_u [kNm]	FAILURE MODE
I.	B-1/1	99	125	419	500	FWB
	B-1/2	99	128	429	512	FWB, FB
	B-1/3	49,5	119	398	475	TFB
	B-1/3*	49,5	129	431	514	FWB, DEP
	B-1/4	74,25	125	417	498	FWB
	B-1/5	24,75	130	435	519	FWB, FB, DEP
	B-1/6	99	128	428	511	FWB, FB, DEP
	C-3/1	155	133	444	545	FWB
	C-3/2	77,5	126	419	514	FWB
	C-3/3	38,75	116	386	474	FWB
II.	B-1TM	99		337	402	TBB
	C-3TM	155		387	475	FWB

ABBREVIATIONS:

FWB	BOTTOM FLANGE BUCKLING AND WEB BUCKLING
FB	FRACTURE OF TENSION BOLT
TFB	THREAD FRACTURE OF TENSION BOLT
DEP	SIGNIFICANT DEFORMATION OF END-PLATE
TBB	LATERAL-TORSIONAL BUCKLING OF BEAM

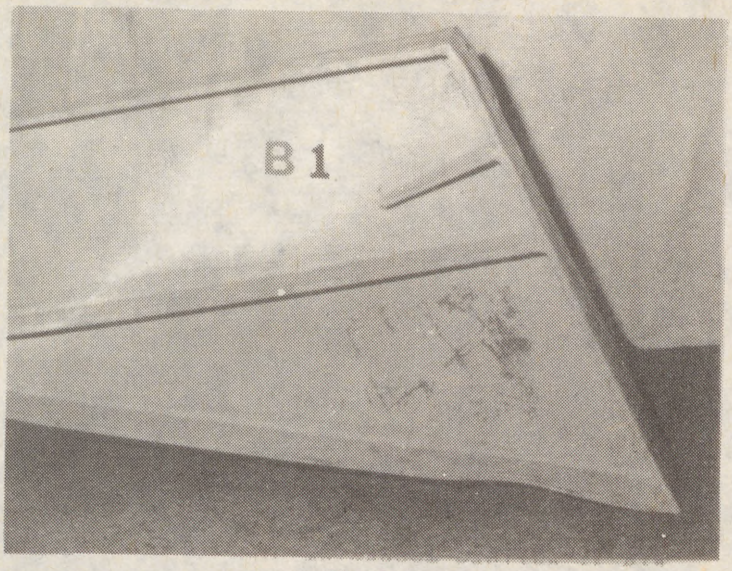

Fig.5.

The variation of bolt prestressing has no significant effect on the load which causes failure, although the normal forces which occur in the haunching could show a considerable difference with bolts relaxation. (Fig.6.)

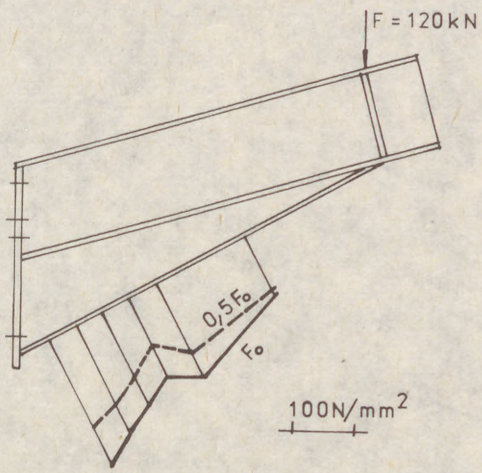

FIG.6.

Conclusions

Whilst the local buckling showed in Fig. 3,4 and 5 being examined, the failure on all cases occured in the plastic range, slowly around the calculated plastic moment capacity. Since the calculated moment capacity

(6)

for the tested specimens was a defining value, then for this reason, in the test sequence, the quotient of the haunched beam and beam section plastic moment capacity in the function of that of the hauching length and height for the tested specimens is shown on Fig.7.

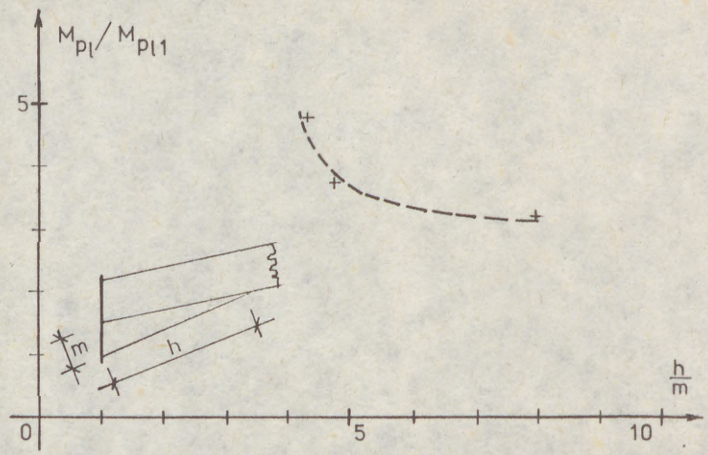

FIG.7.

The curve drawn from the experiments results can give a useful information to the designers (On the diagram each point represents data obtained from different experimental works, see [2], [3] and [6] .)

Further on there would be a need of bringing such a collapse mechanism which precisesly considers both the haunching web and the flange plate local plastic buckling. A possible failure mechanism is shown on Fig.8.

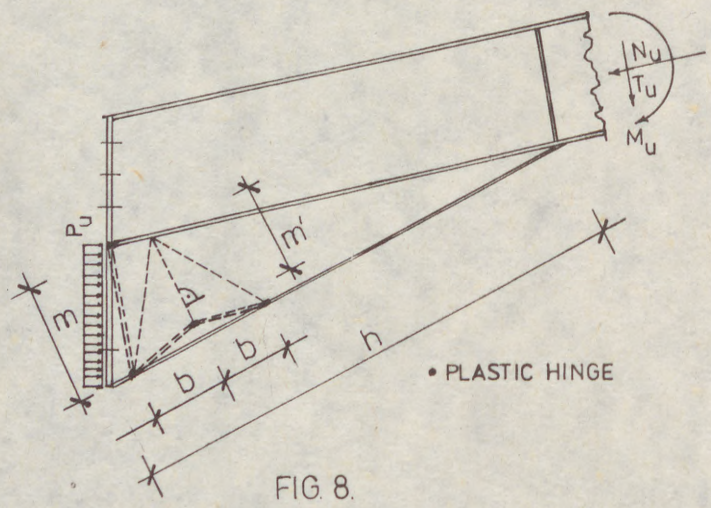

FIG. 8.

(7)
References

[1] **HALÁSZ O. - IVÁNYI M:** Test with Simple Elastic-Plastic Frames. Periodica Polytechnica. Civil Engineering. Vol.23. No. 3-4. 1979. pp.151-182. Budapest

[2] **IVÁNYI M. - SZABÓ B:** Experimental Analysis of High - Strength Bolted End-Plate and Flange Plate Connections. International COLLOQUIUM. Bolted and Special Structural Connections. USSR. MOSCOW. 1989. Proceedings Volume 2. pp. 84-88.

[3] **SZABÓ B::** Experimental Analyísis of End-Plate Connections. Mélyépítéstudományi Szemle 35. 1985.6. pp. 250-254. Budapest (in Hungarian)

[4] **KOVÁCS CS.:** Experimental Analysis of Frame Corner. Diploma work. Budapest. 1987. (in Hungarian)

[5] **MASIKA R.J.:** Tests with Semi-Rigid Column - Beam Frame Connections. Scientific Students' Circle Work. Budapest. 1989. (in Hungarian)

[6] **DEVESCOVI GY.:** Design Problems of End-Plate Connections of Frame Corners of Typical Frames. Diploma work. Budapest. 1979. (in Hungarian)

(1)
SZATMÁRI, ISTVÁN x

A NEW NUMERICAL APPROACH FOR THE CALCULATION OF 3D BAR SYSTEMS

INTERNATIONAL COLLOQUIUM
STABILITY OF STEEL STRUCTURES
BUDAPEST, HUNGARY, 1990
PRELIMINARY REPORT

Summary

A method is presented for the solution of spatial frameworks of rigid connections. Bars of the framework are thin-walled with open and closed cross-section. As material steel is assumed.
The computer program handles above the particular problems induced by torsion the second-order effects as well.

1. Description of the Problem

The program determines the displacements and stresses of spacial thin-walled steel frames.
The structure is made up from members of arbitrary arrangement, with rigid connections. Cross-section of the members can be open or closed, whose data are calculated by the program, with the approximation usual at thin-walled sections, i.e. the cross section is substituted by the area circumferred by the central line of the wall, and elongations or stresses are considered constant over the thickness of the wall.
Open sections are continuous in material, though can be of any shape. Closed cross-sections have to closed loops, and besides it, they might contain open completions.
The structure may be devided into sections by arbitrarily taken nodes. An important precondition that external loads can be applied on the structure only at the nodes. The program consideres the given loading system so-called one-parameter load, and the actual load is reached, when the load parameter "p" reaches the value, p = 1.00. Loads, acting on the nodes are consisted from 7 components, namely, from 3 forces, 3 bending moments and a bi-moment.
The result of the program, the displacements of the nodes, namely the three deflections, 3 rotations and the warping, furthermore the noral and shear stresses in the perpendicular plane, on the middle of the bar.

---

x Assoc. Prof., Department of Steel Structures TU Budapest

(2)

2. Theoretical bases

As it is known, according to the principle of the conservation of the energy, in a physical system, Π is the sum of the potential, and E_k is the sum of the kinetic energies, respectively (provided that the system does not either gain nor loses other energy).

$$\Pi + E_k = \text{const.} \tag{1}$$

The system in equilibrium is in still condition (in a chosen system of co-ordinates), therefore

$$E_k = 0, \tag{2}$$

while in any other cases $E_k > 0$, since the kinetic energy is by far positive.
Therefore, if potential energy belonging to the equilibrium state is Π_0, after disturbing the equilibrium

$$\Pi_0 + \delta\Pi + \delta E_k = \Pi_0 \tag{3}$$

that is

$$\delta\Pi + \delta E_k = \Pi_0 \tag{4}$$

Therefore the condition of equilibrium is

$$\delta\Pi = 0 \tag{5}$$

or

$$\Pi = \text{extr!} \tag{6}$$

The method of the solution that determines the static state internal forces of structures by the above mentioned principle, is called the "slope-deflection" method based on the extreme value of the potential energy.
Writing down the second variation of energies

$$\delta\Pi + \delta^2\Pi + \delta E_k + \delta^2 E_k = 0 \tag{7}$$

from this

$$\delta^2\Pi + \delta^2 E_k = 0 \tag{8}$$

It can be proved that by disturbing the original equilibrium, the system could return into this equilibrium state only if $\delta^2 E_k < 0$, therefore the condition of the stable equilibrium is that

$$\delta^2\Pi > 0 \tag{9}$$

or

$$\Pi = \text{min!} \tag{10}$$

Total potential energy Π is equivalent with the work of the internal and external forces:

$$\Pi = L_b + L_k \tag{11}$$

In the following it is assumed that the structure is loaded by cylinders hydraulic jacks connected to a common hydraulic system, where the system is infinitely rigid and the hydraulic fluid is incompressible. The total potential energy, Π can be written in the form of

$$\Pi = L_b - p(\underline{A}^* \cdot \underline{u} - V) \tag{12}$$

(3)

where

p is the pressure of the system,
A_i is surface like charachteristics proportionla to the loading force (the cross sectional area of the "cylinder"),
u_i is the displacement on the structure in the direction of the operation of the cylinder,
V is the volume of the fluid fed into the hydraulic system.

Equation (12) can be written in a different form, as a conditional extreme value problem.
Let's find that equilibrium mode of the structure, when the volume of the fluid taken by the cylinders is equivalent with the volume of the fluid fed in, i.e.

$$\underline{A}^{*} \cdot \underline{u} - V = 0 \tag{13}$$

The extreme value problem to be solved, by using the Lagrange multiplicator is:

$$F = L_b + \lambda (\underline{A}^{*} \cdot \underline{u} - V) = \text{extr!} \tag{14}$$

It can be proved that int this case

$$\lambda = - p \tag{15}$$

Sincle $L_b = L_b (\underline{u})$, i.-e. that the internal work is the function of the

displacement vector $\underline{u}$ solution is given by the following equations

$$\frac{\partial F}{\partial u_i} = 0 \tag{16}$$

and

$$\frac{\partial F}{\partial \lambda} = 0 \tag{17}$$

Determination of the internal work L_b can be as of the following.
Internal work L_b on a structure of the volume U is

$$L_b = \int_{(U)} \int_{(\varepsilon)} \sigma(\varepsilon) \, d\varepsilon \, dU \tag{18}$$

1st simplification: the volume U can be divided amoug the nodes to volume parts of U_i, such as

$$U = \Sigma U_i \tag{19}$$

or

$$L_b = \Sigma L_{bi} \tag{20}$$

To determine L_{bi} let us assume that by using the stress as the mean value, in the mid-plane perpendicular to the axis of the bar between the nodes I and J:

$$L_{bi} = 2 a \int_{(F)} \int_{(\varepsilon)} \sigma(\varepsilon) \cdot d\varepsilon \cdot dF \tag{21}$$

2nd simplification: Within the cross section F in the sub-area F_i the stress can be substituted by the mean stress, i.e.

$$F = \Sigma F_i \tag{22}$$

and

$$P_i(\varepsilon_i) = F_i \cdot \sigma(\varepsilon_i) \tag{23}$$

(4)
Therefore

$$L_{bi} = 2\,a \sum_{(\varepsilon)} \int P_i(\varepsilon_i)\,d\varepsilon_i \tag{24}$$

and the total internal work can be calculated by using Formula (20).
In order to solve the problem one has to put down the following compatibility equation:

$$\underline{\varepsilon} = \underline{\underline{G}} \cdot \underline{u} \tag{25}$$

3rd simplification: let's assume that deformations $\underline{\varepsilon}$, are functions maximum of second degree of the displacements $\underline{u}$:

$$\underline{\varepsilon} = (\underline{\underline{G}}_1 + \underline{\underline{G}}_2(\underline{u})) \cdot \underline{u} \tag{26}$$

and $\underline{\underline{G}}_2$ is the linear function of displacements $\underline{u}$. Condition of equilibrium (16) by the aboves:

$$\frac{\partial F}{\partial u_i} = \frac{\partial L_b}{\partial u_i} + \lambda A_i = 2a_i \sum P_j(\varepsilon_j) \frac{\partial \varepsilon_j}{\partial u_j} + \lambda A_i \tag{27}$$

By the relationship (26)

$$\frac{\partial \underline{\varepsilon}}{\partial \underline{u}} = \underline{\underline{G}}_1 + \underline{\underline{G}}_2(\underline{u}) + \frac{\partial \underline{\underline{G}}_2}{\partial \underline{u}} \cdot \underline{u} = \underline{\underline{G}}_1 + 2\,\underline{\underline{G}}_2 \tag{28}$$

If

$$\underline{\underline{DG}} = \frac{\partial \underline{\varepsilon}}{\partial \underline{u}} \tag{28/a}$$

and

$$\underline{H} = \begin{bmatrix} \underline{\underline{DG}}^* \cdot \underline{P} \\ \underline{A}^* \quad \underline{u} \end{bmatrix} + \lambda \cdot \begin{bmatrix} \underline{A} \\ 0 \end{bmatrix} - \begin{bmatrix} 0 \\ \underline{V} \end{bmatrix} \tag{29}$$

the condition of the equilibrium is

$$\underline{H} = 0 \tag{30}$$

Condition (30) can be satisfied by an iterative method, such as the Newton-Raphson method. In order to have a better review let's introduce the notation

$$\underline{F}_1 = \frac{\partial \underline{\varepsilon}}{\partial \underline{u}} \cdot \underline{P} \tag{31}$$

than

$$\frac{\partial \underline{F}_1}{\partial \underline{u}} = \frac{\partial^2 \underline{\varepsilon}}{\partial \underline{u}^2} \cdot \underline{P} + \frac{\partial \underline{\varepsilon}}{\partial \underline{u}} \cdot \frac{\partial \underline{P}}{\partial \underline{u}} \tag{32}$$

Parts of the expression (32) are the followings:

$$\frac{\partial^2 \underline{\varepsilon}}{\partial u^2} = 2 \frac{\partial \underline{\underline{G}}_2}{\partial \underline{u}} = 2 \cdot \underline{\underline{GH}} \tag{33}$$

(5) $$\frac{\partial P}{\partial \underline{u}} = \frac{dP}{d\underline{\varepsilon}} \cdot \frac{\partial \underline{\varepsilon}}{\partial \underline{u}}$$

(34)

Arranging the $\frac{dP}{d\varepsilon}$ differential quotients into a diagonalt matrix, and applying the notation (28a), one can compile the

$$\underline{\underline{D}} = \left[\begin{array}{c|c} \underline{\underline{DG}}^{*} \cdot \left[\frac{dP}{d\varepsilon}\right] \cdot \underline{\underline{DG}} + 2\underline{P} \cdot \underline{\underline{GH}} & \underline{A} \\ \hline \underline{A}^{*} & 0 \end{array}\right]$$

(35)

coefficient matrix.

Equation of the correction is

$$\underline{\underline{D}} \cdot \left[\frac{\Delta u}{\Delta \lambda}\right] = \underline{H}$$

(36)

and

$$\left[\frac{u}{\lambda}\right]^{(k+1)} = \left[\frac{u}{\lambda}\right]^{(k)} - \left[\frac{\Delta u}{\Delta \lambda}\right]$$

(37)

where k means the number of repetition of solving equation (36).

Iteration can be interrupted, if in case of m unknowns, the

$$h = \frac{1}{\sqrt{m}} \cdot \sqrt{\underline{H}^{*} \cdot \underline{H}} \qquad (38)$$

least square error becomes adequately small.

The application for the computer program is presented in Szatmári - Tomka 1990, and Szabó - Szatmári (1990) in this proceeding.

References

Szabó, Gy. - Szatmári, I. (1990) Comparison of Numerical and Experimental Results of Bars Subjected to Lateral-Torsional Buckling

Szatmári, I. - Tomka P. (1990) Analytical and Numerical Study on the Lateral Instability of a Plated Bridge

(1)
TOADER, Ioan Horea Iosif (1)

A GENERALISATION OF LIVESLEY'S STABILITY FUNCTIONS

INTERNATIONAL COLLOQUIUM
STABILITY OF STEEL STRUCTURES
BUDAPEST, HUNGARY, 1990
PRELIMINARY REPORT

Summary: The paper presents a generalisation of Livesley's stability functions for members with semi-rigid joint connections.

INTRODUCTION

One of the most difficult problems in the design of steel frames is the effect of partial restraint of the members, which depends on the solution adopted for joint connections. Thus, site welding provides perfect restraint, while some of the bolted joints behave like hinged connections. As a rule, the actual restraint degree for a given system has to be determined by laboratory tests. A rigorous analysis should take into account the influence of this restraint. Modern computer programs, now available to the majority of designers, allow a more sophisticated treatment of joints without an appreciable increase in calculation costs.

MEMBER WITH SEMI-RIGID JOINT CONNECTIONS. SECOND-ORDER ANALYSIS

Unless specifically stated otherwise, the following assumptions, consistent with structural theory and with the geometry of steel frames, will hold throughout the investigation

(1) Associate Professor, Polytechnic Institute of Cluj-Napoca, Romania, M.IABSE.

(2)

of the straight member semi-rigid connected at the ends:

a) The structural material is linearly elastic-rigid plastic;

b) The member has a double symmetric and constant cross section;

c) Loads are acting on joints;

d) The displacements of the member are small;

e) The effect of shear deflections is disregarded;

f) The torsional buckling and local instability do not occur.

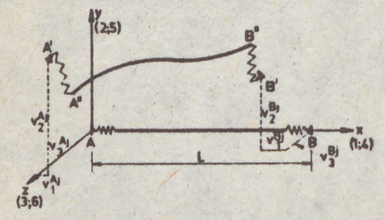

Fig.1

Figure 1 shows the bar AB of a space frame, semi-rigid connected at the ends, before and after deformation.

The constants k_i of the spring stiffness i (i=1,2,...,6) at the joint which vary form 0 to ∞ may be replaced through the "fixity factors" η_i which vary from 0 to 1, Fig.2.

This replacing is advantageous for current available computer oriented methods, Refs 2 and 6, which lies in the basic relationship required for either stiffness or flexibility approach :

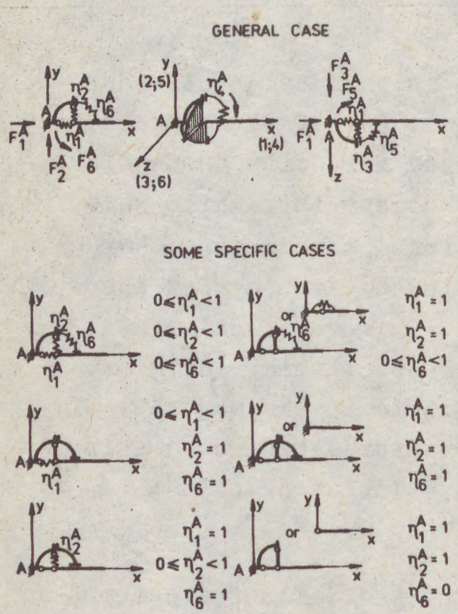

Fig.2

$$\eta_1 = \frac{k_1}{k_1 + \frac{AE}{L}} \; ; \quad \eta_2 = \frac{k_2}{k_2 + \frac{12EI_2}{L^3}}$$

$$\eta_3 = \frac{k_3}{k_3 + \frac{12EI_3}{L^3}} \; ; \quad \eta_4 = \frac{k_4}{k_4 + \frac{GJ}{L}}$$

$$\eta_5 = \frac{k_5}{k_5 + \frac{4EI_2}{L}} \; ; \quad \eta_6 = \frac{k_6}{k_6 + \frac{4EI_3}{L}} \qquad (1)$$

(3)

In Eqns (1) AE is the axial stiffness, GJ is the torsional stiffness, EI_2 and EI_3 are flexural stiffness about y and z axis, respectively and L is the bar length. The fixity factor η_i^A of the elastic connection i between member end Am and joint Aj is defined through the ratio between displacement v_i^{Am} of the bar end Am in the i direction and displacement v_i^{Aj} of the joint Aj in the same direction, provided that all the other displacements are zero, Ref.2.

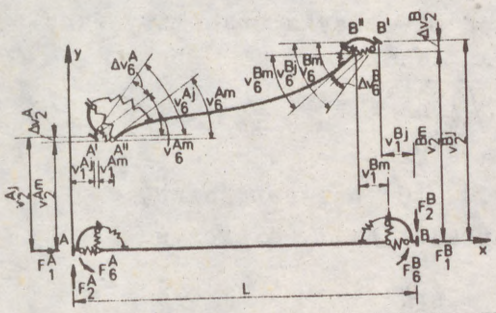

Fig.3

The coordinate system Axyz of the bar AB with x axis along the member length before its deformations, are shown in Figs 2 and 3.

The linear displacements in the plane Axy are v_1^{Aj}, v_1^{Am}, v_2^{Aj}, v_2^{Am}, v_1^{Bj}, v_1^{Bm}, v_2^{Bj}, v_2^{Bm} and the angular ones are v_6^{Aj}, v_6^{Am}, v_6^{Bj}, v_6^{Bm}, Fig.3. The indices "j" and "m" are referred to joints and ends of the member, respectively.

The member end forces are bending moments F_6^A and F_6^B, transverse shear forces $F_2^A = -F_2^B$ and the axial force $F_1^A = -F_1^B = N$.

In the second order theory the transverse shear forces and the rotations of the member ends A and B are:

$$F_2^A = -F_2^B = \frac{1}{L}(F_6^A + F_6^B) + \frac{N}{L}(v_2^{Am} - v_2^{Bm}) \qquad (2)$$

$$v_6^{Am} = v_6^{AA} F_6^A + v_6^{AB} F_6^B + \frac{1}{2}(v_2^{Bm} - v_2^{Am}) \qquad (3)$$

$$v_6^{Bm} = v_6^{BA} F_6^A + v_6^{BB} F_6^B + \frac{1}{L}(v_2^{Bm} - v_2^{Am}) \qquad (4)$$

where v_6^{AA}, v_6^{BB}, v_6^{AB} and v_6^{BA} are flexibility coefficients of the member:

$$v_6^{AA} = v_6^{BB} = \frac{L}{3EI_3}\alpha(\varepsilon) \qquad (5)$$

$$v_6^{AB} = v_6^{BA} = -\frac{L}{6EI_3}\beta(\varepsilon) \qquad (6)$$

(4)

and $\alpha(\varepsilon)$ and $\beta(\varepsilon)$ are functions depending on the axial force N. For example, for axial compression force N:

$$\alpha(\varepsilon) = \frac{3}{\varepsilon}\left(\frac{1}{\varepsilon} - \frac{1}{\tan\varepsilon}\right) \tag{7}$$

$$\beta(\varepsilon) = \frac{6}{\varepsilon}\left(\frac{1}{\sin\varepsilon} - \frac{1}{\varepsilon}\right) \tag{8}$$

The variable ε is the argument of Livesley's stability functions:

$$\varepsilon = L\sqrt{\frac{|N|}{EI_3}} \tag{9}$$

The differences Δv_i (for i=1,2,...,6) between joint, and member end displacements are mathematically expressed by the relationships:

$$\Delta v_i^A = v_i^{Aj} - v_i^{Am} = \frac{F_i^A}{k_i^A} \tag{10}$$

$$\Delta v_i^B = v_i^{Bj} - v_i^{Bm} = \frac{F_i^B}{k_i^B} \tag{11}$$

With the notations:

$$d_2 = \frac{1}{\eta_2^A} + \frac{1}{\eta_2^B} - 1 \tag{12}$$

$$e_2 = 1 - \frac{\varepsilon^3}{12}(d_2-1) \text{ for } N \leq 0 \tag{13}$$

$$e_2 = 1 + \frac{\varepsilon^3}{12}(d_2-1) \text{ for } N \geq 0 \tag{14}$$

$$a_2 = \alpha(\varepsilon)e_2 \tag{15}$$

$$b_2 = \beta(\varepsilon)e_2 \tag{16}$$

Equations 3 and 4 become:

$$\frac{6EI_3}{L} e_2 v_6^{Aj} = R_1 F_6^A - R_2 F_6^B + \frac{6EI_3}{L^2}(v_2^{Bj} - v_2^{Aj}) \tag{17}$$

$$\frac{6EI_3}{L} e_2 v_6^{Bj} = -R_2 F_6^A + R_1 F_6^B + \frac{6EI_3}{L^2}(v_2^{Bj} - v_2^{Aj}) \tag{18}$$

(5)

where R_1, R_2 and f_2 are:

$$R_1 = \tfrac{1}{2}\left(d_2 + \frac{3e_2}{\eta_6^A} + f_2\right) \tag{19}$$

$$R_2 = \tfrac{1}{2}\left(2b_2 - d_2 + 1\right) \tag{20}$$

$$f_2 = 4a_2 - 3e_2 - 1 \tag{21}$$

It may be computed from Eqns (17) and (18) the moments F_6^A and F_6^B:

$$F_6^A = \frac{4EI_3}{L} C_{1z}^A v_6^{Aj} + \frac{2EI_3}{L} C_{2z} v_6^{Bj} + \frac{6EI_3}{L^2} C_{3z}^A v_2^{Aj} - \frac{6EI_3}{L^2} C_{3z}^A v_2^{Bj} \tag{22}$$

$$F_6^B = \frac{2EI_3}{L} C_{2z} v_6^{Aj} + \frac{4EI_3}{L} C_{1z}^B v_6^{Bj} + \frac{6EI_3}{L^2} C_{3z}^B v_2^{Aj} - \frac{6EI_3}{L^2} C_{3z}^B v_2^{Bj} \tag{23}$$

Equation (2) becomes:

$$F_2^A = -F_2^B = \frac{6EI_3}{L^2} C_{3z}^A v_6^{Aj} + \frac{6EI_3}{L^2} C_{3z}^B v_6^{Bj} + \frac{12EI_3}{L^3} C_{4z} v_2^{Aj} - \frac{12EI_3}{L^3} C_{4z} v_2^{Bj} \tag{24}$$

In Eqns (22),(23) and (24) C_{1z}^A, C_{1z}^B, C_{2z}, C_{3z}^A, C_{3z}^B and C_{4z} are generalized Livesley's stability functions:

$$C_{1z}^A = \frac{3e_2}{K_z}\left[(d_2+f_2)\eta_6^B + 3e_2\right]\eta_6^A \tag{25}$$

$$C_{1z}^B = \frac{3e_2}{K_z}\left[(d_2+f_2)\eta_6^A + 3e_2\right]\eta_6^B \tag{26}$$

$$C_{3z}^A = \frac{2}{K_z}\left[(2b_2+f_2+1)\eta_6^B + 3e_2\right]\eta_6^A \tag{27}$$

$$C_{2z} = \frac{6e_2}{K_z}(2b_2 - d_2 + 1)\eta_6^A\eta_6^B \tag{28}$$

$$C_{3z}^B = \frac{2}{K_z}\left[(2b_2+f_2+1)\eta_6^A + 3e_2\right]\eta_6^B \tag{29}$$

$$C_{4z} = \frac{1}{e_2}\left(\frac{C_{3z}^A + C_{3z}^B}{2} - \frac{\varepsilon^2}{12}\right) \tag{30}$$

where

$$K_z = \left\{\left[f_2^2 - (2b_2+1)^2\right]\eta_6^A\eta_6^B + d_2\left[2(2b_2+f_2+1)\eta_6^A\eta_6^B + 3e_2(\eta_6^A+\eta_6^B)\right] + 3e_2 f_2(\eta_6^A + \eta_6^B) + 9e_2^2\right\}. \tag{31}$$

The variation of generalized Livesley's stability functions for

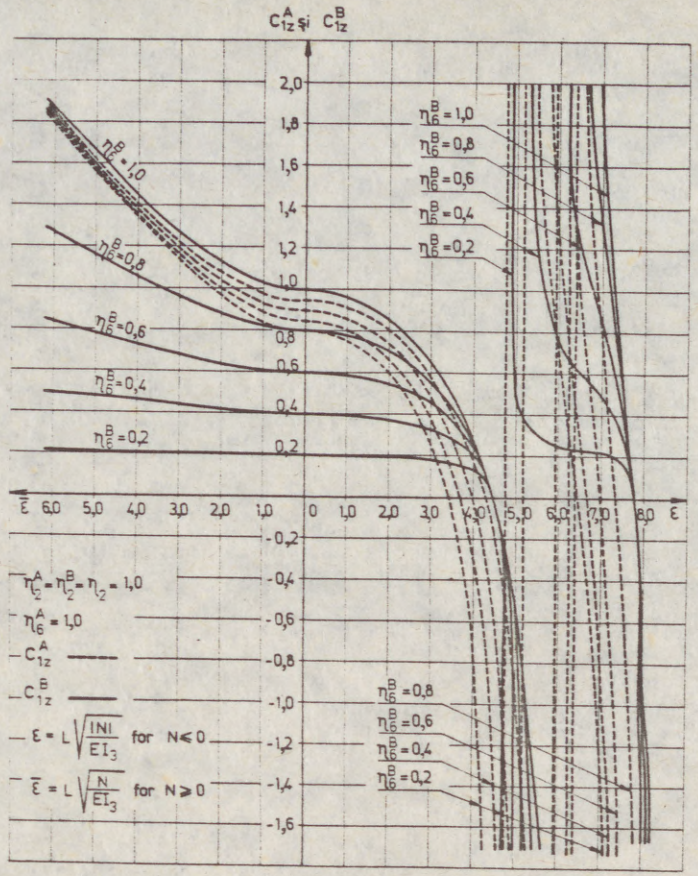
C_{1z}^A şi C_{1z}^B
$\eta_6^B = 1,0$
$\eta_6^B = 0,8$
$\eta_6^B = 0,6$
$\eta_6^B = 0,4$
$\eta_6^B = 0,2$
$\bar{\varepsilon}$ 6,0 5,0 4,0 3,0 2,0 1,0 0 1,0 2,0 3,0 4,0 5,0 6,0 7,0 8,0 ε
$\eta_2^A = \eta_2^B = \eta_2 = 1,0$
$\eta_6^A = 1,0$
C_{1z}^A
C_{1z}^B
$\varepsilon = L\sqrt{\frac{|N|}{EI_3}}$ for $N \leq 0$
$\bar{\varepsilon} = L\sqrt{\frac{N}{EI_3}}$ for $N \geq 0$

Fig.4

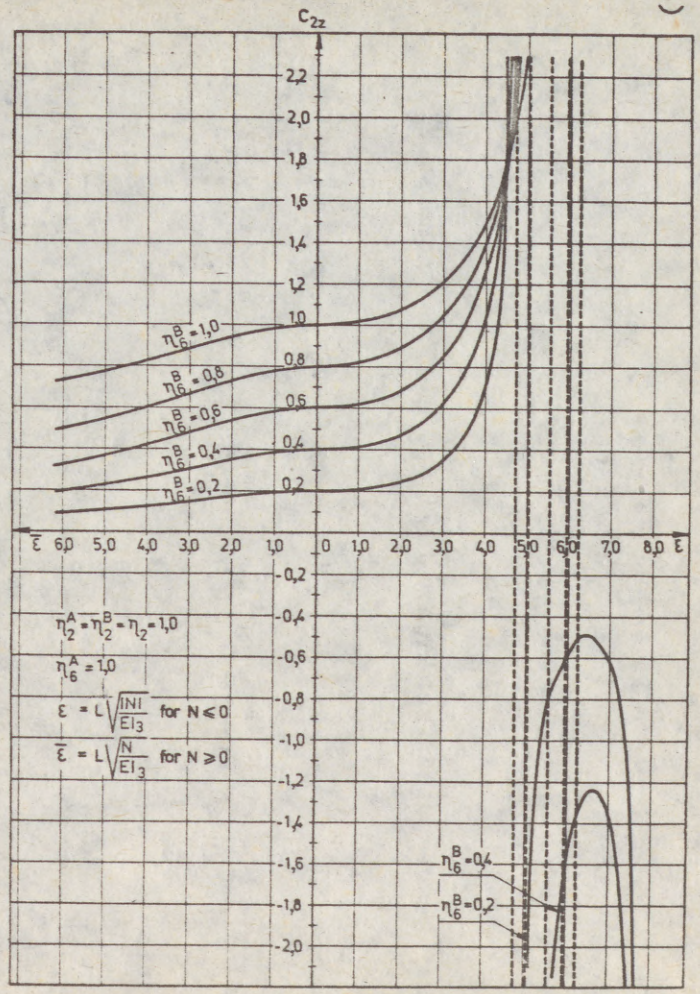
C_{2z}
$\eta_6^B = 1,0$
$\eta_6^B = 0,8$
$\eta_6^B = 0,6$
$\eta_6^B = 0,4$
$\eta_6^B = 0,2$
$\bar{\varepsilon}$ 6,0 5,0 4,0 3,0 2,0 1,0 0 1,0 2,0 3,0 4,0 5,0 6,0 7,0 8,0 ε
$\eta_2^A = \eta_2^B = \eta_2 = 1,0$
$\eta_6^A = 1,0$
$\varepsilon = L\sqrt{\frac{|N|}{EI_3}}$ for $N \leq 0$
$\bar{\varepsilon} = L\sqrt{\frac{N}{EI_3}}$ for $N \geq 0$

Fig.5

C_{3z}^A şi C_{3z}^B

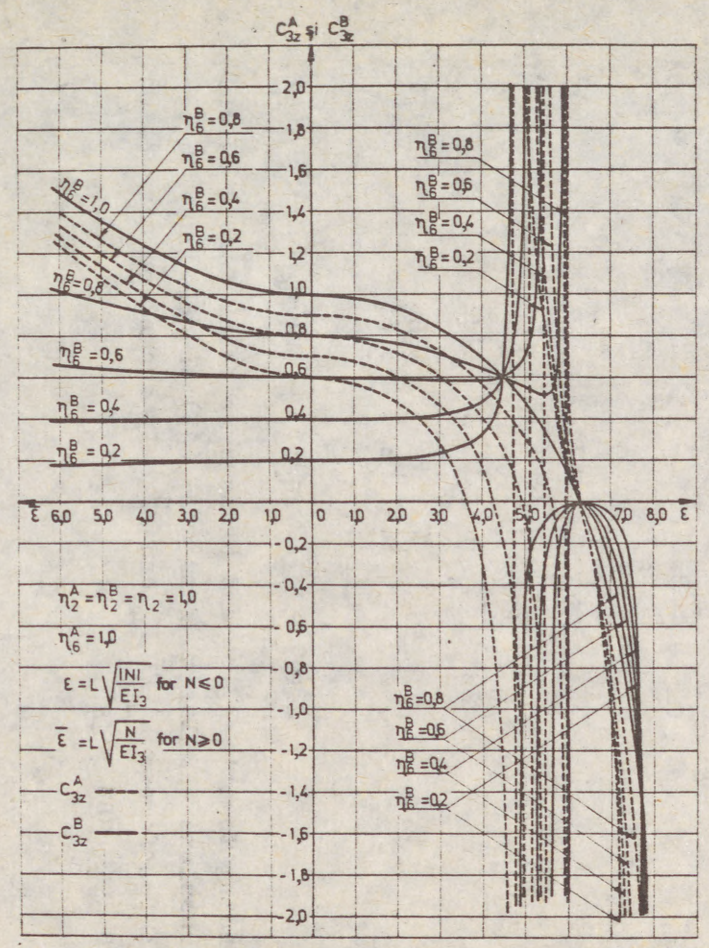
C^A_{3z} şi C^B_{3z}
$\eta^B_6=0,8$
$\eta^B_6=0,6$
$\eta^B_6=0,4$
$\eta^B_6=0,2$
$\eta^B_6=1,0$
$\eta^A_2=\eta^B_2=\eta_2=1,0$
$\eta^A_6=1,0$
$\varepsilon=L\sqrt{\frac{|N|}{EI_3}}$ for $N\leq 0$
$\bar{\varepsilon}=L\sqrt{\frac{N}{EI_3}}$ for $N\geq 0$
C^A_{3z}
C^B_{3z}
ε

Fig.6

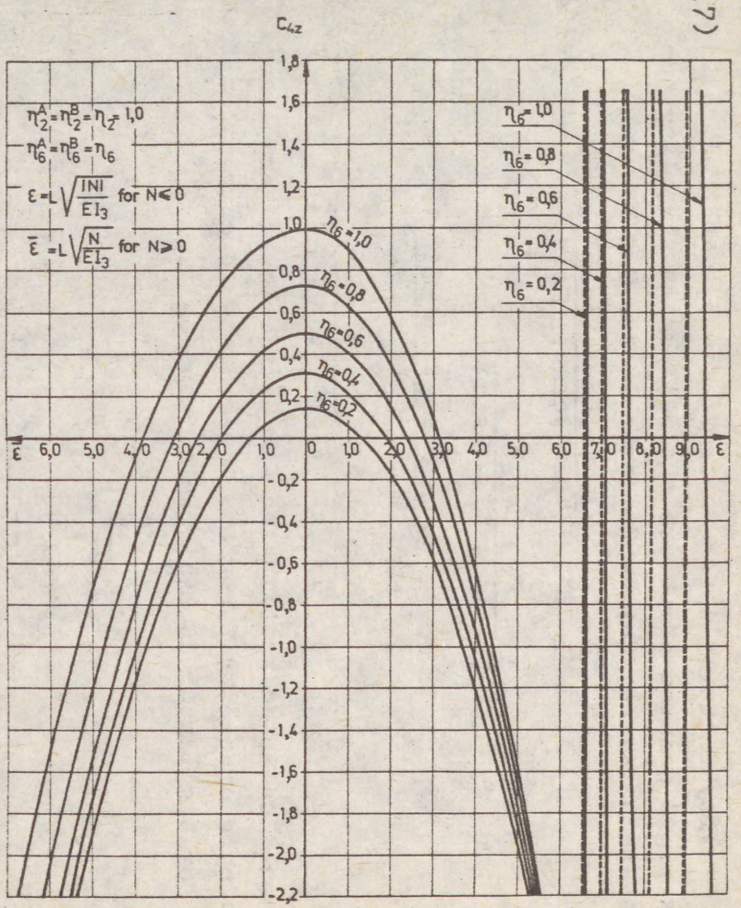
C_{4z}
$\eta^A_2=\eta^B_2=\eta_2=1,0$
$\eta^A_6=\eta^B_6=\eta_6$
$\varepsilon=L\sqrt{\frac{|N|}{EI_3}}$ for $N\leq 0$
$\bar{\varepsilon}=L\sqrt{\frac{N}{EI_3}}$ for $N\geq 0$
$\eta_6=1,0$
$\eta_6=0,8$
$\eta_6=0,6$
$\eta_6=0,4$
$\eta_6=0,2$
ε

Fig.7

(7)

(8)

some "fixity factors" is shown in Figs 4,5,6 and 7.

For a rigid jointed structure the well known stability functions are obtained, Ref.4. For example for $N \leqslant 0$

$$C_1^A = C_1^B = C_1 = \frac{1}{4} \frac{(\sin\varepsilon - \varepsilon\cos\varepsilon)}{2(1-\cos\varepsilon) - \varepsilon\sin\varepsilon} \tag{32}$$

$$C_2 = \frac{1}{2} \frac{\varepsilon(\varepsilon - \sin\varepsilon)}{2(1-\cos\varepsilon) - \varepsilon\sin\varepsilon} \tag{33}$$

$$C_3^A = C_3^B = C_3 = \frac{1}{6} \frac{\varepsilon^2(\varepsilon - \sin\varepsilon)}{2(1-\cos\varepsilon) - \varepsilon\sin\varepsilon} \tag{34}$$

$$C_4 = C_3 - \frac{\varepsilon^2}{12} = \frac{1}{12} \frac{\varepsilon^3}{2(1-\cos\varepsilon) - \varepsilon\sin\varepsilon} \tag{35}$$

It should be noted that in the $N = 0$ case the generalized Livesley's stability functions are reduced to correction factors for the linear analysis, Refs 2 and 6:

$$C_{1z}^A = \frac{\eta_6^A}{K_z}(d_2\eta_6^B + 3) \tag{36}$$

$$C_{1z}^B = \frac{\eta_6^B}{K_z}(d_2\eta_6^A + 3) \tag{37}$$

$$C_{2z} = \frac{2\eta_6^A\eta_6^B}{K_z}(1 + \eta_6^A) \tag{38}$$

$$C_{3z}^A = \frac{2\eta_6^A}{K_z}(1 + \eta_6^B) \tag{39}$$

$$C_{3z}^B = \frac{2\eta_6^B}{K_z}(1 + \eta_6^A) \tag{40}$$

$$C_{4z} = \frac{1}{K_z}(\eta_6^A + \eta_6^B + 2\eta_6^A\eta_6^B) \tag{41}$$

where

$$K_z = d_2(\eta_6^A + \eta_6^B + 2\eta_6^A\eta_6^B) - 3(\eta_6^A\eta_6^B - 1) \tag{42}$$

For bending moments F_5^A, F_5^B and transverse shear forces F_3^A and F_3^B, expressions similar to Eqns (22),(23) and (24) may be obtained. The forces F_1^A, F_1^B, F_4^A and F_4^B only depend on correction factors α_{11} and α_{44}

(9)

$$F_1^A = -F_1^B = \frac{EA}{L}\alpha_{11}(v_1^{Aj} - v_1^{Bj}) \qquad (43)$$

$$F_4^A = -F_4^B = \frac{GJ}{L}\alpha_{44}(v_4^{Aj} - v_4^{Bj}) \qquad (44)$$

where

$$\alpha_{11} = \left(\frac{1}{\eta_1^A} + \frac{1}{\eta_1^B} - 1\right)^{-1} \qquad (45)$$

$$\alpha_{44} = \left(\frac{1}{\eta_4^A} + \frac{1}{\eta_4^B} - 1\right)^{-1} \qquad (46)$$

CONCLUSIONS

The force displacement relationships for the members elastically (semi-rigid) connected at the nodes which express the twelve force components [F] acting on the member in terms of the twelve possible joint displacement components [v] can be written in the form of a matrix equation :

$$\begin{bmatrix}
\frac{EA}{L}\alpha_{11} & & & & & & -\frac{EA}{L}\alpha_{11} & & & & & \\
& \frac{12EI_3}{L^3}C_{4z} & & & & \frac{6EI_3}{L^2}C_{3z}^A & & -\frac{12EI_3}{L^3}C_{4z} & & & & \frac{6EI_3}{L^2}C_{3z}^B \\
& & \frac{12EI_2}{L^3}C_{4y} & & -\frac{6EI_2}{L^2}C_{3y}^A & & & & \frac{12EI_2}{L^3}C_{4y} & & -\frac{6EI_2}{L^2}C_{3y}^B & \\
& & & \frac{GJ}{L}\alpha_{44} & & & & & & -\frac{GJ}{L}\alpha_{44} & & \\
& & \frac{6EI_2}{L^2}C_{3y} & & \frac{4EI_2}{L}C_{1y} & & & & \frac{6EI_2}{L^2}C_{3y} & & \frac{2EI_2}{L}C_{2y} & \\
& \frac{6EI_3}{L^2}C_{3z} & & & & \frac{4EI_3}{L}C_{1z} & & -\frac{6EI_3}{L^2}C_{3z} & & & & \frac{2EI_3}{L}C_{2z} \\
-\frac{EA}{L}\alpha_{11} & & & & & & \frac{EA}{L}\alpha_{11} & & & & & \\
& -\frac{12EI_3}{L^3}C_{4z} & & & & -\frac{6EI_3}{L^2}C_{3z}^A & & \frac{12EI_3}{L^3}C_{4z} & & & & -\frac{6EI_3}{L^2}C_{3z}^B \\
& & \frac{12EI_2}{L^3}C_{4y} & & \frac{6EI_2}{L^2}C_{3y}^A & & & & -\frac{12EI_2}{L^3}C_{4y} & & \frac{6EI_2}{L^2}C_{3y}^B & \\
& & & -\frac{GJ}{L}\alpha_{44} & & & & & & \frac{GJ}{L}\alpha_{44} & & \\
& & \frac{6EI_2}{L^2}C_{3y}^B & & \frac{2EI_2}{L}C_{2y} & & & & \frac{6EI_2}{L^2}C_{3y}^B & & \frac{4EI_2}{L}C_{1y}^B & \\
& \frac{6EI_3}{L^2}C_{3z}^B & & & & \frac{2EI_3}{L}C_{2z} & & -\frac{6EI_3}{L^2}C_{3z}^B & & & & \frac{4EI_3}{L}C_{1z}^B
\end{bmatrix}
\begin{bmatrix} v_1^{Aj} \\ v_2^{Aj} \\ v_3^{Aj} \\ v_4^{Aj} \\ v_5^{Aj} \\ v_6^{Aj} \\ v_1^{Bj} \\ v_2^{Bj} \\ v_3^{Bj} \\ v_4^{Bj} \\ v_5^{Bj} \\ v_6^{Bj} \end{bmatrix}
=
\begin{bmatrix} F_1^A \\ F_2^A \\ F_3^A \\ F_4^A \\ F_5^A \\ F_6^A \\ F_1^B \\ F_2^B \\ F_3^B \\ F_4^B \\ F_5^B \\ F_6^B \end{bmatrix}
\qquad (47)$$

where the equivalent stiffness matrix $[K_E]$ takes into account the influence of the elastic connection on the behaviour of the bar, Ref.6. The equivalent stiffness matrix may be used to analyse the elastic behaviour of steel frames. Their function is not restricted to analyzing stability problems, there might equally well be used simply to find the deflections of a fra-

(10)

mework under a load or a stress in its members in a non-linear analysis.

REFERENCES

1. BIJLAARD,F.,S..K., NETHERCOT,D.,A., STARK,J.,W.,B., TSCHEMMERNEGG,F. and ZOETEMEIJER,P., 1989, Structural Properties of Semi-Rigid Joints in Steel Frames, IABSE SURVEYS S-42/89, Periodica 2/1989, pp 1-31.

2. BOTIZAN,P., 1978, Etablissement de la matrice de rigidité d'un élement barre avec liaisons imperfaites aux noeds, CONSTRUCTION MÉTALLIQUE, No.1, pp

3. CYWINSKI,Z., 1986, On Buckling of Thin-Walled Frames,Second Regional Colloqium on Stability of Steel Structures,September, 25-26,1986, Hungary, Final Report, pp 157-160.

4. FORMAN,S.,E. and HUCHINSON,J.,W., 1970, Buckling of Reticulated Shell Structures, International Journal of Solids and Structures, Vol.6, 1970, pp 909-932.

5. LOTHERS,J.,E., 1960, Advanced Design in Structural Steel, Prentince Hall International, pp 367-406.

6. TOADER,I.H.,I., 1982, Generalized Stability Functions for Structural Frameworks 3 rd International Colloqium on Stability, Proceedings of the First Session, Timişoara, Romania, 16 th October 1982, pp 73-82.

7. VOGEL,U., 1986, General Report for the Session on Frames, Second Regional Colloqium on Stability of Steel Structures, September 25-26, 1986, Hungary, Final Report, pp 135-148.

(1)
URBAN, Karsten (1)
THIELE, Rolf (2)

ON THE INFLUENCE OF FLEXIBLE BEAM-COLUMN CONNECTIONS ON BIFURCATION LOADS OF PLANE, DISPLACEABLE, TWO-LEGGED STEEL STOREY FRAMES

INTERNATIONAL COLLOQUIUM
STABILITY OF STEEL STRUCTURES
BUDAPEST, HUNGARY, 1990
PRELIMINARY REPORT

Summary: The influence of flexible connections on the bifurcation loads of steel storey frames is shown by some examples.

Taking account of the influence of flexible connections on the load level of so-called rigid structures is important for reasons of economy and safety.

According to the GDR Code a tensile test (based on the theory of the second order) and a test on bifurcation loads are required for steel frame structures. In addition /3/ offers an alternative test. When determining the bifurcation load by disregarding horizontal loads, the predeformation required for the calculation according to a second-order method can be reduced from 1/200 of the storey height to 1/800, regarding it as an undesired displacement of the beam. By using an analysis according to a second-order method a correspondingly lesser bending moment increase results.

(1) Dr.-Ing. Assistant of Mechanics, Techn.Hochschule Leipzig
(2) Professor of Mechanics, Technische Hochschule Leipzig

(2)

According Fig. 1 the mere normal load level can be attained by two-, three-, and four-storey frames with pinned (curves 1, 2, 3) as well as restrained base points (curves 4, 5, 6) caused by vertical loads F in all free nodes.

Depending on the degree of flexible restraint c_M between beams and columns (c_M-values are the same for all beam-column connections of a frame), the value of $F = F_{ki}$ has been plotted, which is decisive for the failure by buckling in the frame plane.

As the c_M-value increases, F_{ki} increases as well. The greatest increase is to be seen in the range $0.1 \cdot 10^{11} \leq c_M \leq 0.5 \cdot 10^{11}$ Nmm/rad and $1 \cdot 10^{11} \leq c_M \leq 5 \cdot 10^{11}$ Nmm/rad, which is less clearly to be seen from the logarithmic representation.

The c_M-range plotted on the abscissa corresponds to the zone in which F_{ki} most significantly changes.

For $50 \cdot 10^{11}$ Nmm/rad $\leq c_M \leq \infty$ the F_{ki}-values remain almost unchanged.

c_M-values $\leq 0.01 \cdot 10^{11}$ Nmm/rad for frames with pinned base points are to be regarded as impractical.

The path of curves for frames with restrained base points are markedly flatter and thus they have a comparatively less steep gradient for F_{ki}-values.

At last another aspect is to be mentioned, i.e. the overlapping of the curves 1 and 2 as well as 4 and 5 in Fig. 1.

With low c_M-values the F_{ki}-values of two-storey frames are above those of three-storey frames, which is mainly caused by the two additional vertical loads of the three-storey frame despite the differences in geometry and stiffness between the two frames. With increasing c_M-values this tendency is reversed, as beam stiffness, above all of the lower beam, increases. In the chosen examples the I_R-value of a three-storey frame is, as stated, considerably greater.

In Fig. 2 the path of F_{ki}, depending on the value of the moment of inertia of beams (I_R) and legs (I_S) respectively, is represented for a special stiffness variation of a three-storey frame with restrained base points.

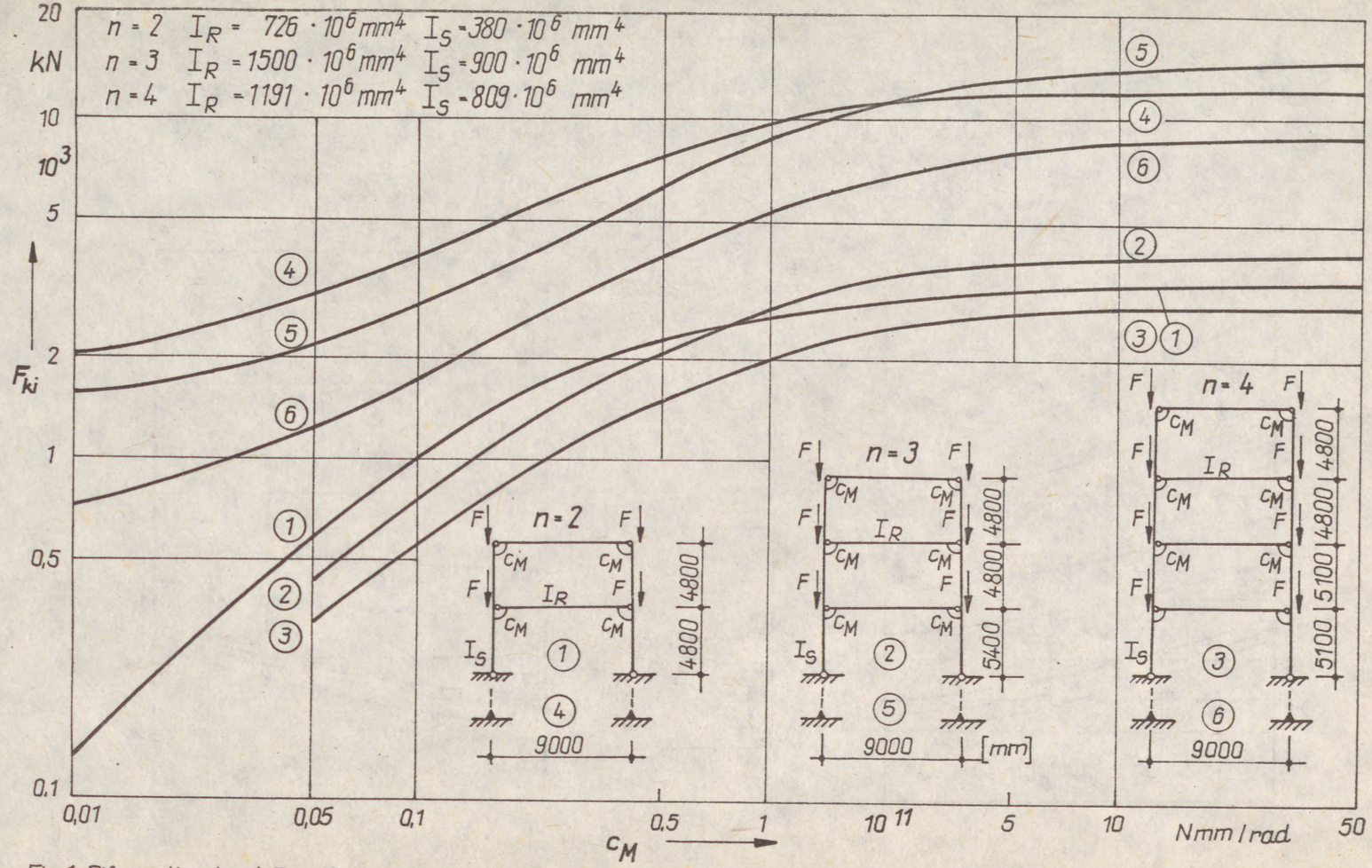

Fig.1 Bifurcation load F_{ki} of frames depending on flexible beam-column-connections (c_M - value).

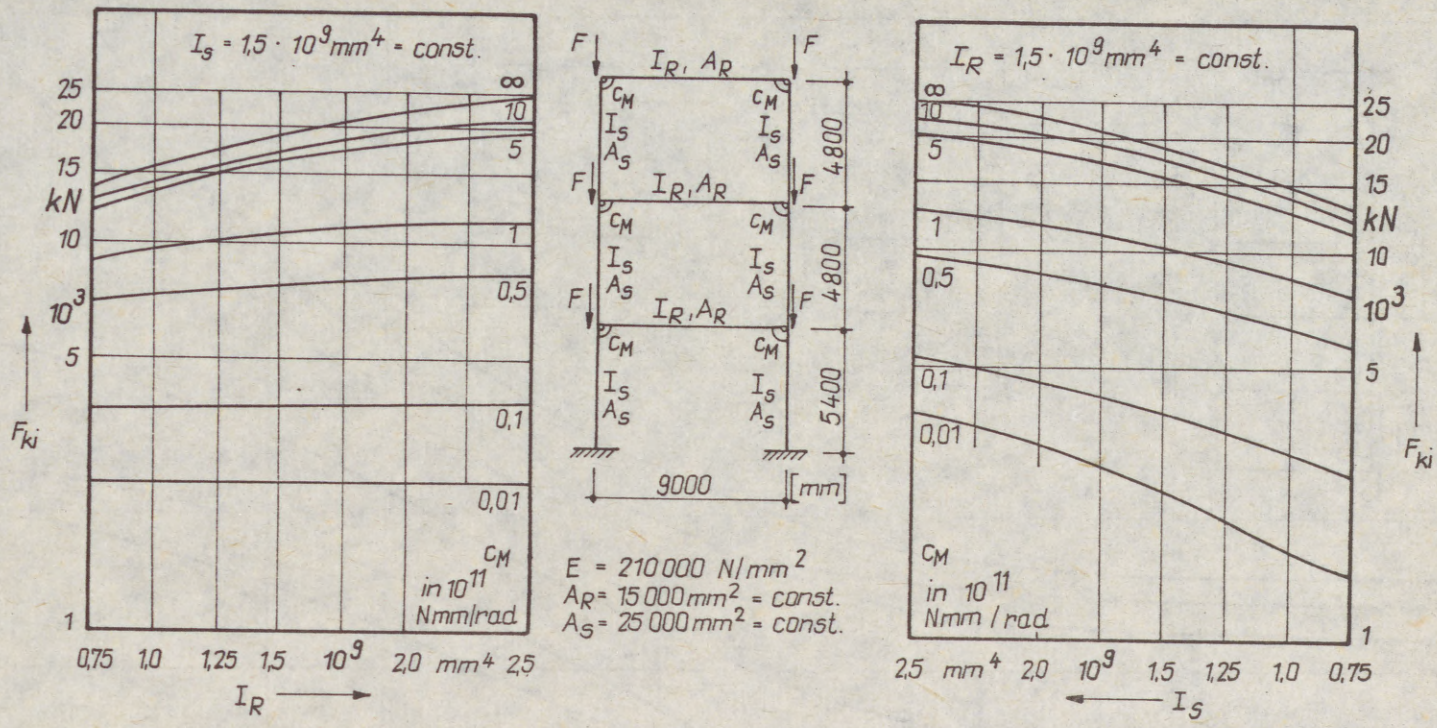

Fig. 2 Bifurcation load F_{ki} of a three-storey frame with restrained base points depending on flexible beam-column-connections (c_M-value) and moment-of-inertia values of beams (I_R) and columns (I_S) respectively.

The individual curves represent selected c_M-values, which are the same for all column-connections of any frame.
It becomes clear that the variation of I_R with constant I_S exerts an influence on F_{ki} for values $c_M \geq 0.5 \cdot 10^{11}$ Nmm/rad only.
This tendency becomes plausible, if c_M-values $< 0.5 \cdot 10^{11}$ Nmm/rad are assumed to be a borderline case of a pinned beam-column-connection. The variation of I_S with constant I_R influences F_{ki} markedly, covering the whole c_M-range.

Bibliography

/1/ Thiele, R.: Baumechanische Simulierung drehelastischer Wirkungen und ihr Einfluß auf den Anstrengungszustand von Stab- und Flächentragwerken. - 1986
Leipzig, Technische Hochschule, Sektion Bauingenieurwesen, Diss. B

/2/ Urban, K.: Schnittgrößenumlagerung und Verformungsentwicklung ebener, zweistieliger, verschieblicher Stockwerkrahmen mit drehelastischen Riegel-Stützen-Verbindungen und Fußpunktlagerungen bei elasto-statischer Berechnung nach Theorie II. Ordnung. - 1989
Leipzig, Technische Hochschule, Sektion Bauingenieurwesen, Diss. A

/3/ TGL 13503, Blatt 1 und 2, Stahlbau - Stabilitätsfälle

VENKOV, LIUBCHO (1)
BELEV, BORISLAV (2)

NON-LINEAR ANALYSIS OF STEEL FRAMES REINFORCED IN LOADED STATE

INTERNATIONAL COLLOQUIUM
STABILITY OF STEEL STRUCTURES
BUDAPEST, HUNGARY, 1990
PRELIMINARY REPORT

SUMMARY : THIS PAPER PRESENTS A METHOD FOR INVESTIGATING STEEL FRAMES REINFORCED IN LOADED STATE BY ENLARGEMENT OF THE ELEMENT CROSS SECTIONS. THE HISTORY OF LOADING, GEOMETRIC AND MATERIAL NON-LINEARITIES ARE INCLUDED IN THE FINITE ELEMENT ANALYSIS. THE PROPOSED METHOD WAS APPLIED TO STUDY THE IN-PLANE BEHAVIOUR AND THE OUT-OF-PLANE STABILITY OF A PORTAL FRAME.

1. INTRODUCTION

THE RENOVATION OF THE MANUFACTURING TECHNOLOGIES USUALLY RESULTS IN INCREASE OF LOADING ON THE INDUSTRIAL BUILDING STRUCTURES. OFTEN STRENGTHENING OF THESE STRUCTURES IS REQUIRED TO ENSURE THEIR FURTHER UTILIZATION.

TWO BASIC METHODS OF STRENGTHENING ARE IMPLEMENTED - ENLARGEMENT OF THE ELEMENT CROSS SECTIONS AND MODIFICATION OF THE STRUCTURAL SCHEME (BY CHANGING THE SUPPORT CONDITIONS, ADDING NEW MEMBERS, ETC.). WHEN PRODUCING THESE OPERATIONS A PART OF THE LOADING (USUALLY DEAD LOAD) IS ACTING UPON THE STRUCTURE.

THE DESIGN CODES GENERALLY DO NOT PROVIDE ADEQUATE FORMULAS TO EVALUATE THE STRENGTH OF STEEL STRUCTURES REINFORCED IN LOADED STATE. TO ALLOW FOR THE HISTORY OF LOADING, GEOMETRIC AND MATERIAL ,NON-LINEARITIES, COMPUTER BASED INVESTIGATION IS RECOMMENDED [REBROV/1988].

---

(1) ASSOC. PROF. OF STEEL STRUCTURES, HIGHER INSTITUTE OF ARCHITECTURE AND CIVIL ENGINEERING, SOFIA, BULGARIA.
(2) POSTGRADUATE STUDENT

THIS PAPER PRESENTS A METHOD FOR ANALYZING THE IN-PLANE BEHAVIOUR AND THE OUT-OF-PLANE STABILITY OF STEEL PLANAR FRAMES REINFORCED IN LOADED STATE BY ENLARGEMENT OF THE ELEMENT CROSS SECTIONS.

2. BASIC DEFINITIONS AND ASSUMPTIONS

THE STEEL FRAMES UNDER CONSIDERATION ARE ASSUMED TO BE LOADED IN THEIR PLANE OF SYMMETRY. THE LOADS, ACTING ON THE ORIGINAL STRUCTURE DURING THE REINFORCING ARE REFERED TO THE INITIAL LOADING. THE LOADS APPLIED AFTER THE REINFORCING ARE REFERED TO THE ADDITIONAL LOADING. IF WELDING IS USED TO CONNECT THE REINFORCEMENT TO THE ORIGINAL STRUCTURAL MEMBERS, A COMPLEX ALTERATION OF THE INITIAL STRESS-AND-STRAIN STATE TAKES PLACE. IN THIS STUDY THE CASE OF BOLTED AND ADHESIVE CONNECTIONS IS CONSIDERED.

STEEL IS TREATED AS A MATERIAL WITH BILINEAR σ-ε CURVE. THE STRAIN REVERSAL IS NEGLECTED. THE ORIGINAL STRUCTURAL MEMBERS AND THE REINFORCEMENT CAN POSSESS DIFFERENT YIELD STRESSES σ_y AND $\sigma_{y,r}$ (FIG. 1).

THE OUT-OF-PLANE STABILITY ANALYSIS ASSUMES THAT THE MEMBERS ARE FREE OF GEOMETRICAL IMPERFECTIONS (LATERAL DEFLECTION, TWIST). THEREFORE THE PREBUCKLING AND THE BUCKLING DISPLACEMENTS ARE UNCOUPLED. FOR PREDICTING THE LATERAL BUCKLING LOADS A PRELIMINARY IN-PLANE ANALYSIS IS REQUIRED [BARSOUM, GALLAGHER/1970].

THE FINITE ELEMENT METHOD FOR ANALYZING BOTH THE IN-PLANE BEHAVIOUR AND THE OUT-OF-PLANE STABILITY IS ADOPTED HEREIN.

3. IN-PLANE ANALYSIS

IN ORDER TO INCLUDE THE MATERIAL NON-LINEARITY, THE STRUCTURAL MEMBERS ARE APPROXIMATED BY SERIES OF FINITE ELEMENTS OF SMALL LENGTH AND UNIFORM SECTION PROPERTIES. THE EXTERNAL LOADS ARE APPLIED AS SEQUENCES OF SUFFICIENTLY SMALL INCREMENTS. THEN THE INCREMENTAL NODAL DISPLACEMENTS $\{\Delta Z_i\}$ FOR STEP NUMBER i CAN BE FOUND FROM THE LINEAR EQUATION SYSTEM

$$[K_t(Z_{i-1})]\{\Delta Z_i\} = \{\Delta F_i\} \qquad (1)$$

WHERE $\{\Delta F_i\}$ IS THE NODAL LOAD INCREMENT AND $[K_t(Z_{i-1})]$ IS THE TANGENT STIFFNESS MATRIX, BASED ON DISPLACEMENT STATE $\{Z_{i-1}\}$.

TO DECREASE THE NUMERICAL ERROR ACCUMULATION, A MODIFIED SOLUTION SCHEME INCLUDING PRELIMINARY AND FINAL SUBSTEPS IS SUGGESTED :

$$\{\Delta Z_i^*\} = [K_t(Z_{i-1})]^{-1}\{0.5\Delta F_i\}$$
$$\{\Delta Z_i\} = [K_t(Z_{i-1}+\Delta Z_i^*)]^{-1}\{\Delta F_i\} \qquad (2)$$

THE PRELIMINARY SUBSTEP PROVIDES AN "AVERAGE" TANGENT STIFFNESS OF THE STRUCTURE.

KNOWING THE STRAIN VALUES FOR THE PREVIOUS LOAD LEVEL, THE STRAIN INCREMENTS FOR A GIVEN STEP ARE OBTAINED FROM THE EQUILIBRIUM CONDITIONS

$$M_{ext} = M_{int} \quad , \quad N_{ext} = N_{int} \qquad (3)$$

IN ACCORDANCE WITH THE BERNOULLI-NAVIER HYPOTHESIS. THE STRESS RESULTANTS

$$M_{int} = \sum_i y_i \sigma_i \Delta A_i \quad , \quad N_{int} = \sum_i \sigma_i \Delta A_i \qquad (4)$$

ARE COMPUTED VIA THE CROSS SECTION DISCRETIZATION SHOWN IN FIG. 2. IN (4) ΔA_i IS THE ACTIAL AREA OF THE RECTANGLE NUMBER i AND σ_i IS THE CORRESPONDING NORMAL STRESS.

WHEN THE STRAIN INCREMENTS FOR A GIVEN STEP HAVE BEEN ALREADY FIXED, EFFECTIVE SECTION PROPERTIES ARE CALCULATED USING THE EFFECTIVE AREAS

$$\Delta A_{i,t} = (E_{i,t}/E)\Delta A_i \quad . \qquad (5)$$

HERE $E_{i,t}$ REPRESENTS THE CURRENT VALUE OF THE TANGENT YOUNG'S MODULUS. THE EFFECTIVE FINITE ELEMENT RIGIDITIES ARE MEAN VALUES OF THE EFFECTIVE SECTION PROPERTIES OBTAINED FOR THE NODAL CROSS SECTIONS.

IN ORDER TO ALLOW FOR THE MATERIAL NON-LINEARITY AND THE MOMENTARY CHANGE IN CROSS SECTION SHAPE (DUE TO REINFORCING), AN ELEMENT STIFFNESS MATRIX FORMULATED WITH RESPECT TO AN ARBITRARY COORDINATE SYSTEM [ROIK, KINDMANN/1982] IS USED. IN MATRIX NOTATION

$$[\, K^e \,] = [\, K_L^e \,] + [\, K_G^e \,] \qquad (6)$$

WHERE $[\, K_L^e \,]$ IS THE LINEAR STIFFNESS MATRIX AND $[\, K_G^e \,]$ IS THE GEOMETRIC STIFFNESS MATRIX. THE MATRIX $[\, K^e \,]$ OF ORDER 14 IS SPLITTED INTO TWO MATRICES TO PERFORM CONSECUTIVELY THE IN-PLANE AND THE OUT-OF-PLANE ANALYSIS.

THE FINITE DISPLACEMENTS OF THE STRUCTURE ARE TAKEN INTO ACCOUNT BY CONTINUOUSLY UPDATING THE NODAL COORDINATES.

TWO LIMIT STATE CRITERIA ARE INCLUDED IN THE IN-PLANE ANALYSIS. AT FIRST, THE GLOBAL TANGENT STIFFNESS MATRIX SINGULARITY INDICATES THAT THE ULTIMATE POINT ON THE LOAD - DISPLACEMENT CURVE IS REACHED. THE SECOND CRITERION USED RESTRICTS THE PLASTIC STRAIN VALUE [CHERNOV, STRELETSKII, LIUBAROV/1984] :

$$\varepsilon_p \leq \varepsilon_{p,lim} \qquad (7)$$

IN THE NUMERICAL STUDY DESCRIBED BELOW, $\varepsilon_{p,lim} = 0.003$, IS ADOPTED.

(4)

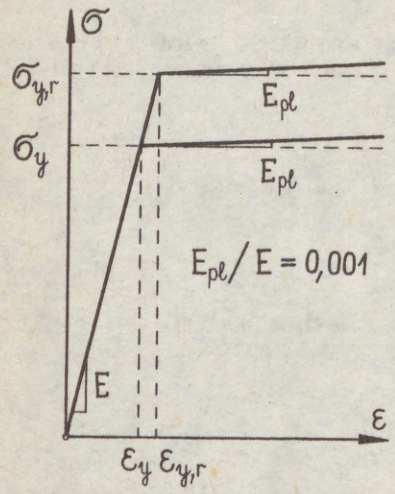

Fig.1

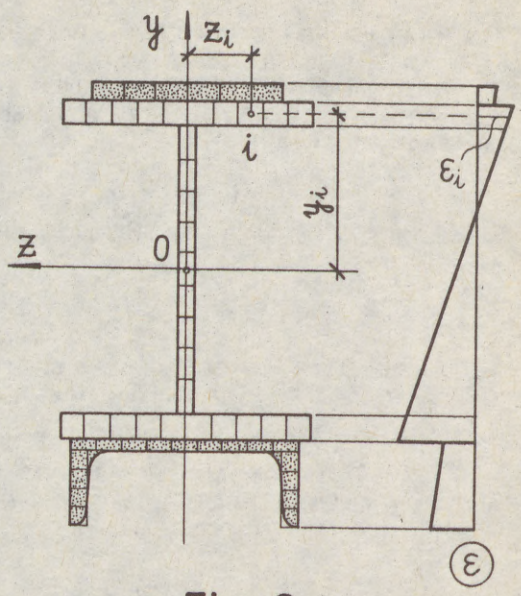

Fig. 2

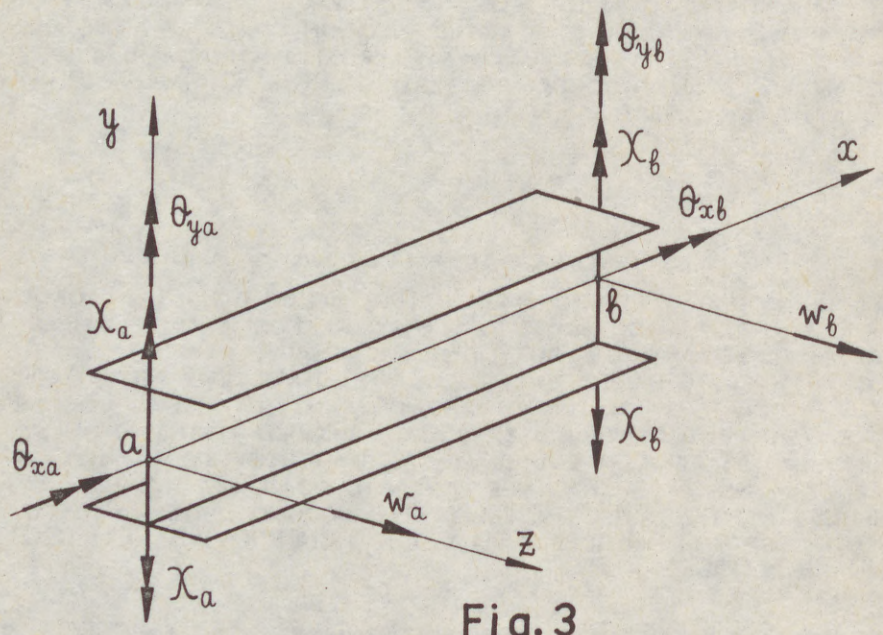

Fig. 3

4. OUT-OF-PLANE ANALYSIS

THE NODAL BUCKLING DISPLACEMENTS ARE SHOWN IN FIG.3. IN ORDER TO INCLUDE THE WARPING EFFECTS IN THE THIN-WALLED SECTIONS, A DEGREE OF FREEDOM $\chi = -\theta'_x$ IS ADDED. THE LATERAL BUCKLING LOAD IS DETERMINED ACCORDING TO THE TANGENT MODULUS CONCEPT. THE REQUIRED EFFECTIVE SECTION PROPERTIES ARE COMPUTED WITH THE VALUES OF $\Delta A_{i,t}$, CORRESPONDING TO THE STATE OF STRAINS REACHED. IN THIS WAY, THE MAGNITUDE OF THE INITIAL LOADING IS TAKEN INTO ACCOUNT. TO OBTAIN THE BUCKLING LOAD, A CHECK FOR SINGULARITY OF THE GLOBAL TANGENT STIFFNESS MATRIX MUST BE PERFORMED.

5. NUMERICAL STUDY RESULTS

THE METHOD PROPOSED WAS APPLIED TO STUDY THE BEHAVIOUR OF A STANDART PORTAL FRAME SHOWN IN FIG. 4. TWO LOADING BRIDGES OF 125 kN CAPACITY ARE INSTALLED IN THE BUILDING. IT IS SUGGESTED THAT THE NEW EQUIPMENT REQUIRES LOADING BRIDGES OF GREATER CAPACITY.

THE LOAD COMBINATION CONSIDERED INCLUDES DEAD AND SNOW LOADS AS INITIAL LOADING AND WIND PRESSURE AND LOADING BRIDGES EFFECTS AS ADDITIONAL LOADING. THE LOADING BRIDGES EFFECTS CONSIST OF FORCES D_{max}, D_{min} AND H (FIG. 5) AND THEIR MAGNITUDES HAD BEEN INCREASED PROPORTIONALLY UNTIL THE ULTIMATE POINT WAS REACHED.

TWO SCHEMES OF REINFORCING WERE ADOPTED TO IMPROVE THE STRENGTH AND THE RIGIDITY OF THE STRUCTURE (FIG. 6). THE HORIZONTAL DISPLACEMENT U_{10} OF NODE NUMBER 10, WHERE THE FORCE H IS APPLIED, WAS FOUND TO BE REPRESENTATIVE. THE LOAD - DISPLACEMENT CURVES FOR THE ORIGINAL (A) AND THE REINFORCED (B, C) FRAME ARE SHOWN IN FIG. 7. THE RELATIVE MAGNITUDE OF THE LOADING BRIDGES EFFECTS WITH RESPECT TO THE DESIGN CODE VALUE D_d IS DENOTED D/D_d. ALL CALCULATIONS WERE CARRIED OUT ON IBM - PC/XT COMPUTER.

THE PROPOSED NUMERICAL METHOD COULD BE SUCCESSFULLY APPLIED FOR ESTIMATING THE EFFECTIVITY OF VARIOUS SCHEMES OF REINFORCING.

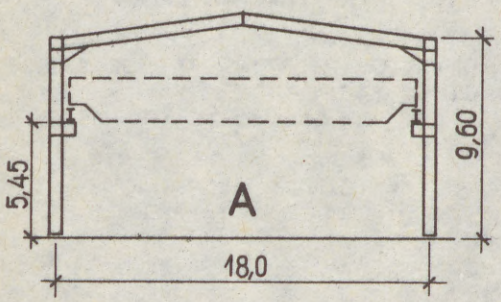

Fig. 4

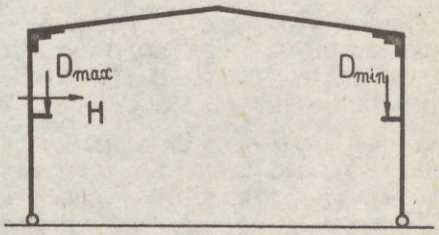

Fig. 5

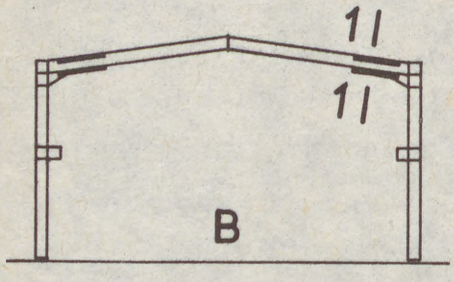

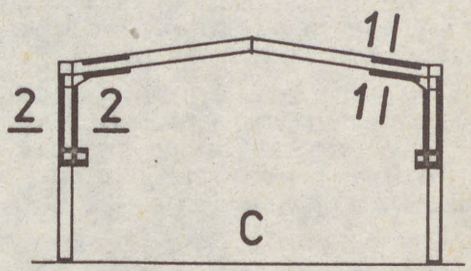

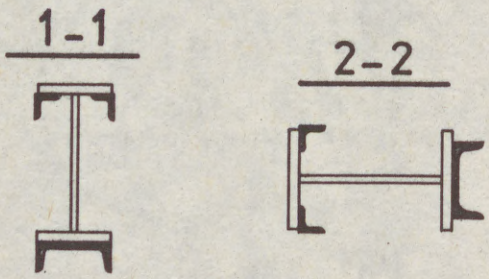

Fig. 6

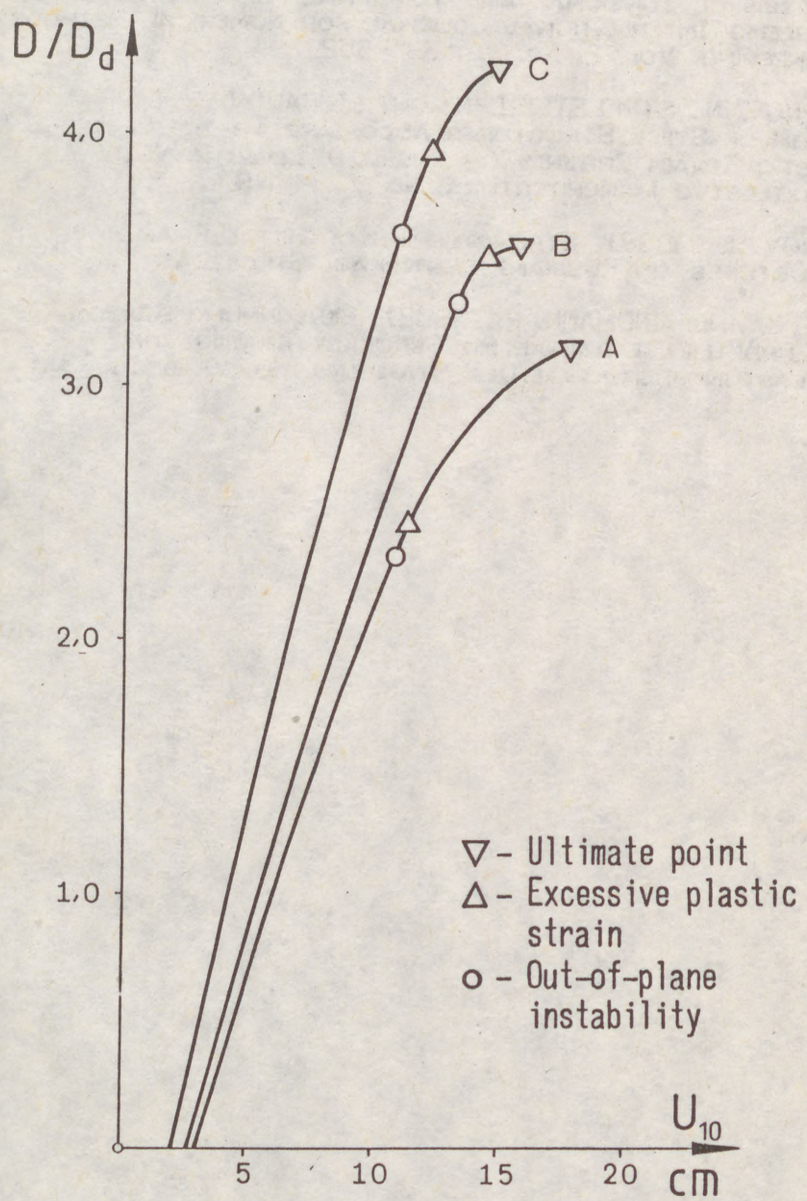
D/Dd
4,0
3,0
2,0
1,0
C
B
A
▽ - Ultimate point
△ - Excessive plastic strain
o - Out-of-plane instability
U10
5
10
15
20
cm

Fig. 7

(8)

6. REFERENCES

1. BARSOUM, R., AND GALLAGHER, R. [1970]. FINITE ELEMENT ANALYSIS OF TORSIONAL AND TORSIONAL-FLEXURAL STABILITY PROBLEMS. INTERNATIONAL JOURNAL FOR NUMERICAL METHODS IN ENGINEERING, VOL. 2, NO. 3, P.335-352.

2. CHERNOV, N., STRELETSKII, N. AND LIUBAROV, B. [1984]. DESIGN OF STEEL STRUCTURES ACCORDING TO THE LIMITED PLASTIC STRAIN CRITERIA. (IN RUSSIAN). IZVESTIA VUZ. STROITELSTVO I ARCHITECTURA, NO. 7., P. 1-9.

3. REBROV, I. [1988]. STRENGTHENING OF METAL FRAME STRUCTURES. (IN RUSSIAN). LENINGRAD, STROIIZDAT.

4. ROIK, K. AND KINDMANN, R. [1982]. BERECHNUNG STABILITÄTSGEFÄHRDETER STABWERKE MIT BERÜCKSICHTIGUNG VON ENTLASTUNGSBEREICHEN. DER STAHLBAU, NO. 10, S. 310-318.

(1)
WALD, František

SENSITIVITY OF SEMI-RIGID FRAMES TO INITIAL IMPERFECTIONS

INTERNATIONAL COLLOQUIUM
STABILITY OF STEEL STRUCTURES
BUDAPEST, HUNGARY, 1990
PRELIMINARY REPORT

Summary: The effects of imperfections are presented for the limit state concept design philosophy of structural steel buildings with flexible beam-column connections. The sensitivity of calibrating frames with four types of connections was tested on second order elastic in plane model with semi-rigid connections expressed as a second order experimental equation. It is demonstrated that for design application of real frames the sensitivity of semi-rigid frames to imperfections is quite adequate to rigid ones.

INTRODUCTION

In a limit states approach to design, it is essential to consider all structural components which may affect the limit states behaviour of the structure. The force-deformation behaviour of the beam-to-column connections in a steel building frame can have a substantial effect on the structural behaviour of the frame. This fact has been recognized at least since 1917, when Wilson and Moore conducted tests on riveled connections. Yet hundreds of tests have been conducted on beam-to-column connections. But it is rather difficult to asses the behaviour of the various types of connections accurately. The most commonly used connections exhibit non-linear behaviour. As a result, non-linear structural analysis techniques are often entailed for a semi-rigid procedure.

We have variety of design methods for rigid frame design with its own brightness of use and accuracy. Each of them brings reasonable results but a lot ones are very complicated. It seams that second order elastic direct methods are most accurate for many cases and best for computer supported design. The effects of imperfections shall be allowed for in frame analysis by means of an equivalent geometric imperfection in the form of an initial sway. Taking into consideration connection flexibility in the analysis and design process represents an important step towards the manifestation of the limit states concept. The problem of second order direct design is in calibrating the imperfections, which we know for local element and need for frame. Against the background of this information, probabilistic methods may be used to derive and define the maximum load-carrying capacity of a given type of structural member. The shape of dangerous imperfection is after first buckling made and is fór building frames similar to sway (Eurocode No.3.- 1989). On the other hand for frame design supported by computer there is no reason for separation of frames on sway and nonsway, rigid and partially restrained.

Assistant Professor, Czech Technical University
166 29 Prague 6, Thakurova 7, Czechoslovakia

(2)

IMPERFECTIONS

Among the various factors that affect the strength of a column in a framework the following are considered to be important: initial crookedness end restraints, residual stresses, load excentricities, variation in mechanical properties of material over cross section, stress-strain characteristicks of material, loading, unloading and reloading of yielded fibres. All of them are substitute as a geometric imperfection - the initial sway of frame. This calibration from known element imperfection to unknown imperfection of frame establish the accuracy of method and its limits of use (Eurocode No.3. - 1989). The value of imperfection should be smaller when we are including the residual strasses in frame model and the same when we are taking into account the end restraints.

CALIBRATING FRAMES

For sway frames with rigid joints was established set of models which should be used as calibrating system in order to check the reliability of different computer programs or new simplified approaches or approximations for the ultimate limit state calculation (Vogel - 1985). For frames with semi-rigid joints will be necessary to have the same set. In this study was used Vogel - 1985 set with rigid and semi-rigid connections for his simplicity and commonly use. Fig. 1.

MODELING OF SEMI-RIGID CONNECTIONS

We know that linear models are simple but inaccurate, polynomial nay encounter a negative stiffness and cubic B-spline needs a large amount of test data. Power model have too many parameters and exponential can not fit well test curves that do not flatten out near the final loadings. Because all these methods can easily be implemented in a computerized method of analysis the exponential combined piece-wise model for calculation (Kishi and Chen - 1986) as very refined was used in study. The need of simple describtion of connection rigidily influence was solved by introducing the modified initial stiffness (Kishi et al.-1988).

Five types of connections are used in the analysis. They are labeled connections S, H, T, E, R. Fig. 2. Connection S is a single web angle connection, connection H is a header plate connection both tested by Wald and Janda 1989, connection T is a top and seated angle connection with double web cleats tested by Azizinamin et al. (1985) and connection E is a extended end plate connection tested by Johnson and Walpole (1981). The size of connection T, E is not exactly for this frame but is very closed to optimum and rotational deformation of any connection never exceeds 0,05 rad.

MODELING OF BEAM-COLUMN ELEMENT

The behaviour of flexible connections is represented by discrete nonlinear rotational spring $M = R_c(\theta_r, M) \cdot \theta_r$, where $R_c(\theta_r, M)$ is a function corresponding to the secant stiffness of the connection. In the unloading case the connection behaviour is assumed to unload linearly following the initial stiffness R_i of connection. The relative rotation θ_{ri} at node i is expressed as rotational degree of freedom of the member minus rotational degree of freedom of the connection. Substituting this into the element stiffness matrix formulation

$$|K_e + K_g| \{d\} + \{F_f\} = \{F\}$$

(Chen and Lui - 1987) we have a reasonable base for iterative solution. Because we have applied the polynomial of third degree for displacement function and only linear for axial deformation along the element we have to cat the compressed element into four elements.

(3)

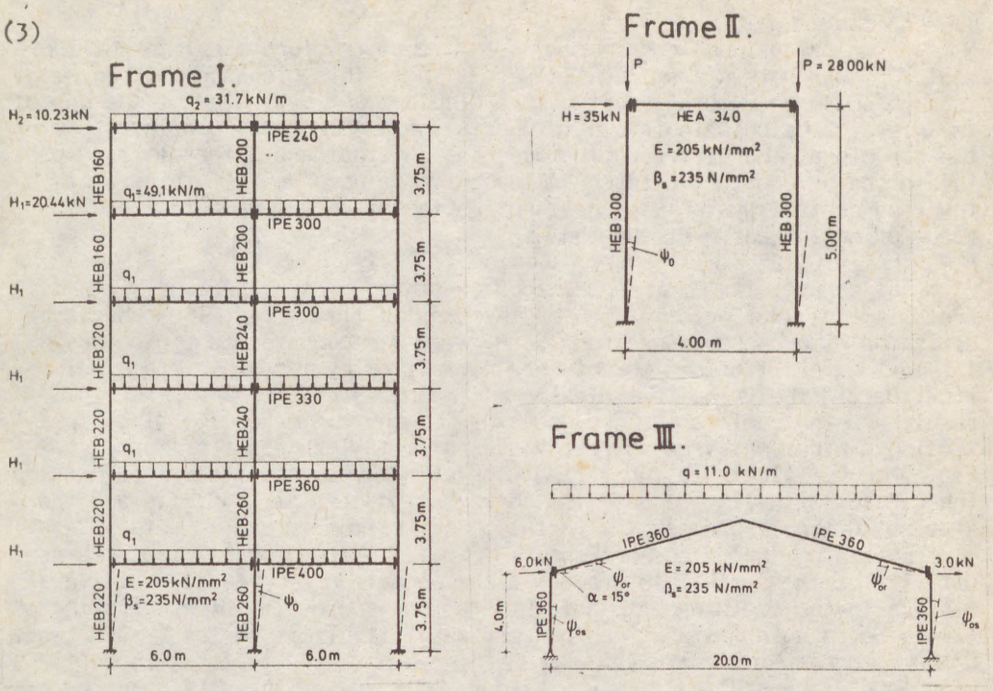

Fig. 1. Calibrating Frames

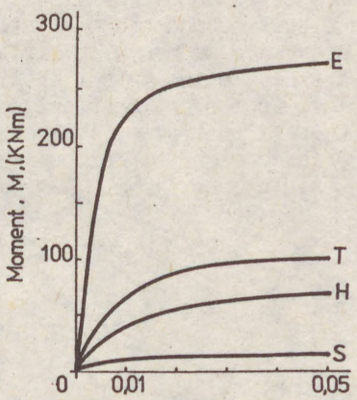

Fig. 2. Connections Behaviour

(4)

COMPUTATION TECHNIQUE

For a prescribed load increment $\{R_s\}$ the structure displacement increment $\{D_s\}$ was solved from eqn $\{R_s\} = [K_s] \cdot \{D_s\}$. This displacement increment is then added to cumulative structure displacement evaluated at the end of the previous calculation cycle to update the displacement configuration of the structure. The difference between the internal and external force vectors gives an unbalanced force vector which is used as R_s to correct D_s. The load control Newton-Rapson iterative technique was used to trace the load-deflection curve of the frame.

NUMERICAL STUDIES

The sensitivity of imperfections for three typical frames I, II, III from Vogel - 1985 was examined on the elastic limit load. The behaviour of frames with connections types S, H, T, E was compared to rigid one R. The maximum drift column moments are normalized by the rigid frame solutions. Herein the value is the ratio of the difference between the rigid result and the real semi-rigid behaviour to the rigid results. The imperfection was parametrized as real value ratio to the height of frame. Fig. 3 to 5. illustrate the variantions of analysis results for each frame. The circle-solid line represents the variation of maximum drifts and the star-solid line expresses the variation of maximum column moments.

Examining the values enclosed in Fig. 3. to 5. we can say that the sensitivity of the semi-rigid frames to the geometric imperfections is very similar to the rigid ones to some boundaries of rigidity. There are the frames reasonable designed to the serviceability limit states (H/300 resp. H/500 Eurocode No 3 - 1988). To show these boundaries is for this particular mode expressed the same variation. Modified initial stiffness C_{ko} was used for each frame with imperfections after Eurocode No 3 - 1988. The stiffness was expressed as relative $\overline{C} = C_{ko} \cdot L/EI$, where L is length, E modulus of elasticity and I moment of inertia of connected beam.

CONCLUSIONS

The most complex, accurate and reasonable difficult design model for rigid and semi-rigid frames is direct second order elastic design. There is no reason for using some approximate method with difficulties on boundaries. All these models is necessary tested on calibrating frames.

The sensitivity of semi-rigid frames on imperfections is very similar to the rigid frames for reasonable stiff frames. That means that frames which are in recommendet limits for horizontal deflection have the same sensitivity on imperfections as rigid ones.

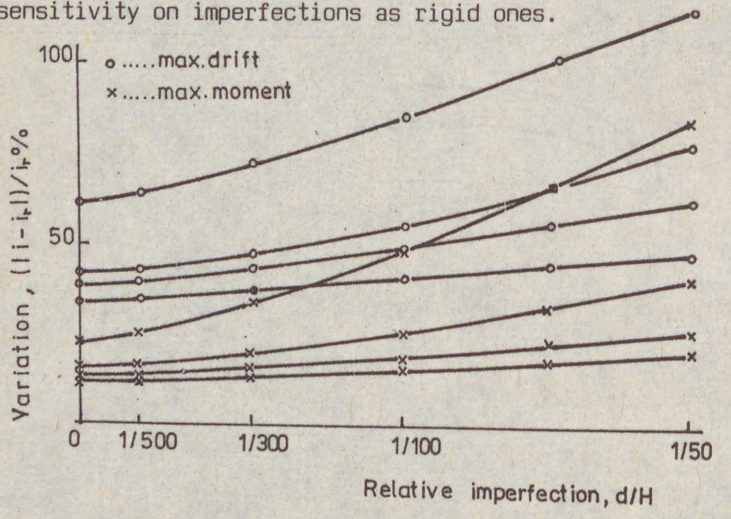

Fig. 3.

The Variation of Analysis Results for Frame I

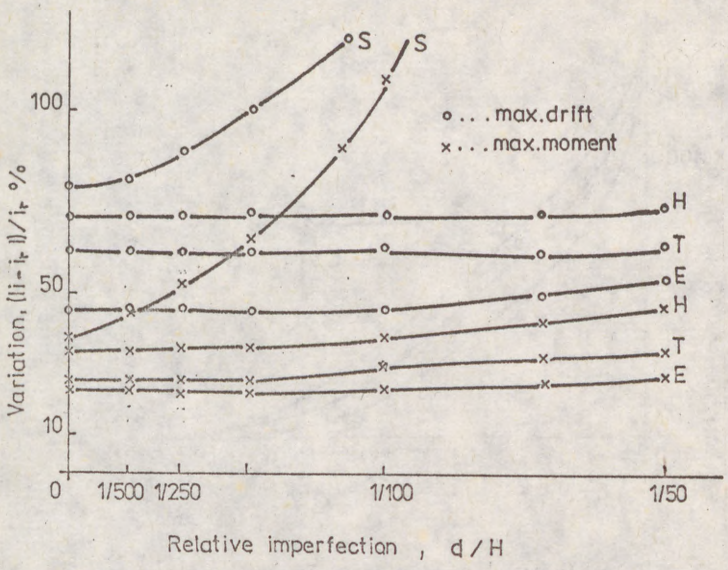

Fig. 4. The Variation of Analysis Results for Frame II

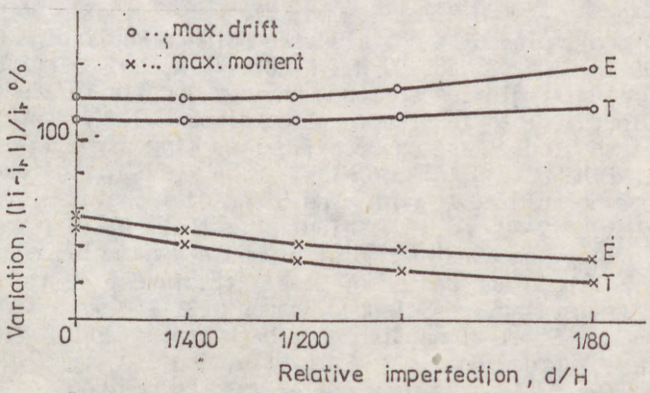

Fig. 5. The Variation of Analysis Results for Frame III

(6)

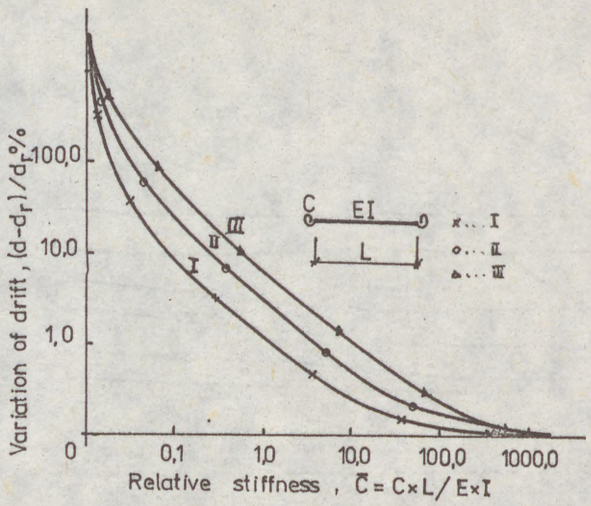

Fig. 6. The Variation of Sway for Modified Initial Stiffness

References

1. EUROCODE No. 3 (1989), Design of Steel Structures, Final Draft December 1988, Liaison Engineers, February.-2. AZIZINAMIN,A., BRADBURN, J.H. and RADZIMINSKI, J.B. (1985): Static and cyclic behaviour of semi-rigid steel beam-column connections, Dept. of Civ. Engrg. Univ. of South Carolina, Columbia, S.C., USA.-3. BJORHOUDE, R., BROZETTI, J. and COLSON, A. (1987): Classification of connections, Connections in Steel Structures, Elsevier A.S., London, 388-396 pp.-4. CHEN, W. F. and LUI, E. M. (1987): Structural Stability - Theory and Implementation, Elsevier Science Publishing Co., New York, N.Y., 490 pp. - 5. JONES, S. W., KIRBY, P. A. and NETHERCOT, D.A. (1981): Modeling of semi-rigid connection behaviour and its influence on steel column behaviour. Joints in Structural Steelwork, J. H. Hewlett, W.M. Jenkins and R. Stainsby, eds. Pentech Press, United Kingdom, 5.73 - 5.78. - 6. JONES, S. W., NETHERCOT, D. A. and KIRBY, P. A. (1987): Influence of connection stiffness on column strength, The Structural Engineer, Volume 65A, No. 11, November, 399-405 pp. - 7. KISHI, N. et al. (1988): Moment - Rotation Relation of Top- and Seat-Angle with Double Web-Angle Connections and the Behaviour, Strength and Design of Steel Structures, R. Bjorhoude, et. al. Editors, Elsevier Applied Science, London, 121-134 pp. - 8.KISHI,N. and CHEN, W. F. (1986): Steel connection data bank program. CE-STR-86-18, School of Civ. Engrg., Purdue Univ., W. Lafayette, Ind., USA. - 9.KISHI, N. and CHEN, W. F. (1986): Data base of steel beam-to-column connections, CE-STR-86-26, School of Civ. Engrg., Purdue Univ., W. Lafayette, Ind., USA. 10. MORRIS, G. A., PACHER, J. A. (1987): Beam-to-column connections in steel frames, Can J. Civ. Eng., Vol. 14, 68-76 pp; Dalen, K. V., Dalen, M. V.: Discussion, Nethercot, D. A., Zandonini, R.: Discussion, Can. J. Civ. Eng. 15, 280-284 pp, 1988. - 11. NETHERCOT, D. A., KIRBY, P. A. and DAVISON, J. B. (1988): Structural Performance of Steel Frames with Semi-Rigid Connections, IABSE, Congress Report, Helsinki, 681-686 pp. - 12. SHEN, Z. Y.,

(7)
LU, L. W. (1983): Analysis of Initially Crooked, End Restrained Steel Column, Journal of Constructional Steel Research, Vol. 3, No 1, 10-18 pp. - 13. VOGEL, U. (1985): Calibrating Frames, Vergleichsberechnungen an verschieblichen Rahmen, Stahlbau 54/1985, S. 295-301. - 14. WALD, F. (1983): Non-Linear Analysis of Steel Frames (with Special Consideration of Deflection), ABK paper, Serie R, No 158, Department of Structural Engineering, Technical University of Denmark. - 15. WALD, F. (1989): Rotational Stiffness Characteristics of Semi-Rigid Steel Beam-Column Connections, Acta Polytechnica, ČVUT, Praha, 1989 in printing.

TABLE OF CONTENTS

VOLUME I.

Session 1. "General Design Concepts"

Session 2. "Compression Members"

Session 3. "Built- Up Members"

Session 4. "Beams"

Session 5. "Beam-Columns"

VOLUME II.

Session 6. "Plate and Box Girders"

VOLUME III.

Session 8."Arches"

Session 9. "Triangulated Structures"

Session 10. "Tubular Structures"

Session 11. "Shells"

Session 12. "Cold Formed Members and Interactive Buckling"

VOLUME IV.

Session 13. "Composite Members"


Insignia Liberæ Regiæ Me
tropolitanæ Civitatis Budensis

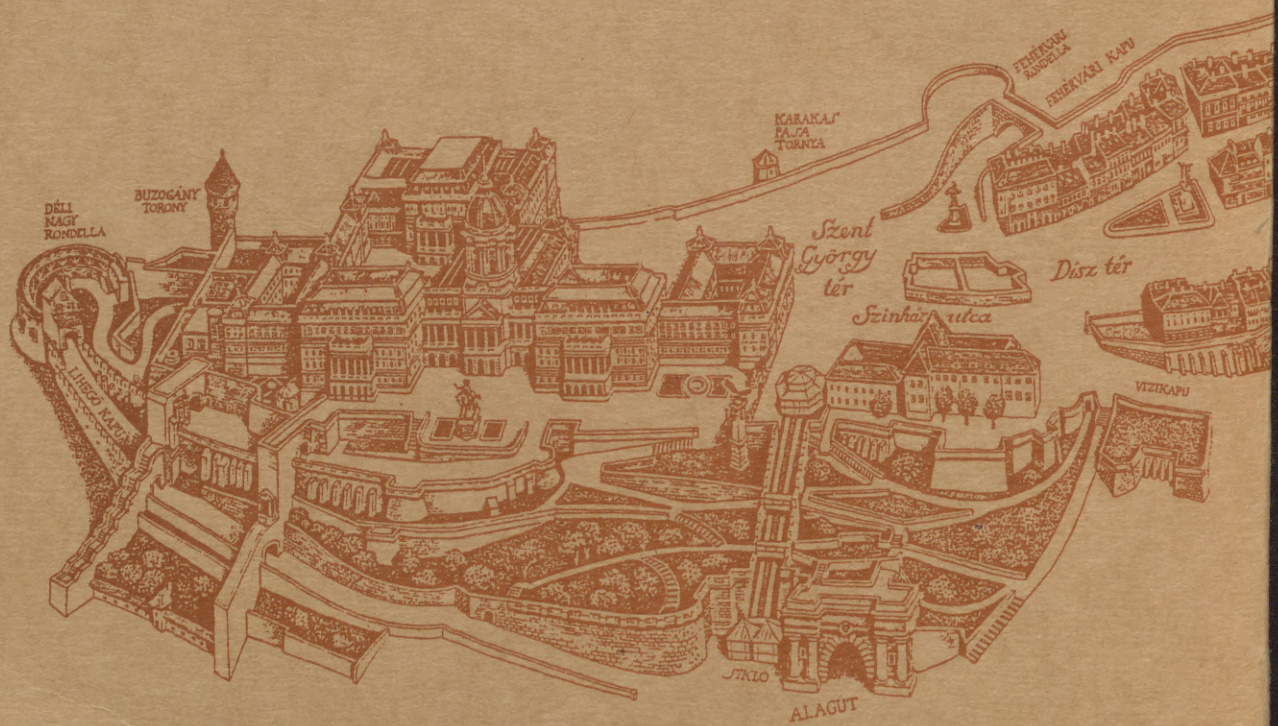
FEHÉRVÁRI RONDELLA
FEHÉRVÁRI KAPU
KARAKAS PASA TORNYA
DÉLI NAGY RONDELLA
BUZOGÁNY TORONY
Szent György tér
Dísz tér
Színház utca
LIHEGŐ KAPU
VÍZIKAPU
SIKLÓ
ALAGÚT

INTERNATIONAL COLLOQUIUM

STABILITY OF STEEL STRUCTU

HUNGARY, BUDAPEST 1

PRELIMINARY REPORT

VOLUME II.